



GoBiGas demonstration – a vital step for a large-scale transition from fossil fuels to advanced biofuels and electrofuels

CHALMERS
UNIVERSITY OF TECHNOLOGY

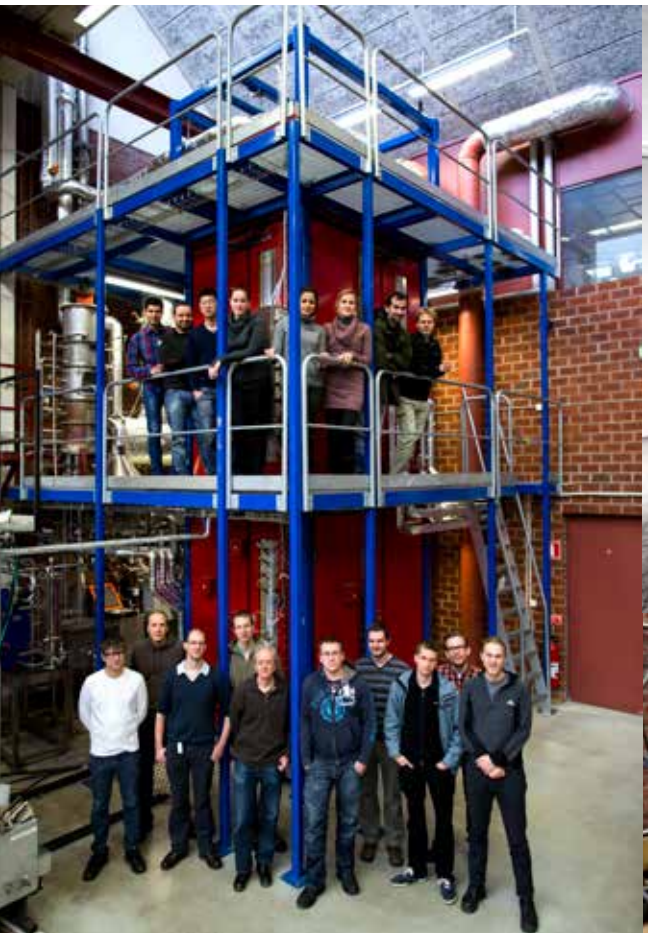


Preface

“The GoBiGas project is the most advanced project on thermochemical conversion of biomass to biomethane on a global scale at present. This shows that innovation and state of the art gasification technologies are very advanced in the EU and actually places the EU ahead of all other in this technology area.

I have being following closely the developments over the past years as the innovation and knowledge the GoBiGas project has generated is very important for the entire industry in terms of both credibility and bankability while driving costs down by the learning effect.

The GoBiGas is really a pioneer, first-of-a-kind-plant that shows the way forward for others to follow. The plant wouldn't have been built if it was not for the determination and foresight of Goteborg Energi.”

– *Kyriakos Maniatis, Principal Administrator, European Commission, DG ENER*

GoBiGas demonstration –
a vital step for a large-scale transition from fossil fuels
to advanced biofuels and electrofuels.

Editor: Henrik Thunman

ISBN: 978-91-88041-15-9

Table of contents

Executive Summary

This report summarises the technical and economic demonstration of the GoBiGas-project, a first-of-its-kind industrial demonstration of advanced biofuel production via gasification. The principal result of the GoBiGas demonstration is an advanced biofuel plant with a production capacity of 20 MW of biomethane* from woody biomass, which shows that the technology is commercially mature and is ready for large-scale deployment.

Transportation fuel can be produced at an attractive cost level: The demonstration was designed to fulfil the requirements of an industrial installation, meaning that costs and experiences are directly transferable to a commercial project. Moreover, the project gave insights into how to integrate advanced biofuel production into existing infrastructure, how to efficiently utilise advanced biofuel production to make electrofuels and the importance of building in efficient logistics for sustainable biomass and/or waste materials to feed this type of plant. The preferred plant size for the technology is around 200 MW of advanced biofuel output, operating for at least 8,000 hours/year. This corresponds to an annual feedstock requirement of around 450,000 dry tonnes of biomass; comparable to the biomass needs of an averagely sized pulp mill. The production costs of the advanced biofuel are in the equivalent range of EUR 0.55 per litre of petrol (EUR 60/MWh) at a current feedstock price of EUR 15/MWh. This is based on the lower heating value for the dry part of an average 45% of moist biomass delivered to the plant. At present feedstock prices, the feedstock corresponds to 35% of the total production costs.

Network of experienced industries: The demonstration plant was built by Göteborg Energi, supported by the Swedish Energy Agency. In principle, it comprised two steps. The first is the gasification step; converting biomass to gas. In the second step, the gas is converted to specific hydrocarbon(s), methane in the case of the GoBiGas-plant. Cutting-edge multinational companies where contracted for the construction. Valmet (formerly Metso Power) was selected to deliver the gasification section. The company to have built the world's largest commercial biomass-fuelled gasifiers. Valmet has over 40 years' experience in this field and operates on all continents. The methanation section of the technology was delivered by Haldor Topsoe. This firm has provided the technology and designed the largest commercial installations in the world for synthesising methane from syngas. Jacobs was contracted for detailed engineering and for construction of the methanation section. Jacobs is one of the largest Engineering Company in the world in this discipline. In total, the project required 300,000 M/h of engineering and 800,000 M/h of construction.

Research under industrially relevant conditions: An extensive research programme was launched support the demonstration, led by Chalmers University of Technology. This involved erecting a 2-4 MW research gasifier on the Chalmers campus. A spectrum of vital competences was gathered under the research programme. This provided the necessary knowledge to solve all manner of technical challenges, whilst developing the necessary tools to evaluate process performance. The major technical breakthrough in the project related to balancing and controlling the chemistry of the gasification process during start-up, plus stable operation to overcome fouling issues (mainly tar in the convection path; a generally recognised showstopper for this technology).

Technology ready to go full-scale, but market conditions lacking: From the evaluation programme, it can be concluded that the high performance goals of the process could be achieved for woody biomass (as seen in theoretical process evaluation). The new findings from the demonstration show that the technology is now ready for commercial-scale implementation. However, to provide an economic situation

**Also called Synthetic Natural Gas, SNG, or biogas via gasification.*

favouring such an implementation, there are still numerous questions. These issues were not included in the demonstration, but must be answered (or would increase the competitiveness of the technology if they were):

- How can a robust regular system be established which facilitates investment in large-scale advanced biofuel production?
- How can the vast quantities of sustainable biomass necessary for large-scale introduction of advanced biofuels be organised and assured?
- How can the overall process be optimised to favour higher value chains?
- How can the conversion process be optimised to give a direct mixture of valuable hydrocarbons without using the carbon monoxide and hydrogen route?
- How can biochemical processes be used in combination with chemical processes to produce high-value molecules and increase overall economy of the plant?
- How can the process be adapted for low-value fuels (such as waste materials), including problematic inorganic components?
- How can the process be adapted to make all components ingoing with the biomass or waste end up as valuable products?
- How can present infrastructure be used to enable the cost-effective introduction of advanced biofuel production?

Current status of the GoBiGas plant: on 27th March 2018, the board of Göteborg Energi decided that the demonstration had achieved its goals and that continued operation of the plant could only be justified if the plant were run on a commercial basis. Technically, the plant has been built so that it can go from demonstration to commercial operation. However, the current price of biomethane for a producer in the region is below SEK 600/MWh (~EUR 60/MWh). This is less than the variable costs of operating the plant as a standalone. For pellets, this is EUR 80-90/MWh, for forest residue EUR 65-72/MWh (plus additional investment of around EUR 5 m) and for recovered wood EUR 50-60/MWh (this requires a new environmental permit and additional investment similar to that for forest residues). Based on this information, a commercial operation under present conditions would not work. Had the original plan been fulfilled, the demonstration plant would have shared personnel with a commercial plant five times its size. This would have lowered the variable costs by EUR 20-22.5/MWh for all fuels. The plant has now been mothballed and can be recommissioned (if market conditions change) or rebuilt for other purposes.

Content of this report: a popular-science presentation of the project and the research groups involved is given, plus a collection of full-length papers published or submitted for publication in peer-reviewed scientific journals. These detail the experiences and evaluation of process performance, plus a summary of the various integration options. There is also a reference list of relevant works from involved research groups.

Introduction

The climate issue is one of the greatest challenges of our time. In this context, increased global temperatures due to anthropogenic greenhouse gases emissions (from combusting fossil fuels such as oil, gas or coal) will have an uncontrolled effect on the climate. The anticipated outcome is more extreme weather, resulting in all kinds of societal disturbances. The image below shows what might be considered be a mild (or even harmless) example; a cycle path has become a "canoe path". However, this kind of flooding will cause soil erosion at tremendous cost to society.

Since fossil fuels account for some 80% of all global energy sources, replacing most of them with energy-efficiency measures or renewables by 2050 (in keeping with the Paris Agreement) is a tremendous challenge. The expectation is that a large proportion of the fossil fuels will be replaced by solar or wind-generated electricity and perhaps nuclear power. However, there are a number of areas which will have to be produced from renewable carbon. These include aviation, long-distance shipping and heavy haulage in rural areas plus various materials and chemicals. These will mainly go over to biomass, complemented with fuels produced from carbon dioxide directly captured from the air or extracted from shallow seawater. The sustainable biomass used for these purposes will be by-product of the extraction of more valuable products like timber and pulp. From a global perspective, this means that even the selection of markets mentioned above will be huge; equivalent to practically all the estimated available biomass.

Photo: Henrik Thunman.

The limitations imposed by short supply portend a situation in which processes using biomass as production feedstock will need to be: 1) highly efficient from the economic and energy perspectives, 2) able to use heterogeneous feedstock, 3) able to produce substantial quantities and 4) able to convert all ingoing carbon into hydrocarbon products, as direct or indirect replacements for fossil alternatives. Hydrocarbons produced in such process are known as "advanced biofuels".

In the last 40-50 years, gasification has been identified as the technology that meets these requirements. The technology found similar use during WWII in Germany and during the embargo against apartheid-era South Africa. At those times, coal was the preferred feedstock, as with the large coal gasification plants in modern-day China. In terms of technology, the processes developed for coal cannot generally be used for biomass, because the basic conversion characteristics, heterogeneity and ash behaviour are all different. This means dedicated biomass processes must be developed. Large-scale biomass gasification was considered during the oil crises of the 1970s and 80s. Sweden, for example, wanted to switch to methanol as vehicle fuel and become independent of oil. A major domestic programme was launched and the technology was piloted. However, development was all but halted by the discovery of North Sea oil and diversification of the market. Still, the programme did result in several demonstration projects, the best-known of which is the biomass integrated gasification combined cycle (BIGCC) in Värnamo.

Development resumed in the mid-1990s, as awareness of climate issues grew. During this period, a great many commercialisation plans were laid, including Chemrec, a black liquor gasification process with subsequent synthesis to DME (DiMethyl Ether). This was successfully piloted (3MW) in Piteå Sweden, with gasification from 2005 and DME synthesis from 2011. However, no-one in the world has built a plant on a suitable industrial scale until the GoBiGas plant, described and analysed here. The GoBiGas is an abbreviation for **Go**thenburg **Bi**ogas **Gas**ification project. Even if the second part of the project (erection of a commercial sized plant) were cancelled in 2015, what so far has been built would meet the requirements of an industrial plant: a production unit in commercial operation for 8,000 hours a year for at least 20 years.

The technology used in advanced biofuel production via gasification includes all the processes which enable intermittent production of electrofuels. Thus, it can benefit from the increased intermittent electrical production in the energy system from solar and wind sources. The process in the GoBiGas demonstration contain of two main steps: 1) gasification, converting biomass to gas and 2) conversion of that gas to one or more specific hydrocarbons. The chemical composition of the biomass is such that the gas produced, when it is converted to specific hydrocarbons, releases the oxygen from the biomass as carbon dioxide. By mixing hydrogen into the gas mixture exiting the gasification process, principally all carbon in the biomass can be converted to the desired hydrocarbon(s). Here, the hydrogen is favourably produced from water splitting by electrolysis..

So, if the price relation between electricity and biomass favours electrofuel production (electrofuel mode), the principle reaction is as follows:

Water (moisture in biomass) + Electricity + Biomass + heat => hydrocarbon(s) + oxygen

Biomethane: 1.28 H_2O + Electricity + $CH_{1.44}O_{0.66}$ + heat=> CH_4 + 0.97 O_2

0.28 H_2O + Electricity + $CH_{1.44}O_{0.66}$ + heat => $(CH_2)_n$ + 0.47 O_2 (Liquid fuels)

In the case of an electricity-biomass price relation unfavourable to electrofuel production, biomass mode:

Water (moisture in biomass) + Biomass + heat=> hydrocarbon(s) + Carbon dioxide

0.310 H_2O + $CH_{1.44}O_{0.66}$ + heat=> 0.515 CH_4 + 0.485 CO_2 (Biomethane)

0.033 H_2O + $CH_{1.44}O_{0.66}$ + heat=> 0.687$(CH_2)_n$ + 0.313 CO_2 (Liquid fuels)

Where the heat needed for the process is mainly produced by electricity (in electrofuel mode) and from combusting part of the biomass (in biomass mode). As a rule of thumb, in electrofuel mode half the fuel produced in the process will be allocated to electrical energy and half to the energy provided by the biomass. With practically no additions, other than the electrolysers used for water splitting, the GoBiGas process could operate with intermittent electrofuel production; switching between the electrofuel and biomass modes. This therefore opens up an attractive route of electrofuel production.

Feasible large scale production of advances biofuels

Results from the GoBiGas demonstration published in scientific journals confirm that large-scale production of advanced biofuel via gasification is feasible. This has been suggested in a large number of theoretical studies and predictions, and has formed the basis of many political decisions to transition from fossil to renewable fuels and meet local and global climate targets. The technology provides an opportunity to produce advanced biofuel on a TWh rather than a GWh scale and thereby opens the way to production that can make a difference globally. The demonstration also confirms that the technology is ready for commercial production and that, using tried and tested components, the process can be built to reach high levels of energy efficiency.

The analysis shows a techno-economic energy efficiency of around 70% (conversion of energy in the dry part of the biomass to energy in the advanced biofuel). It also confirms the economics associated with advanced biofuel production. Based on the assumptions in this work, the cost of producing advanced biofuels in a commercial-scale plant (preferably with 200 MW output and 1.6 TWh annual production), plus an assumed economic lifetime of 20 years and 5% interest) result in a production cost of advanced biofuels of EUR 60/MWh, where the biomass is priced at EUR 15/MWh (fresh forest residue, February 2018 and fuel energy content calculated based on the dry mass of fuel received) correspondrelate to roughly 35% of that cost. This corresponds to EUR 0.545/litre petrol (USD 2.5/gallon at an exchange rate of USD 1.25 to EUR 1).

From a technical standpoint, the GoBiGas demonstration is a success. However, the demonstration also shows that market conditions are not ready for the introduction of large-scale processes, which could make a significant difference. All incentives in this direction currently rely on some sort of subsidiary. If the technology is introduced on a large scale, this becomes too expensive for society. Another drawback is the lack of clear separation between the fossil fuel and its renewable alternative. This means the fossil fuel would outcompete the renewable alternative if it were cheap enough. This implies a contradiction. If the Paris agreement were to be observed, the market for fossil alternatives would disappear; their prices heading towards zero.

Photo: Rob Vanstone

*The GoBiGas Plant. GoBiGas is an abbreviation for **Go**thenburg **Bi**ogas **Gas**ification.*

The GoBiGas Plant

The GoBiGas project originated with the air pollution problem of Gothenburg in the 1970s and 80s. The City decided to replace coal and heavy oil for heat production, as well as introduce gas-powered buses to overcome the problem of soot and other major emissions.

Natural gas was initially used as fuel, but heightened awareness of climate issues resulted in a major programme to produce biogas via fermentation. However, at the start of the 2000s, the substrate available for fermentation in the region was no longer able to cope with demand. It was decided to go for a technology which could deliver vast quantities of biogas from forest residue at high levels of efficiency, making Gothenburg fossil-free.

The GoBiGas plant uses gasification on an industrial scale to convert biomass into advanced biofuel. The current plant was built as a demonstration, but with the aim of being commercially and economically viable when run in combination with a plant five times larger, once the demonstration phase ended. This set the plant's performance bar very high; the target was 65% energy efficiency from biomass-to-biomethane and 90% from ingoing energy streams for saleable biomethane or district heating. Furthermore, the plant was built to operate for at least 20 years, with an availability of 8,000 hours per year. The plant is a first-of-its-kind installation and has played its part in achieving several developmental milestones.

For example:

- April 2014. Artificial activation of biomass gasification for the first time, allowing the gasifier to start up without clogging the downstream heat exchanger with tar (condensable and, in most cases, reactive hydrocarbons).
- December 2014. Biomethane produced via gasification for high-pressure gas grid.
- Autumn 2015. First continuous operation of advanced biofuel production for over 1,000 hours, achieving over 90% of design capacity.
- 2016 to autumn 2017. Successful gasification of bark, wood chips, waste wood.
- Summer 2017. Feasibility of product gas condensation using coated-plate heat exchanger.
- February 2018. Achieved over 1,800 hours of continuous operation and 100% of designed capacity.

The personnel of the GoBiGas-plant during the first year.

The control room at the GoBiGas plant during one of the early start-ups of the gasifier. Åsa Burman (centre, standing) oversees the progress.

The plant has operated for over 15,000 hours in total since being commissioned in November 2014.The GoBiGas plant was built by Göteborg Energi. The demonstration costs totalled SEK 1.6 bn, of which SEK 222m was a grant from the Swedish Energy Agency. Göteborg Energi contracted cutting-edge multinational companies for the construction project. Valmet (formerly Metso Power) was selected to deliver the gasification section. This is the company that have built the world's largest commercial biomass-fuelled gasifiers. Valmet has over 40 years' experience in this field and operates on all continents.

The methanation section of the technology was delivered by Haldor Topsoe. This firm has provided the technology and designed the largest commercial installations in the world for synthesising methane from syngas, which are 1000 times larger than the one in the GoBiGas-demonstration and fed by syngas from gasification of coal in China. Jacobs was contracted for detailed engineering and for construction of the methanation section. Jacobs is one of the largest Engineering Company in the world in this discipline. In total, the project required 300,000 M/h of engineering and 800,000 M/h of construction. Åsa Burman headed the project during the construction phase, aided by Malin Hedenskog (in charge of the gasification section) and Freddy Tengberg (leading the methanation and auxiliary systems sections). Ingemar Gunnarsson had played a central role in the project since its inception in 2005. Up to 2010, he had overall responsibility for the project and was actively involved until his retirement in February 2018. Åsa Burman left the project in the autumn of 2014, with Freddy Tengberg taking over her role.

Staffan Andersson from the project team, Anton Larsson from Chalmers/Göteborg Energi and Claes Breitholtz from Valmet all had crucial roles in the commissioning and process performance development. Larsson and Breitholtz were trained to operate a dual gasification process by helping commission the dual fluidised bed gasifier at Chalmers (described below) during its first five years of operation (from the end of 2007). This connection proved vital to the interaction and exchange of information between the GoBiGas demonstration plant and the research gasifier at Chalmers.

The GoBiGas project also included a demonstration examining the full lifecycle of the gas that was produced. The fuel was delivered to the plant by a Volvo truck running on liquid biogas. The ConGas project was a larger-scale joint project between Volvo AB, Chalmers and Göteborg Energi. Its aims were to develop engines and examine the well-to-wheel benefits of using biogas for heavy transport.

The text translates to: "Five tonnes are enough to fuel this lorry for a 100 kilometers", and "Now we are creating biogas from forest residue".

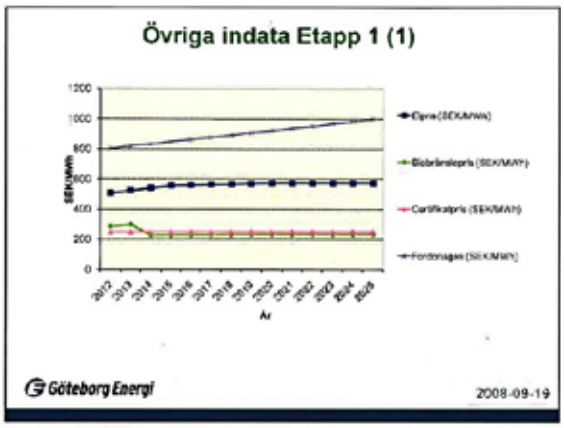

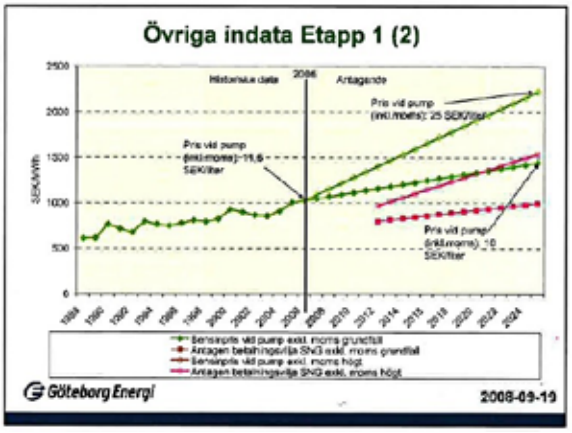

Left: Price forecast for the economic consideration connected to the GoBiGas demonstration from September 2008. The left figure shows the predicted electricity price on the Swedish market (Elpris), the price of biomass (biobränslepris), the certificate price for renewable electricity (Certificatpris) and biomethane for vehicles (Fordonsgas). All figures exclude VAT.

Right: comparison of petrol (bensin) and biomethane (SNG) at tap (vid pump) excluding VAT (moms) for a high and low price on transport fuels. Here, the biomethane price was estimated at SEK 900-1350/MWh.

Economic forecast

In this type of project, the factors that determine whether a plant will be built or not are the economic forecast and capacity to handle the economic risk. In the Figures above the predicted prices are shown and can be compared with current prices ten years later.

Current prices with predicted prices for 2018 made in 2008 in brackets are: electricity SEK 300 (550)/MWh, biomass SEK 170 (230)/MWh, certificate SEK 70 (250)/MWh and biomethane for vehicles 980 (900) SEK/MWh. This shows that the price development of biomethane was very well predicted. However, regulatory changes and Danish biogas with in feed-in support were unforeseen. Given the current price of biomass feedstock, this means the current price (February 2018) of biogas from the GoBiGas plant is less than SEK 600/MWh, the breakeven price of a commercial-sized plant

As shown in the paper relating to the economics of the 20 MW GoBiGas plant, the variable cost coverage for the demonstration unit operated as stand-alone needs a biomethane price of at least SEK 750/MWh to breakeven (production cost for the GoBiGas plant are with present fuel prices; for wood pellets SEK 800-900/MWh, for forest residue SEK 650-720/MWh and for recovered wood SEK 500-600 MWh, both forest residue and recovered wood demand some additional investments, in addition recovered wood need an updated environmental permit). The breakeven cost is then at present configuration substantially higher than the local market price of biomethane. The market failure is largely due to biomethane being traded on a rather limited regional market. The gas market that are natural gas with a negligible amount of renewable gas in the form of biomethane, however, is global. This makes it hard to handle market risks and local disruptions for the biomethane, such as Danish gas on the Swedish market. Although the quantity is a small proportion of all the gas traded on the Danish/Swedish market, it can create a huge effect for specific plants in the region.

This means that regular financial instruments are out of play and extends the time needed to achieve a stable market situation. A situation like this is especially problematic to the introduction of biomethane from large units, such as those based on gasification. In this context, a commercial-sized plant will produce roughly 1.6 TWh of biomethane annually; this would practically double the available biomethane on the Swedish/Danish regional market. Building a plant in the present market situation would cause a major disturbance. The recovery would take quite a few years and cause economic loss to all players in the biomethane market. However, 1.6 TWh of gas on the North European market is almost negligible. This clearly illustrates the need to see how biogas can transform natural gas market across a larger region; preferably ones such as the European Union, North America and so on. This allows creation of a liquid market and allows regular financial tools such as those used in the fossil market. It also means there is a need to separate the producer of renewable gas from the user, which also separates the timings of production and use.

Chalmers Power Central

A major part of the success of the GoBiGas plant's technical demonstration was the availability of and connection to Chalmers Power Central, which provides an experimental plant on a semi-industrial scale.

Chalmers Power Central has been in operation since 1947 and in the beginning of the 1980s, when Bo Leckner had academic oversight, the installation of the first bubbling fluidised bed research boiler was made. Prof. Leckner is still active at Chalmers as an emeritus professor. At the time, this boiler was a highly innovative construction. Several design details originating with this boiler appear in today's commercial boilers. Chalmers Power Central is run as part of Chalmers' strategic infrastructure and incorporates an industrial circulated fluidised bed boiler with attached steam gasifier. This steam gasifier (known as Chalmers 2-4 MW) was built by Valmet (formerly Metso Power) and funded by Göteborg Energi as part of the GoBiGas project. The gasifier was based on an original design by Henrik Thunman who, since 2005, has been responsible for coordinating and implementing the scientific work connected to the GoBiGas project.

In addition to the fluidised bed systems at Chalmers Power Central an oxyfuel fired pilot unit and three connected labs. The bubbling fluidized bed boiler shown on the picture above is at present replaced with a new suspension-fired research boiler. Klas Andersson is the infrastructure manager and managed also the construction of the oxyfuel unit in the start of the 2000s. This was built as part of Vattenfall's oxyfuel aims which resulted in the first-of-its-kind 30 MW demonstration unit in Schwartzepumpe, Germany, a demonstration that ended 2011. The Oxyfuel unit at Chalmers is currently mostly used with industrial partners to help with fuel switching and emission control.

Left: Chalmers Power Central, which delivers heat to the Chalmers campus. A series of contracts between Chalmers, Akademiska Hus and Göteborg Energi has created a unique collaboration enabling industrial-scale generic research at marginal cost.

Right: Installation of the first bubbling fluidized bed research boilers in the Chalmers Power Central 1982. Photo: Martin Seemann(2011)/Bo Leckner (1982).

The pilot gasifier, Chalmers 2-4 MW gasifier, has been in operation since December 2007 and the photo below is from the very first operation. This is, a steam blown dual fluidized bed gasifier, which was built to practice, educate and act as test facility for solving unforeseen technical issues in the GoBiGas-project. Chalmers 2-4 MW gasifier offer a unique operational flexibility, where gasification process in an industrial relevant scale can be followed in detail. During the time of the GoBiGas-project the research at the Chalmers Gasifier has been an integrated part of the demonstration, where result from the research has been implemented in the demonstration unit without unnecessary delay, often within weeks or months.

Photo: Henrik Thunman

Appearing in the photo: from the left, Malin Jessen (operator), Karl-Erik Brink (head of gasifier technical design for Metso Power (now Valmet)), Raymond Hansson (operator), Per Löveryd (now with Akademiska Hus but at the time plant manager of Chalmers Power Central), Kent Davidsson (at the back, RISE researcher), two unnamed guests, Johannes Öhling (at the front, Chalmers research engineer), Fredrik Lind (Chalmers' first PhD in gasification and currently heading the spinoff oxygen carrier-aided combustion (OCAC) activity as well as managing the research engineers), Martin Seemann. Seated, from the left: Mikael Reis (operator), Olle Wennberg (S.E.P. process engineer), Hanna Strand Göteborg Energi (project leader for erecting the gasifier) and Rustan Marberg Chalmers (research engineer).

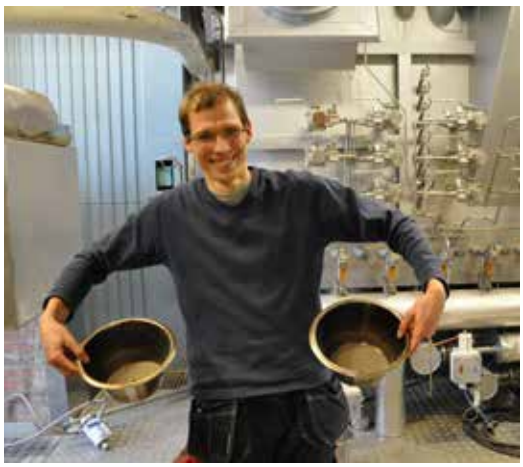

Photos: Henrik Thunman/Huong Nguyen.

The picture to the left Martin Seemann show some of the first bed material samples extracted from the in and out going solid material streams from the gasifier, to the right show from the left Johannes Öhling, Jelena Maric and Sébastian Pissot extracting bed samples from the gasifier.

In any biomass gasification process operating at medium temperatures (700-900 °C), the production of unwanted tar components is considered a showstopper. A major part of the research is therefore directed at this topic. One of the greater breakthroughs was made by developing artificial control of the chemistry inside the gasification system. This allows controlled startup of the process and maintenance of the correct gas quality for downstream systems to handle over suitably long timespans.

Pictured: the measurement procedure to determine the tar concentration of gas produced by the Chalmers gasifier, a procedure exported to the GoBiGas plant.

Top left: Isabel Cañete Vela and Teresa Berdugo Vilches controlling the operational conditions to determine the proper time for tar sampling.

Right: Jelena Maric takes the sample and delivers it to Teresa.

Bottom right: Jessica Bohwalli extracts tar from the sample.

Bottom left: GC-FID analysis to determine the concentration.

Photos: Huong Nguyen/Isabel Cañete Vela.

Left: Isabel Cañete Vela introducing gas into the high temperature oven. Right: Teresa Berdugo Vilches in the front and Huong Nguyen in the back preparing an experiment in the external reactor that are fed with gas from the gasifier to allow dedicated investigations to give a more detailed understanding of the process.

An additional factor often overlooked in laboratory-scaled gasification research is the need to close the mass balance. This may seem trivial, as it is chapter one of any rudimentary chemistry book. However, doing this in a gasification process, especially on an industrial scale, is a huge task. The first five years of activity at the Chalmers gasifier were dedicated to finding solutions and measurement methods to achieve this. The reactor that was developed and finally solved this problem was the high temperature reactor (1700 °C), which converts all gases to simple components and that define elemental streams of carbon, hydrogen and oxygen. Components that can be measured using simple methods. The system was developed as part of Mikael Israelsson's PhD work. A system was thus created in which, for the first time, the elemental mass balance could be closed to a high degree of accuracy and with relatively high time resolution (every three minutes, compared to the tar measurement procedure, which takes at least 24 hours). It thereby provided totally new insights into this type of process.

Operating a gasification plant on industrial scale introduce a large number of practical issues that need to be handled, here some picture where the plant manager Richard Block, Akademiska hus, inspect the Chalmers gasifier during a planned stop.

Prominent visitors

Since their construction, Chalmers' gasifier and GoBiGas plant have received thousands of visitors from all over the world. The first visitor to the Chalmers gasifier was James D. Boyd, then Commissioner and Vice Chair of the California Energy Commission. He visited the plant a couple of weeks before it became operational.

From the left: Karin Markides at the time president and CEO of Chalmers, Jan Björklund at the time vice Prime Minister of Sweden, and Henrik Thunman, Chalmers.

Ibrahim Baylan Energy Minister of Sweden, also with Henrik Thunman.

All photos: Jan-Olof Yxell

From the left: Anders Ådahl (then Director of Chalmers' Energy Area of Advance), Henrik Thunman (Chalmers head of academic gasification research connected to the Chalmers gasifier and the GoBiGas plant, HM King Carl XVI Gustaf, Tomas Kåberger Chalmers (Deputy Director of the Energy Area of Advance and formerly Director General of the Swedish Energy Agency where, in 2008, he inaugurated the Chalmers 2-4 MW gasifier), Lars Bäckström (then County Governor of Västra Götaland), Stefan Bengtsson (current President and COE of Chalmers). Seated, from the left: Rikard Block (Akademiska Hus and current Plant Manager of Chalmers Power Central and Johannes Öhling Chalmers (process engineer).

Swedish Gasification Centre - SFC

Swedish Gasification Centre (SFC) is a research center where a number of academic stakeholders cooperate with the industry. The purpose of SFC is to create a national skills base for research, development and postgraduate education in the biomass gasification technology and related fields. This is achieved by gathering skilled groupings among universities, industry and other stakeholders for commercialization of the technology.

Photo: Kentaro Umeki.

The management group and international expert group of SFC. Left: Henrik Thunman (Chalmers University of Technology), leading the node CIGB connected to dual fluidised bed gasification, Kevin Whitty (University of Utah, expert in dual-bed combustion and gasification systems, US representative in IEA Bioenergy Task 33 Thermal Gasification of Biomass and Waste and expert in the international reference group connected to SFC); Joakim Lundgren (head of the SFC); Rikard Gebart (Luleå University of Technology, leader of the Bio4Gasification node on suspension gasification and leader of LTU Green Fuels, which operates the DME from black liquor plant in Piteå Sweden); Klas Engvall (Royal Institute of Technology and leader of the CleanSyngas node connected to pressurised fluidised bed gasification and currently focusing mostly on syngas upgrading and cleaning) and Lars Waldheim, Swedish representative in IEA Bioenergy Task 33 Gasification of Biomass and Waste, Chairman of Working Group 2 examining conversion of ETIP Bioenergy and member of the Advanced Renewable Transport Fuel Forum.

Photo: Joakim Lundgren.

Right: Hermann Hofbauer (Technical University of Vienna and second expert in the international expert group. He was responsible for the basic research and design of the Güssing gasifier, which was scaled up for the GoBiGas project's gasifier). The photo was from a workshop in Vienna between Bioenergy 2020+ and SFC in May 2017.

Strong governmental support

The Swedish government has strongly promoted the development of biomass gasification processes, via mainly the Swedish Energy Agency. This is being done to facilitate future large-scale national production of advanced biofuels and make Sweden independent of fossil fuels in the transportation sector before 2030.

The Swedish Gasification Centre (SFC) was formed in 2011 as a direct response to this policy. The Centre comprises several Swedish stakeholders from academia, industry and the Swedish Energy Agency. The programme duration is ten years with a total budget of SEK 540 m. Coordinated from Luleå University of technology via three separate research nodes, the programme was originally directed towards three planned commercial plants:

- The GoBiGas project, Göteborg Energi, phases 1 and 2, with the first phase granted SEK 222 m via the Swedish Energy Agency. The second phase was designated a European Union NER300 project, with dual fluidised bed gasification as its gasification technology.
- The E.ON, B2G project, aiming to produce 200 MW of biomethane in southern Sweden via pressurised oxygen blown fluidised bed gasification. The Swedish part of E.ON (formerly Sydkraft) had internal expertise from its efforts in developing and installing a first-of-its-kind biomass integrated gasification combined cycle in Värnamo in the 1990s. B2G was also designated a NER300 project.
- The third technological track aiming at commercialisation was the Chemrec black liquor suspension gasification with downstream Methanol/DME production project, a process demonstrated as a first-of-its-kind pilot in Piteå (pictured below). The commercial plant was planned for construction in Örnsköldsvik and aimed for ~120 MW DME. The project received SEK 500 m in government support, under the same funding scheme that gave SEK 222 m to GoBiGas phase 1.

However, due to uncertainties about the market conditions for advanced biofuels in recent years, all these projects (except GoBiGas phase 1) have been put on hold or been abandoned. Thanks to the Swedish Gasification Centre, the knowledge built up from the above three commercial tracks has been preserved. The Centre is ready to support large-scale introduction of the technology, once market conditions become more favourable.

The gasifier within the GoBiGas demonstration is based on a dual fluidized bed reactor system. The dual fluidised bed system has several different application areas, where Chemical Looping Combustion [CLC] is one other strong area of research at Chalmers.

Rikard Gebart (Luleå University of Technology, leader of the Bio4Gasification node on suspension gasification and leader of LTU Green Fuels, which operates the DME from black liquor plant in Piteå Sweden) Photo: Thomas Bergman.

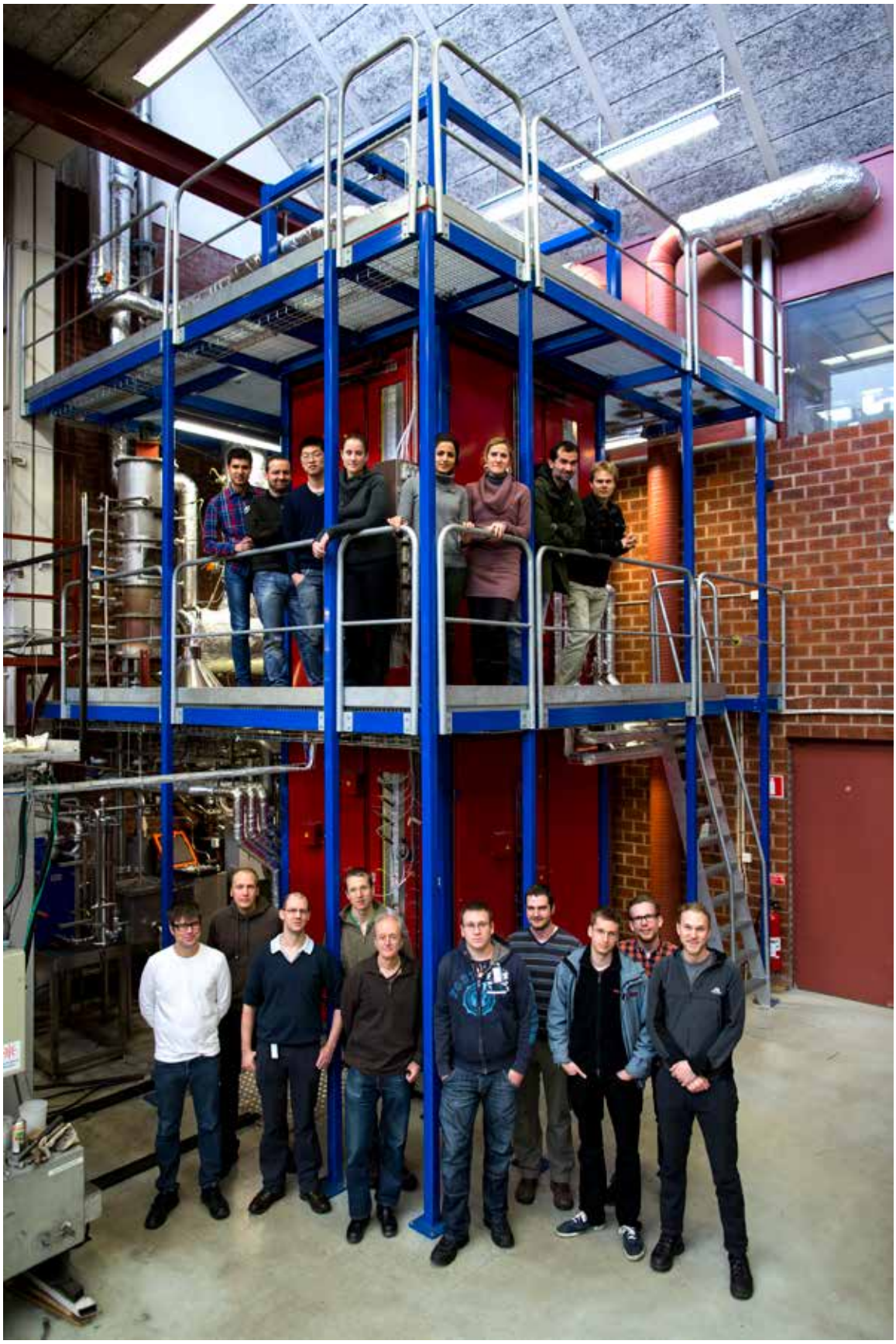

December 2012, celebration of 30 hrs of successful operation of the 100 kW solid-fuel chemical-looping combustor at Chalmers. Top row from left: Mehdi Arjmand, Matthias Schmitz, Dazheng Jing, Malin Hanning, Golnar Azimi, Pavleta Knutsson, David Pallarés and Pontus Markström.

Bottom row from left: Tobias Mattisson, Magnus Rydén, Henrik Leion, Carl Linderholm, Anders Lyngfelt, Sebastian Sundqvist, Georg Schwebel, Martin Keller, Jesper Aronsson and Patrick Moldenhauer.

Photo: Daniel Bäckström.

Chemical Looping Combustion

The Chemical Looping Combustion (CLC) group is led by Anders Lyngfelt and Tobias Mattisson. It was the first group to operate the CLC process, initially for gaseous fuels, then solid and liquid.

In the CLC process the dual bed is used to separate the oxygen from the nitrogen in the combustion process, which allows the combustion products (carbon dioxide and water) to exit the combustion unit in a concentrated stream, with virtually no energy penalty for the oxygen separation process. Its activity began back in the 1990s and provided basic knowledge for the design and construction of the research activity for dual fluidised bed gasification. Mattisson also devised the chemical looping reforming CLR process. This process has also been applied to the Chalmers gasifier to produce clean syngas by Fredrik Lind followed by Nicolas Berguerand and has been further studied in dedicated lab tests by Martin Keller in collaboration with Henrik Leion. A spin-off from the work with the CLR process and the oxygen carrying materials taken forward within the CLC group is the oxygen carrier-aided combustion (OCAC) process allowing greater efficiency and better emissions control for existing fluidised bed boilers.

Two more people in the CLC group photo who link the dual-bed gasification and combustion activity at Chalmers are David Pallarés, the head of fluid dynamic research and Pavleta Knutsson. Knutsson provides expertise in the inorganic chemistry involved in the process and also leads the advanced material characterisation (at Chalmers Material Analysis Laboratory (CMAL) and the Max lab (Synchrotron) in Lund). She also bridges the combustion and gasification activities to the Competence Centre Recycling at Chalmers. This means the group can examine the inorganic species appearing in the processes. This asset has been used extensively by the GoBiGas project and has provided key information for understanding the activation of bed material in the gasification process.

This photo is from the press release about the OCAC process, an invention resulting from the chemical looping reforming activity and allowing greater efficiency and better emissions control for existing fluidised bed boilers.

Left: Bengt-Åke Andersson (E.ON), who pushed for commercialisation of the concept via the formation of the spinoff company Improbed, Angelica Corcoran (the PhD student in the project) and inventors Henrik Thunman and Fredrik Lind.
Photo: Oscar Mattsson

The chemical looping reforming reactor connected to the Chalmers gasifier as part of Fredrik Lind's PhD project.
Photo: Henrik Thunman.

Chalmers Energy Initiative

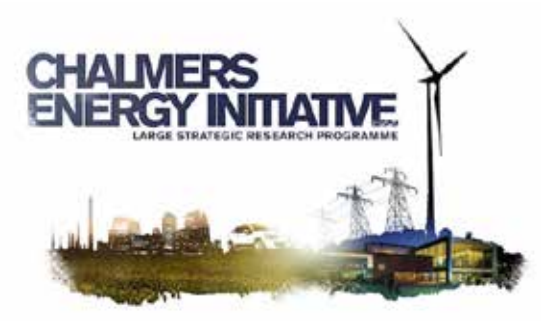

An important factor behind the technical successful GoBiGas demonstration was its access to expertise and research infrastructures. This meant it was able to deal with the wide range of questions arising from a first-of-its-kind project. The expertise was largely provided by Chalmers via the Chalmers Energy Initiative (CEI), a result of a 2008 government call promoting collaboration between strong research groups on various strategic governmental goals.

One of these goals was promoting large-scale introduction of advanced biofuels to achieve the goal of a fossil-free Swedish transport sector by 2030. The establishment of CEI was coordinated by Thore Berntsson, who in the preparation phase represented process integration and industrial energy systems. Other key people in this work were Filip Johnsson (representing regional and global energy systems, including biomass systems and multi-phase flows), Lisbeth Olsson (representing biochemical processes), Hans Theliander (representing separation and catalytic processes) and Henrik Thunman (representing combustion/gasification/fast pyrolysis processes and high-temperature corrosion).

Theliander and Olsson also represented related activities in biobased materials and are key Chalmers representatives at the Wallenberg Wood Science Center, a national initiative. Its mission is to promote innovative future value creation from forest raw materials, with the aim of further strengthening the Swedish forestry industry. The initiative enabled the organisation of leading groups in Chalmers relating to:

- Thermal conversion of solid fuels.
- Fluidised bed technology.
- Carbon Capture and Storage, oxyfuel and chemical looping combustion.
- Multi-phase flow.
- High-temperature corrosion.
- Internal combustion engines.
- Biochemical processes.
- Material recycling.
- Chemical process engineering within the forestry industry.
- Process integration analysis.
- Energy System Modelling.
- Life-cycle assessment (LCA).
- Resource management of biomass.

It also made their expertise and networks available to the GoBiGas project when needed; networks which include a large number of national competence centres and research infrastructures, including:

- Swedish Gasification Centre.
- Centre for Combustion Science and Technology (CeCost).
- High Temperature Corrosion Centre (HTC).
- Chalmers Material Analysis Laboratory (CMAL)
- Swedish National Infrastructure for Computing
- Chalmers' Fluid Dynamics Laboratory.
- Chalmers Materials Analysis Laboratory.
- Competence Centre Recycling.
- Wallenberg Wood Science Center.
- Swedish Life Cycle Center.
- IEA bioenergy.
- Graduate School in Energy Systems.
- The European Pathways project.
- Combustion Engine Research Center.
- MyFab The Swedish National Research Infrastructure for Micro and Nano Fabrication

All this activity involves the combined research efforts of several hundred researchers.

The Chalmers Energy Initiative was managed by Thore Berntsson from 2010-2012 and then by Anders Ådahl and Lisbeth Olsson, before being merged into the organisational structure of Chalmers' Energy Area of Advance. In the same call which funded the Chalmers Energy Initiative (CEI), Luleå University of Technology, Umeå University and Swedish University of Agricultural Sciences obtained funding for their Bio4Energy programme, covering the same area. These two initiatives and the Royal Institute of Technology (KTH) later joined forces to establish the competence centre Swedish Gasification Centre (SFC), described above. All programmes receiving funding via the strategic call were evaluated in 2015, with CEI and Bio4Energy receiving top marks and a recommendation for increased funding. CEI was somewhat more highly ranked than Bio4Energy, due mainly to the assessor's judgment of excellent management and structure. This entailed having a clear strategy for using the funding to further improve strong research groups and facilitate synergy between them, plus an openness to including new and emerging strong research groups in relevant areas. Since, 2016 the scope of activities at CEI has been extended and organised under Energy in a Circular Economy.

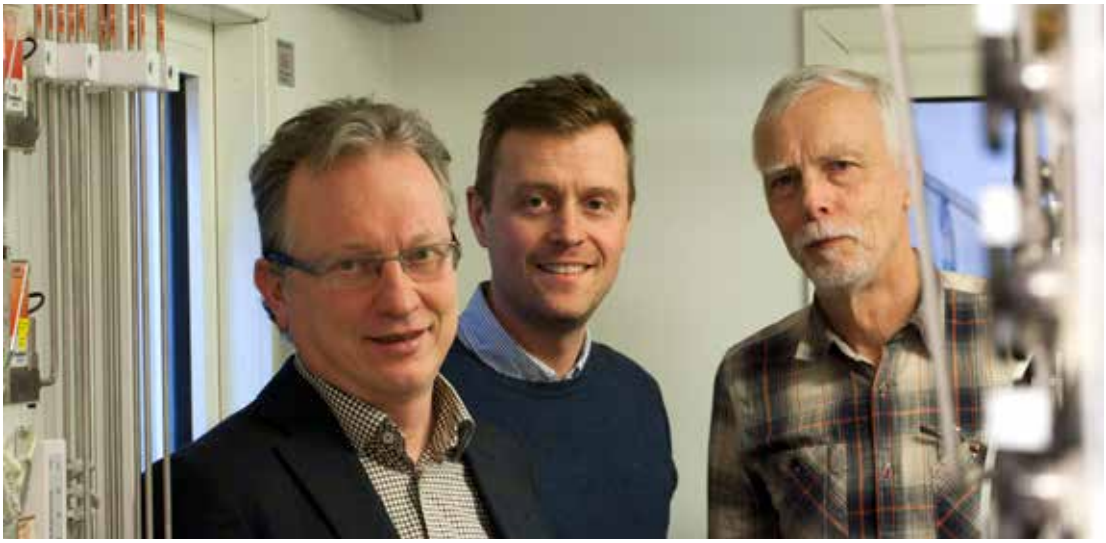

Key people in the field of high-temperature corrosion at Chalmers. From left: Jan-Erik Svensson (Co-director of HTC), Jesper Liske (Project Manager at HTC) and Lars-Gunnar Johansson (Director of HTC). Photo: Anna Pettersson

High Temperature Corrosion

At the start of the GoBiGas project, it was expected that the technology might be challenged by high-temperature corrosion. This was based on past experience of converting coal-fired combined heat and power boilers to biomass firing.

The High Temperature Corrosion Centre (HTC), a competence centre hosted by Chalmers, was launched in 1996 to address corrosion problems in biomass-fired power boilers. Its aim was to mitigate corrosion by developing new, more corrosion-resistant materials, thereby increasing the electrical efficiency of CHP plants.

To address the high-temperature corrosion risks associated with the planned large-scale introduction of biofuels via gasification in the GoBiGas plant, HTC initiated research into high-temperature corrosion in gasification atmospheres. This involved the construction of a specialised lab.

It turned out that high-temperature corrosion in the plant is not severe enough to be a show-stopper. Experience from the GoBiGas plant and HTC's corrosion investigations show that corrosion problems are manageable, given the present process layout and fuel mix. However, this might not be the case if a cheaper (dirtier) fuel were used and/or if the plant tried to improve process economy by extracting high-temperature steam during cooling of gas leaving the gasifier. The newly built high-temperature corrosion lab is designed to run experiments in a wide range of different gasification (and other low oxygen activity) environments, including corrosive alkali chlorides which may be released by cheaper fuel. The specialised HTC lab is probably the best equipped in the world for this type of study and constitutes vital infrastructure for the Chalmers corrosion group.

Example of an experimental setup used in the project to evaluate the flow properties of the fluidised beds. From left: Tove Djerf, Anna Köller and Louise Lundberg, who work under the supervision of David Pallarés. Photo: Huong Nguyen.

Fluid flows and properties

Experimental determination and simulation of fluid flows and properties in a gasification system is vital to cost-effective upscaling and optimisation, plus general understanding of the process.

At Chalmers there are an extensive experimental infrastructure examine multi-phase flow phenomena in fluidized bed, which is connected to wide range of numerical simulations tools ranging from detailed modelling from the first principles to semi-empirical approaches for industrial designs. Here, the experimental work and the semi-empirical modelling is conducted under the supervision of David Pallarés and Filip Johnsson. Henrik Ström is responsible for the advanced numerical multiphase flow simulations, where the group uses high-performance computing resources provided by the Swedish National Infrastructure for Computing (SNIC) and in parallel to the fluidized bed lab has access to Chalmers' Fluid Dynamics Laboratory, a world-class (top 50) fully equipped fluid dynamics and heat transfer lab.

Claes Breitholtz from Valmet applying his experimental expertise and experience. This experiment was conducted during efforts to solve the initial fuel feeding problems of the GoBiGas plant. Problems in its first 18 months limited the duration between maintenance stops to a couple of hundred hours. Claes had a key role in the GoBiGas project and was trained for it during the first year's operation of the Chalmers gasifier. Photo: Anton Larsson.

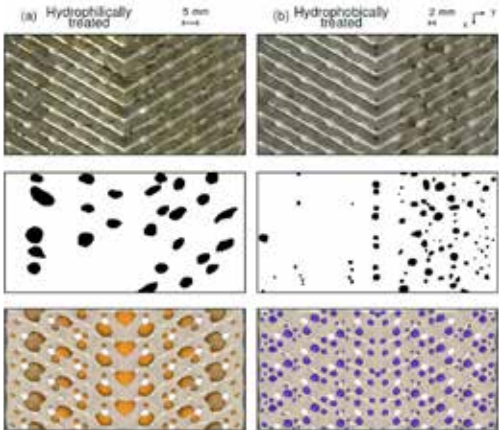

Simulated condensation behaviour of water and tar resulting from steam gasification of biomass on a plate heat exchanger. The comparison photo is of droplet distribution on heat exchanger plates (with different coatings) exposed to raw gas from a steam-blown gasifier. The computations were carried out by Dario Maggiolo.

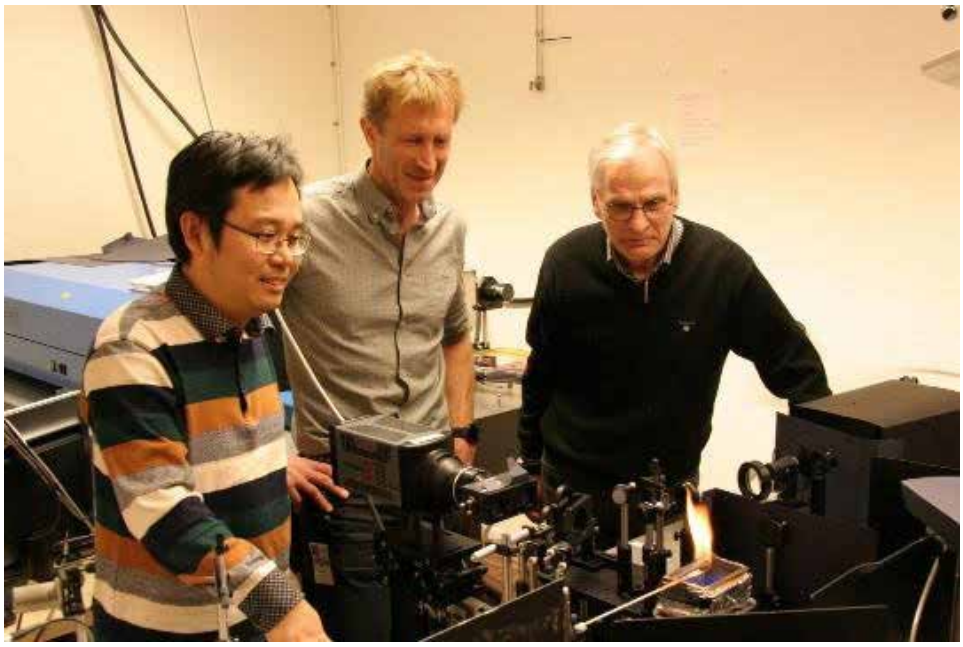

Monitoring the conversion of a biomass particle in time and space, by advanced laser diagnostics Right to left, key people in this development: Marcus Aldén (Programme Director CECOST, Lund University), Per-Erik Bengtsson (Project Leader of SFC project, Lund University) and Zhongshan Li (Project Leader of the CECOST project, Lund University). Photo: CeCost.

Fuel conversion

The understanding of the conversion of single fuel particles is a key to gain fundamental understanding of the gasification process.

A recent development, allowing monitoring in time and space of the conversion of a biomass particle in various atmospheres, plus the gases released and reactions taking place. This means fundamental knowledge can be accrued and fuel conversion inside a gasifier explained. It provides optimisation opportunities which would not be possible using a trial and error approach. This work has been done within the Centre for Combustion Science and Technology (CeCost). CeCost) is a collaboration in the field of combustion (and now also gasification) between Lund University, Chalmers University of Technology and the Royal Institute of Technology (KTH). The Centre has been developing advanced diagnostics in this research field since the mid-1990s. Initially, it focused on combustion but, in the last ten years, has broadened its scope to include gasification. The developments within CeCost together with complementing work within Swedish Gasification Centre enable the transfer of these advanced diagnostics from the lab to pilot and demonstration units. Parallel research, connected to single fuel conversion in small experimental fluidized bed, with the aim to provide more global information of the fuel conversion has been conducted at RISE by Placid Tchoffor Atongka and at the University of Averio by Daniel Neves and Luís Tarelho.

Photo: Julian Borgmeyer.

Laser diagnostics in industrial size gasifiers

Advancing the development of a technology means resolving process details. The development and introduction of new measurement and analysis methods (or application of existing ones) is crucial in this context. GoBiGas and other activities at the Swedish Gasification Centre (SFC) have brought about various ongoing national and international collaborations.

Under the supervision of York Neubauer, a research group at the Technical University of Berlin (TU Berlin) developed and applied an online analysis laser-based method of tar measurement intended for industrial application. This was a parallel European project funded by the ERA-net scheme. The method was developed in two versions, both of which were tested in the Chalmers and GoBiGas gasifiers. During its application in the GoBiGas gasifier, it captured the transient performance of the different gas-conditioning steps within the plant. This information was useful in making significant improvements to the plant's operation and providing clues on how to finally reach 100% of the plant's designed capacity. Most of the development of equipment and results analysis was carried out by Julian Borgmeyer at TU Berlin.

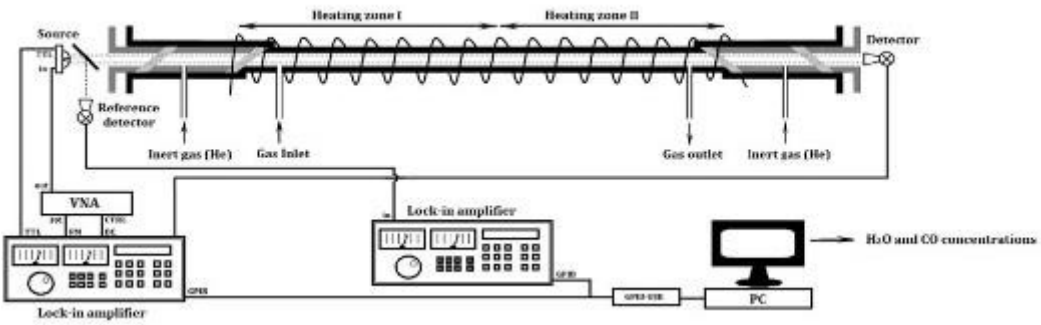

THz experimental setup. Figure: Hosein Bidgoli.

The extraction point for measurements during a measurement campaign at the Chalmers gasifier. Mohit Pushp (left) and Dan Gall (right). Photo: Dan Gall/ Mohit Pushp

A look inside the gasifier

The harsh environment inside a fluidised gasifier limits the accessibility of laser diagnostics for most wavelengths in the optical spectra used in these methods. Other wavelengths were investigated in an attempt to access and view those areas in the gasifier which cannot be reached by such methods.

In this context, the development of transmitters and receivers in the THz region over the last decade are very attractive. Applying these wavelengths makes it theoretically possible to measure temperatures, particle concentrations and individual gas species inside the gasifier, using detectors placed on the outside of the refractory walls. These opportunities were investigated in a collaboration between researchers associated with the Chalmers gasifier, plus Sergey Cherednichenko and Thomas Bryllert at the THz-lab at Chalmers (also connected to MyFab, the Swedish National Research Infrastructure for Micro and Nano Fabrication). This meant detectors and sensors could be developed within the research group. This particular collaborative work was funded via the Chalmers Energy Initiative, with very promising initial results.

Other important information on the gasification process can be obtained by extracting and analysing fine particles or gas components, which form particles as they are cooled. Within the framework of the Swedish Gasification Centre (SFC), atmospheric chemistry experts at Gothenburg University (GU) and the Research Institutes of Sweden RISE have been developing several online methods of extracting measurements from gasification systems. They are supervised by Jan Pettersson (GU) and Kent Davidsson (RISE). Measurements conducted by this group on the GoBiGas gasifier (using a simple device to detect alkali metals) gave critical information on how to dose potassium into the gasification system and achieve good quality gas from the gasifier without clogging the cooler with either tar or potassium carbonate.

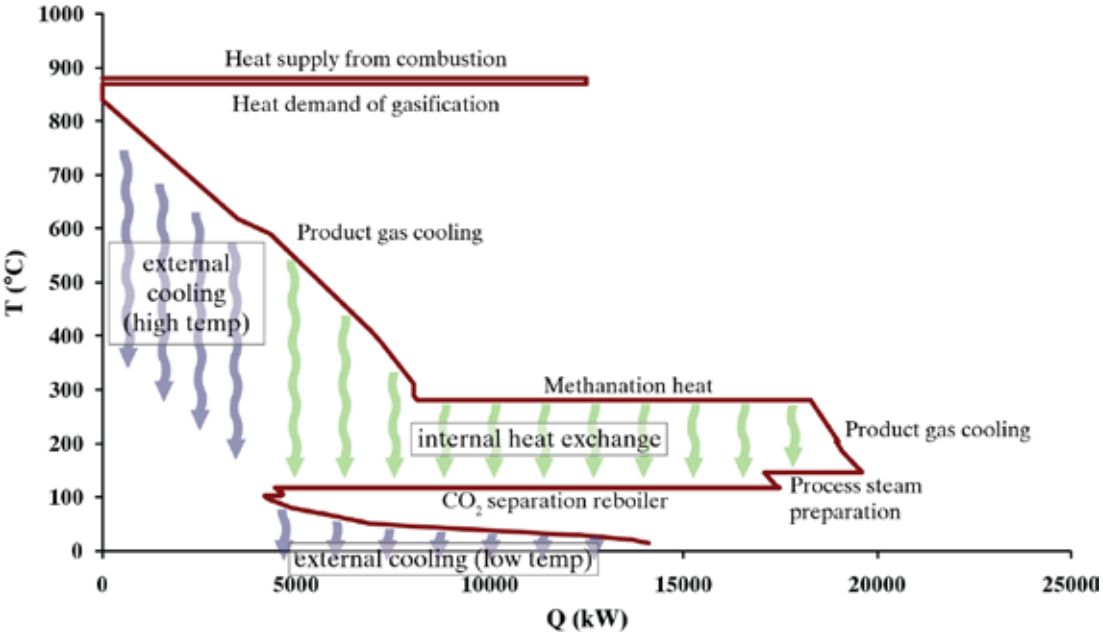

Process integration

The complexity of an advanced biofuel production plant is similar to that of a petrochemical industrial site. This means there is a need to adopt a holistic view of the process, to avoid sub-optimisation. Process integration tools tailored for analysing industrial energy systems are needed. They facilitate understanding of how a change in performance of one part of a process impacts the process as a whole.

Furthermore, such analyses provide insights into how improved performance of core technologies (such as the gasification process) can open new opportunities for advanced biofuel production concepts in other industries wanting to shift from fossil fuels to renewables like biomass. A significant number of process integration studies on integrated biorefinery concepts have been conducted at Chalmers, primarily supervised by Simon Harvey and Thore Berntsson. Berntsson is also the Swedish representative and initiator of the IEA Technology Collaboration Programme "Industrial Energy-related Technologies and Systems" and f3, the Swedish Knowledge Centre for Renewable Transportation Fuels.

General analysis showing the potential of the GoBiGas plant concept was primarily conducted by Stefan Heyne, from whose thesis the above figure is taken, which shows the energy flows in a biomass-to-biomethane process via gasification. Process integration studies based on measurement data collected from the Chalmers gasifier and GoBiGas plant were primarily conducted by Alberto Alamia, supervised by Henrik Thunman.

Introduction of large scale biofuel production

The ramping up of advanced biofuel production will create a new situation in forestry and agriculture, as well as for the energy system. Bioenergy development can vitalise the forestry and agriculture sectors and support the increased use of renewable resources as feedstocks for a range of industrial processes. However, it can also have negative impacts if not developed and deployed properly.

Currently, various forms of bioenergy are enduring strong criticism from some stakeholders and its future role in the energy system is still and open question. In a wider sense, it is likely that the bioenergy sustainability debate will affect the future development of a biobased economy, since much of the debate relates to our present use of biomass resources. It is also clear that sustainability concerns are not limited to feedstock production; the full supply chain and end usage need to be considered.

Chalmers experts have collaborated on research projects to improve the understanding of the possible (positive and negative) effects of biobased systems. Over the years, Chalmers' research into land use and environmental impacts has generated a large body of knowledge. Chalmers also has a strong presence in various organisations and processes relating to the governance of land use and biomass production for food, energy and biomaterials.

Photo: Christian Löwhagen

Key people at Chalmers relating to system related issues relevant for the introduction of biofuel production at large scale. From the left: Göran Berndes works on land and biomass use on scales ranging from local case studies to a globally and with special focus on climate change mitigation. Christel Cederberg is an agronomist working on sustainable food and bioenergy production, focusing on land-use impacts. Filip Johansson works mainly with energy systems, but also conducts significant activities within the field of fluidised bed processes. Anne-Marie Tillman works in quantitative environmental assessment of product chains (life-cycle assessment, LCA) and the closely related field of Life Cycle Management (LCM), covering the governance of product chains for enhanced environmental performance.

The team from Industrial Biotechnology which will realise this opportunity. From the left: Yvonne Nygård, Pawel Piatek, Nikolaos Xafenias and Lisbeth Olsson.

Producing the best value from ingoing feedstock: Biochemical methods

Gas upgrading via the catalytic steps applied in the synthesis process of GoBiGas' plant is a complex and costly process. To make converting gasifier-produced gas into advanced biofuels a viable process, economies of scale must be exploited and production focused on a narrow range of products. New opportunities can be developed by replacing or combining these chemical catalysis methods with biochemical ones. Although biochemical processes are traditionally optimised to use sugars as feedstock, they can equally well be adapted to use gas produced by the gasifier.

Two recognisable developments may be advantageous in this context: i) the development of tolerant microorganisms to handle impurities which traditional catalysts cannot and ii) efficient production of high-value molecule streams as by-products in large scale production of advanced fuels. Supervised by Prof. Lisbeth Olsson (a leading expert on developing microorganisms for biofuel production), the Chalmers gasifier research group is working to develop a strategic collaboration. This collaboration will develop a biochemical process-centred concept, optimised to work with cooled gas from biomass gasification.

A parallel group led by Prof. Jens Nielsen is involved in several ambitious projects. These aim to design cell factories for the biochemical production of major value-added chemicals. A broad toolbox is in development to this end.

(Far right) Jens Nielsen receives the ENI award from the President of Italy (left). The award was for Nielsen's achievements in designing microorganisms to produce drop-in fuels for use in diesel and jet fuel. Photo: ENI.

From the left: Hans Theliander, Magnus Skoglundh, Louise Olsson.

Photos: J-O Yxell and Mats Tiborn

Producing the best value from ingoing feedstock: Chemical methods

In a biomass gasification process, all ingoing biomass is converted to simple molecules. These are assembled into the desired hydrocarbons, using various synthesis processes. This is the most efficient route for a highly heterogeneous feedstock.

In the GoBiGas project, the synthesis process used to convert syngas produced in the gasifier into methane used was delivered by Haldor Topsoe. It was considered mature, as proven by the demonstration. However, although the Chalmers Competence Centre for Catalysis (KCK) was part of the research network, it was not activated.

For better defined feedstocks and the production of more complex molecules, there may be much more attractive process alternatives to gasification. These may be standalone or combined with gasification processes to achieve the best value from ingoing feedstock. Several such processes have been developed and commercialised via the collaborations within Chalmers. Regarding advanced biofuel production, the most interesting complementing developments are the hydrothermal cracking of lignin and direct upgrading of biooil from pyrolysis to petrol and diesel. Hydrothermal cracking of lignin is supervised by Hans Theliander (pictured top left). He is also one of the inventors behind the LignoBoost process, which was commercialised by RISE (formerly Inventia) and Valmet. This process allows the extraction of high quality lignin from a pulp process. It can be used in the hydrothermal process to produce a lignin oil, which can be further hydrogenated in an oil refinery into, say, petrol and diesel.

By operating the dual-bed gasification process at lower temperature, the gasifier becomes a pyrolyser with the main objective of breaking down the ingoing compounds into a biooil instead of a gas. This then allows the production of various hydrocarbons by hydrogenation, in similar fashion to the hydrogenation of lignin oil. However, both routes need hydrogen. This can be produced as a renewable feedstock, if it is produced by gasification of the solid carbon-rich residue following pyrolysis or cracking, or from renewable electricity via electrolysis. For the pyrolysis route, the dual fluidised bed system provides an opportunity to combine pyrolysis and gasification of the solid residue by temperature staging. Activity to obtain this has already begun. This effort will be combined with the hydrogenation activity at KCK, supervised by Louise Olsson and Magnus Skoglund.

Inspiration for future engineers

An extensive introduction of large scale production of advanced biofuels will require a great number of engineers. To inspire engineering students, specific efforts are made within the GoBiGas-demonstration, as well the gasification area in general. The teaching use GoBiGas as a case of inspiration and the students are offered master and bachelor thesis projects in the area.

One example is a yearly bachelor's project where students are challenged to design, build and evaluate one operational unit of a lab-scale biomethane plant. The long term goal is to produce the required amount of fuel for the student built car entering the Eco Marathon competition (picture to the left), via these bachelor thesis projects. These projects are cross-disciplinary and includes students from different educations as well as supervision from different departments. In this way the education will be connected to research centre within catalysis (KCK) and internal combustion engines (CERC). Furthermore, these activities are supported by the Area of Advance Energy. Over the last five years, groups of six students has been engaged each year to construct one part of the process and, thereby, gradually build up an entire process. Currently, around half of the process is in place. These projects are supervised by Jonas Sjöblom from the department of Mechanics and Maritime Sciences and Martin Seemann from the department of Earth, Space and Environment. The picture on the right shows this year's student group who are designing the fuel feeding system and optimize the gasification process.

Paper 1:

Advanced biofuel production via gasification – lessons learned from 200 man-years of research activity with Chalmers' research gasifier and the GoBiGas demonstration plant.

Energy Science & Engineering

Open Access

IN THE FIELD

Advanced biofuel production via gasification – lessons learned from 200 man-years of research activity with Chalmers' research gasifier and the GoBiGas demonstration plant

Henrik Thunman[1], Martin Seemann[1], Teresa Berdugo Vilches[1], Jelena Maric[1], David Pallares[1], Henrik Ström[2], Göran Berndes[3], Pavleta Knutsson[4], Anton Larsson[5], Claes Breitholtz[6] & Olga Santos[7]

[1]Division of Energy Technology, Chalmers University of Technology, 412 96 Göteborg, Sweden
[2]Division of Fluid Dynamics, Chalmers University of Technology, 412 96 Göteborg, Sweden
[3]Division of Physical Resource Theory, Chalmers University of Technology, 412 96 Göteborg, Sweden
[4]Division of Energy and Materials, Chalmers University of Technology, 412 96 Göteborg, Sweden
[5]Göteborg Energi AB, Göteborg, Sweden
[6]Valmet Power AB, Göteborg, Sweden
[7]Alfa Laval AB, Lund, Sweden

Keywords
Biofuel, biomass, dual fluidized bed, gasification, GoBiGas, Electrofuels

Correspondence
Henrik Thunman, Division of Energy Technology, Chalmers University of Technology, 412 96 Göteborg, Sweden.
E-mail: henrik.thunman@chalmers.se

Funding Information
Swedish Gasification Center (Grant/Award Number: 34721-3); European Union's Seventh Framework Program for Research, Technological Development and Demonstration (Grant/Award Number: 321477); Energimyndigheten (Grant/Award Number: 42206-1).

Received: 19 September 2017; Revised: 11 January 2018; Accepted: 11 January 2018

***Energy Science and Engineering* 2018; 6(1): 6–34**

doi: 10.1002/ese3.188

[Correction added on 28 February 2018 after first online publication: Figure 7 was incorrect and has been corrected in this version.]

Abstract

This paper presents the main experiences gained and conclusions drawn from the demonstration of a first-of-its-kind wood-based biomethane production plant (20-MW capacity, 150 dry tonnes of biomass/day) and 10 years of operation of the 2–4-MW (10–20 dry tonnes of biomass/day) research gasifier at Chalmers University of Technology in Sweden. Based on the experience gained, an elaborated outline for commercialization of the technology for a wide spectrum of applications and end products is defined. The main findings are related to the use of biomass ash constituents as a catalyst for the process and the application of coated heat exchangers, such that regular fluidized bed boilers can be retrofitted to become biomass gasifiers. Among the recirculation of the ash streams within the process, presence of the alkali salt in the system is identified as highly important for control of the tar species. Combined with new insights on fuel feeding and reactor design, these two major findings form the basis for a comprehensive process layout that can support a gradual transformation of existing boilers in district heating networks and in pulp, paper and saw mills, and it facilitates the exploitation of existing oil refineries and petrochemical plants for large-scale production of renewable fuels, chemicals, and materials from biomass and wastes. The potential for electrification of those process layouts are also discussed. The commercialization route represents an example of how biomass conversion develops and integrates with existing industrial and energy infrastructures to form highly effective systems that deliver a wide range of end products. Illustrating the potential, the existing fluidized bed boilers in Sweden alone represent a jet fuel production capacity that corresponds to 10% of current global consumption.

Introduction

According to the Intergovernmental Panel on Climate Change (IPCC), scenarios that have a good chance of restricting global warming to less than 2°C involve substantial cuts in anthropogenic greenhouse gas (GHG) emissions, implemented through large-scale changes in energy systems. The use of renewable energy sources and fossil fuels, in combination with carbon capture and storage (CCS), could help to reduce GHG emissions in the

energy sector. Electricity can be produced from noncarbon sources, such as wind, hydro, and solar energy, and from carbon-based feedstocks, which are also needed for the production of fuels, chemicals, and various materials.

There are three main alternatives for producing carbon-based feedstocks: (1) biomass harvesting, that is, relying on photosynthesis as the mechanism for capturing CO_2 from the atmosphere; (2) CO_2 capture via physical or chemical processes from the atmosphere or seawater; and (3) recycling, through the utilization of suitable materials, such as recycled paper and plastics, waste wood, or through CO_2 capture from flue gases. The future potential of the latter option depends on whether burning of hydrocarbons to produce process heat and/or electricity will remain common, which is uncertain.

The future magnitude of biomass resources is currently debated, and estimates of bioenergy potentials vary widely due to differences in the approaches adopted to consider important factors, which in themselves are uncertain [1, 2]. Moreover, biomass supply may be limited by a scarcity of resources, such as land and water, and society may want to avoid over-reliance on biomass harvesting due to concerns regarding negative environmental and socio-economic impacts. Therefore, it is reasonable to expect that future biomass use will be prioritized for applications for which alternatives at similar cost levels are not available.

For example, heat can be produced and stored based on geothermal heat and renewable electricity. As another example, biomass-based electricity may not be needed at locations and during time periods when other renewable or fossil-free alternatives are available. Widespread application of various storage and demand management strategies, together with renewable supply options, such as wind and solar energy, could limit the periods of the year that are suitable for fuel-based thermal electricity generation to hundreds rather than thousands of hours, and might restrict the periods for continuous operation of such plants to days or weeks instead of months.

In such a scenario, it will be advantageous to combine the continuous production of renewable fuels, materials, and chemicals with intermittent generation of heat and electricity. Biorefinery concepts that are based on large-scale gasification represent one such combined production solution. In contrast, large thermal production plants that produce only electricity and/or heat are unlikely to be economically viable. In this context, it will be desirable to introduce novel solutions that exploit the infrastructure that has been built up in recent decades for biomass-based heat and combined heat and power (CHP) production.

The Nordic countries of Sweden, Finland, and Denmark have been forerunners in the development of large thermal production plants using biomass for electricity and/or heat production. In Sweden, more than 60 units, with a thermal capacity of >50 MWth (250 dry tons of biomass/day) biomass or waste (with 40 units of >100 MWth, 500 dry tonnes of biomass/day), have been built at a cost of more than 100 M€ per 100-MWth unit. The main technology used in this sector is bubbling or circulating fluidized bed combustors, and Sweden alone has a total installed thermal capacity of 6400 MWth (1200 MMBtu/hour). If the utilization of those fluidized bed units can be extended, these would represent an asset available for the introduction of a large production capacity for biomass to biofuels.

In this paper, the results of research and development activities conducted in two industrial-scale demonstration units are used to formulate a strategy for how fluidized bed boilers can be converted to gasifiers, in a manner similar to that used in the 1990s to convert coal-fired grate boilers in the Nordic countries to biomass-fired fluidized bed boilers. The conversion offers a low-cost route for the production of alternative fuels, materials, and chemicals (instead of heat or CHP) from carbon-based feedstocks and hydrocarbons based on renewable electricity. It is also described how the gasification concept can be implemented in pulp, paper and saw mills, as well as in oil refineries and the petrochemical industries, as well as the potential of electrification of the processes. The results of 200 man-years of research activity, carried out over the last decade are summarized in this paper.

The research results obtained and experiences gained concerning the gasification process are summarized in *Description of and Results from the Technical Demonstrations*. This section contains brief descriptions of materials that have been published elsewhere, as well as more detailed descriptions of results that have not been published previously. The applications and descriptions of routes for introducing the examined gasification technology into the energy system and industrial systems including the potential for electrification of the processes are presented in *Introduction of the Technology into the Existing Infrastructure*.

Description of and Results from the Technical Demonstrations

With the vision of establishing local production of around 1 TWh/year (86,000 TOE) of advanced biofuels in Gothenburg before Year 2020, the **Go**thenburg **Bi**omass **Gas**ification (GoBiGas) project was initiated in Year 2005. The GoBiGas project currently comprises a 32-MWth dual fluidized bed (DFB) gasifier (150 dry tonnes of biomass/day, 9.5 MMBtu/hour), complemented by state-of-the-art synthetic natural gas (SNG) synthesis,

producing up to 20 MW of biomethane (5.9 MMBtu/hour). It is a first-of-its-kind plant for industrial-scale production of advanced biofuels from woody biomass, whereby methane was identified as the desired end-product due to local conditions. To support the GoBiGas project, a research program with a 2–4-MW (10–20 dry tonnes of biomass/day) DFB gasifier was established in 2007 at Chalmers University of Technology, hereinafter referred to as the Chalmers gasifier. As the research gasifier was constructed by retrofitting an existing boiler, it is an example of the conversion of a boiler to a gasifier. The project has acquired experience from around 10,000 h of operation of the GoBiGas demonstration plant and more than 25,000 h of operation of the research gasifier at Chalmers [3–5].

The gasifier in the GoBiGas demonstration plant is one of two, third-generation dual fluidized bed gasifiers that originated from the 8–MWth (40 dry tonnes of biomass per day) CHP plant that was built in Güssing, Austria, in Year 2000, based on research conducted at the Technical University of Vienna under the supervision of Professor Hermann Hofbauer. This was followed by the construction of a CHP plant of the same size in Oberwart, Austria, which employed integrated fuel drying and an organic cycle to improve the electrical efficiency [6–8]. The other third-generation gasifier is a 16-MWth (80 dry tones of biomass/day) CHP plant in Senden, Germany, which was designed to use forest residues as fuel, that is, similar fuel use but half the capacity of the gasifier in the GoBiGas project. The unique property of the GoBiGas plant is that it is designed for advanced biofuel production via a syngas synthesis process. The Chalmers gasifier builds on the same principles, although the gasifier is built as an add-on to an existing boiler. A similar gasification system of the same size was in the same time period developed and built (under the TIGAR trademark) by IHI Corporation of Yokohama, Japan. This was later scaled up to a 15-MWth (30 dry tonnes of biomass/day) demonstration unit in Kujan, Indonesia and brought into operation in 2015, whereby lignite was used as the fuel and the intended product for a subsequent demonstration plant is ammonia [9, 10].

The research associated with the GoBiGas and Chalmers gasifiers had as its initial goal to demonstrate – on a commercial scale – the feasibility of converting biomass with 50% moisture to methane with a conversion efficiency >75% (higher heating value basis, which is similar to the efficiency on a lower heating value basis when a dry fuel is used). With the successful operation of the GoBiGas plant and the extrapolation of its performance to a commercial unit (5–10-times larger), this goal has been realized [11]. The performance level of the plant was achieved thanks to an improved understanding of how the process chemistry is affected by the key ash species of potassium, sulfur, and calcium [5]. In particular, research using the Chalmers gasifier has provided essential validation data, which have been complemented by investigations in laboratory-scale reactors of the release of alkali compounds from single biomass particles [12].

The abilities of certain bed materials to capture and release these active ash species, with potassium being identified as the most important, were found to be crucial in limiting the yield of tar from the gasifier [13]. The beneficial properties of potassium are exploited in a way that is similar to that in the process developed by Exxon at the end of the 1970s for the direct production of methane using potassium-impregnated coal [14]. However, the latter process never reached the commercial implementation stage. One issue is the high silicon content of the coal ash consuming the potassium catalyst. Even though similar reactions occur with biomass ash, the consequences are negligible considering the high abundance of potassium in most woody biomasses.

The research findings at Chalmers explain how the biomass ash contributes to a suitable chemistry for the conversion process. This process should be regarded as a steam reforming process rather than a traditional gasifier, as it enables steam reforming processes that are commonly used to produce syngas (H_2, CO, CO_2) for a variety of industries based on lower-value, ash-rich fuels and waste streams. In addition to syngas, the DFB gasification process yields a variety of side products, such as light hydrocarbons and aromatic hydrocarbons, which can be utilized in the production of various chemicals and materials or heat.

In general, the applied process can be divided into three conversion steps (Fig. 1): Heat Generation (1); Gasification (2); and Synthesis (3). In addition, there are two bridging process units for compression (4) and BTX removal (5), which connect the conversion of the solid fuel to an intermediate gas with the upgrading of the gas to the final product. The heat generation and gasification processes are described in *Gasification system*, and optimization of the gasification and heat generation processes are discussed in *Optimization of the gasification process*. The synthesis, bridging process steps, and the material consumption and waste streams are briefly described and discussed in *Synthesis process*, *Bridging processes*, *Material consumption and waste streams during operation of the GoBiGas plant*.

Gasification system

A DFB gasifier of the type applied in the GoBiGas plant is primarily a circulating fluidized bed (CFB) boiler used

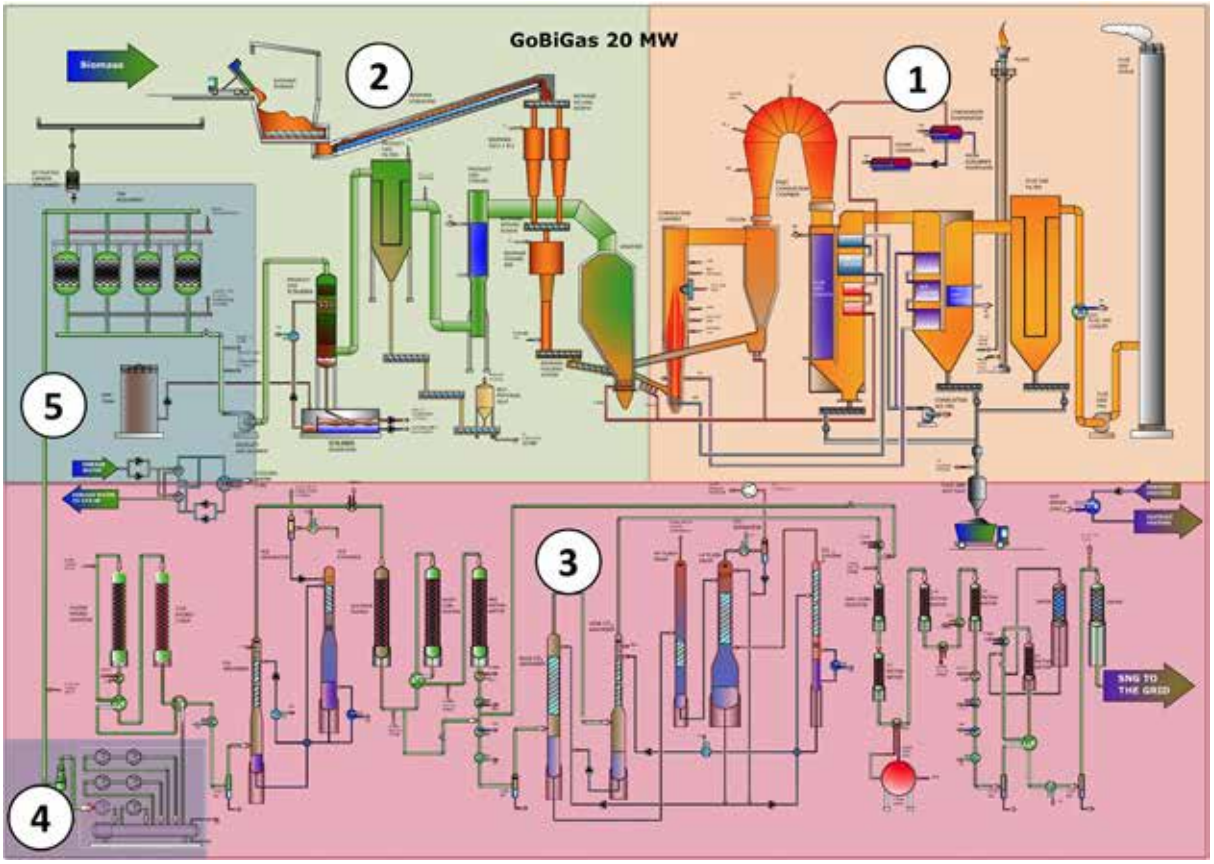

Figure 1. Schematic of the process layout for the GoBiGas demonstration unit, which is a complete system that converts raw biomass to a high-quality biofuel, that is, bio-SNG. In comparison to a commercial plant, the only missing part is the drying of the fuel, which is performed elsewhere. Process layout provided by Göteborg Energi AB.

for heat generation, which is connected to a bubbling fluidized bed (BFB) boiler that is used as the gasifier. For it to be used as a gasifier, the connected boilers have the conventional design of boilers that are intended for fuels with a high moisture content (≥50% moisture in the received fuel). This means that the walls of the combustion and gasification chambers are covered by refractory materials to retain the heat within the process. Even though the GoBiGas plant is large for a biomass gasifier, the small size of the plant is apparent when one compares it to standard CFB and BFB boilers. For example, the CFB reactor (5–10 MWth capacity, 25–50 dry tonnes of biomass/day) is 5–10-times smaller than the smallest commercial CFB boilers on the market. The BFB reactor (10–15 MWth capacity, 50–75 dry tonnes of biomass/day) is within the capacity range of the smallest commercial boilers. The gasification is described in the following section, and the consequences of the small size of the fluidized beds, as well as aberrations that emanate from the standard equipment in the applied design are discussed.

Combustion section

Despite the small size of the GoBiGas plant, the outline of the "CFB boiler" follows that of a commercial system designed for a complex fuel with a high moisture content upon reception; see Figure 2 for a schematic of an 88-MWth (440 dry tonnes of biomass/day) multi-fuel boiler from Valmet, which is comparable to the CFB boiler in the GoBiGas plant.

In contrast to a conventional CFB boiler used in commercial systems, there is no external solid fuel feed to the combustor in the GoBiGas plant. In addition, there is no flue gas condenser, which is installed in systems optimized for district heating, since the moisture content of the flue gas from the gasification system will be very low (a few percent, on a volume basis). Furthermore, the GoBiGas setup includes a large postcombustion section. The process outline of the combustion part of the GoBiGas plant is described in below, treating the convection path (including filtering) and the combustor separately.

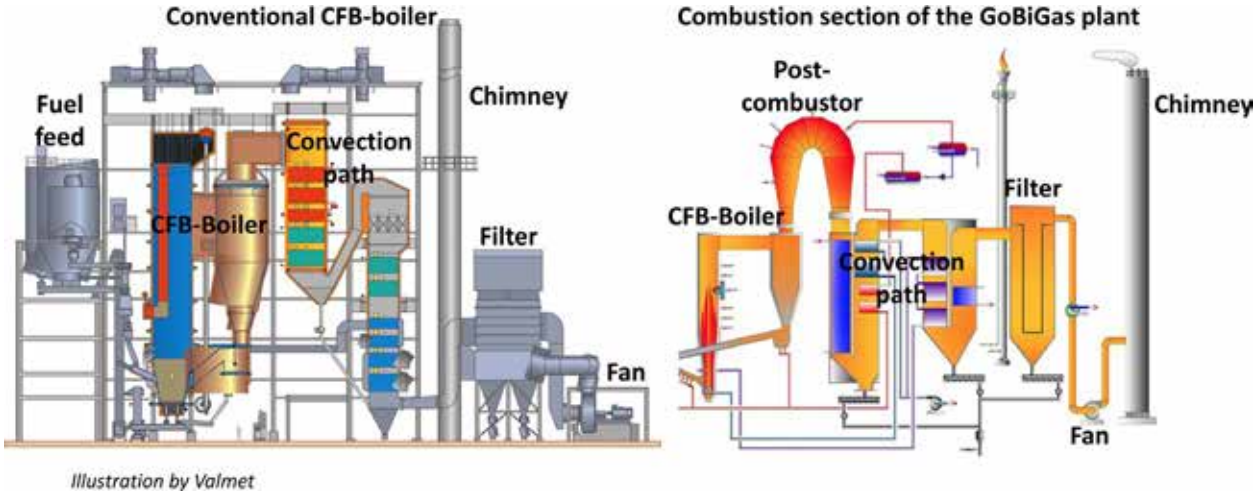

Figure 2. The 88-MW (440 dry tonnes of biomass/day) CFB Multi-Fuel Boiler from Valmet (left panel, illustration published with permission from Valmet), and an outline of the combustion section of the GoBiGas plant (right panel).

The convection path of the GoBiGas process is designed to handle a flow that exhibits an uneven particle load. A significant fraction of the particles in the flue gas flow is alkali salts, which condense during the cooling process inside the convection path. To handle this, the first chamber is an empty downdraft chamber with cooled walls, which gradually reduces the temperature and provides sufficient residence time for the particles to become non-sticky. During the cooling process, alkali can condense onto larger particles. These larger particles, coarse fly ash, consist of small particles of bed material and ash fragments that were generated through attrition, and they are gravity-separated from the flue gas when the flow is redirected to an updraft chamber. Heat transfer surfaces are introduced in the updraft chamber to preheat the combustion air and to produce superheated steam at 320°–350°C (600°–660°F).

Thereafter, the gas is sent to a second downdraft chamber, where the air that enters the combustion chamber is preheated. Here, more particles of the same type as those separated in the bottom of the first chamber are separated from the gas by gravity as the gas is directed to the final updraft chamber, where water is preheated. Downstream of the convection path, the remaining particles, mainly fly ash and free alkali particles, are removed by passage through a filter before the flue gas is finally vented to the atmosphere through the chimney at a temperature of around 140°C (280°F). This stepwise removal of particles enables selective particle recirculation to the gasification process. At GoBiGas, important ash components are thus reintroduced to the process through recirculation of particles from the two downdraft chambers to the process. This setup could be further optimized in a commercial plant [15]. The design resembles that of a conventional CFB boiler, and it has been operated without major issues since it was first commissioned. The efficiency of energy recovery could be further optimized by introducing a flue gas condenser.

The combustor is optimized for its main purpose of producing high-value heat for the various processes, most notably the gasification. The reactor walls are insulated by refractory materials and the incoming air is preheated. In the present design, the temperature in the outer walls of the reactor is kept above the condensation point (120°–140°C, 250°–280°F), to avoid condensation on the steel sealing, which would otherwise entail corrosion issues. This design was a consequence of the small reactor size, which did not motivate the installation of water-filled panel walls to extract and recycle part of the heat that is transferred through the refractory [4]. In a commercial-sized reactor, the area-to-volume ratio is more favorable, which significantly reduces heat losses through the walls and ensures that the incorporation of water-filled panel walls is reasonable.

Unconverted char from the gasifier is used as the main fuel for the combustor, and recirculated by-products from the downstream process are used as supplementary fuel. In addition, the temperature of the process is regulated by combusting part of the gas produced in the gasification process or, during start-up, by combusting natural gas. While this solution is reasonable for a small pilot-scale unit, it is unlikely to be optimal for the size of the present system and certainly not for a commercial-scale plant. As will be discussed in *Controlling the gas quality using potassium*, this solution creates problems when adjusting the chemistry of the process, especially during

start-up. For future units of size equivalent to or larger than the GoBiGas plant, it will be convenient to feed solid biomass also to the combustion side. This would simplify the start-up, increase the flexibility of the fuel feed to the gasifier, and reduce the operational costs, since both natural gas and the product gas currently used at GoBiGas have a higher market value than raw biomass. Further, during the start-up phase, and during operation with a fuel that has an unfavorable ash composition, the biomass burned to heat up the system would ensure the necessary ash balance in the system.

To obtain complete combustion of the gases that exit the combustor, a postcombustion chamber needs to be added. The construction of such a chamber depends on the planned mode of operation and the choice of fuel. If the plan is to use waste as fuel and the gasifier is to be operated within the European Union, the afterburner chamber needs to have a residence time of 2 sec at 850°C (1560°F) [16]. In the absence of such design requirements, the experience with the Chalmers DFB system suggests that the size of the afterburner chamber can be reduced significantly while still meeting the requirement to control the potassium-sulfur balance so as to obtain full conversion of the fuel. As will be discussed in *Controlling the gas quality using potassium*, a process that has a potassium-sulfur equilibrium will experience a problem with unconverted CO in the flue gas. This means that in a combustor that is equipped with a potassium-saturated bed, the CO will not be fully converted unless a small amount of sulfur is added [13], for example in the form of elemental sulfur or ammonium sulfate; the latter can conveniently be added to the afterburner chamber. Furthermore, the costs for construction and maintenance can be reduced by constructing the afterburner chamber with straight panel walls, in line with the design of regular combustors, instead of using the complicated macaroni shape of the GoBiGas system, which has its origin in a small pilot-scale system.

Gasification section

The second reactor in the gasification system is the BFB reactor, which functions as a gasifier in the GoBiGas process, but is comparable to a BFB boiler. The differences between these two systems are mainly evident in the convection pathway (gas cooling and cleaning) and in the fuel feeding (Fig. 3). These differences will be discussed in relation to five areas based on the functionality of the system: (1) the convection path, including filtering and condensation of water and polyaromatic hydrocarbons (PAHs); (2) heat transfer; (3) chemistry; (4) primary fuel conversion; and (5) fuel feeding.

The convection pathway in the gasification part of the GoBiGas process (Repotec design) is very basic compared to the convection pathway on the combustion side (Valmet design). The design of the cooling step applied in GoBiGas, with the gas being passed through hundreds of (externally located) water-cooled tubes, resembles the design of the heat exchangers used for tar and alkaline-poor product gases produced from mainly liquid or gaseous fuels. As

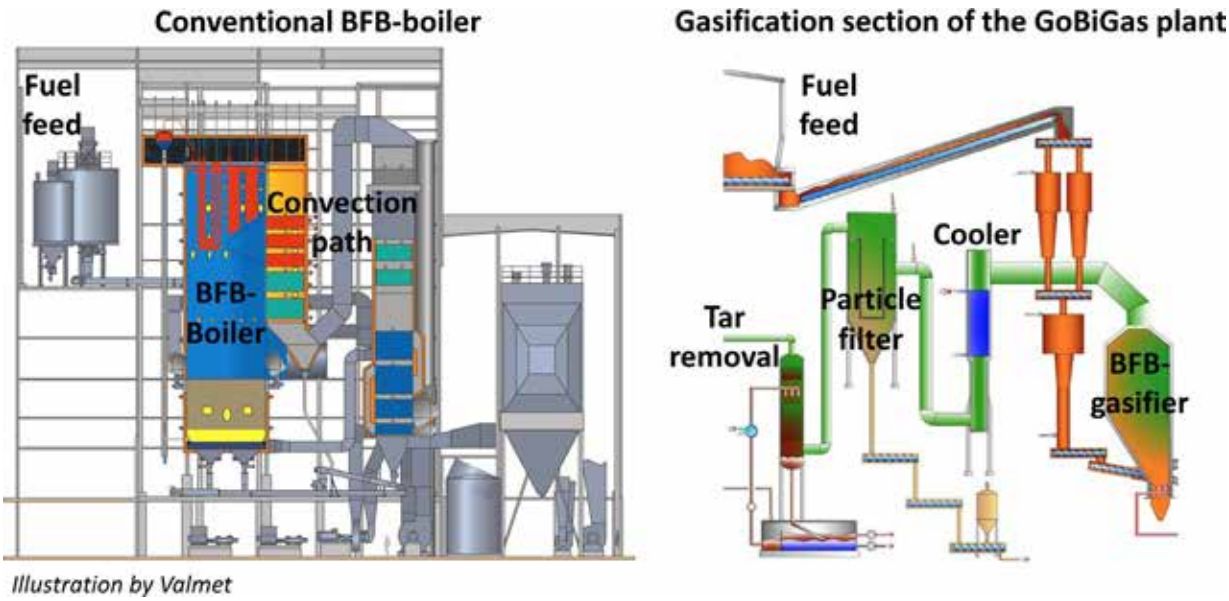

Figure 3. The second reactor in the gasification system is the BFB reactor, which functions as a gasifier in the GoBiGas process, but is comparable to a BFB boiler. The differences between these two systems are mainly evident in the convection pathway (gas cooling and cleaning) and in the fuel feeding (Fig. 3).

described for the CFB convection path, a more robust design is required for solid, ash-rich fuels. By gradually lowering the temperature, to avoid temperature windows in which various components can condensate (as is done in the CFB and BFB boilers), operational issues related to fouling by tar and alkaline can be handled.

The current GoBiGas design creates a challenge for process start-up, until the activity of the bed material has been reached, as fouling from either alkali salts or large PAH deposits on the surfaces of the heat exchangers occurs readily. The surface temperature of the heat exchangers in the gasification section need to be maintained within a narrow temperature range of 140–200°C (285–390°F), and the cooler will work properly only if the catalytic activity of the bed material is sufficient, since it will otherwise become clogged with tar within a few hours [5]. However, the most common cause of clogging of the cooler is alkaline deposits at the top of the cooler during start-up, when the bed material is saturated to avoid high tar yields, as will be described in *Controlling the gas quality using potassium*.

The experience gained from the research conducted with the Chalmers gasifier suggests that the convection path of the gas exiting the gasifier should follow the same layout principles as those that apply to the combustion side, that is, the employment of an empty downdraft chamber before the heat exchanger, to cope more effectively with the alkaline components of the gas. Furthermore, the outlet temperature from the initial cooling stage should ideally be adjusted from 140 to 200°C (285°–390°F) to around 400°C (750°F) during start-up and disturbances. It would also be preferable to extract particles at several steps, as is done on the combustion side, to permit more stringent control of the chemical circulation of fines and to reduce the particle loads on the downstream filters.

At GoBiGas, the particles are separated from the product gas using textile bag filters that are coated with limestone to form a filter cake. The added limestone provides the system with additional calcium, which is an important ash component for the process, as described in detail in *Controlling the gas quality using potassium*. With the present design, the filter tolerates temperatures of up to approximately 230°C (450°F), thereby imposing a restriction on the outlet temperature of the gas from the convention pathway. As previously discussed, for a future system, it would be advisable to upgrade the filters so that they can handle temperatures up to 400°C (750°F), at least for short periods of time.

Downstream of the textile bag filters, steam and PAHs are, in the present process, removed by passage through a scrubber. To simplify the separation, rapeseed oil methyl ester (RME) is used as a scrubber agent to absorb the PAHs. However, the composition of the gas at this stage of the process is typically >30% volume steam and <1% PAHs. A typical composition of the PAHs and the separation efficiencies of the different tar components in the RME scrubber are listed in Table 1 (see *Cooling and cleaning of the product gas*). Thus, the scrubber acts mainly as a product gas condenser. The RME used to absorb and separate the PAHs should in future plants be replaced by a less-expensive scrubbing agent or separation method,

Table 1. Typical compositions of the major PAHs that influence the dew-point of the gas entering the RME scrubber in the GoBiGas plant, using wood pellets as the fuel. (n.d.: no significant change determined).

Component	Typical concentration [g/Nm^3]	Average removal, RME-scrubber (%)	Test at Chalmers [g/Nm^3]
Benzene	13.24	n.d.	8.41
Toluene	0.54	n.d	3.00
Xylene	0.00	n.d.	0.00
Styrene	0.13	n.d.	0.95
Indene	0.16	29	0.91
Naphthalene	2.66	72	2.15
2-MethylNaphthalene	0.03	91	0.39
1-MethylNaphthalene	0.02	98	0.27
Biphenyl	0.04	100	0.16
Acenaphthylene	0.52	98	0.60
Acenaphthene	0.02	100	0.57
Dibenzofuran	0.04	98	0.11
Fluorene	0.06	100	0.18
Phenanthrene	0.43	100	0.50
Anthracene	0.04	100	0.08
Fluoranthene	0.13	100	0.10
Pyrene	0.12	100	0.08
Crysene	0.05	100	0.04

as the RME used presently accounts for 5–10% of the operating costs.

Optimization of the gasification process

The experience gained from both the GoBiGas plant and the Chalmers gasifier has led to a comprehensive picture of how best to optimize the DFB gasification technology for the production of advanced biofuels. The optimization measures are founded based on a thorough understanding of the carbon balance of the Chalmers gasifier. This has been possible thanks to the advances in raw gas characterization methods, which include: He tracing to derive the total yield of gas [17]; Gas Chromatography for measurement of the concentrations of permanent gases; and SPA method for characterization of aromatic tar [18]. More recently, the development of a High Temperature Reactor (HTR) provided an independent method to quantify the total carbon in the raw gas [19]. The HTR enabled the closure of the carbon balance of the Chalmers gasifier, as well as the validation of an improved SPA method [20].

The main aspects of the optimization discussed here are related to: the solid circulation of the process; ways to control the gas quality of the process; improvements to the cooling and cleaning of the product gas; ways to optimize the chemical efficiency of the gasifier; and the design of the fuel feeding.

Solid circulation in a DFB gasifier

The material flows in indirect gasifiers, built according to the example of the Güssing plant, employ two material cycles, as illustrated in Figure 4. In the figure, the material flows are distinguished as the *primary circulation* of bed material between the gasifier and the combustor (blue), and the *secondary circulation* of ash fractions (green and orange).

The primary circulation is the flow of bed material between the gasifier and the combustor through a seal in the bottom of the gasifier and a cyclone at the exit of the boiler with the main function of using the bed material as heat carrier, catalyst and carrier of reactive species. At GoBiGas, the bed material consists of olivine with a particle size distribution between 180 and 500 μm. The circulation flow of bed material depends mainly on the gas velocity through the bed section of the combustor [21]. It therefore depends on the fuel load of the system and the amount of air added to the system. A slight adjustment of the flow can be achieved by adjusting the quotation between primary and secondary air but not

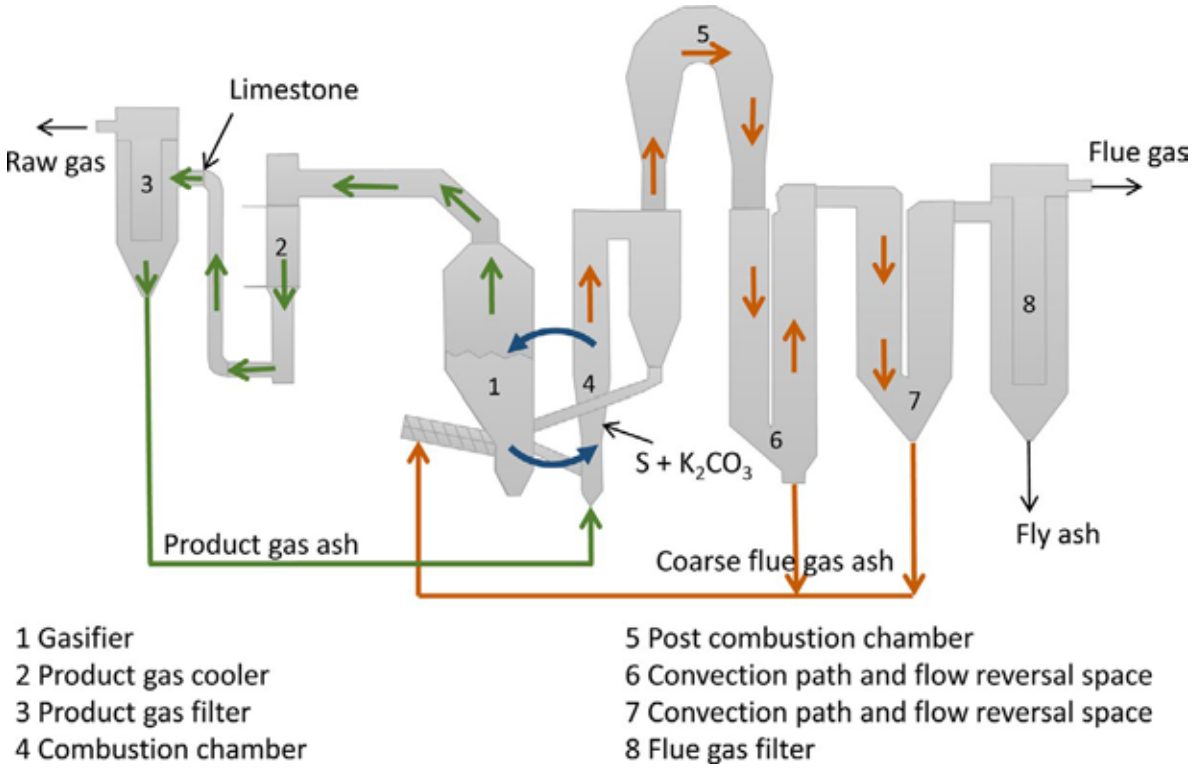

Figure 4. Illustration of the flows in the gasification section of the GoBiGas plant of the bed material (blue), product gas ash (green), and coarse flue gas ash (umber).

enough to keep the circulation flow constant as the load is changed in the system. Thus, both the heat transfer and the transport of active components change with the fuel load and this can limit the operational window of the process. For example, both the excess air ratio and the temperature difference are coupled to the load of the combustor.

To circumvent the limitations cause by changes in the bed material flow and to improve the process control, recirculation of flue gas to the combustion chamber should be included. This possibility is available in the Chalmers system where circulation flow of bed material can be controlled much more specific and the effect of changing the bed material flow has been investigated [17].

The secondary circulation consists of the recirculated material that is trapped in the product gas filter (3) and the coarse ash from the flue gas train. The ash in the product gas is rich in carbon (around 10–15%mass), so it is reintroduced into the combustor for carbon/energy recovery. The other main constituents of the product gas ashes are entrained bed material particles (≤100 μm in diameter), the limestone added as precoat material for the filters, and biomass ash. The ashes from the two flow reversal space (6, 7) are recycled to recover the entrained bed material (mean particle size >100 μm). The main functions are the recovery of entrained bed material, important ash components, and the carbon in the product gas ash (PG-ash). Since the commissioning of the GoBiGas plant, both the bed material and the ash chemistry have been optimized to achieve a high gas quality.

As mentioned above, all the heat needed for fuel conversion in the gasifier is provided by the primary cycle of the bed material, which transports the heat from the combustion side to the gasification side, while at the same time facilitating the return of the unconverted char fraction with the bed material to the combustion side. With conventional circulating bed systems, the experience is that it is favorable to minimize the size of the bed particle so as to avoid erosion and to create a high circulation flux. However, for a combined bubbling and circulating bed system, the gas velocity in the bubbling bed needs to be considered, so as to avoid entrainment of the bed material in the gasifier. As the gas velocity in the combustor is determined by the designated air ratio, a larger particle size distribution of the bed material results in a low circulation flux and, consequently, in a large temperature difference between the two reactors, and *vice versa* for a smaller particle size distribution. This coupling could be reduced by applying flue gas recirculation to the combustion section in a commercial-scale gasifier. The bed material at GoBiGas was changed in Year 2016 from Austrian olivine (pretreated olivine, 100–800 μm; Magnolithe GmbH) to Norwegian olivine (Vanguard 180–500 μm; Sibelco). The main reason for this change is related to reduced transport costs and avoiding energy-intensive pretreatment, which affect both the overall cost and CO_2 emissions related to the bed material. Furthermore, the new olivine had a narrower and on average smaller particle size distribution of 180–500 μm compared with the 100–800 μm of the previous olivine. No significant effect on gas quality was linked to the change of bed material, although the ash components were affected, as will be discussed in *Controlling the gas quality using potassium*.

An unwanted effect of the bed circulation that is often overlooked is that all the bed material used in a DFB system will eventually transfer a certain amount of oxygen from the oxygen-rich combustion reactor to the reducing gasification reactor, either through oxidation/reduction of the bed material itself or ash components attaching to the surface of the bed material [22, 23]. This will result in oxidation of some of the produced gas in the gasifier, and for the process, an increase in the amount of CO_2 that needs to be separated in the synthesis process, most likely via the energy-intensive amine process. Therefore, when considering the whole process from fuel input to synthesized fuel as the output, precautions need to be taken to minimize the oxygen transport.

As expected, when particles of a smaller average size distribution are used there is a noticeable increase in the circulation flux, as was also observed when the olivine was changed from the Austrian to the Norwegian version. For instance, in the Chalmers gasifier, it was shown that this affects the circulation flux of the bed material, which in turn affects both the heat transfer and the oxygen transport [24]. Furthermore, the chemical balance of inorganic species between the gasifier and combustor is affected by the bed material circulation flux, as the rates of uptake and release of species that mediate the catalytic activity will differ at different temperatures. This means that both the overall temperature level in the gasification process and the temperature difference between the combustor and the gasifier are parameters that can be used for optimization of the process. In particular, a lower overall temperature and smaller temperature difference between the combustor and the gasifier will have positive effects on the thermal efficiency of the process, although a small temperature difference between the combustor and the gasifier entails a high circulation flux and increased oxygen transport, which lower the chemical efficiency of the process.

Controlling the gas quality using potassium

A conclusion from the commissioning of the GoBiGas plant is that, for a cooler operating at temperatures <200°C

(390°F), it is crucial to produce a gas of sufficient quality that can be handled by that cooler. Such gas quality can only be achieved if the bed material has a sufficiently high catalytic activity. Complete catalytic conversion of volatiles is, however, unlikely due to mixing limitations.

Previous experiences with smaller demonstration units, for example, the plants in Güssing, Oberwart, and Senden [8, 25], which cumulatively have been in operation for more than 100,000 h, indicate that catalytic activation of the bed is achieved with continuous operation. However, during the commissioning of the GoBiGas plant, which took place at the end of Year 2013 and beginning of Year 2014, it was not feasible to operate the gasifier continuously for a sufficiently long period to obtain a catalytically active bed without clogging the cooler.

This focused the work in the Chalmers research gasifier to finding a solution, whereby the bed could be artificially and sufficiently catalytically activated. From the evaluation of the results obtained from the experimental campaigns conducted between Year 2007 and the beginning of Year 2014, it became clear that it was necessary to saturate the system with potassium. The amount of potassium carbonate (K_2CO_3) needed to saturate the bed material and the refractory material in the demonstration plant was estimated at about 1000 kg, which was the quantity that in April 2014 was dissolved in water and pumped into the combustion side of the GoBiGas gasifier. This resulted in the first successful operation of the demonstration plant with a gas composition and a load of larger polyaromatic hydrocarbons (PAHs), which were handled without clogging the cooler.

Since then, much effort has been expended toward attaining a better understanding of the activation process and ways to control the chemistry in the gasification process [26]. Based on the many experiments performed in the Chalmers gasifier and during the operation of GoBiGas, our current hypothesis is as follows: in the combustor, the bed material becomes saturated with potassium, enabling potassium salt to form on the bed material and the calcium layer formed on the surface of the bed material enhances the storage capacity of such salts. The bed material together with the potassium salts enters the gasifier, where these components are then released through exposure to steam and a reducing atmosphere. As they are released, they transform and interact with the radical pool, providing the necessary catalytic activity. A side-effect of the increased levels of potassium is a dwindling CO-burnout on the combustor side, which has been observed in a context of high catalytic activity [26].The addition of sulfur or silicon to the combustor removes the effect on the burnout. Sulfur also reinforces the catalytic effect on tar formation, in contrast to silicon, which eliminates this effect.

Figure 5 shows a typical example of how the concentration of unconverted CO in the flue gas of the Chalmers boiler increases as the activity of the olivine bed increases. The addition of a continuous flow of 1.0–1.2 kg/h (i.e., 1 mg/kg dry fuel) of elemental sulfur to the bed immediately confers complete combustion of CO, while the CO emissions increase progressively when the sulfur supply is terminated.

The amount of potassium salts on the bed material can be quantified by leaching in water, followed by analysis of the leachate. Figure 5 depicts the relationship between the level of water-soluble potassium in the bed material particles and the catalytic activity of the bed, which can be qualitatively assessed based on the tar concentration of the product gas and the level of CO emissions in the combustor. Here, the drop in the level of tar and the increase of CO emission from the boiler are seen over a very narrow range of concentrations of leachable potassium, leading to the interpretation that the bed material becomes saturated. The active components exit together with the gas from the gasifier and condense as salts in the convection path. The salts are collected in the filter, wherefrom they are returned to the combustor. In the combustor section, alkali components are once again made available for reactions, that is, they are adsorbed or absorbed onto the bed particles to the saturation level, while the remaining excess of alkali is collected in the filter and removed from the system with the fly ash.

As potassium is an essential catalytically active component, the selection of bed material needs to be made with some care. The main criterion is to avoid an excess

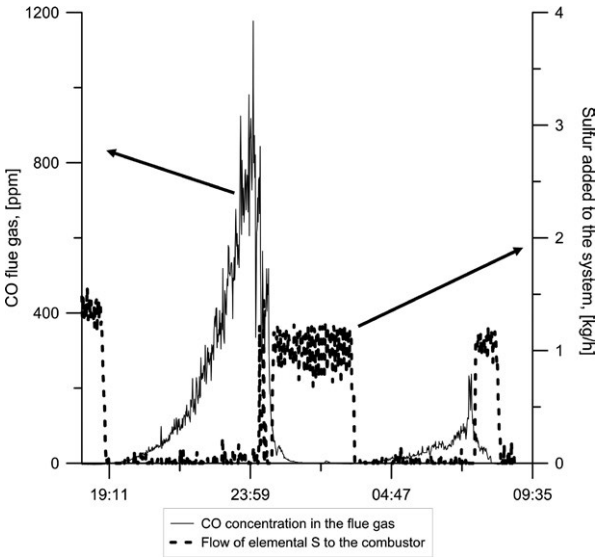

Figure 5. CO emissions from the boiler. Elemental sulfur was added to mitigate the incomplete burning of CO. The test was conducted in the Chalmers gasifier with wood as the fuel on a bed of Norwegian olivine.

of free silica, which will capture the active potassium very efficiently and permanently as silicates, thereby diminishing the activity of the bed material. Figure 6 summarizes the evidence for the loss of activity of a bed of olivine when a silicon-rich material (silica sand) is added to the system. The tar concentration increased 1.7-fold after the addition of 600 kg of silica sand to a bed of 3 tonnes of material in the Chalmers system, as compared to the tar concentration before the addition. Note how the CO burnout in the boiler also improves with the addition of silica sand, as the catalytically active potassium reacts with the silica. When this happens, not only the catalytic activity will be diminished, but also the bed particles will start to agglomerate due to the formation of low-melting-point eutectics of potassium silicates. Therefore, care should be taken to avoid silica sand, either as a bed material or as inert impurities (e.g., soil) in the biomass feed, in cases where the biomass was not handled correctly before being delivered to the plant. Favorable bed materials that can be used in the process are olivine, alkali feldspar, and low-iron-content bauxite [13, 22, 24].

It is crucial to identify the window of operation within which the appropriate proportions of potassium, sulfur, and calcium, together with the aging bed material give the optimal level of catalytic activity. Too little potassium or sulfur leads to too-high levels of large PAHs (*cf.* Fig. 7, *Tar-CO-leachable potassium*), while too much potassium leads to a large fraction of potassium salts in the gas. In both situations, the heat exchanger will become clogged and eventually cause the process to stop. The key to creating a stable process is, therefore, to exploit the flexibility offered by the process design to control the levels of the above-mentioned species.

Data from GoBiGas have shown that there is a correlation between the tar concentration and the methane concentration in the dry gas [5]. Measurements obtained from the system at Chalmers have shown that the fraction of carbon in the fuel that is converted to methane is close to constant, regardless of any operational changes. However, a more active bed increases the conversion of both PAHs and char to mainly H_2 and CO, as well as increasing the shift from CO and H_2O to H_2 and CO_2, thereby reducing the dry methane concentration and providing an online indication of the activity of the bed. The correlation is illustrated in Figure 8, and it is clear that different fuels yield different correlations. Based on operational experience, limitations with regard to the methane concentration are established, as indicated by the dotted lines in Figure 8, where operation with a higher concentration of CH_4 yields tar deposits in the cooler, mainly reducing the heat exchange capacity, whereas a lower concentration of CH_4 yields alkaline deposits at the entrance of the cooler, mainly increasing the pressure drop.

The strategy that is currently applied to control the gas quality is described as follows. When the concentration of methane gradually increases, this indicates that

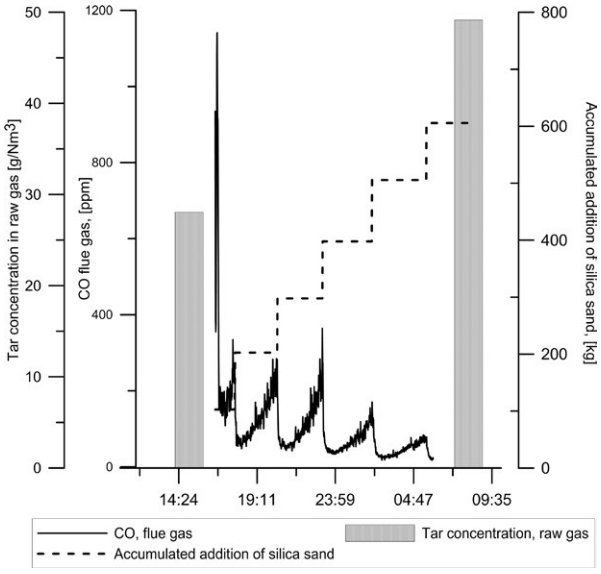

Figure 6. Tar concentrations (including BTX) before and after the addition of 600 kg of silica sand to a bed of 3 tonnes of olivine. The silica sand was added in six steps, and the corresponding CO emissions in the combustor side are shown. The tests were conducted in the Chalmers gasifier with wood as the fuel.

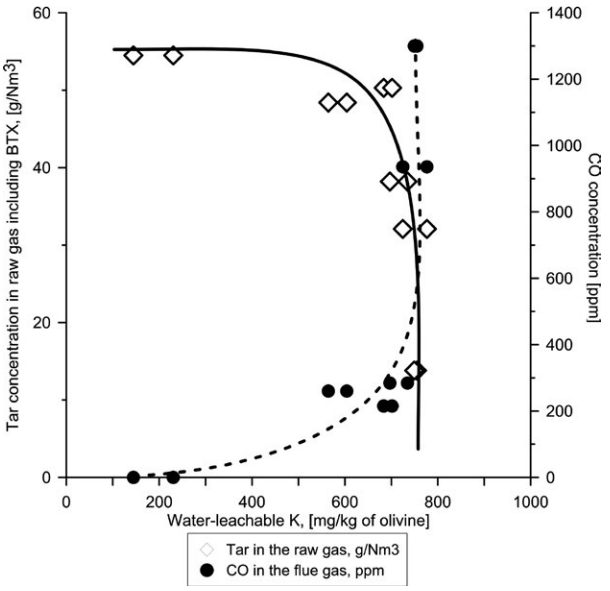

Figure 7. Relationship between the levels of water-leachable potassium in the bed material transferred from the combustor to the gasifier and the signs of catalytic activity (i.e., the levels of CO emissions in the combustor and the tar concentration in the raw gas). The tests were conducted in the Chalmers gasifier with wood as the fuel and Norwegian olivine sand as the bed material.

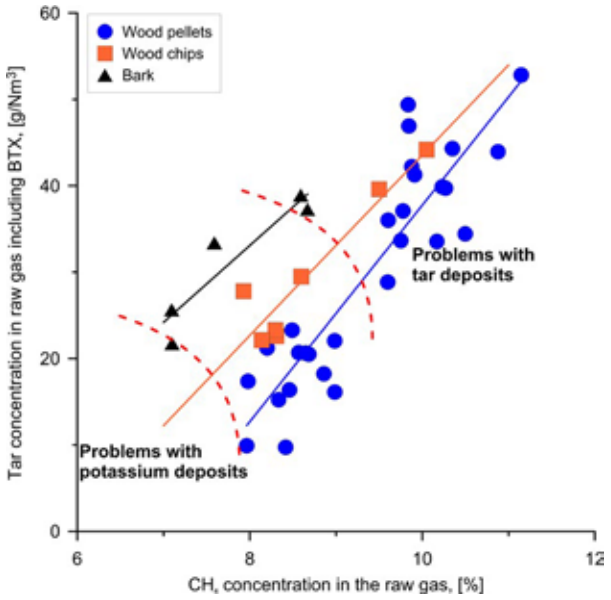

Figure 8. Correlations between the concentrations of methane and tar for various fuels and limits, for which actions related to bed activity are taken. Data from the GoBiGas plant.

the activity of the bed is reduced. In this case, the addition of potassium carbonate to the combustion chamber is increased. If further activation is required, recirculation of particles from the flue gas can be increased, or elemental sulfur can be added to the combustor as well. In a situation in which the dry concentration of methane drops to a level that is too low, the activity of the bed needs to be reduced to prevent the potassium salts falling out as deposits upon the heat exchanger surfaces. In this case, the flow of potassium to the combustor and the recirculation of fines from the flue gas to the gasifier are reduced. If the increased recirculation rate is not sufficient, bed material is removed and replaced with new material. While wood chips and pellets often require addition of alkali, forest residues and bark are self-sustaining, provided a low content of silicon carrying impurities.

Nevertheless, as shown in Figure 8, the limits within which the bed activity needs to be controlled are fuel-dependent. Therefore, the functionality of the strategy will rely on the ingoing fuel having a reasonably stable composition. However, biomass and waste, which are the intended fuels for the technology, are by their nature heterogeneous, so controlling the composition is not a viable option. To overcome this limitation, online measurements of tracer species that indicate changes in the tar concentration/composition and alkali concentration are important, keeping in mind the linkage of low tar levels with high concentrations of alkali. Several developments aimed at achieving this are ongoing and have even been tested within the context of the project. For online tar monitoring, spectroscopic methods, such as laser-induced fluorescence and UV-vis spectroscopy have demonstrated the ability to give reliable responses for a shift in the tar composition toward larger molecules [27, 28]. Even measurement after a high temperature conversion of a slip stream to assess the overall carbon amount gives information about the yield of condensable hydrocarbons [19]. For alkali species, spectroscopic methods are under development but are not yet ready for application [29, 30]. Surface ionization detectors for alkali species have been developed by different groups [31–33] and shown to be applicable for measurements.

As stated above, the ash in the biomass to some extent compensates for the loss of active components during steady-state operation. However, extra additives might be required during start-up or in the case of a fuel with an unfavorable ash composition. The start-up strategy currently applied in the GoBiGas plant is that the initial activation is carried out by adding calcine and potassium, while heating the system through the combustion of natural gas on the combustion side. Here, the present layout of the process entails a special challenge, as the gasification reactor during the stop phase and initial start phase is fed pure nitrogen, before it is turned over to steam. Operation without adding new ash components to the system leads to a gradual loss of potassium and sulfur from the system and need to be compensated to assure sufficient activity of the bed. The amount of supplementary potassium carbonate and elemental sulfur that have to be added to the bed before start-up has to be estimated based on the interpolation and extrapolation of experiences from previous start-ups. This procedure could be modified by incorporating a recycle stream of preactivated bed material and ash fractions [34].

The combustion side of the process also serves as a regenerator of the catalysts in the system, in which the bed material and ash components are partially oxidized. Furthermore, the bed material takes up the ash components that provide the catalysts for the gasifier in the combustor, which also include supplemented ash components, such as potassium, sulfur, and calcium [35, 36]. For instance, net transport of sulfur from the combustor to the gasifier has been observed in the Chalmers gasifier. Figure 9 shows the levels of sulfur that originated from the H_2S in the raw gas in the Chalmers gasifier during tests conducted with an ash-free fuel, as well as a test conducted with wood pellets when the process was operated with olivine or silica sand as the bed material. For the case in which wood pellets were gasified, the difference in sulfur concentration between the raw gas and the fuel feed proves that the silica sand and olivine bed materials can transport sulfur from the combustor to the gasifier. This was further confirmed

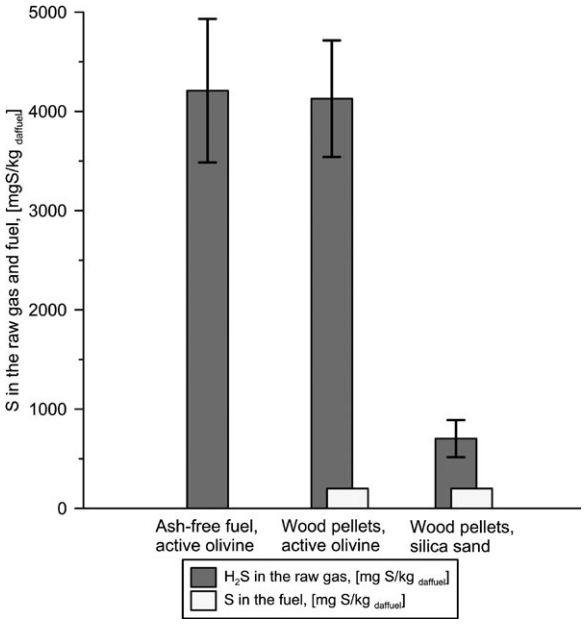

Figure 9. Sulfur transport and release from the bed material (olivine or silica sand) in the gasifier, as well as the levels of sulfur in the fuel (ash-free or wood pellets) fed to the gasifier.

in the test that involved gasification of the ash-free fuel, where the H_2S measured in the raw gas could only originate from the bed material coming from the combustor. Similar transport phenomena for inorganic species, in particular potassium, transferring from the combustor to the gasifier, have been observed in the Güssing plant [35].

In summary, the gas quality is mainly a function of the catalytic activity in the DFB system, which is controlled by:

- the primary circulation of the bed material;
- the secondary circulation of recirculated particles;
- the addition and removal of the bed material;
- the fuel-ash temperature levels of the bed materials in the gasifier and combustor;
- the steam-to-fuel ratio and fuel load; and
- artificial supplementation with potassium, sulfur, and calcium.

Cooling and cleaning of the product gas

Controlling the cooling of the producer gas from a steam-blown gasifier is challenging because of the impending risk of tar fouling on the heat exchanger surfaces. The fouling of heat exchanger surfaces is a well-known industrial problem globally, and it has been estimated to cost industrialized countries approximately 0.25% of their GDP [37]. One approach to mitigating physically the fouling without changing the overall heat exchanger design or operation is to modify the interactions of the deposit-forming precursors with the heat transfer surface [38]. By taking advantage of recent developments in coating technology, thin and stable coatings that involve ceramics can be produced that outperform the previous generations of pure fluoropolymer coatings [39]. These functional coatings can be made both erosion-resistant and oil- or water-repellant, and they are already used commercially, for example, in the oil and gas industries [40].

A major milestone in progress toward improving product gas cleaning was reached in March 2017 when it was shown an RME scrubber could be replaced by a regular plate heat exchanger with coated surfaces, upon which both steam and aromatic structures with two or more rings could be condensed. Testing was performed using a slipstream of product gas from the Chalmers gasifier, which was cooled in a down-scaled plate heat exchanger. Validating tests was performed in July 2017 at the GoBiGas-plant. This proof-of-concept work, as illustrated in Figure 10, represents a major breakthrough for the technology, as it allows the removal of an otherwise costly and troublesome process unit. The coated heat exchanger plates used in the experimental evaluation in the Chalmers gasifier are inspired by the concept of self-cleaning surfaces [41], in which modifications of the surface chemistry and roughness create a situation in which the liquid water flow that results from the condensing steam effectively keeps the surface clean [42, 43]. The functionality is highly complex, arising from the interplay of the molecular and continuum properties of the gas–liquid mixture and the coated plates. Furthermore, the corrugation of the surfaces of the plates has been shown to affect the flow at both the macro- and microscales [44].

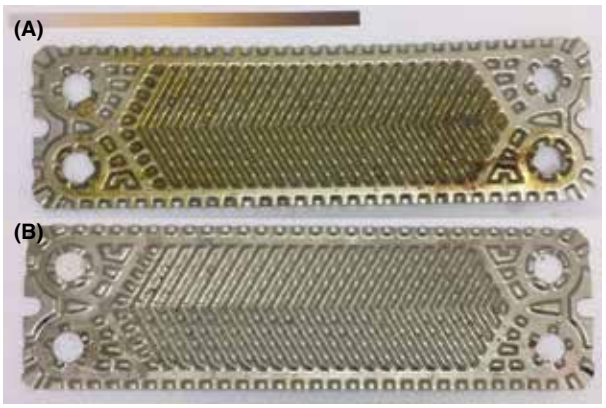

Figure 10. Comparison of a conventional (A) and a novel, coated (B) heat exchanger plate after several hours of exposure to a raw gas side stream in the Chalmers research gasifier. The degradation of the uncoated plate by a yellow-brownish tar residue is clearly visible. In contrast, the coated plate has remained virtually unaffected.

The tar concentrations to which the heat exchanger was subjected during the tests in the Chalmers gasifier are summarized in Table 1, where they are also compared to typical tar concentrations in the gas before the RME scrubber at GoBiGas, and an indication is given as to how well these components are removed in the RME scrubber. The components are presented in order of increasing dew point, starting with benzene, which has the lowest dew-point, and ending with chrysene, which has the highest dew point. The levels of performance of the RME scrubber for the most relevant hydrocarbons are presented in Table 1, which shows that the scrubber efficiently removes components with higher dew points than naphthalene, while a significant fraction of the naphthalene and almost all of the more volatile components remain in the product gas. The remaining components are removed by active carbon beds, see *Bridging processes*. The more components with higher dew points than benzene, such as naphthalene, that enter the carbon beds, the more difficult it becomes to regenerate the beds. Therefore, any new or existing systems need to be considered together to optimize the overall gas cleaning. Improved control of the distribution of tar components via the operation of the gasifier might also offer the possibility to lighten the burden on the carbon beds by producing a tar that is more easily removed in the plate heat exchanger unit.

Optimizing the chemical efficiency of a DFB gasifier

Typical gas compositions and energy fractions from the GoBiGas demonstration operating with wood pellets as fuel are shown in Table 2. Based on the chemically bound energy in the gas, as distinct from the chemically bound energy in the fuel, it is evident that the overall reaction in the gasifier is endothermic, showing an increase in chemical bound energy of 2.3%. In the present GoBiGas system, the heat for the gasification process is provided by the combustion of char, larger polyaromatics, and part of the dry product gas. The BTX (Benzene, Toluene, Xylene) species and the part of the naphthalene that is not captured by the scrubber are at present combusted in the postcombustor at GoBiGas. This represents a loss of more than 3.5% of the chemically bound energy. Thus, to increase the efficiency, these components should be better utilized (see the *Bridging processes* on the removal of BTX). Furthermore, the heat demand of the process should be minimized, so as to optimize the chemical efficiency of the gasifier. This can be achieved by: applying reactor walls that lower the heat losses; preheating the ingoing air and steam streams to higher temperatures; decreasing the overall gasification temperature; lowering the moisture content of the fuel; and preheating the ingoing fuel. Through these measures, the heat demand could be reduced by as much as 20% in a future

Table 2. Wet and dry gas compositions and energy distributions for a gasifier operated with wood pellets and a bed temperature of 870°C. The data shown are extracted from validation experiments at GoBiGas [3].

Component	Wet gas $\%_{vol}$	Dry gas $\%_{vol}$	Energy $\%_{daf}$[1]
H_2	27.7	39.9	30.1
CO	16.6	24.0	21.3
CO_2	13.8	19.9	
CH_4	6.0	8.6	21.4
C_2H_4	1.4	2.0	8.2
C_2H_2, C_2H_6, C_3H_6	0.2	0.3	1.4
Inertization gas (CO_2; during production), N_2 (validation experiments))	3.7	5.3	
H_2O	30.2		
BTX[2]	0.3		3.5
Tar[3]	0.1		2.1
Char			14.3
		Sum	102.3
Potential CO and H_2 production from remaining char			19.0
	kg/kg_{daf}	mol/mol_{stoic}[4]	Loss of chemical bound energy %[5]
Oxygen transport	0.07	0.049	5.3

[1]Dry ash-free fuel (daf).
[2]BTX represented by benzene.
[3]Tar represented by naphthalene.
[4]Stoichiometric combustion (stoic).
[5]Calculated from the average gas composition.

commercial plant, thereby increasing the chemical efficiency of the gasifier to the same extent (for more details see [45]). In addition, by introducing an alternative external heat source, for example, direct heating by electricity, the energy content of the produced gas could be increased even further, up to about 120% compared to the chemically bound energy of the ingoing fuel [11].

Given the relatively narrow time window for the release of volatile matter and the typical rates of lateral mixing of fuels in fluidized beds, the layout of the process provides, at all times, for scales larger than laboratory units and sufficient residence times for the biomass to be pyrolyzed in the gasification chamber. As most of the chemically bound energy in the biomass is stored in the volatile fraction of the fuel, the volatiles will, therefore, represent the major share of the gas released on the gasification side of the process. However, for an optimized biofuel plant, part of the produced char needs to be gasified, so as not to release too much heat on the combustion side of the process.

To control the extent of char conversion in the gasification chamber, several alternative methods are available. The most intuitive option is to increase the overall residence time for the char and the circulated bed material by increasing the volume of bed material in the gasification reactor (given by the cross-sectional area and the bed height). However, the optimal height of a fluidized bed is in the range of 30–60 cm, as the bubbles in taller beds will coalesce to form larger bubbles, which greatly reduce the gas-solids contacts and confer no further benefit in terms of the overall performance of the mass transfer [46]. Furthermore, the pressure drop across beds that are taller than 60 cm requires a specially designed, high-pressure drop gas distributor to ensure good fluidization and to avoid partial defluidization of the emulsion phase located in-between the bubble paths [47]. Similar problems will be experienced following the introduction of tapered walls into the reactor along the height of bubbling bed, which is the case for the present design of the GoBiGas gasifier, as the bed located in the region of the tapered walls will not be properly fluidized or even defluidized.

For the GoBiGas process, if this issue is not addressed sufficiently, it can create a very unfavorable flow profile and suboptimal mixing conditions. An alternative method for increasing the inventory of bed material in the gasifier is to increase the cross-sectional area, which is not an attractive option, as it increases the cost of the plant. A more straightforward strategy to increase the residence time in the gasifier is to increase the temperature difference between the combustor and the gasifier, thereby increasing the heat-carrying capacity and allowing the process to operate with a lower volumetric flow of circulating solids. However, this option also has its limitations, as the temperature difference between the combustion and gasification reactors is restricted to around 100°C, so as to maintain the process below the temperature at which there is a risk of agglomeration.

The remaining options are either to modulate the rate of char gasification or to decouple the residence time of the char from that of the bed material. We start with changing the reaction rate of the char gasification, which is significantly increased by the potassium released from the activated bed material on the gasification side and that diffuses into the char particles [48]. In the demonstration plant, this effect is substantial, where the char that is converted is around 50% and will be sufficient to fulfill the mass balance for most applications [11]. If there is a need to increase the char conversion beyond a level that can be realized by the catalytic activity, the significant differences in density and size between the bed material and the char offer the possibility to decouple the mixing, and thereby the residence time, of the char from that of the bed material. This can be achieved by optimizing the pressure drop over the distributor plate in combination with the fluidization flow and fuel size and shape, such that the char particles float on the bed surface (see Figure 11), and by physically creating an enclosure for the char particles using, for example, baffles [49].

Design of the fuel feeding to the gasification section

The fuel feeding system warrants close attention in the quest to obtain a process with high availability. Here, there is a strong influence of scale, and the experience

Figure 11. Photograph of fuel particles (black dots) floating on the surface of the bubbling fluidized bed in the research gasifier operating at 820°C (1500°F) and using wood pellets as fuel. Source: Erik Sette, Rustan Marberg, Chalmers University of Technology.

from laboratory-scale fluidized bed gasifiers is of a preference for mechanical in-bed feeding over feeding the fuel by gravity fall on-top of the fluidized bed. The same experience was obtained for fluidized bed combustors in the late 1970s and the beginning of the 1980s. To investigate if this also applied to industrial units, the first industrial-sized (16-MWth) bubbling fluidized bed combustion system installed at Chalmers in 1982 was equipped with both in-bed and on-top feeding. The experience from that exercise, which remains unpublished, but has been transferred to and adopted by the major boiler manufacturers [50], was the opposite of the experience with the laboratory units. Here, feeding by dropping the fuel onto the bed surface always gave better results than in-bed feeding.

If there is an ambition to drag the fuel down into the bed in an industrial system, where the cross-sectional area allows fully developed fluidization, it is much more advantageous to increase the fluidization velocity in the area within which the fuel feed is located. Fuel that is fed into the bed via an in-bed feeding system rises very rapidly to the bed surface and remains there, as a consequence of the density difference and the released moisture and volatile matter, which create so-called 'endogenous bubbles' around the fuel particle, helping it to rise towards the bed surface [51]. Despite this knowledge, the technology provider of the demonstration gasifier was not willing to change the design, as the gasifier in the GoBiGas plant was scaled up from the existing unit in Güssing. That decision has created significant problems related to availability for the current unit.

The availability problems related to the in-bed fuel feeding system have to a large extent been related to the transport of heat by the bed material into the fuel feeding system (see Figure 12), which causes the fuel to pyrolyze inside the screw. The tar produced in this region will condense and start to build up inside the screw, which eventually results in a momentum that is too high for the engine driving the feeding screw and eventual blockage of the fuel. This has not been as big a concern in the smaller units in Güssing and Oberwart in Austria as in the GoBiGas demonstration plant, which to a large extent is attributed to the use of a fuel with a relatively high moisture content (typically around 20%), as compared to the fuel with a moisture content of 8% used in the demonstration plant. The higher moisture content introduces a cooling to the fuel-feeding system, as the heat that is transported into the screw is absorbed by the heat of evaporation of the moisture. In addition, the larger geometrical dimensions of the fuel feeding system exacerbate this problem.

In the research gasifier at Chalmers, the fuel is dropped onto the surface of the bed by gravity, so the problem of heat transfer into the fuel feeding system is not an issue. The main motivation for getting the fuel into the bed is to assure good gas–solids contacts, as the catalytic activity was originally thought to be a heterogeneously catalyzed reaction that involved the volatiles and the coarse bed material. According to specific investigations in the Chalmers gasifier only 48–69% of the volatiles meet the surface of the bed material particles, while the rest of volatiles do not interact with the bed [52]. This means that, if gas–solid contact is required, full catalytic conversion of volatiles to syngas is not achievable, regardless the catalyst applied. Despite the different approaches, both the in bed feeding by screw (GoBiGas) and the gravimetric on-bed feeding (Chalmers) yield the same low levels of tar. As described above, the findings in the present work imply that with a potassium-activated bed material, homogeneous reactions play a significant role, beyond the importance of gas-solid contacts.

This was validated by changing the bed height in the GoBiGas gasifier during operation with a potassium-activated bed material. As shown in Figure 13, there were no significant changes in the gas quality, here indicated by the methane concentration, of the dry product gas. The notion that the fuel feeding depth has a negligible effect is further supported by the finding that an equivalent gas quality can be obtained in the research gasifier, where the fuel is dropped from the top of the gasifier down to

Figure 12. Left photograph: Cold flow model showing how the bed material is pushed into the fuel feeding screw. Source: Claes Breitholtz, Valmet AB. Right photograph: Feeding screw used in the GoBiGas plant, exhibiting mainly graphite-like deposits.

the fluidized bed, as in the demonstration plant, where the fuel is fed into the bed. Nevertheless, if there is a need in future reactor designs to force the volatiles into contact with the bed material to obtain the required gas quality this can be achieved by an integrated feeding chamber [53].

During 2016, a new external fuel feeding system was put into operation at the GoBiGas plant, which allows wood chips or bark as fuel. The experience to date is that after solving the initial mechanical issues, these fuels can be gasified in a satisfactory way if the fuel is predried according to specification. At the moment, the most serious problem connected to changing the fuel type is the variability in moisture content of the batches of fuel delivered to the plant (at present no dryer is installed at the GoBiGas project, as it was planned for the second commercial phase of the project). This emphasizes the importance of incorporating a dryer onsite, instead of relying on external drying capability. A similar experience was gained from the Güssing plant, leading to the incorporation of a dryer in the Oberwart and Senden plants.

Considering the vulnerability of the overall process, where a stop in the fuel feeding will result in several days production stop in downstream synthesis process, in combination with the well-known sensitivity of biomass-feeding systems, at least a second line is recommended for a future plant. This is especially important bearing in mind the general trend toward adopting low-grade fuels. Further, at least two feeding lines allow one to take full advantage of the co-gasification of fuels with chemical synergy effects, for example, a char-rich fuel plus a fuel with low char content. Even though theoretically these fuels could be blended and fed together through the same port, their different flow properties, arising from shape, surface, and density differences, would create unwanted load fluctuations. Further, additional ports will improve the redundancy of the overall process.

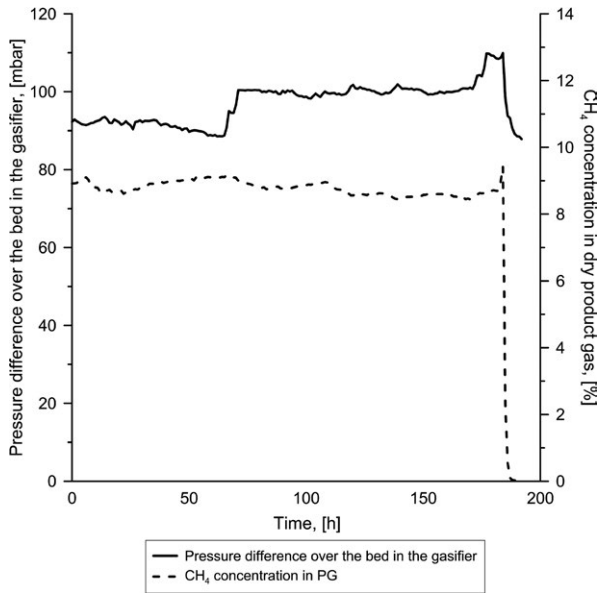

Figure 13. Methane concentrations and the pressure drops over the fluidized bed of the gasifier during 200 h of operation as the bed height was increased in two steps.

Synthesis process

Methane synthesis is the standard way to produce synthetic natural gas from coal. This process is currently up and running in commercial plants at several locations in China and in the US. The biggest concern for the demonstration unit was its small scale and the risk associated with down-scaling the process units (typically by a factor of 10–100, compared to the scale that is usually applied in today's commercial units). A more detailed description of the synthesis process can be found elsewhere [54].

When pure syngas or hydrogen is the desired product, methane and ethane can be converted in standard operation units. This reaction is quite endothermic and needs a supply of heat at temperatures >800°C (1475°F), which can be provided by catalytic partial oxidation or catalytic steam reforming [55–57]. These units run preferentially at high pressure and using relatively clean gas, meaning that they are placed further downstream in the process chain. However, even the application of catalytic tar cleaning catalysts will decrease the amount of methane in the gas, as has been demonstrated previously [55]. In addition, coking and catalyst poisoning are issues of concern.

Nonetheless, looking at the gasification process as a steam reforming process offers more energy and most likely cost-efficient integration strategies for the production of mixed alkenes, methanol or mixed alcohols. The GoBiGas process is optimized for the production of pure methane, which means that the process was designed with the aim of keeping the methane concentration as high as possible in the gas entering the synthesis step. To achieve this, the char gasification with steam to CO and H_2 needs to be optimized so that the char leaving the gasifier just covers the heat demand for the process, so as to avoid dilution.

The temperature of the process can be controlled through the amount of char that is gasified, although this is impractical, as it is a slow process and the char reactivity of the ingoing fuel can vary over time. Instead, the process is setup to ensure that more char than is necessary is gasified, and the process is controlled by the recirculation of some of the cooled produced gas, as illustrated by Alternative 1 in Figure 14.

In the refinery and petrochemical industries, methane is, however, regarded as the hydrocarbon of least value

and it has a lower value than the syngas from which it is produced. To valorize the CO and H_2 in the produced gas, hydrocarbons of higher value should be produced. Thus, the integration strategy would change, in that as much char as possible should be gasified and as little gas as possible should be internally combusted by the oxygen that is transported by the bed material from the combustion to the gasification side of the gasifier. The latter occurs because the oxygen transported by the bed material to the gasifier will most likely favor the conversion of H_2 and CO over hydrocarbons, as observed previously [24]. In this way, the maximum amounts of CO and H_2 will leave the gasifier for the synthesis process.

In the synthesis processes shown for Alternatives 2 and 3 in Figure 14, the gas can be shifted efficiently to the preferred H_2/CO ratio, dried, and cleaned of excessive CO_2 before the gas proceeds to a second compression step that increases the pressure to the level designated for the intended synthesis process. Downstream of the compressor, it is preferable to have a one-step synthesis process that converts as much as possible of the CO and H_2 to the sought-after hydrocarbon, where methane and shorter alkanes act as inert gases. The gasification process is balanced by part of the off-gas from the synthesis reactor, and the remaining off-gas is upgraded to methane, as methanation offers close to 100% conversion. The principal integration scheme is illustrated as Alternative 2 in Figure 15.

Examples of suitable one-step synthesis processes are methanol production, as demonstrated for several thousand hours of operation in the DME plant in Piteå using syngas from black liquor gasification [58] or the FT synthesis process developed and demonstrated in connection with the Güssing plant in Austria [59]. The one-step methanol process developed by Haldor Topsøe requires that the pressure in the second step is increased to 130 bar [58], which might offer a possibility to take out the produced methane produced from the off-gas in liquid form. In the FT process developed by Velocys in connection with the Güssing plant, the pressure is slightly raised to around 20 bar, and the synthesis is performed in a slurry reactor, providing good overall conversion of the gas from a DFB gasifier [59]. Both processes are module-based, and the modules operated in both demonstrations are of the same scale as the intended commercial scale.

If there is no market for the methane or there is an excess of electricity available for the process it would be beneficial to carry out steam reformation of the off-gas

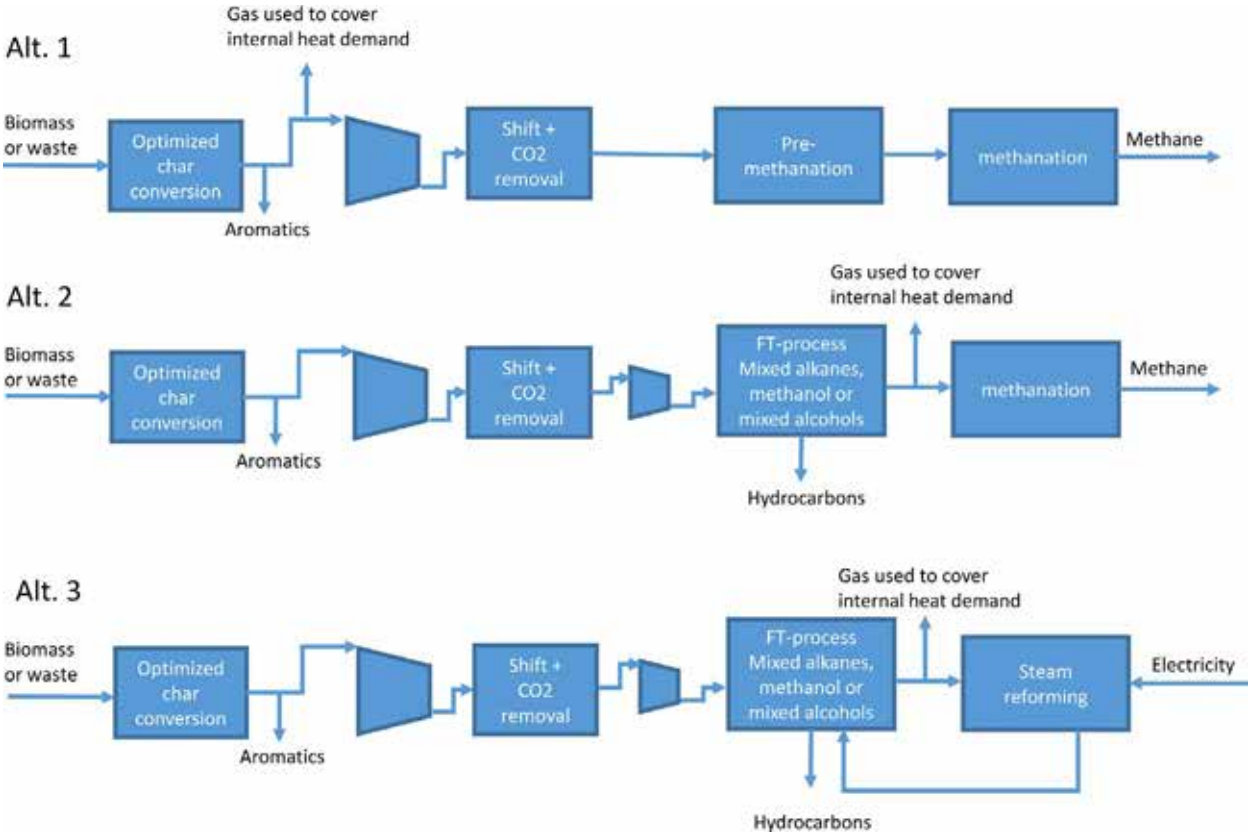

Figure 14. Different integration strategies for different end-products.

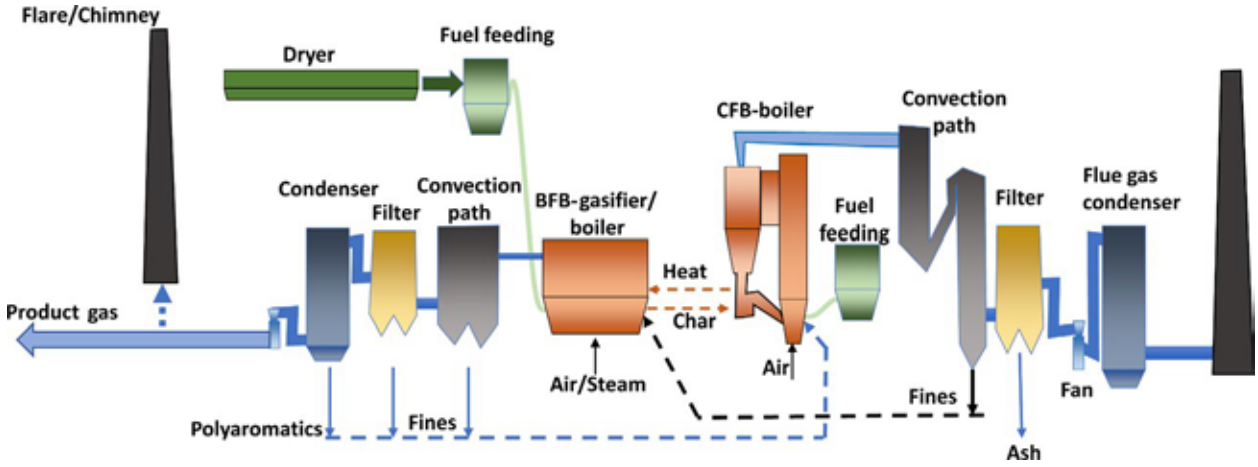

Figure 15. Integration of CFB and BFB boilers to create a dual fluidized bed gasifier.

from the synthesis to CO and H_2, rather than producing pure methane to increase the production of hydrocarbons of higher value, as shown in Alternative 3 in Figure 14. Here, extraction of the gas for heating the gasification process would be beneficial for the overall process, as it would minimize the accumulation of inert gases in the synthesis process, which otherwise would limit the amount of gas that it is possible to synthesize.

Bridging processes

The production of advanced biofuels via gasification merges two industrial branches that traditionally have developed their processes independently with very limited exchange of knowledge. Large-scale biomass gasification has mainly been developed in the energy sector, with the main goal being efficient production of electricity. The focus has been on solid fuel conversion to obtain a gas quality that at atmospheric or moderate pressures can be handled by gas turbines and gas engines, or simply to replace a burner in a regular boiler. In contrast, the synthesis processes are developed for gases that are refined to an extremely high quality and at high pressure. To connect the gasification process with the synthesis process, the "clean" gas from the gasification needs to be compressed and further upgraded to meet the requirements of the synthesis process. This imposes two costly additional steps:

- Compression
- BTX condensation and the removal of other impurities

We start with the compressor, which in the GoBiGas process is an integrally geared centrifugal compressor that takes the gas from atmospheric pressure to 16 bar in six consecutive steps. From the gasification process applied in the GoBiGas demonstration unit, the produced cold gas contains a substantial amount of BTX and naphthalene, which together with small amounts of HCl, ammonia, and H_2S are preferentially separated from the gas upstream of the compressor. Typical compositions of the BTX for two different gasification temperatures are listed in Tables 1 and 2.

In the GoBiGas demonstration plant, the separation is performed in a configuration that comprises four active carbon beds, which can be operated in any order. Typically, the beds are operated as follows: the gas enters the first bed, which has as its main function the removal of all larger aromatic structures and impurities from the gas leaving the RME scrubber. Thereafter, the gas passes through one additional bed, where it removes the main part of the BTX and impurities, such as H_2S, before the gas leaves for compression. The other two parallel beds cycle between acting as the bulk BTX remover and being regenerated with steam.

The regeneration is performed using steam, and the off-gases are led to the afterburner of the combustor for destruction of the BTX components released during the regeneration. During the regeneration, the steam is condensed in the carbon beds, causing a gradual increase in the temperature of the carbon bed, such that the BTX components are released to the off-gases. This means that most of the BTX is released in a very short time period, as the propagating steam condensation front reaches the opposite side of the bed under regeneration.

As a consequence of the substantial quantity of BTX that is removed and the intermittent release of the individual species, a stability problem arises in the combustor. The released fuel will consume all the available oxygen, creating a large increase of combustion air required, which the operating system attempts to handle. When most of the BTX is released from the bed under regeneration, the

steam tends to cool the postcombustion, which converts unburnt fuel in the flue gas. Currently, this is controlled by the combustion of part of the product gas in the postcombustor during regeneration, which can be dynamically controlled to compensate for the rapid pulse of BTX. However, in this case, there is efficiency penalty in the order of 5–10 percentage points. As the regeneration is intermittent this also cause undesired variations throughout the hole process chain.

To resolve this issue, the steam and BTX components from the regeneration can be condensed instead of the mixture being sent to the postcombustor. By doing so, the BTX can be extracted, separated from the steam, and evenly fed into and combusted in the primary combustor chamber rather than the postcombustor, thereby creating a valuable heat source for the process. Furthermore, the significant cooling effect of the steam feed to the postcombustor can be avoided, so that the combustion of product gas is no longer required in the postcombustor. The separation also opens up the possibility for extraction and utilization of the BTX fractions as green aromatics sold as a product from the plant.

The designed regeneration strategy limits the regeneration temperature of the active carbon to 160°C (320°F), which means that the active carbon will not be fully regenerated, and this reduces the capacity of the carbon beds. To avoid a further reduction of the capacity due to components that are larger than naphthalene entering the bulk adsorbers and not being removed adequately via regeneration, the preadsorber is replaced in intervals. The duration of operation of the preadsorber is based on the product gas flow, the tar levels in the gas (which at GoBiGas depend on the performance of the RME-scrubber), and the temperature and pressure of the product gas.

At present, the preadsorber needs to be replaced every 2.5 months of full operation, and the used carbon is sent as waste for incineration. However, the removed active carbon can more or less be fully regenerated, if it is regenerated at a higher temperature, that is, 400°–500°C (750°–930°F). Therefore, if beds with active carbon are chosen for the removal of BTX in a larger plant it is recommended to include an external high-temperature regeneration step for the recovery of spent active carbon, or to optimize the tar removal prior to the carbon beds, so as to decrease the levels of components that are larger than naphthalene (see *Cooling and cleaning of the product gas*), and, thereby, the need to replace the activated carbon.

The active carbon beds actually exhibit the desired functionality, although due to some design errors, the capacities of the carbon beds in the present installation are too small. As the active coal bed system represents a complex and expensive installation, intensive efforts have been made to optimize the system beyond the design specifications. This has gradually allowed increases in the gas throughput, without compromising the gas quality. Presently, 93% of the design capacity of the plant is reached, and there are further suggestions as to how the capacity can be increased to allow the plant to reach full capacity.

The overall experience with the carbon beds is that it would be beneficial to cool the gas entering the active carbon beds to <30°C (86°F), to condense out more of the water and the remaining hydrocarbons in the product gas. Lower temperature will additionally result in an increase of the loading capacity of the activated carbon. Furthermore, a redesign of the process so as to incorporate a separate unit that would remove the BTX while operating at around 10°C (50°F) should be considered. This would create a smaller active carbon bed system that has the function of a guard bed rather than that of a temperature-swing adsorption system. In this context, the breakthrough of using coated heat exchangers is crucial, as it can reduce the temperature to the desired level in a cost- and energy-efficient way.

Material consumption and waste streams during operation of the GoBiGas plant

The material consumption and waste streams during operation are vital, as they affect the production costs of the plant. The levels of consumption of the different materials used at the GoBiGas plant during start-up and stable operation are summarized in Table 3. It takes about 32 h to heat up the process before the fuel can be fed into the gasifier, and it takes about 24 h for the gasifier to reach stable operation. Once stable operation of the gasifier has been established, methanization can be started, which takes an additional 60–80 h, and during this time the product gas must be flared. To ensure economic viability, the start-up time of the process makes it crucial to avoid starts and stops, meaning that efforts have to be made to attain high availability for the process.

For a new plant or the redesign of an existing plant, several improvements can be made to reduce the level of consumables, with the major improvements (details of which can be found in the sections above) being:

- the condensation of the regeneration steam and BTX components from the carbon beds, which would lower the heat demand of the gasifier and increase the efficiency;
- the feeding of solid fuel to the combustion side of the gasifier, which would reduce the need for natural gas during start-up;

Table 3. Summary of the consumables used during the start-up and during stable operation of the GoBiGas plant when operated at 80% of capacity.

Consumable	Unit	Start-up	Stable operation
Wood pellets	tonnes/h	0	6.2
Natural gas	m_n^3/h	450	100
Nitrogen	m_n^3/h	608	4
Olivine	kg/h	0	65
Rapeseed methyl ester (RME)	kg/h	0	70
Calcine	tonnes/h	1	0.11
Potassium carbonate solution	l/h	5	5
Ash	tonnes/h	0	0.3
Electricity	MW	1	2
Active carbon	kg/h	0	2.7
Waste water	m_n^3/h	0.7	0

- the introduction of an ash-rich fuel, such as bark or forest residues, which would eliminate the need for potassium carbonate supplementation;
- the introduction of coated heat exchangers, which would remove or minimize the need for RME;
- the introduction of a steam cycle, which would allow production of the electricity internally in the process; and
- the on-site, high-temperature regeneration of active carbon, which would minimize the need for replacement by at least a factor of 10.

Introduction of the Technology into the Existing Infrastructure

The GoBiGas demonstration plant and the research gasifier at Chalmers, together with the plants in Güssing, Oberwart, and Senden have contributed to establishing a comprehensive strategy for the design and control of biomass gasification for the production of advanced biofuels based on a variety of biomass sources. Collectively, they show how one can handle these types of processes during start-up and disturbances, which cause low availability and failures in many demonstration and pilot projects around the world. Here, it can be mentioned that the plant in Senden has reached an availability level of more than 6000 h/year, and with recent modifications taken forward in collaboration with the Technical University of Vienna, availability for 8000 h/year seems to be reachable.

A vital insight from the research summarized in this paper is that the ash components of the biomass itself, which are often considered as agents that make biomass problematic as a fuel, are instead the solution to some of the problems. Furthermore, experience from both the demonstration plant and the research gasifier shows that the basic layout and temperature levels of a combustion reactor (including the convection path and filter) in a conventional fluidized bed setup designed for wet biomass corresponds to the desired design of a biomass gasifier. This means that a DFB gasifier can be constructed from two regular fluidized bed boilers placed next to each other, thereby providing a process that can be operated as a DFB gasifier or two parallel boilers (one CFB and one BFB) for biomass or waste.

The principal integration scheme for this type of system is shown in Figure 15, where the CFB system is a schematic of the Valmet boiler shown in Figure 2, complemented with a flue gas condenser. Starting from the CFB boiler, the recirculation of the bed material separated in the cyclone is directed to the BFB boiler instead of directly back to the combustion chamber (as is the case when the CFB boiler is operated as a boiler rather than as one of the interconnected reactors in a DFB gasifier). This flexibility can be ensured by the introduction of a particle distributor, as demonstrated in the Chalmers research gasifier (item 9 in Figure 16). The functionality is as follows: the pipe to the loop seal connecting the CFB boiler with the BFB boiler is located at a lower position than the pipe that is connected to the combustor. In the absence of fluidization in the loop seal, there is no flow of solids through the seal, which means that they build up the bed level in the distributor until it starts to flow back to the CFB instead. If the seal is fluidized the solid flow will go through the seal, thereby adjusting the bed level in the distributor below the height of the pipe to the CFB and directing the entire solid flow to the BFB reactor. To return the solid material to the CFB reactor from the BFB, there is a second loop seal, through which the solid material enters via a weir, whereby turning on or off the fluidization in the two seals controls the flow between the reactors, as further described elsewhere [60]. With this design, the CFB and the BFB systems can be operated as two separate boilers or as a DFB gasifier.

To operate the BFB reactor as a gasifier, the fuel has to be dried (as discussed above in *Description of and Results from the Technical Demonstrations*) and the combustion air needs to be replaced by steam. Furthermore, the circulation of the coarser fines, which in a regular fluidized bed boiler would be returned to the combustion chamber, should be redirected from the CFB reactor to the BFB reactor. From the BFB reactor, all flows of fines (both the coarser fines that in the boiler mode are returned back to the boiler and the finer fractions that are sent to the ash bin) should in gasification mode be redirected to the CFB reactor. This ensures the recirculation of ash components that control the chemical activity, as

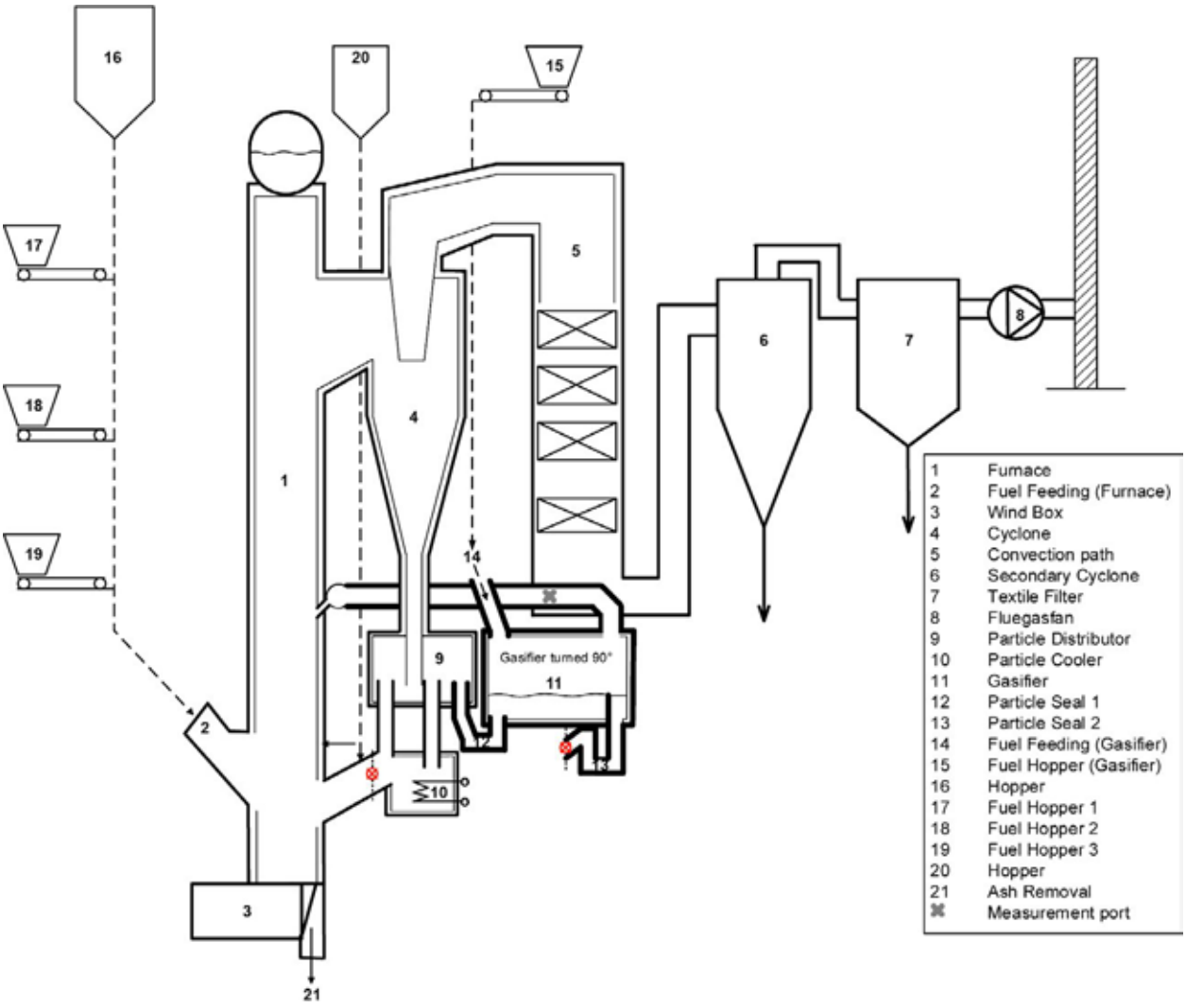

Figure 16. The Chalmers 12-MWth boiler – a 2–4-MWth gasification system.

well as the full conversion of the converted particles of char and soot, as well as tars that are captured in the filter cake. Furthermore, waste streams from the downstream cleaning steps will be directed to the CFB reactor for destruction, which in Figure 15 is depicted as the polyaromatics being separated from the product gas stream in the condenser.

Based on the closure of the heat and mass balance of the GoBiGas demonstration plant [3], it is concluded that for a stand-alone DFB gasifier there is an optimum size relationship between the CFB and the BFB boiler. As role of thumb, a CFB boiler of one energy unit of fuel input and a BFB-boiler of two energy units of fuel input can be combined to a DFB gasifier of up to eight energy units of fuel input. However, this number will be typically between 5 and 8, where the upper number relate to a plant that is fully optimized toward gasification and the lower number to a plant with, more or less, full flexibility to be used as one gasifier or two parallel boilers.

Fluidized bed boilers in district heating networks or bark boilers in pulp mills are typically operated at an annual rate corresponding to 1500–3000 full-load hours (the annual delivered energy in MWh divided by the full load capacity in MW). This corresponds to load factors of 17– 35%, when operated as a boiler. Considering these boilers potential as DFB gasifiers both the time of operation and ability as fuel converters would increase. The goal for the operation of a gasifier for advances biofuel production will be around 8000 h per year, which also was one of the initial goals of the GoBiGas plant, and be independent of other system needs, for example district heating. The potential as fuel converter will, as explained above, increase with 8/3 when converting from a combustion to a gasification system, which also imply that the

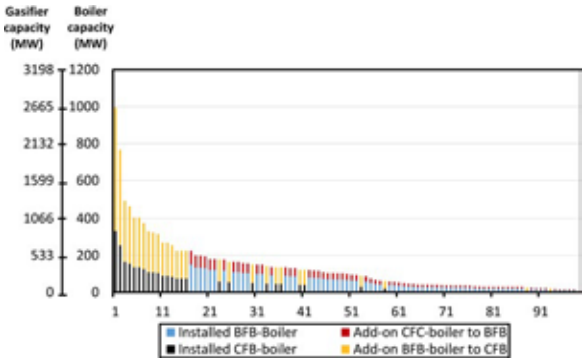

Figure 17. Existing installed capacity of fluidized bed boilers in the Swedish energy system and the corresponding additional boiler sizes needed to realize their conversion to dual fluidized bed gasifiers, Data provided by Christer Gustavsson.

system is complemented with a second boiler. Thus, converting such a boiler to an optimized DFB gasifier can increase the utilization of the plant by 700–1500%.

Thus, the presented process provides a technology that can gradually transform existing infrastructures, such as district heating networks, pulp and paper mills, and saw mills. The production processes in these units can also yield a renewable feedstock for oil refineries and petrochemical industries, as well as enable large quantities of intermittent electricity to be stored as fuel/products (further described in *Electrification and use of intermittent electricity within the process*). Such a transformation of the energy system is in line with the scenario presented in the *Introduction*, in which the most valuable assets are the existing sites and the surrounding infrastructures.

Within these assets, environmental permits are in place and the land is already exploited for this type of activity, which is a value that is hard to assess. Considering that many of the locations are situated at, or close to, the coastline or near water, it is difficult to envisage new claims for virgin land for this type of industrial production. If such new claims were needed, the costs would most likely be significantly higher for the land than for the equipment that is going to be installed, and very long political and legal processes would be required to secure the required permits. The conclusion from this is that the only feasible way to transform the energy system within the timeframe proposed by the Paris agreement is to make the transformation at sites that are currently being utilized by process or energy industries.

Incorporation into the existing district heating infrastructure

In Sweden and Finland, the main application for fluidized bed boilers is for district heating and in the pulp and paper industry, and in Figure 17, the fluidized boilers currently installed in the Swedish energy system are visualized, together with the types and sizes of boilers with which they need to be combined to realize their full potential as DFB gasifiers. In summarizing the potential, it is clear that to the 6400-MWth (1200 MMBtu/h) installed boilers one needs to add 6800 MWth (1275 MMBtu/h) of boiler capacity to create a gasification potential of 35,000 MW (6550 MMBtu/h). With an assumed annual operation of 8000 h, this correspond to a fuel demand of 280 TWh of biomass (59 million dry tonnes of biomass per year), which can produce between 170 TWh and 200 TWh (14.6–17.2 MTOE) of advanced biofuels or materials. This corresponds to a potential production that is 5-times greater than the Swedish target for biofuel production in a fossil-free nation in Year 2045. However, due to logistic problems, it will for most locations not be feasible to have units with fuel inputs >500 MW (2500 dry tonnes of biomass/day), which reduces the potential by around 30%, decreasing the annual potential fuel demand to around 200 TWh (42 million dry tonnes of biomass). This is, nevertheless, a substantial demand for fuel and corresponds to the total forest growth in Sweden, implying that there will need to import biomass if this is to be realized.

In terms of the required level of investment, retrofitting an existing boiler from district heating or the combined production of electricity and district heating to a gasifier with full downstream synthesis would reduce the cost of the investment by 10–20% compared to a new stand-alone plant. This estimation is based on the projected cost for an n^{th} commercial plant with full synthesis process extrapolated from the costs of the different process units in the GoBiGas plant with available scaling factors [3]. Note that this estimate does not include the potential savings linked to permits and land use.

Incorporation into existing pulp, paper, and saw mills

The integration of biomass/waste gasification with the downstream extraction of hydrogen or synthesis of hydrocarbons for the production of fuels, chemicals, and materials in the forest industry (pulp or saw mill) can be carried out in a stepwise manner using the dual bed gasification technology.

The first step is to change the bark boiler to a fluidized bed of suitable size. Here, a bubbling bed is the most likely system to be used to produce steam for the mill. The second step is to connect the bubbling bed to a circulating bed, transform the BFB boiler to a gasifier, and introduce a primary dryer that reduces the moisture content of the fuel in the process to <30%. The outcome

is a system that provides the mill with steam and a combustible gas with a high heating value, which can be used in, for example, a lime kiln.

The next step is to select the end-products and an appropriate synthesis process. This step also includes a secondary dryer, which decreases the moisture content to well below 10%. This step requires large additional investments, whereas the previous steps in the development can more or less be part of the continuous upgrading of the mill and can be operated independently, regardless of whether the mill decides to produce the refined end-products or not. Therefore, the investment decision for the synthesis or the hydrogen separation process can wait until the dual bed system has proven its performance and the markets for the produced end-products are assured.

Incorporation into existing oil refineries and petrochemical industries

To introduce the production of advanced biofuels, chemicals, and materials into an oil refinery or petrochemical industry that currently lacks both a biomass boiler infrastructure and established logistics for using biomass as fuel, requires a novel strategy for applying the technology. In both these types of industries, there is a large steam demand that is currently covered by combusting the gases that emanate from the internal distillation or conversion process. As the compositions of the gases burned in present processes to cover the heat demand are similar to those of the gases that are produced in a biomass gasifier, they can be upgraded to a syngas and further synthesized to desired hydrocarbons or extracted as hydrogen.

For these processes, it would be a natural first step to incorporate a biomass boiler for part of the steam production. In this way, the synthesis process for the intended system could be put into operation using the excess gases already produced within the industry, where the heat demand is covered by intensified heat integration and the combustion of biomass. This integration also provides the opportunities to increase gradually the demand for biomass and to build up the logistic infrastructure needed to receive biomass at the plant by starting with the installation of a CFB boiler. With a CFB that initially can be operated at 30% of maximum capacity, which correspond to just 4% of the final DFB gasifier capacity, the level of biomass utilization on-site can be gradually increased.

When the supply chain is able to provide biomass/waste corresponding to 80–90% of the capacity of the CFB boiler, the BFB boiler can be constructed, and the biomass could once more be increased at the same time as more and more process internal gas is made available for the synthesis process. Once 80–90% of the combustion capacity of the two boilers is reached, it is time to connect the boilers to each other and to build a primary biomass dryer, which reduce the moisture content of the ingoing fuel from the initial 50% to 20–30%.

This will increase the conversion capacity of the biomass and, thereby, the production of both steam and gas from the unit. The produced gas can initially be burned in the steam boilers that were originally used to combust the internal gas, bringing the fuel capacity of the DFB gasification system up to 50–60% of the final need. The next steps are as follows: to introduce a second dryer that reduces the moisture content to 3–10%; to clean the gas of BTX; and to compress the gas to the pressure required for the synthesis process. At this stage, all the gas produced from the biomass/waste is going to the production of advanced biofuels, and the refinery or petrochemical industry goes back to using the internally produced gas of fossil origin to produce the steam needed for their processes.

Electrification and use of intermittent electricity within the process

As previously described, in a future energy system, the carbon atoms accumulated through photosynthesis will become a valuable resource, which means that as much carbon as possible needs to be converted to products. In the present process, around 50% of the carbon is released from the process as carbon dioxide. The majority of this comes from the CO_2 separation step in the synthesis process, and this reflects the composition of the biomass, which for woody biomass normalized to the carbon atom typically is $CH_{1.44}O_{0.66}$. This means that there is an excess of oxygen atoms that need to be removed as either carbon dioxide ($0.67\ CH_{2.15} + 0.33\ CO_2$) or as water ($CH_{0.12} + 0.66\ H_2O$).

For most hydrocarbons, such as alkenes and alkanes, the H/C-ratio is around 2. The H/C ratio for aromatics ranges between 0.8 and 1, and for methane it is 4. For the production of methane (as in the GoBiGas demonstration plant), the right balance is achieved by inherent chemical splitting of water by the water gas reaction and, thereby, providing more hydrogen to the hydrocarbon molecule, while at the same time removing some more carbon as CO_2. To be able to convert all the carbon in the biomass to hydrocarbons, there is a need to split water outside the process, through for example, renewable electricity using electrolysis, and to provide pure hydrogen to the gas produced from the biomass in the DFB gasifier. By doing so, the oxygen in the biomass is removed from the downstream synthesis process as water instead

of carbon dioxide, while at the same time there is external production of pure oxygen.

Therefore, this method can be used to store renewable electrical energy in the form of hydrocarbons, whereby all the carbon can be converted into methane if one provides 1.94 H_2 per carbon atom in the biomass (1.94 H_2 + 0.67 $CH_{2.15}$ + 0.33 CO_2 => CH_4 + 0.66 H_2O). When producing methane, the stored energy in the methane can be as high as 173% of the chemically stored energy of the ingoing biomass. For alkene production, the corresponding ratio is 0.94 H_2 per carbon atom in the biomass (0.94 H_2 + 0.67 $CH_{2.15}$ + 0.33 CO_2 => ½ C_2H_4 + 0.66 H_2O), and the energy stored in the alkenes corresponds to 139% of the energy of the ingoing biomass. The energy in the electricity supplied for the water splitting comprises the energy of the vaporization of the water (14%), chemically bound energy (61%), and heat losses (25%). This means that around 60% of the electrical energy is converted to chemical energy in the generated end products.

The use of electrolysis to increase the yield from the process entails a significant additional investment and this should be seen as a second step in the electrification of the process. A rough estimate is that large electrolysis processes at the present costs will be of interest if the mean cost for electricity for a major part of the year is half of that of the ingoing fuel, biomass or waste. Given the uncertainties concerning both the future evolution of electricity generation and the cost structure for biomass and waste, investors might be held back due to not seeing a solid business case.

A more straightforward method to introduce electricity into the process is to install electrical heaters to replace the fuel that is burned, so as to produce the heat in the process. This entails a much lower level of investment, and the marginal energy efficiency from electricity to product would be close to 100%, as direct heating with electricity implies that all the introduced energy is converted to heat, while heat generation that originates from combustion will introduce flue gas losses, together with other mechanical losses, example, a primary air fan [45]. Thus, installation of direct heating could increase the production and will be economically beneficial if the cost of the electricity is similar to or lower than the biomass or waste fuel for an extended period of the year. The feasible level of direct heating that could be applied would, however, be lower than that of the theoretical scenario, as combustion also serves other needs for the process, such as achieving 100% fuel conversion, the destruction of slipstreams from the synthesis process, and the regeneration of the catalytic process.

Based on the hydrogen and heat demands of the conversion process [3], the electricity demand in relation to the energy in the biomass used for pure methane production would be in the range of 1.4–1.6, and for alkenes it would be in the range of 0.7–0.9. Building on the example above in regard to the potential for retrofitting fluidized bed boilers in the Swedish energy system (Sweden has 10 million inhabitants, 0.13% of the world population), which has a potential for gasification of 200 TWh biomass annually, an additional 180–300 TWh electricity could be stored through DFB gasification. This corresponds to 120–200% of the present annual electricity production in Sweden.

If the goal is to utilize essentially 100% of the carbon, the introduction of hydrogen and electrical heating will not be sufficient, as there will be a small amount of CO_2 leaving with the flue gases. In such a carbon-optimized case, the CO_2 may need to be separated from the flue gases in an amine scrubber, which could be integrated with the CO_2 cleaning in the synthesis process, and the heat integration could be integrated with the electrolyzer for the reboiling of the amine (see Figure 18). However, this is an extreme scenario which implies that the carbon atoms in the biomass are much more valuable than the energy, and the cost for electricity is in relation to the biomass more or less negligible. During such circumstances, there is no need to optimize the process toward energy and it would most likely be more cost effective to burn the biomass/waste with the pure oxygen from the electrolyser to produce a pure carbon dioxide in a relatively simple combustion unit compared to the complex gasification process described in this paper. The carbon dioxide can thereafter be synthesized together with hydrogen to the desired hydrocarbon. For the production of alkenes from 50% moist biomass, the involved reactions can be summarized as follows:

Combustion: $CH_{1.44}O_{0.66}$ + 1.33 H_2O (moisture) + 1.06 O_2 => CO_2 + 2.05 H_2O;

Electrolysis: $3H_2O$ + electricity => $3H_2$ + 1.5 O_2;

Synthesis: CO_2 + $3H_2$ => CH_2 + $2H_2O$,

where the combined reaction would be the same independently if applying a combustor or a gasifier for the initial thermal conversion of the biomass and could be written as $CH_{1.44}O_{0.66}$ + 1.33 H_2O (moisture) + electricity => CH_2 + 1.05 H_2O + 0.94 O_2.

However, taking the combustion path would require around twice as much electrical energy.

In summary, advanced biofuels, chemicals, and materials can be produced in large amounts through this process. As an example, a maximum level of production of methane of 346 TWh by retrofitting fluidized bed boilers in Sweden alone, corresponding to 32 bcm of natural gas, could be achieved, and this can be compared with the

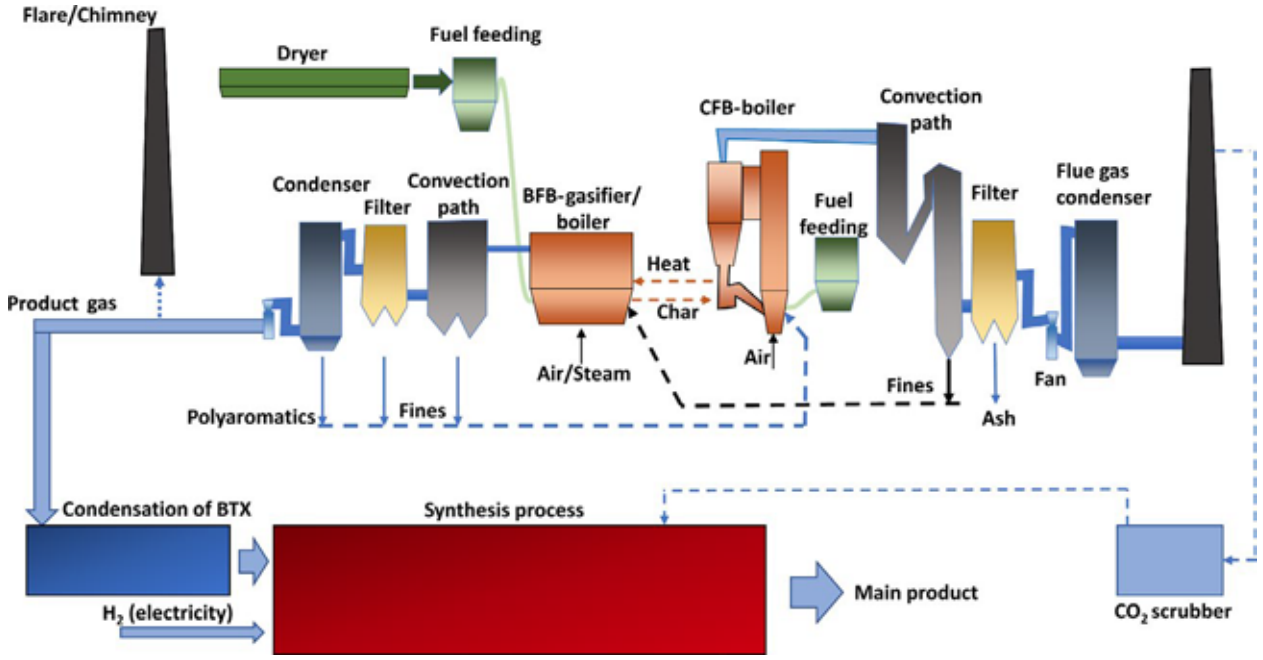

Figure 18. Process layout for a process with close to 100% carbon utilization.

world consumption (2013) of 3350 bcm of natural gas. Alternatively, one could achieve a maximum production level of alkenes of 278 TWh, which corresponds to approximately 23 million tonnes of alkanes, and this can be compared with world consumption (2014) of jet fuel alkanes of 225 million tonnes. These examples show the potential for producing substantial quantities of renewable fuels, chemicals, and materials through application of the technology presented in this paper and within the existing infrastructure.

Conclusions

The experience gathered from the first-of-its-kind demonstration project, GoBiGas, in combination with experimental results obtained from experiments in the Chalmers gasifier have augmented our knowledge on how to control the gas quality and how to design a gasification process such that problems related to fouling on heat exchangers for medium-temperature gasification of biomass can be avoided. The key roles are played by alkali and earth alkali metals (mainly potassium), which come naturally with the biomass ash and previously have been regarded as components that make biomass a problematic fuel in highly efficient thermal processes. Here, we show instead that in combination with specific bed materials and balanced by sulfur and calcium, potassium catalyzes the conversion process to produce a gas from the gasifier that is of sufficient quality to avoid downstream problems. Furthermore, we show how coated heat exchangers can be used to condense out the steam and hydrocarbons after the gas is cleaned of particles, allowing significant simplification of the gasification process.

Together with new insights on fuel feeding and reactor design, presented in this paper, these solutions form the basis for a comprehensive process layout that can be used to transform fluidized boilers into fluidized bed gasifiers. This route represents an example of how biomass conversion can develop and be integrated with existing industrial and energy infrastructures to form highly effective systems that can deliver a wide range of products. By retrofitting existing district heat, pulp, paper, and saw mills, as well as oil refineries and petrochemical industries, renewable fuels, chemicals and materials can be produced from biomass and waste at increasing scale. To illustrate the potential, transforming existing fluidized bed boilers in the Swedish energy system alone would allow the production of jet fuels corresponding to 10% of the present world consumption.

Acknowledgments

This work was supported by the Swedish Gasification Center (SFC) (project number 34721-3) and was conducted within the BioProGReSs project, which has received funding from the European Union's Seventh Framework Program for Research, Technological Development and Demonstration under grant agreement 321477. Financial

support from the Swedish Energy Agency (project number 42206-1) and the European Union's Horizon 2020 Research and Innovation Program through the ADVANCEFUEL project (grant agreement 764799) are also gratefully acknowledged. The authors thank Dr. Dario Maggiolo for his assistance in the evaluation of the coated heat exchanger plates. Furthermore, the work was supported by Akademiska Hus AB, Alfa Laval AB, E.ON, Göteborg Energi AB, and Valmet Power AB.

Conflict of Interest

None declared.

References

1. Slade, R., A. Bauen, and R. Gross. 2014. Global bioenergy resources. Nat. Clim. Chang. 4:99–105.
2. Creutzig, F., N. H. Ravindranath, G. Berndes, S. Bolwig, R. Bright, F. Cherubini et al. 2015. Bioenergy and climate change mitigation: an assessment. GCB Bioenergy 7:916–944.
3. Hedenskog, M. 2015. The GoBiGas Project: Bio-Methane from Forest Residues – from Vision to Reality. Presentation at SVEBIO2015.
4. Alamia, A., A. Larsson, C. Breitholtz, and H. Thunman. 2017. Performance of large-scale biomass gasifiers in a biorefinery, a state-of-the-art reference. Int. J. Energy Res. 41:2001–2019.
5. Larsson, A., M. Hedenskog, and H. Thunman. 2015. Monitoring the bed material activation in the GoBiGas-Gasifier. *in* Nordic Flame days.
6. Rauch, R., H. Hofbauer, K. Bosch, I. Siefert, C. Aichernig, K. Voigtlaender et al. 2004. Steam gasification of biomass at CHP plant Guessing-Status of the demonstration plant.
7. Pfeifer, C., S. Koppatz, and H. Hofbauer. 2011. Steam gasification of various feedstocks at a dual fluidised bed gasifier: impacts of operation conditions and bed materials. Biomass Convers. Biorefin. 1:39–53.
8. Kotik, J. 2010. Über den Einsatz von Kraft-Wärme-Kopplungsanlagen auf basis der wirbelschicht-dampfvergasung fester biomasse am beispiel des biomassekraftwerks oberwart. Vienna University of Technology, Vienna (in German).
9. Suda, T., Z. Liu, M. Takafuji, K. Hamada, and H. Tani. 2012. Gasification of lignite coal and biomass using twin IHI Gasifier (TIGAR®).
10. Paethanom, A. 2016. Twin IHI Gasifier (TIGAR®) – current status of Indonesian demonstration project and its business plan. *in* Gasification and Syngas Technologies Conference. Vancouver, BC.
11. Alamia, A., S. Òsk Gardarsdòttir, A. Larsson, F. Normann, and H. Thunman. 2017. Efficiency comparison of large-scale standalone, centralized, and distributed thermochemical biorefineries. Energy Technol. 5:1435–1448.
12. Tchoffor, P. A., K. O. Davidsson, and H. Thunman. 2013. Transformation and release of potassium, chlorine, and sulfur from wheat straw under conditions relevant to dual fluidized bed gasification. Energy Fuels 27:7510–7520.
13. Marinkovic, J., H. Thunman, P. Knutsson, and M. Seemann. 2015. Characteristics of olivine as a bed material in an indirect biomass gasifier. Chem. Eng. J. 279:555–566.
14. Nahas, N. 1983. Exxon catalytic coal gasification process: fundamentals to flowsheets. Fuel 62:239–241.
15. Biomass product gas reforming solutions. Available at http://bioprogress.se/
16. EUR-Lex. 2011. COMMISSION REGULATION (EU) No 142/2011.
17. Larsson, A., M Seemann, D Neves, and H Thunman. 2013. Evaluation of performance of industrial-scale dual fluidized bed gasifiers using the Chalmers 2–4-MWth gasifier. Energy Fuels 27:6665–6680.
18. Israelsson, M., M. Seemann, and H. Thunman. 2013. Assessment of the solid-phase adsorption method for sampling biomass-derived tar in industrial environments. Energy Fuels 27:7569–7578.
19. Israelsson, M., A. Larsson, and H. Thunman. 2014. Online measurement of elemental yields, oxygen transport, condensable compounds, and heating values in gasification systems. Energy Fuels 28:5892–5901.
20. Israelsson, M., T. Berdugo Vilches, and H. Thunman. 2015. Conversion of condensable hydrocarbons in a dual fluidized bed biomass gasifier. Energy Fuels 29:6465–6475.
21. Johnsson, F. L., and B. Leckner. 1995. Vertical distribution of solids in a CFB-furnace. *in* 13. International Conference on Fluidized-bed Combustion. Orlando, FL (United States).
22. Berdugo Vilches, T., J. Marinkovic, M. Seemann, and H. Thunman. 2016. Comparing active bed materials in a dual fluidized bed biomass gasifier: olivine, bauxite, quartz-sand, and ilmenite. Energy Fuels 30:4848–4857.
23. Lancee, R. J., A. I. Dugulan, P. C. Thüne, H. J. Veringa, J. W. Niemantsverdriet, and H. O. Fredriksson. 2014. Chemical looping capabilities of olivine, used as a catalyst in indirect biomass gasification. Appl. Catal. B 145:216–222.
24. Berguerand, N., and T. Berdugo Vilches. 2017. Alkali-Feldspar as a catalyst for biomass gasification in a 2-MW indirect gasifier. Energy Fuels 31:1583–1592.
25. Rauch, R., C. Pfeifer, K. Bosch, H. Hofbauer, D. Swierczynski, C. Courson, and A. Kiennemann. 2004. Comparison of different olivines for biomass steam

gasification, 6th International Conference on Science in Thermal and Chemical Biomass Conversion, Victoria, Canada, August 2004.
26. Marinkovic, J. 2016. Choice of bed material: a critical parameter in the optimization of dual fluidized bed systems. Chalmers University of Technology, Gothenburg.
27. Sun, R., N. Zobel, Y. Neubauer, C. C. Chavez, and F. Behrendt. 2010. Analysis of gas-phase polycyclic aromatic hydrocarbon mixtures by laser-induced fluorescence. Opt. Lasers Eng. 48:1231–1237.
28. Edinger, P., J. Schneebeli, R. P. Struis, S. M. Biollaz, and C. Ludwig. 2016. On-line liquid quench sampling and UV–Vis spectroscopy for tar measurements in wood gasification process gases. Fuel 184:59–68.
29. Leffler, T., C. Brackmann, M. Aldén, and Z. Li. 2017. Laser-induced photofragmentation fluorescence imaging of alkali compounds in flames. Appl. Spectrosc. 71:1289–1299.
30. Qu, Z., E. Steinvall, R. Ghorbani, and F. M. Schmidt. 2016. Tunable diode laser atomic absorption spectroscopy for detection of potassium under optically thick conditions. Anal. Chem. 88:3754–3760.
31. Davidsson, K. O., K. Engvall, M. Hagström, J. G. Korsgren, B. Lönn, and J. B. Pettersson. 2002. A surface ionization instrument for on-line measurements of alkali metal components in combustion: instrument description and applications. Energy Fuels 16:1369–1377.
32. Wellinger, M., S. Biollaz, J. Wochele, and C. Ludwig. 2011. Sampling and online analysis of alkalis in thermal process gases with a novel surface ionization detector. Energy Fuels 25:4163–4171.
33. Tran, K. Q., K. Iisa, M. Hagström, B. M. Steenari, O. Lindqvist, and J. B. Pettersson. 2004. On the application of surface ionization detector for the study of alkali capture by kaolin in a fixed bed reactor. Fuel 83:807–812.
34. Pissot, S., T. Berdugo Vilches, H. Thunman, and M. Seemann. 2017. Recirculation of reactive fines – an optimization strategy for existing dual fluidized bed gasification Systems. *in* European Biomass Conference & Exhibition. ETA-Florence Renewable Energies, Stockholm.
35. Kirnbauer, F., M. Koch, R. Koch, C. Aichernig, and H. Hofbauer. 2013. Behavior of inorganic matter in a dual fluidized steam gasification plant. Energy Fuels 27:3316–3331.
36. Marinkovic, J., M. Seemann, G. L. Schwebel, and H. Thunman. 2016. Impact of biomass ash-bauxite bed interactions on an indirect biomass gasifier. Energy Fuels 30:4044–4052.
37. Müller-Steinhagen, H., M. R. Malayeri, and A. P. Watkinson. 2005. Fouling of heat exchangers-new approaches to solve an old problem. Heat Transfer Eng. 26:1–4.
38. Müller-Steinhagen, H., M. R. Malayeri, and A. P. Watkinson. 2011. Heat exchanger fouling: mitigation and cleaning strategies. Heat Transfer Eng. 32:189–196.
39. Zettler, H. U., M. Wei, Q. Zhao, and H. Müller-Steinhagen. 2005. Influence of surface properties and characteristics on fouling in plate heat exchangers. Heat Transfer Eng. 26:3–17.
40. Thulukkanam, K. 2013. Heat exchanger design handbook, 2nd ed. CRC Press, Boca Raton, FL.
41. Blossey, R. 2003. Self-cleaning surfaces – virtual realities. Nat. Mater. 2:301–306.
42. Bhushan, B., and Y. C. Jung. 2011. Natural and biomimetic artificial surfaces for superhydrophobicity, self-cleaning, low adhesion, and drag reduction. Prog. Mater Sci. 56:1–108.
43. Ho, T. A., D. V. Papavassiliou, L. L. Lee, and A. Striolo. 2011. Liquid water can slip on a hydrophilic surface. Proc. Natl Acad. Sci. USA 108:16170–16175.
44. Jaeger, R., J. Ren, Y. Xie, S. Sundararajan, M. G. Olsen, and B. Ganapathysubramanian. 2012. Nanoscale surface roughness affects low Reynolds number flow: experiments and modeling. Appl. Phys. Lett. 101:184102.
45. Alamia, A., A. Larsson, C. Breitholtz, and H. Thunman. 2017. Performance of large-scale biomass gasifiers in a biorefinery, a state-of-the-art reference. Wiley-VCH, Weinheim.
46. Aronsson, J., D. Pallarès, and A. Lyngfelt. 2017. Modeling and scale analysis of gaseous fuel reactors in chemical looping combustion systems. Particuology 35:31–41.
47. Whitehead, A. B. 1971. Some problems in large-scale fluidized beds. Pp. 781–811 *in* J. F. Davidson and D. Harrison, eds. Fluidization. Academic Press, London.
48. Berdugo Vilches, T., J. Maric, P. Knudsson, D. C. Rosenfeld, H. Thunman, and M. Seemann. 2017. Bed material as a catalyst for char gasification: the case of ash-coated olivine. Fuel.
49. Larsson, A. 2014. Fuel conversion in a dual fluidized bed gasifier. Chalmers University of Technology, Gothenburg.
50. Leckner, B. Personal communication Prof. Emeritus Bo Leckner (resaech leader) and Per Löveryd (manager of the operation of the boiler).
51. Bruni, G., R. Solimene, A. Marzocchella, P. Salatino, J. G. Yates, P. Lettieri et al. 2002. Self-segregation of high-volatile fuel particles during devolatilization in a fluidized bed reactor. Powder Technol. 128:11–21.
52. Berdugo Vilches, T., and H. Thunman. 2015. Experimental investigation of volatiles–bed contact in a 2–4 MWth bubbling bed reactor of a dual fluidized bed gasifier. Energy Fuels 29:6456–6464.

53. Zhao, K., H. Thunman, D. Pallarès, and H. Ström. 2017. Control of the solids retention time by multi-staging a fluidized bed reactor. Fuel Process. Technol. 167:171–182.
54. Alamia, A. 2016. Large-scale production and use of biomethane. Chalmers University of Technology, Gothenburg.
55. Simell, P., I. Hannula, S. Tuomi, M. Nieminen, E. Kurkela, I. Hiltunen et al. 2014. Clean syngas from biomass—process development and concept assessment. Biomass Convers. Biorefin. 4:357–370.
56. González Arcos, A. V., M. Diomedi, R. Lanza, and K. Engvall. 2015. Effect of potassium electrochemical promotion in biomass-tar reforming.
57. Rostrup-Nielsen, J. R. 2002. Syngas in perspective. Catal. Today 71:243–247.
58. Landälv, I., R. Gebart, B. Marke, F. Granberg, E. Furusjö, P. Löwnertz et al. 2014. Two years experience of the BioDME project—A complete wood to wheel concept. Environ. Prog. Sustain. Energy 33:744–750.
59. Sauciuc, A., Z. Abosteif, G. Weber, A. Potetz, R. Rauch, H. Hofbauer et al. 2012. Influence of operating conditions on the performance of biomass-based Fischer-Tropsch synthesis. Biomass Convers. Biorefin. 2:253–263.
60. Larsson, A., H. Thunman, H. Ström, and S. Sasic. 2015. Experimental and numerical investigation of the dynamics of loop seals in a large-scale DFB system under hot conditions. AIChE J. 61:3580–3593.

Paper 2:

Performance of large-scale biomass gasifiers in a biorefinery, a state-of-the-art reference

INTERNATIONAL JOURNAL OF ENERGY RESEARCH

INTERNATIONAL JOURNAL OF ENERGY RESEARCH
Int. J. Energy Res. (2017)
Published online in Wiley Online Library (wileyonlinelibrary.com). DOI: 10.1002/er.3758

Performance of large-scale biomass gasifiers in a biorefinery, a state-of-the-art reference

Alberto Alamia[1,*,†], Anton Larsson[2], Claes Breitholtz[3] and Henrik Thunman[1]

[1]Department of Energy and Environment, Chalmers University of Technology, Gothenburg, Sweden
[2]Göteborg Energi AB, Gothenburg, Sweden
[3]Valmet AB, Gothenburg, Sweden

SUMMARY

The Gothenburg Biomass Gasification plant (2015) is currently the largest plant in the world producing biomethane (20 $MW_{biomethane}$) from woody biomass. We present the experimental data from the first measurement campaign and evaluate the mass and energy balances of the gasification sections at the plant. Measures improving the efficiency including the use of additives (potassium and sulfur), high-temperature pre-heating of the inlet streams, improved insulation of the reactors, drying of the biomass and introduction of electricity as a heat source (power-to-gas) are investigated with simulations. The cold gas efficiency was calculated in 71.7%LHV_{daf} using dried biomass (8% moist). The gasifier reaches high fuel conversion, with char gasification of 54%, and the fraction of the volatiles is converted to methane of 34%$_{mass}$. Because of the design, the heat losses are significant (5.2%LHV_{daf}), which affect the efficiency. The combination of potential improvements can increase the cold gas efficiency to 83.5%LHV_{daf}, which is technically feasible in a commercial plant. The experience gained from the Gothenburg Biomass Gasification plant reveals the strong potential biomass gasification at large scale. © 2017 The Authors. *International Journal of Energy Research* published by John Wiley & Sons Ltd.

KEY WORDS

biomass gasification; GoBiGas; dual fluidized bed; mass balance; power-to-gas; biomethane; SNG

Correspondence

*Alberto Alamia, Department of Energy and Environment, Chalmers University of Technology, Hörsalsvägen 7, S-412 96 Gothenburg, Sweden.

†E-mail: alamia@chalmers.se

Received 26 October 2016; Revised 21 March 2017; Accepted 26 March 2017

INTRODUCTION

Societal ambitions to create a circular economy necessitate more sustainable use of our biomass resources [1–4]. In particular, biomass residues, such as stew, bark and branches, can be converted into valuable energy products, in factories that are generally referred to as 'biorefineries'. Both thermochemical and biochemical conversion can be integrated in a biorefinery, although the latter is not particularly efficient at decomposing lignin and hemicellulose, with only thermochemical processes, involving gasification, achieving full conversion of the residues of woody biomass [2,5]. With gasification, the carbon matrix of the lignocellulose is broken down into simple molecules, such as carbon monoxide and hydrogen, which are subsequently synthesised to create high-value biofuels or chemicals. Because of its high efficiency and feedstock flexibility, gasification has been identified as a core process in any circular economy scenario [2,6], and different technologies have been tested over the past decades in several pilot plants [7,8]. However, no industrial unit intended for commercial operation has been built to date.

A first-of-its-kind demonstration plant for the gasification of forest residues on a commercial scale with full downstream synthesis to biofuel was constructed within the Gothenburg Biomass Gasification (GoBiGas) project [9] in Sweden. The GoBiGas plant is the largest plant of its kind and is the first to convert solid biomass to high-quality biomethane, for injection into the national gas grid [9]. The purpose of the GoBiGas project is to establish the performance of the commercial plant and to acquire experience towards the construction of a large-scale (>100 MW) process. For these reasons, the plant is equipped with several measurement points and control options, making the data obtained from GoBiGas the first real reference to support techno-economic analyses and

energy system modelling, both of which have been conducted over the past decades [10–14].

The plant, which is owned by Göteborg Energi (a local utility company that produces heat and power), is designed to target the following high-performance parameters: the production of 20 MW of biomethane, operation for 8000 h/year, ≥65% biomass to biomethane efficiency (η_{bCH4}) and total efficiency (biomass plus district heating) of ≥90%. The total cost to date for the project has been M€165, of which M€24 was provided as governmental support through the Swedish Energy Agency. Table I provides a summary of the investment costs for the different parts of the process, defined according to the main component, where the cost includes all the surrounding systems and equipment of the plant, including scale factors to enable estimation of the costs associated with plants of different scales.

The planning of the GoBiGas project started in May 2005, together with an ambitious research programme funded by the government and industry, which also included the building of a 2–4-MW research gasifier that was commissioned in December 2007 on the campus of Chalmers University of Technology. Construction of the GoBiGas plant started in 2011 and was completed in November 2013, requiring 300 000 man-h of engineering and 800 000 man-h of construction, with an associated labour cost of M€90. The construction of the gasification section was assigned to Valmet AB (former Metso Power), on licence from Repotec GmbH. The subsequent commissioning process took 21 months, during which several major challenges were overcome. Two major breakthroughs occurred during the commissioning phase. First, at 6 months, potassium was added to saturate and stabilise the chemistry that controls the catalytic effect, to assure the quality of the produced gas [15,16], thereby avoiding any clogging of the product gas cooler. Second, the bed height of the gasifier was lowered so that the fuel could be fed closer to the surface of the bubbling bed in the gasifier, thereby reducing the heat transfer and clogging of the fuel-feeding screw and enabling more than 1600 h of continuous operation. At the time of writing, October 2016, the plant is operational and delivers biomethane to the gas grid. Further research is needed to optimise the performance of the plant and improve the efficiency of the process. The present study focuses on establishing the mass and energy balances of the gasification section, so as to evaluate its performance and identify pathways towards optimisation, as well as on creating a reference for the techno-economic and energy system analyses.

Table I. Summary of the costs of the different parts of the process, including the estimated SF, which is defined as *C*/Cref = (*P*/Pref)SF, where *C* is the cost, *P* is the power and 'ref' indicates the values of the reference pant

Part of process	Cost (M€)	Scale factor
Gasifier section (total)	32.8	
Fuel feeding	8.25	0.62
Gasifier	11	0.80
Product gas cooler, filter and scrubber	4.5	0.79
Flue gas cleaning	8.25	0.55
Methanation section (total)	65.5	
Carbon beds	13.7	0.62
Syngas compressor	13.7	0.60
Hydrogenation and sulfur removal	7.2	0.62
Shift and pre-methanation	10	0.62
CO_2 separation	7.2	0.62
Methanation and drying	13.7	0.62
Buildings and construction (total)	21	0.40

SF, scale factor.

A schematic of the GoBiGas biomass-to-biomethane process is shown in Figure 1 (a high-resolution figure is provided in the Supporting Information), in which the plant is presented in a simplified form as two macro-sections: gasification, where the solid fuel is converted to the product gas, and methanation, where the product gas is refined to biomethane. The actual building contains 5000 m^3 of concrete; 800 t of rebar; 1300 t of structural steel; 25 km of piping; 90 km of electric cables; 130 pumps, compressors, fans and conveyers; 200 towers, reactors, heat exchangers, tanks, and vessels; 2500 instruments; and 650 valves [17]. The gasification section comprises an up-scaled version of a dual fluidised bed (DFB) gasification technology, whereby the gasifier has a capacity that is approximately twofold that of the plants in Senden [18], fourfold that of the thermal power plants in Güssing [19] and eightfold that of the gasifier at Chalmers University of Technology. The design of the GoBiGas gasifier is based on the Güssing pilot plant, rather than a downscale version of the commercial combustion units, as is the case, for example, for the gasification system at Chalmers. Nevertheless, the GoBiGas technology shares features with circulating fluidised bed combustors that have an external heat exchanger, which are commercially available at the scale of several hundreds of MW. In this analogy, the circulating bed used as the combustor in the GoBiGas gasifier corresponds to a 10-MW_{th} combustor, and the bubbling bed used as the gasifier corresponds to an external heat recovery unit of around 5 MW_{th}. Building this type of reactor system in small scale is challenging and requires several simplifications that affect efficiency. The methanation section is based on well-proven processes and technologies, which are downscaled to fit the size of the gasification section.

This paper presents the first evaluation of the GoBiGas plant that focuses on the gasification section, because the efficiency of DFB systems limits the performance of the overall biomethane production process. This study uses the results obtained in the first measurement campaign with full operation of the gasifier using wood pellets as the fuel. The evaluation is based on the process parameters extracted from the measurements and incorporated into a simulation, in which the effects of various identified improvements for a commercial-size unit are investigated. The overall scope of the present study is to assess the efficiency of the gasification section in a large-scale plant based on the experience gained from the GoBiGas demonstration plant.

Int. J. Energy Res. (2017) © 2017 The Authors. *International Journal of Energy Research* published by John Wiley & Sons Ltd.
DOI: 10.1002/er

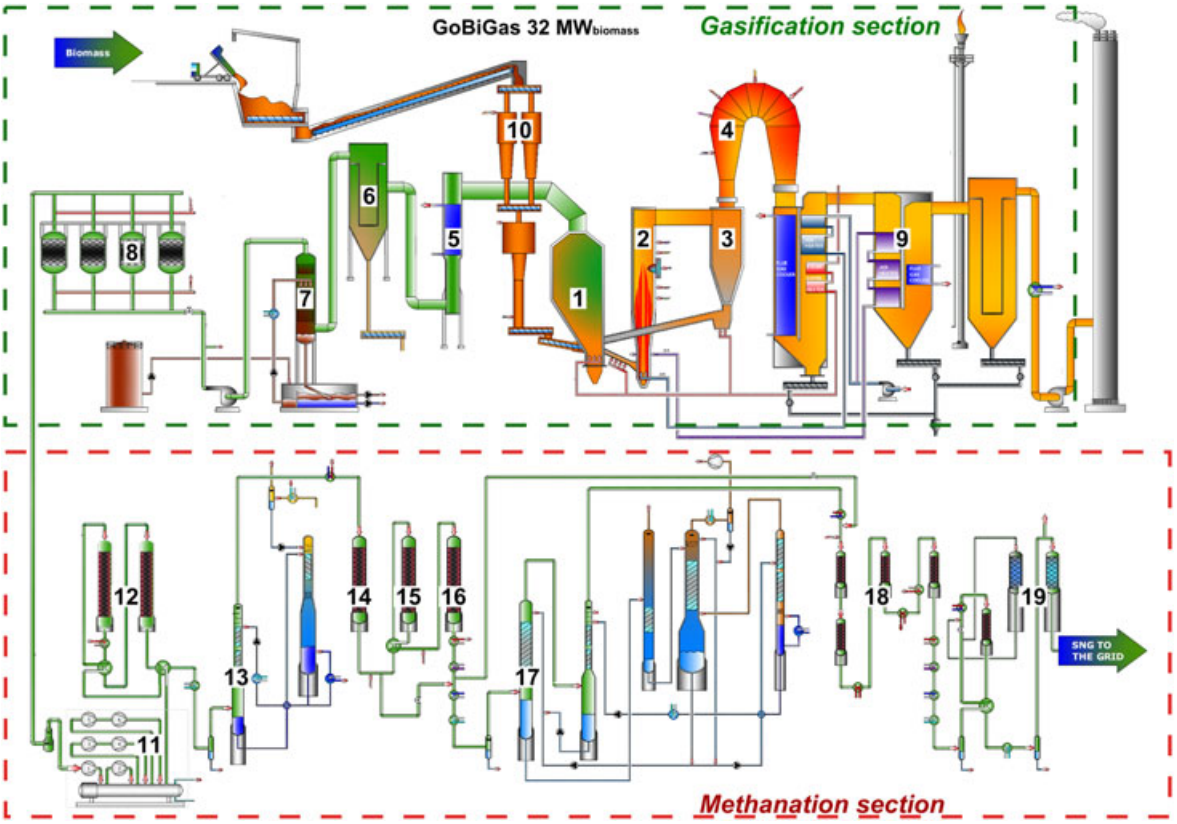

Figure 1. Process schematic of the Gothenburg Biomass Gasification (GoBiGas) biomass to biomethane plant: 1, gasifier; 2, combustion chamber; 3, cyclone; 4, post-combustion chamber; 5, raw gas cooler; 6, raw gas filter; 7, rapeseed methyl ester scrubber; 8, carbon beds; 9, flue gas train; 10, fuel feeding system; 11, product gas compressor; 12, hydration of olefins and COS; 13, H_2S removal; 14, guard bed; 15, water–gas shift reactor; 16, pre-methanation; 17, CO_2 removal, 18, methanation; and 19, drying. [Colour figure can be viewed at wileyonlinelibrary.com]

DESCRIPTION OF THE GOBIGAS PLANT

The GoBiGas plant can be operated with either wood pellets or chipped woody biomass as fuel; wood pellets were used during the commissioning of the plant. The fuel is fed to the gasification reactor (number 1, Figure 1), wherein the major part is converted into gas through devolatilization and partial gasification of the char. The remaining char is transported with the bed material to the combustor (number 2), where it is burnt to produce heat. The transportation of heat between the combustor and the gasifier is achieved through circulation of the bed material.

When biomass is gasified, numerous solid-phase and gas-phase compounds are produced. The distribution and composition of the raw gas depend on the operating conditions, as well as the catalytic activity of the bed material, ash components or additives. DFB gasifiers yield a rather high percentage of methane already in the produced raw gas (6–12% vol.) [20,21] because of the relatively low operating temperature of <900 °C. When the target product is biomethane, this is one of the major advantages of the DFB process over other gasification technologies, which are operated at higher temperatures. Because using a low temperature for the process can lead to a significant level of tar, limiting the tar yield becomes a major challenge with the DFB technique. A common approach to limiting the tar yield is to use an active bed material [21–23], thereby avoiding fouling or deactivation in the downstream equipment [24–26].

Olivine is a natural magnesium-iron-silicate ore that is commonly used as the bed material in DFB gasifiers because of its ability to reduce the yield of tar and its tendency not to agglomerate at these process temperature levels [15,23,27,28]. However, to achieve the desired catalytic behaviour, olivine needs to be activated. There are different approaches to activate olivine; the one used in the GoBiGas plant is based on the addition of potassium [15,28,29].

A continuous flow of fresh rapeseed methyl ester (RME) (0.03–0.035 MW_{RME}/MW_{fuel}) is fed to the scrubber to avoid saturation of tar, especially naphthalene, which can be problematic as it crystallises when the RME is saturated. The used RME and the extracted tar are fed to the combustion side of the gasifier for destruction and heat recovery. After the scrubber (P3), there remains mainly

Int. J. Energy Res. (2017) © 2017 The Authors. *International Journal of Energy Research* published by John Wiley & Sons Ltd.
DOI: 10.1002/er

light cyclic hydrocarbons, such as benzene, toluene and xylene (referred to as BTX), and a small fraction of the naphthalene, as well as trace amounts of larger tar components. As the slip of tar is proportional to the volume of fresh scrubbing liquid, there is a trade-off between avoiding the slip and minimising the use of scrubbing liquid. Downstream of the scrubber, a fan increases the pressure of the gas, enabling the re-circulation of part of the product gas to the combustor, which is necessary to fulfil the heat demand of the DFB system.

At this point (P3), the quality of the product gas is sufficiently high to be used in several applications, for example, internal combustion engines. However, further cleaning is required for synthetic applications. In brief, the remaining BTX and tar components are removed in a series of three fixed beds that are filled with activated carbon. The plant has four active carbon beds, enabling regeneration of one bed at all times using steam. Currently, the off gases from the regeneration are introduced into the post-combustion chamber for destruction and heat recovery. However, a system is being developed that will allow condensation of the steam and recovery of the tar compounds, which then can be fed to the combustor. The product gas that exits the gasification section (P4) is compressed to 16 bar before it undergoes further cleaning and synthetic steps in the methanation section, which include hydration of olefins and COS (number 12, Figure 1); H_2S removal (13); passage through the guard bed for removal of trace components (14); water–gas shift reaction (15); pre-methanation (16); CO_2 removal (17); four-stage methanation (18); drying (19); and final compression to 30 bar before feeding into the natural gas grid.

Experimental data

For this work, the data were collected at the end of the commissioning period, during which wood pellets were used as the fuel, with the aim of evaluating the performance of the gasification section. The locations of the measurements points in the process are shown as points 1–10 (P1–10) in Figure 2, and the type of measurement that was performed at each point is listed in Table II. The evaluation is based on one operational point with 90% load (wood pellets, 8% moisture) and potassium carbonate (K_2CO_3) as the activation agent [15,28,30], corresponding to ~0.2 kg/t wood pellets. This results in a tar concentration that is below the operability threshold of the plant (around 35 g/Nm [3] dry gas, including BTX and heavy tars). This is the base case in the evaluation and is hereinafter referred to as the *K-activated* (*K-act*) case. The composition of the used wood pellets is given in the Supporting Information (Table S1), and the major operating parameters are summarised in Table III, while the gas and tar measurements are listed in Tables IV and V. The fuel flow to the gasifier (P6 in Figure 2) was calculated based on the carbon balance of the gasification section (P4 and P5) and compared with the scale measurement of the ingoing fuel (Table S1). To simplify the evaluation of the gasification section, the fuel feed was purged with nitrogen (CO_2 produced in the methanation section was used during normal operation, and the methanation section and regeneration of the active carbon beds were not operated to simplify the carbon balance).

MEASURES TO IMPROVE THE EFFICIENCY OF THE DUAL FLUIDISED BED GASIFICATION PROCESS

As described previously, GoBiGas is a demonstration plant for the DFB technology, and the design is not yet optimised for maximum performance in terms of efficiency and availability. Because of the relatively small scale of the demonstration plant and the previous knowledge gap (now filled with the construction of the plant), several measures have been identified to improve the process towards the creation of a commercial plant. The measures evaluated in this work focus on improving the efficiency of the gasification section.

Improvements based on the heat demand of the Gothenburg Biomass Gasification gasifier

The efficiency of a gasification process correlates strongly with the heat demands of the process. The impact on the gasification performance of reducing the total heat demand through different practical measures was assessed. The measures that yielded the greatest effect on the total heat demand were identified as the level of pre-heating of the steam and combustion air; the moisture content of the fuel; heat losses; and the operational temperature. Furthermore, part of the total heat demand could be covered by an additional heat source, such as electricity, as a power-to-gas concept.

The steam used to fluidise the gasifier and the air for the combustor are pre-heated by heat recovery in the flue gas train; during the evaluation, both streams were heated to about 350 °C. Both streams could in principle be heated to a higher temperature, either by heat recovery at elevated higher temperature in the flue gas train or by the addition of an additional heat source. Based on the choice of material, the maximum temperature investigated is 550 °C, which is feasible using steel with material number 1.4401 (3016L). An even higher temperature would increase the material costs considerably and is therefore not considered. Note that in the absence of an additional heat source, the maximum temperature is instead restricted by the temperature of the super heaters that recover the heat from the flue gas train.

The wood pellets used as fuel in the present work have moisture contents of about 8%. However, wood pellets

Int. J. Energy Res. (2017) © 2017 The Authors. *International Journal of Energy Research* published by John Wiley & Sons Ltd.
DOI: 10.1002/er

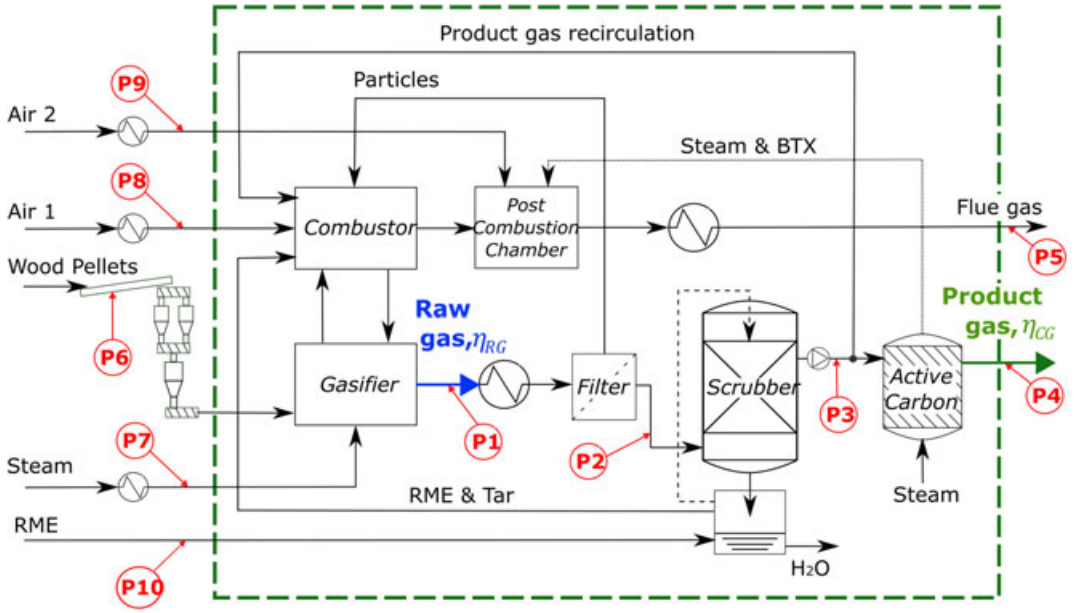

Figure 2. Schematic of the gasification section showing measurement points P1–P10. RME, rapeseed methyl ester; BTX, benzene, toluene and xylene. [Colour figure can be viewed at wileyonlinelibrary.com]

represent a pre-processed fuel, which is more expensive than other biomass-based fuels, such as wood chips or forest residues. To improve the economics of the plant, it is, therefore, relevant to consider fresh biomass that is not pre-treated and has a moisture content of up to 40%. As a higher moisture content is deleterious to process efficiency, a moisture content >40% is not relevant for gasification, at least without the introduction of dryers upstream of the gasifier. Drying on-site is certainly beneficial and can be achieved by exploiting the excess heat in the process. Several drying concepts are available [31], with low-temperature drying (with air and steam) being more suited for integration. For steam gasification, extended drying with recovery of the moisture as gasification media is of interest [32], as this confers dual benefits in terms of drying and pre-evaporation of the gasification steam. The maximum size of the fuel particle is limited by the feeding system to 7–10 cm.

The heat losses are here calculated as the differences in sensible and chemical energy between the inlets and outlets of the DFB gasifier. The heat losses of the GoBiGas plant are higher than those of a regular biomass boiler owing to the small size and the design of the insulation walls (Figure S2). The reactors do not have heat transfer panels coupled to insulation blocks, which would allow control of the temperature of the gas sealing (outer steel lagging), which needs to be higher than the condensation temperature at atmospheric pressure, so as to avoid condensation and corrosion. Instead, the external walls are designed to be cooled by the surrounding air in the building housing the gasifier, where temperatures as high as 140 °C have been measured. As a consequence, there are significant heat losses. Nevertheless, the heat insulation can be easily improved in a large-scale plant using a conventional reactor wall design for commercial fluidised bed combustors.

Table II. Measurements made in the gasification section

Sampling point – sample type	Measured compound(s)	Type of measurement
P1 – hot raw gas	Tar	SPA, temperature
P2 – particle-free gas	Tar	SPA
P3 – cold gas	Tar and permanent gases	NDIR, flow and SPA
P4 – product gas	Permanent gases	GC
P5 – flue gas	Permanent gases	FTIR, flow, temperature and pressure
P6 – fuel feed	Proximate and ultimate analysis	Moisture (offline) and composition (offline)
P7 – steam feed	Steam	Flow, temperature and pressure
P8 – air feed	Air	Flow, temperature and pressure
P9 – air feed	Air	Flow, temperature and pressure
P10 – RME	RME	Flow and heating value (offline)

RME, rapeseed methyl ester; SPA, solid phase adsorption method; NDIR, nondispersive infrared; FTIR, Fourier transform infrared spectroscopy.

Int. J. Energy Res. (2017) © 2017 The Authors. *International Journal of Energy Research* published by John Wiley & Sons Ltd.
DOI: 10.1002/er

Table III. Operational parameters

Operational parameter	Mean	SD
Gasifier bed temperature (°C)	870	2
Raw gas temperature (°C)	815	2
Combustor temperature (°C)	920	3
Steam temperature (°C)	345	14
Air temperature (°C)	348	10
Flue gas temperature (°C)	140	2
Fluidisation steam (Nm^3/h)	4255	53
Combustion air* (Nm^3/h)	8830	109
Post-combustion air (Nm^3/h)	1709	164
Flue gas (Nm^3/h)	13 049	491
Fresh rapeseed methyl ester flow (kg/h)	100	2
Fuel feeding (kg_{daf}/h)†	5820	142

*Including the fluidisation air.
†Calculated form carbon balance.

While the temperature of the gasification section is important for the eventual quality of the gas, it also has a strong impact on the total heat demand of the gasifier.

This creates a trade-off whereby a lower temperature leads to a lower quality gas with higher tar yield, which at the same time enables higher efficiency. With improved catalysis in the gasifier, the temperature can be decreased while retaining the quality of the gas, thereby improving efficiency. During the experiments presented in the present study, the GoBiGas gasifier was operated with a temperature of the gasifier of 870 °C using potassium (K) as the activation additive. As described in previous studies, the addition of sulfur increases further the catalytic effect of potassium, decreasing the tar yield substantially [28,33–35] and decreasing the risk of corrosion [36]. Initial tests have shown that with sulfur addition, the temperature of the gasifier can be decrease to 820 °C while retaining gas quality (as assessed by CH_4 concentration). Therefore, a case with an operating temperature of the gasifier of 820 °C was investigated, to illustrate the potential of decreasing the temperature and, thereby, the heat demand of the process.

To date, the gasifier was operated for more than 8000 h with potassium addition including 5000 h with sulfur addition, without sings of corrosion in the reactors and heat exchangers.

Electricity that can be produced in a steam cycle that recovers the excess heat from the plant is estimated to be in the range of 3–10% of the energy of the dry fuel [10,37–39], while consumption is in the range of 3–5% [9,10,39]. The electricity can be sold to the grid or re-used as a heat source for the gasifier to enhance biomethane production. The simplest way to introduce electricity into the gasification section is through either direct heating of the reactors or further pre-heating of the inlet streams. Introducing a power-to-gas technology makes the gasification process suitable for the storage of renewable electricity from intermittent energy sources (wind and solar) in the form of biomethane.

Case study – performance of a commercial-scale dual fluidised bed gasifier

To understand the potential performance of a commercial-scale DFB gasifier, a case study based on the measures described previously in Improvements based on the heat demand of the Gothenburg Biomass Gasification gasifier section was conducted. The notations and descriptions of the different cases are summarised in Table VI, where the different improvements incorporated in each case are indicated. In the base case potassium is used as activation additive in the GoBiGas gasifier (referred to as *K-act*, in contrast to the *K,S-act* notation, which refers to both *K* and *S* being used as additives). For the *K,S-act* case, the measurements reveal a different gas composition and a reduction in the level of tar, as compared with the *K-act*

Table IV. Permanent gas measurements

	P3		P4		P5	
	Mean	SD	Mean	SD	Mean	SD
H_2 ($vol\%_{dry}$)	39.9	0.49	42.1	0.49	–	–
CO ($vol\%_{dry}$)	24.0	0.3	24.6	0.3	0.02	0.02
CO_2 ($vol\%_{dry}$)	19.9	0.21	18.3	0.21	11.53	1.23
CH_4 ($vol\%_{dry}$)	8.6	0.12	6.8	0.12	–	–
C_2H_2 ($vol\%_{dry}$)	0.13	0.00	0.13	0.00	–	–
C_2H_4 ($vol\%_{dry}$)	2.0	0.07	2.0	0.07	–	–
C_2H_6 ($vol\%_{dry}$)	0.19	0.01	0.19	0.01	–	–
C_3H_6 ($vol\%_{dry}$)	0.001	0.00	0.01	0.00	–	–
N_2 ($vol\%_{dry}$)	5.28‡	0.81	4.0‡	0.81	56.9	5.35
H_2O (vol%)	6.33	–	14.1†	–	27.2	2.55
O_2 (vol%)	–	–	–	–	4.35	1.20
Flow ($Nm^‡/h$)	7998†	9	7157†	6	13 049	491

*Dry flow.
†Saturated.
‡From purge gas.

Int. J. Energy Res. (2017) © 2017 The Authors. *International Journal of Energy Research* published by John Wiley & Sons Ltd.
DOI: 10.1002/er

Table V. Tar measurements

	P1		P3		P4	
	Mean	SD	Mean	SD	Mean	SD
Tar, including BTX (g/Nm^3)	20.5	0.5	13.3	0.3	–	–
Tar, excluding BTX (g/Nm^3)	7.8	0.2	0.7	0.0	–	–
$H/C_{total\ tar}$ (mol/mol)	0.92	–	0.99	–	–	–
$O/C_{total\ tar}$ (mol/mol)	3/10^4	–	5/10^4	–	–	–
H/C_{BTX} (mol/mol)	0.99	–	0.99	–	–	–
O/C_{BTX} (mol/mol)	5/10^4	–	5/10^4	–	–	–
Flow (Nm^3/h)	7998*	9	7998*	9	7157*	6

BTX, benzene, toluene and xylene.
*Dry flow.

Table VI. Designs investigated in the simulation of the gasifier

	K-act	*K,S-act*	*K,S-act LT*	*K,S-act LT, PH, Ql*	*K,S-act LT, PH, Ql, El*	*K,S-act LT, PH, Ql, El_{int}*
Activation with *K*	x					
Activation with *K* and *S*		x	x	x	x	x
Low gasification temperature (820 °C)			x	x	x	x
Pre-heating of air and steam to 550 °C				x	x	x
Minimised heat loss				x	x	x
Power-to-gas from the grid					x	
Power-to-gas from excess heat						x

case. The increased catalytic effect achieved through the use of both *K* and *S* could be used to reduce the operating temperature instead of further improving the gas quality and decreasing the tar concentration. When the gasification temperature is reduced to 820 °C (referred to as the *K,S-act LT* case), the resulting gas composition and tar level (Table IX) are assumed to be equal to those in the *K-act* case, albeit with the benefit of a lower heat demand in the reactors. Further improvement to the design are invstegated, such as improved pre-heating of the inlet streams to 550 °C (denoted as case *PH*), reduction of the heat losses to 33% of the original (*Ql*), adding externally produced electricity (*El*) and adding internally produced electricity (El_{int}), with both of the latter corresponding to 3% of the energy in the fuel. All the cases were investigated for a plant that used dried biomass (8% moisture w.b.) and for a plant that used fresh biomass (40% moisture w.b.).

METHODOLOGY

A black-box model of the mass and energy balances, based on a stochastic analysis of the measurements, is used to calculate a set of key performance parameters that describe the fuel conversion, the efficiency of the process and the levels of uncertainty. The methodology applied has been described previously [40] and is briefly summarised in Mass balance and statistical analysis of the experimental data section.

Key performance parameters

The overall performance of the DFB gasifier is assessed using a set of five efficiencies, calculated using the lower heating value (LHV) on dry ash-free fuel (Table VII). The following three efficiencies are defined based on the energy content of the fuel, E_f: (1) the raw gas efficiency (η_{RG}); (2) the cold gas efficiency (η_{CG}); and (3) the biomethane efficiency (η_{bCH4}) (as defined by Eqs. (1)-(3) in Table VII). The raw gas efficiency represents the energy of the raw gas from the gasifier (including tar) and is a direct measure of the fuel conversion in the gasification reactor (P1 in Figure 2). The cold gas efficiency includes only the permanent gases that exit the gasification section, excluding

Table VII. Definitions based on the LHV of dry ash-free biomass to describe the efficiencies of the η_{RG}, raw gas; η_{CG}, cold gas; η_{bCH4}, biomethane; μ_{sect}, gasification section; η_{plant}, plant; and η_{P2G}, power-to-gas

$$\eta_{RG} = \frac{E_{RG}}{E_f}[\%\mathrm{LHV_{daf}}] \quad (1)$$

$$\eta_{CG} = \frac{E_{CG}}{E_f}[\%\mathrm{LHV_{daf}}] \quad (2)$$

$$\eta_{bCH4} = \frac{E_{bCH4}}{E_f}[\%\mathrm{LHV_{daf}}] \quad (3)$$

$$\eta_{sect} = \frac{E_{CG}}{E_f + E_{RME} + El}[\%E_{tot}] \quad (4)$$

$$\eta_{plant} = \frac{E_{bCH4}}{E_f + E_{RME} + El_{tot}}[\%E_{tot}] \quad (5)$$

$$\eta_{P2G} = \frac{E_{bCH4} - E'_{bCH4}}{El_{sect}}[\mathrm{MW_{bCH4}/MW_{el}}] \quad (6)$$

LHV, lower heating value.

Int. J. Energy Res. (2017) © 2017 The Authors. *International Journal of Energy Research* published by John Wiley & Sons Ltd.
DOI: 10.1002/er

Table VIII. Fuel conversion reactions [40]: R1, devolatilisation; R2, gasification; R3, syngas combustion; R4, volatile conversion; R5, volatile combustion; and R6, char combustion

$\sum Z_i + \lambda_v = 1 - Y_{ch}$	(R1)
$(\dot{X}_g - \lambda_{ch}) \cdot [(n_C,\ n_H, n_O)_{ch} + d_1 \cdot H_2O \quad \rightarrow\ a_1 \cdot CO + b_1 \cdot H_2]$	(R2)
$\lambda_{ch} \cdot \left[(n_C,\ n_H, n_O)_{ch} + d_2 \cdot H_2O + \overline{n}_{O,ch} \rightarrow a_2 \cdot CO_2 + b_2 \cdot H_2O\right]$	(R3)
$Z_i \cdot [(n_C,\ n_H, n_O)_v \rightarrow\ a_{3,i} \cdot CO_2 + b_{3,i} \cdot H_2O + c_{3,i} \cdot C_{p,i}H_{q,i}O_{k,i}]$	(R4)
$\lambda_v \cdot \left[(n_C,\ n_H, n_O)_v + \overline{n}_{O,v} \rightarrow a_4 \cdot CO_2 + b_4 \cdot H_2O\right]$	(R5)
$(1 - X_g) \cdot \left[(n_C,\ n_H, n_O)_{ch} + \lambda_a \cdot \overline{n}_{O,f} \rightarrow a_5\ CO_2 + b_5\ H_2O + \overline{n}_{O,f} \cdot \lambda_{Otr} + \overline{n}_{O,f} \cdot \left(\lambda_a - \lambda_{Otr} - \frac{\overline{n}_{O,ch}}{\overline{n}_{O,f}}\right)\right]$	(R6)

the tar and BTX, and the re-circulated product gas, which are separated and fed to the combustor (P4). The biomethane efficiency represents the amount of energy in the fuel that is retained in the final biomethane product (theoretical, as described later). The biomethane efficiency is also the value used for the performance target of the GoBiGas project and is set at $\eta_{b\mathrm{CH4}} > 65\%\mathrm{LHV_{daf}}$. Two additional efficiencies are defined to assess the overall performance of the gasification section (η_{sect} in Eq. (4), Table VII) and of the whole plant (η_{plant} in Eq. (5), Table VII); all the energy inputs (biomass, RME and electricity) are included in the calculation. The biomethane and plant efficiencies are based on the assumption that the conversion from product gas to biomethane follows the general conversion reaction:

$$(n_C,\ n_H, n_O)_{PG} \rightarrow a \cdot CH_4 + b \cdot CO_2 + c \cdot H_2O. \qquad (1)$$

Based on (1), around 85% of the energy in the cold gas measured at P4 can be retained as biomethane. Furthermore, electricity used for the operation of the plant, including the intermediate and final compression stages, is estimated at 3.75%$\mathrm{LHV_{daf}}$, which is included in the plant efficiency.

Unlike other power-to-gas processes, the power-to-methane conversion in the plant cannot be assessed only by an efficiency that is defined as the increase in biomethane production in relation to the electricity input, because the feedstock that is converted has a high energy value. Instead, the power-to-methane efficiency is set as being equal to the plant efficiency (Eq. (5), Table VII). The power-to-gas efficiency of the power-to-methane process (η_{P2G} in Eq. (6), Table VII) is used to assess the electricity conversion to biomethane based on the reference production, $E^{*}_{b\mathrm{CH4}}$.

Mass balance and statistical analysis of the experimental data

The validity of the calculated variables reflects the quality and completeness of the measurements themselves. Therefore, a statistical analysis is used to assess the uncertainty of the calculated variables by establishing a synthetic dataset ($>10^6$ cases) that is based on the uncertainty of the measurements, assuming a normal distribution for all the variables [41]. Systematic errors, such as incomplete characterisation of the raw gas compounds or errors in the measurements, are not included because they are unknown. The overall mass and energy balances are assessed with a black-box approach to handle the high degree of complexity of the reactions in the gasification process and the high degree of freedom in the operation of the double-reactor system. The mass balance is used to estimate three types of fuel conversion variables, which are calculated from the measurements: (1) the degree of char-gasified X_g (Eq. (B1)); (2) oxygen transport by the bed material between the combustion and the gasification side of the gasifier λ_{Otr} (Eq. (B3)); and the fraction of volatile matter that is converted to a given raw gas compound Z_i (Eq. (B2)). The fuel flow to the gasifier, $\dot{m}_f$, is calculated from the amount of carbon in the outgoing flows, $\dot{m}_{C,PG}$ and $\dot{m}_{C,FG}$, (measurement points P4 and P5), the amount of carbon in the RME, $\dot{m}_{C,RME}$, and the fraction of carbon in the fuel, $Y_{C,f}$:

$$\dot{m}_f = \frac{\left(\dot{m}_{C,PG} + \dot{m}_{C,FG} - \dot{m}_{C,RME}\right)}{Y_{C,f}}. \qquad (2)$$

The reactions considered for the fuel conversion in the DFB gasifier are summarised in Table VIII, where the subscripts *f*, *v*, *ch*, *syn, i* and *RG* indicate the fuel, volatile matter, char, syngas from char gasification, the generic raw gas compound and the dry raw gas flow, respectively. Furthermore, *n* represents the molar yields of the generic $C_pH_qO_k$ compound on a dry ash-free fuel basis (mol/$\mathrm{kg_{daf}}$); Y_{ch} is the char yield ($\mathrm{kg_{char}/kg_{daf}}$); *a*, *b*, *c* and *d* indicate the stoichiometric reaction coefficients; and $\bar{n}_{O,f,v,ch}$ are the moles of oxygen for stoichiometric combustion of the fuel, char and volatiles, respectively. The decomposition of the biomass in the gasifier is depicted in the Supporting Information (Figure S1), where the fraction X_g of the char yield (Y_{ch}) is converted by R2 (gasification), the fraction λ_{ch} is combusted by the oxygen transport (R3) and the fraction ($1 - X_g$) is transported to the combustor and converted by R6 (combustion), where λ_a describes the excess of air in the reactor. The conversion of volatile matter is described by R4 and R5. In each R4, a fraction Z_i of the volatile matter is converted to one component of the raw gas that contributes to the heating value of the gas, described by the generic molecule $C_pH_qO_k$, and the reaction is balanced with water and carbon dioxide. A fraction of the volatiles λ_v (Eq. (B5)) is combusted by the oxygen transport according to R5. The total oxygen

transport is described by λ_{Otr} (Eq. 6) as the stoichiometric ratio of the oxygen transported to the gasifier and reacting with the fuel (i.e. present in the raw gas) to the oxygen used for stoichiometric combustion of the fuel.

The mass balance equations include the carbon balance (Eq. (B7)) and the balance of volatiles (Eq. (B8)) (Table S2). The fuel conversion is summarised by the fuel conversion variables X_g, λ_{Otr} and Z_i and is used to calculate the internal heat demand of the gasifier [40]. The degrees of freedom of the mass balance equations depend on the available measurements; if the raw gas flow is measured (i.e. the yields of raw gas species are measured) and all the species are detected, the equation has one solution, and the values of X_g, λ_{Otr} and Z_i can be calculated [40]. In particular, the char gasification is calculated from the carbon balance, and the oxygen transport is calculated comparing the oxygen for stoichiometric combustion of the raw gas with that of the fuel at the net of the char to the combustor [40].

In the GoBiGas plant, the flow measurements are available, and the fuel conversion variable can be calculated with a relatively low degree of uncertainty. Other sources of uncertainty, such as measurement errors, fuel composition and raw gas characterisation, are assessed by stochastic simulation of the mass balance inputs, that is, the experimental data. The measurements (including the flows, concentrations, temperatures, fuel composition and tar yields) are varied within a range that is twice the standard deviation (SD) of their measurements according to normal distributions. For each variation of the input, the fuel flow is re-calculated, and the mass balance is solved. The solutions are considered valid if the calculated values of X_g, λ_{Otr} and Z_i are within physically possible ranges, and the fraction of carbon detected by the measurement is lower than the level of carbon in the fuel [40]. The final results are presented as a mean value and SD calculated from the set of valid solutions.

Energy balance of the dual fluidised bed system

The streams considered and the control volumes used for the energy balance of the DFB system are depicted in Figure 3. In contrast to Figure 2, a solution of water and potassium is added to activate the bed material, and the water content in the RME flow to the combustor is $40\%_{vol}$; these features are relevant for the energy balance, while they can be neglected for the carbon balance. The energy balance can be calculated for either the entire DFB system or for each of the reactors using Eqs. (C1)–(C3) (Table S3).

In the assessment of the GoBiGas gasifier, one of the main unknowns is the heat losses $Q_{l,tot}$, which in the GoBiGas plant are considerable because of its relatively small size. The ratio of the heat losses between the combustor $Q_{l,comb}$ and the gasifier $Q_{l,gasif}$ was previously estimated to be 3 [42], based on the external surface and the temperatures of the reactors.

In the scheme reported in Figure 3, the electricity introduced into the system is located in the gasifier, reducing the internal heat demand of the gasifier and the re-circulation of bed material. Nevertheless, the energy balance equations can be easily re-formulated to introduce electricity into the combustor (increasing the re-circulation of bed material).

The energy balance of the gasifier reactor (Eq. (C2)) enables the calculation of the internal heat demand of the gasifier Q_{iHD}, which is used in the simulation to calculate the fraction of product gas that has to be re-circulated to the combustor. Equations 15–17 are used to calculate the

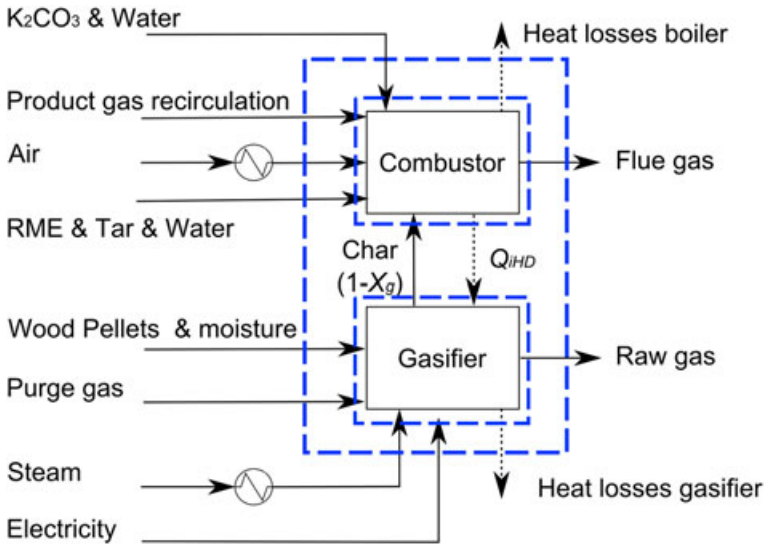

Figure 3. Energy balance of the dual fluidised bed (DFB) system. RME, rapeseed methyl ester. [Colour figure can be viewed at wileyonlinelibrary.com]

Int. J. Energy Res. (2017) © 2017 The Authors. *International Journal of Energy Research* published by John Wiley & Sons Ltd.
DOI: 10.1002/er

heat balance of the gasifier during the extrapolation to new conditions.

Simulation of the dual fluidised bed gasifier

Five key assumptions are made in the simulation algorithm: (1) the circulation of bed material and the oxygen transport are linearly proportional to the internal heat demand of the gasifier (i.e. the oxidation level of the bed material from the combustor is equal for all cases); (2) the RME flow is linearly proportional to the mass flow of the wet raw gas; (3) the average re-circulated flow gas should at a minimum be 1% of the fuel input, to cope with process fluctuations, such as variations in the moisture content; (4) the char gasification can be increased beyond the measured level when the product gas re-circulation is at the minimum level; and (5) the BTX are separated and fed to the combustor. The char gasification depends on several process parameters and on the heat balance of the DFB gasifier. If the heat demand in the combustor is reduced, by, for example, reduced heat losses, the raw gas re-circulation will be reduced.

When the raw gas re-circulation is at the minimum level, the temperature in the gasifier will start to rise, increasing the rate of char gasification. As gasification is endothermal, it moderates the increase in temperature. Through assumption 4, it is assumed that char gasification can be varied within a range (±10 percentage points, pp) and it is calculated from the energy balance while maintaining the temperatures in the reactors. Figure S3 shows the variations of the product gas re-circulation and char gasification used in the simulation algorithm. The first action that can be taken to address a decrease in internal heat demand is to reduce re-circulation of the product gas to the combustor to the minimum level, set according to the need to cope with variations in the process via a rapid regulatory measure. Beyond this point, any further reduction of the heat demand can be compensated by an a reduction of char combustion, making more char available for gasification depending on the design and operational conditions of the gasifier.

In contrast, when the heat demand of the gasifier is increased (e.g. higher moisture content of the fuel), the product gas re-circulation is increased to maintain constant the conditions in the gasifier, including the char gasification. The structure of the simulation algorithm is shown in Figure 4, in which each simulation is defined by a set of independent variables and requires a set of initial values The starting values are initially guessed and thereafter re-calculated through two iterative calculations, one linked to the mass and energy balances of the gasifier to derive λ_{Otr} (step 3) and one linked to the mass and energy balances of the entire system to derive X_g (step 6). Assumption 1, which is concerned with the oxygen transport, and assumption 2, concerning the RME flow, are introduced in steps 3 and 4 of the algorithm, respectively, while assumption 3, which considers re-circulation of the product gas, and assumption 4, which constrains char gasification, are applied in step 6.

To simulate a different chemistry in the reactor, the Z_i values are modified based on the measured composition of the product gas when sulfur is added to the process (Table IX). The distribution of Z_i values is adjusted to match the raw gas composition, assuming that the differences in the concentrations of the measured compounds are related to different rates of conversion of the volatile. Furthermore, the ratio between the C_2H_x and C_3H_x hydrocarbons (not measured) and methane was set as being equal to that of the reference case.

RESULTS AND DISCUSSION

Evaluation of the Gothenburg Biomass Gasification gasifier

The results of the assessment of the DFB gasifier in the GoBiGas plant are reported in Tables X and XI, which show the fuel conversion variables with their associated uncertainties; the results are based on operation using wood pellets as the fuel, with 870 °C as the operating temperature in the gasifier, and potassium-activated olivine as the bed material. The char gasification is 53.8% with an SD of 4.7 pp, and the oxygen transport, λ_{otr}, is estimated as 4.9% (SD, 2.7 pp) of the volume of oxygen required for stoichiometric combustion of the fuel. Calculation of the conversion of volatiles shows that 34.1% of the volatile matter is directly converted to methane, which is favourable for the downstream synthesis processes. The percentages of volatiles converted through the reactions forming tar and BTX are 3.5% and 5.8%, such that in total, 9.3% of the volatiles form unwanted hydrocarbons.

The heat loss of the system, calculated based on the heat balance, corresponds to 5.2% of the energy in the fuel, or about 1.6 MW, of which 0.4 MW is from the gasification side and 1.2 MW is from the combustion. Compared with the heat lost in a typical circulating fluidised bed combustor, which is around 1–2% of the energy of the fuel, the energy lost to the surroundings in the GoBiGas system is considerably higher.

These results highlight the need for better insulation of the reactors, so as to increase the efficiency of the system. The high heat losses affect the energy balance between the two reactors, requiring a high level of re-circulation of the product gas, $E_{PG,rec}$, to maintain the temperature of the process, corresponding to 9.8% of the fuel LHV on a dry basis. The total heat demand of the GoBiGas gasifier is 18% of the energy of the ingoing fuel, whereby about half of the heat demand is covered by the re-circulated gas.

The raw gas efficiency of the gasifier is calculated as 87.3%LHV_{daf} (SD, 1.9 pp), with 71.7%LHV_{daf} (SD, 1.8 pp) of the energy in the fuel being converted into permanent gases and delivered to the methanation section (herein referred to as the 'cold gas efficiency'). Including the energy input from the RME, the efficiency of the

Int. J. Energy Res. (2017) © 2017 The Authors. *International Journal of Energy Research* published by John Wiley & Sons Ltd.
DOI: 10.1002/er

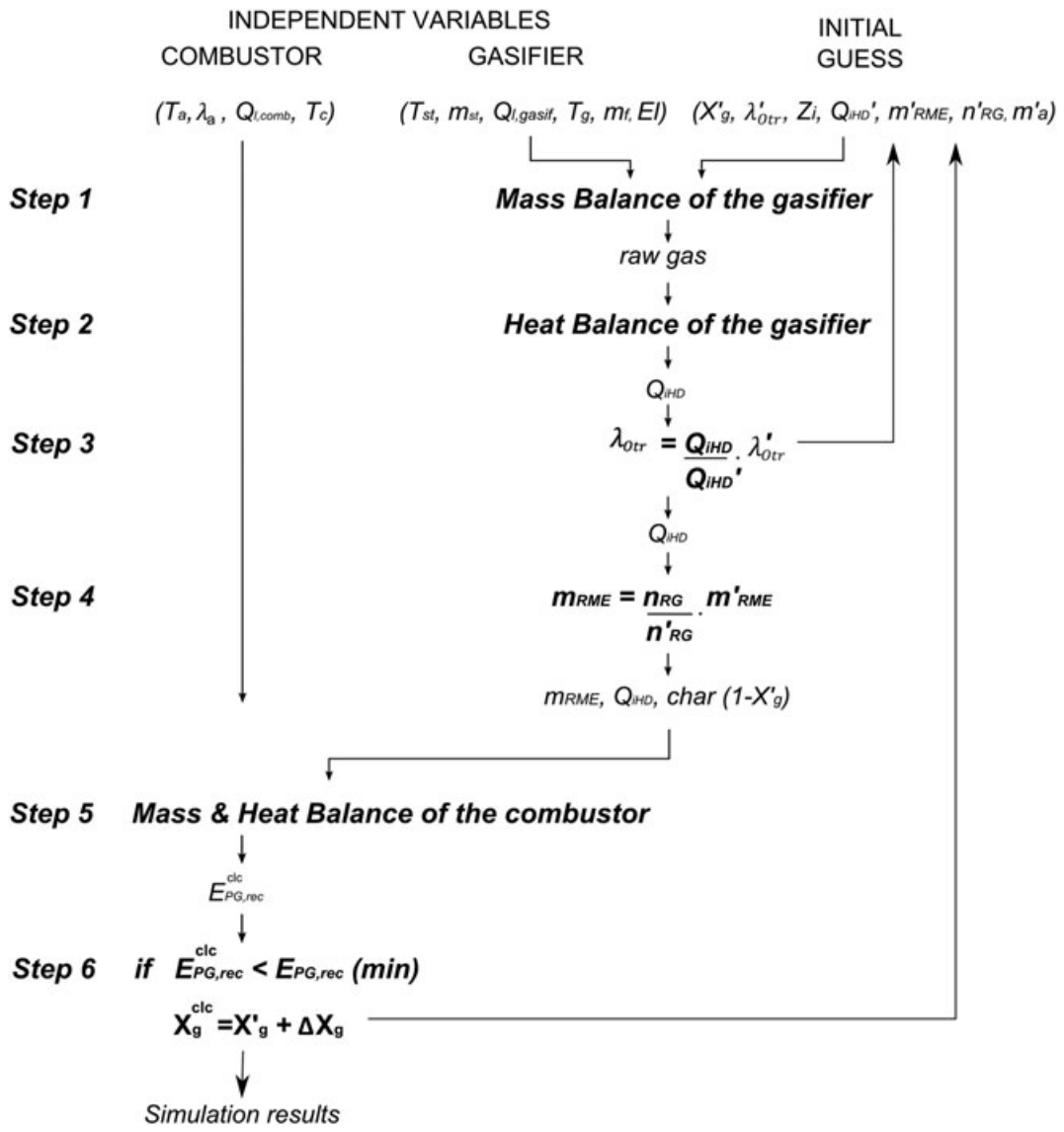

Figure 4. Simulation algorithm.

Table IX. Concentrations of permanent gases and tar following sulfur addition to processes at high and low temperatures

	K,S-act		*K,S-act LT*	
Gasification temperature (°C)	870		820	
Combustion temperature (°C)	920		870	
Measurement point	P1	P3	P1	P3
	Mean	Mean	Mean	Mean
H_2 (vol%$_{dry}$)	n.a.	42.1	n.a.	39.9
CO (vol%$_{dry}$)	n.a.	24.1	n.a.	24.0
CO_2 (vol%$_{dry}$)	n.a.	23.5	n.a.	19.9
CH_4 (vol%$_{dry}$)	n.a.	7.7	n.a.	8.6
Tar (g/Nm^3)	10	6.6	20	13

n.a., not available.

Table X. Mass balance results, X_g, char gasification, Z_i, and volatile matter converted to the *i*-th compound

Parameter (%$_{mass}$)	Mean	SD
X_g	53.8	4.7
λ_{otr}	4.9	2.7
λ_{ch}	0.9	0.5
λ_v	7.8	3.8
Z_{H2}	25.2	1.2
Z_{CO}	9.8	0.8
Z_{CH4}	34.1	0.2
Z_{C2H4}	13.8	0.1
Z_{C3H6}	0.02	0.0
Z_{tar}	3.5	0.2
Z_{btx}	5.8	0.3

Int. J. Energy Res. (2017) © 2017 The Authors. *International Journal of Energy Research* published by John Wiley & Sons Ltd.
DOI: 10.1002/er

Table XI. Energy balance results

	Mean	SD
η_{RG} (%LHV$_{daf}$)	87.3	1.9
η_{CG} (%LHV$_{daf}$)	71.7	1.8
η_{bCH4} (%LHV$_{daf}$)	61.8	1.5
η_{sect} (%)	69.2	1.6
η_{plant} (%)	57.7	1.3
Q_{iHD} (%LHV$_{daf}$)	18	1.0
$E_{PG,rec}$ (%LHV$_{daf}$)	9.8	0.2
$Q_{l,tot}$ (%LHV$_{daf}$)	5.2	0.6
Fuel feed (kg$_{daf}$/h)	5820	142

gasification section is 69.2%E_{tot} (SD, 1.6 pp). The biomethane efficiency, η_{bCH4}, is calculated as 61.8% LHV$_{daf}$ (SD, 1.5 pp), and the plant efficiency, η_{plant}, including all the energy inputs (biomass, electricity and RME) is 57.7%E_{tot} (SD, 1.3 pp) based on the LHV.

Improvements based on the heat demand of the Gothenburg Biomass Gasification gasifier

The sensitivity analysis of the performance of the GoBiGas gasifier aims to identify efficient measures that could be used to improve the efficiency of DFB gasifiers using the GoBiGas gasifier as reference. For this purpose, the air and steam pre-heating, the moisture content of the fuel, the heat losses of the system, the use of sulfur as an additive and the introduction of electricity as a heat source were varied, as described in Simulation of the dual fluidised bed gasifier section, and the results are presented in Figures 5 and 6. The results are expressed as the raw gas efficiency η_{RG}, cold gas efficiency η_{CG}, gasification section efficiency η_{sect} and product gas; the filled markers indicate the relevant reference points from GoBiGas (*K-act* case). Because all of these measures influence the heat demand in the boiler, they affect the required re-circulation of the product gas, as well as the efficiency of the gasification section. Note that as soon as the level of re-circulated product gas reaches the defined minimum, char gasification is increased to fulfil the heat balance, as described in Simulation of the dual fluidised bed gasifier section, and this in turn increases the raw gas efficiency. Because the GoBiGas plant requires a high level of re-circulation of the product gas, owing to the considerable heat losses, most of the measures analysed affect only the re-circulation. Therefore, the only situation in which it is possible to derive a benefit from the significantly increased char gasification is when there is extensive introduction of electricity. Air and steam pre-heating from 300 to 550 °C (Figure 5a) reduces the re-circulation of product gas to about 50% of the reference case, increasing the cold gas efficiency from 71.7%LHV$_{daf}$ to 77.3%LHV$_{daf}$. The reduction of heat losses has an effect similar to that of pre-heating, although the heat losses would need to be reduced by a factor of 5 to increase the η_{CG} to 77.4% LHV$_{daf}$ (Figure 5c). The moisture content depends on the fuel (wood pellets and wood chips) that is being used and the drying process, which is dictated by the economics of the plant, considering both the operational and investment costs for a drying system. A shift from wood pellets (8% moisture) to fresh wood chips (40% moisture, assuming the same chemical composition as the wood pellets) has the effect of reducing η_{CG} from 71.7%LHV$_{daf}$ to 56.3% LHV$_{daf}$ in the current design, while further drying of the fuel to 2% moisture can raise the cold gas efficiency by ~2 pp (Figure 5b). This condition of extreme drying can be achieved with steam dryers, which are connected directly to the feeding system of the DFB gasifier, as suggested previously [31,32]. This type of dryer also pre-heats the biomass to a temperature of 80–100 °C, which further reduces the heat demand in the gasifier [21,32].

Activation with potassium and sulfur affects the gas composition and reduces the tar content, enabling operation of the gasifier across a wider range of conditions. Figure 5d shows the results for the *K,S-act* case with low tar content and the same temperature levels as in the *K-act* case (Table IX) and for the *K,S-act LT* case with the same tar content as the base case, but with the temperature in the reactors reduced by 50 °C (Table IX). In the *K,S-act* case, the lower yield of tar indicates that more energy is stored in the permanent gas, although this is partially compensated for by the higher level of re-circulation of the product gas, which is used to counteract the lower tar flow to the combustor. In the *K,S-act LT* case, the lower temperature in the reactor reduces both the heat demand in the combustor and the product gas re-circulation, while the tar yield is similar to that in the base case. Overall, the cold gas efficiency is increased to 72.9%LHV$_{daf}$ for the *K, S-act* case and to 74.2%LHV$_{daf}$ for the *K,S-act LT* case.

The introduction of electricity into the DFB gasifier affects multiple aspects of the process. Overall, the re-circulation of the product gas is reduced, and it may reach the minimum value (Figure 6). If more electricity is provided, the gasification of char may increase. Using electricity as a heat source in the gasifier reactor improves the rate of fuel conversion, that is, the raw gas efficiency (Figure 6). Initially, this is due to the reduced rate of oxygen transport, whereas later, it is due to the higher level of char gasification. The minimum level of re-circulation of product gas in this case is reached by introducing electricity for 8% of the energy in the fuel, thereby achieving a cold gas efficiency of 82.1%LHV$_{daf}$. An electricity input corresponding to 10% of the LHV of the fuel would enable char gasification to be increased from 53.8% to 60% and would increase the raw gas efficiency to 92.3%LHV$_{daf}$. Unlike the other measures investigated, the introduction of electricity causes the cold gas efficiency and the efficiency of the gasification section to diverge in Figure 6, because in the latter, the electricity is accounted for as an energy input. In particular, for the case in which electricity replaces 8% of the LHV of the fuel, the efficiency of the gasification section increases by ~4.5 pp, while the cold gas efficiency is increased by ~10 pp. The effects of the electricity on the overall plant (power-to-gas efficiency) in combination with the measures described

Int. J. Energy Res. (2017) © 2017 The Authors. *International Journal of Energy Research* published by John Wiley & Sons Ltd.
DOI: 10.1002/er

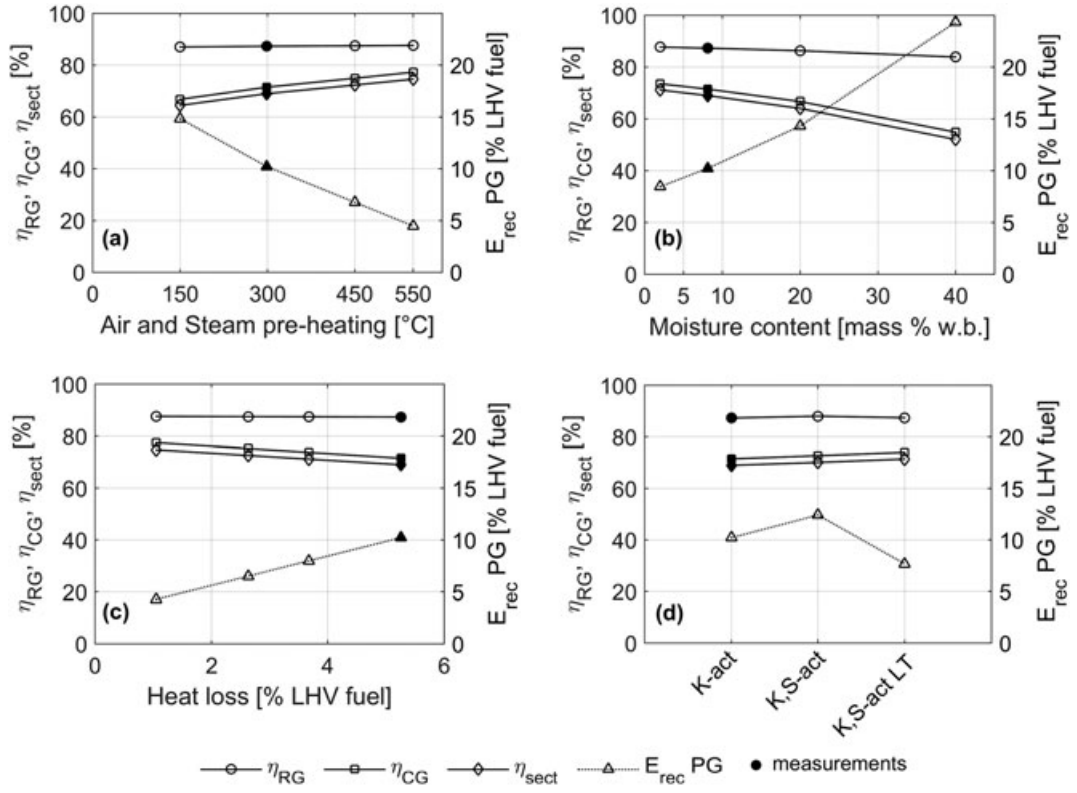

Figure 5. Sensitivity analysis of thermal measures.

previously are investigated in Case study: performance of a commercial-scale gasification plant section.

Case study: performance of a commercial-scale gasification plant

The combined effect of improved thermal measures is investigated with a view to possible designs for a large-scale plant. The results are shown in Figure 7 and Table XII for both dried woody biomass (e.g. pellets or very dry wood chips; 8% moisture w.b.) and fresh wood biomass (e.g. wood chips or forest residues; 40% moisture w.b.). The cases investigated included the (1) *K-act* base case; (2) *K,S-act LT* with addition of sulfur; (3) *K,S-act* with addition of sulfur and low operational temperature; (4) *K,S-act LT, PH* and *Ql* with sulfur addition and low operational temperature, with pre-heating up to 550 °C and heat losses reduced by a factor of 3; (5) *K,S-act LT, PH, Ql* and *El*; and (6) *K,S-act LT, PH, Ql* and El_{int}, the latter two of which introduce electricity from the grid and electricity that is produced internally from heat recovery, respectively. In Figure 7, the results for the DFB gasifier and the biomethane production process are expressed in terms of the cold gas and biomethane efficiencies (based on the LHV of the fuel), as well as the efficiencies of the gasification section and the plant, which include all the energy inputs. In the calculation of the plant efficiency η_{plant}, electricity is included among the energy inputs if it is obtained from the grid and excluded if it is produced locally from waste heat. Electricity is always considered to be an external energy input for the efficiency of the gasification section η_{sect}. A summary of the results for all the cases is reported in Table XII. A comparison of the *K-act* and *K,S*-act *LT* cases shows how the lower temperature achieved in the reactors by sulfur addition leads to increases in η_{CH4} and η_{plant} of about 1 pp, for both dried woody biomass and fresh wood chips. Thus, the

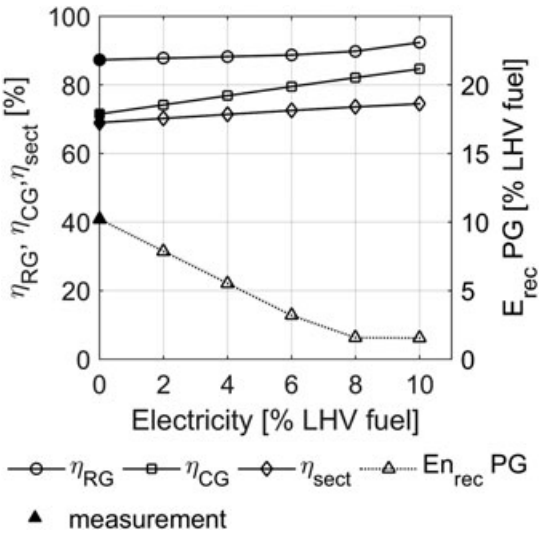

Figure 6. Effects of electricity introduction into the gasifier reactor.

Int. J. Energy Res. (2017) © 2017 The Authors. *International Journal of Energy Research* published by John Wiley & Sons Ltd.
DOI: 10.1002/er

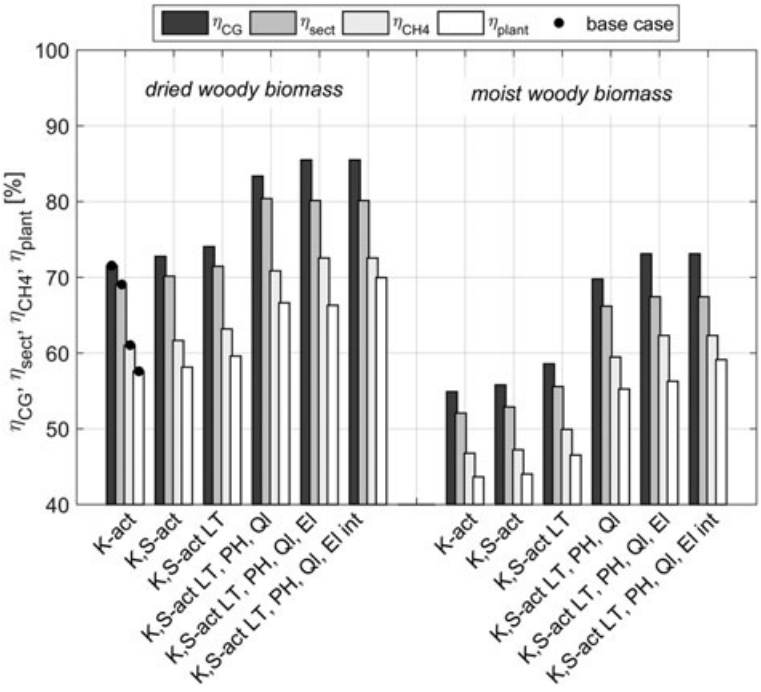

Figure 7. Simulation of the process design cases and efficiencies.

addition of sulfur to the DFB gasifier produces considerable benefits, not only in reducing the operational problems associated with tar clogging but also in significant increases in the efficiencies. With sulfur addition and a lower temperature, the GoBiGas plant achieves a biomethane efficiency of 63.3%LHV_{daf}, approaching the 65%LHV_{daf} target of the project. For the cases of *K,S-act LT, PH* and *Ql*, Figure 7 shows that the combined effect of sulfur addition, extended pre-heating and better insulation of the reactors achieves a biomethane efficiency of 71%LHV_{daf} with dried biomass and 60.5%LHV_{daf} using moist biomass. Compared with the reference case, GoBiGas, the increases in the levels of the cold gas efficiency using wood pellets and fresh wood chips are approximately 11 (83.5%LHV_{daf}) and 14 pp (71%LHV_{daf}), respectively. With this design (*K, S-act LT, PH* and *Ql*), re-circulation of the product gas is reduced to the minimum, whereas char gasification is not increased.

The electricity introduced to the gasifier, in the two cases of *K,S-act LT, PH, Ql* and *El*, and *K,S-act LT, PH, Ql* and El_{int}, corresponds to 3% of the LHV of the fuel and is in the same order of magnitude as the power consumption of the plant (3.75%LHV_{daf}). The total electricity consumption (6.75%LHV_{daf}) is compatible with the electricity production from heat recovery in a large plant, estimated as 3–10% of the energy of the fuel [43]. The results show that by introducing electricity, it is possible to increase the raw gas efficiency when using dried biomass to 94.4%LHV_{daf}, corresponding to a char gasification fraction of 61%. Thus, to achieve this performance, the rate of char gasification should be increased beyond the rate currently obtained at the GoBiGas gasifier.

Several parameters that influence char gasification have been identified, including the catalytic effects of additives and bed materials, residence time, mixing of char in the multiphase flow and temperature. However, the correlations between these parameters and the level of gasification are not fully understood, and there is potential to achieve further improvements in the efficiency of gasification.

When electricity is used in combination with moist biomass, most of the electricity compensates for the higher rate of moisture evaporation in the gasifier. Therefore, the rate of product gas re-circulation is minimised, with a small increase in char gasification and a cold gas efficiency that corresponds to 75%LHV_{daf}. The efficiency of biomethane production is 74.3%LHV_{daf} with dried biomass and 64.0%LHV_{daf} with moist biomass. The plant efficiency is affected by the origin of the electricity, that is, whether it is produced from waste heat or obtained from the grid. In the latter case, the η_{plant} is estimated as 68.2%E_{tot} with dried biomass and as 58.7%E_{tot} with moist biomass. Because of the high-level efficiency of the gasification process, the conversion of electricity to methane is more efficient than current state-of-the-art power-to-methane processes, which employ an electrolyser and further synthesis of hydrogen with renewable CO_2 [44–47]. The efficiency of current state-of-the-art power-to-methane processes is in the range of 45–50% based on LHV [44,45,48] with aims to achieve 55–63% based on LHV

Int. J. Energy Res. (2017) © 2017 The Authors. *International Journal of Energy Research* published by John Wiley & Sons Ltd.
DOI: 10.1002/er

Table XII. Summary of the process efficiencies based on dry ash-free and a.r. biomass (50% moisture), for biomass moisture contents of 40%, 8% and 2% moisture w.b., respectively

		Energy inputs		Efficiencies on LHV_{daf} (%)				Efficiencies on LHV a.r. fresh[§] (%)			
		Rapeseed methyl ester (%MJ_{fuel})	EI_{tot} (%MJ_{fuel})	η_{RG}	η_{CG} (%LHV_{daf})	η_{bCH4}	η_{sect} (%E_{tot})	η_{plant}	η_{RG}	η_{CG} (%$LHV_{a.r.}$)	η_{bCH4}	η_{sect} (%E_{tot})	η_{plant}
Extremely dried wood*	K_{act}	3.3	3.75	87.7	73.6	62.8	71.2	59.4	100.9	93.9	72.2	81.5	67.7
	K, S_{act}	3.3	3.75	88.4	74.8	63.4	72.3	59.9	101.7	98.1	73.0	82.8	68.4
	K, S_{act} *LT*	3.3	3.75	87.8	75.9	64.8	73.4	61.2	101.0	94.0	74.5	84.1	69.9
	K, S_{act} *LT, PH, OI*	3.3	3.75	92.6	85.0	72.1	82.1	67.9	106.5	99.5	83.0	94.0	77.5
	K, S_{act} *LT, PH, OI, EI*[‖]	3.3	6.75	95.9	88.3	75.4	82.9	69.2	110.4	103.3	86.8	94.5	77.7
	K, S_{act} *LT, PH, OI,* EI_{int}[¶]	3.3	0.0	95.9	88.3	75.4	82.9	71.2	110.4	103.3	86.8	94.5	82.7
Dried wood[†]	K_{act}	3.3	3.75	87.3	71.7	61.1	69.2	57.7	100.5	93.5	70.3	79.2	65.9
	K, S_{act}	3.3	3.75	88.0	72.9	61.8	70.3	58.2	101.2	97.6	71.1	80.4	66.4
	K, S_{act} *LT*	3.3	3.75	87.3	74.2	63.3	71.6	59.7	100.6	93.6	72.8	81.9	68.1
	K, S_{act} *LT, PH, OI*	3.3	3.75	91.1	83.5	71.0	80.5	66.7	104.8	97.8	81.7	92.2	76.1
	K, S_{act} *LT, PH, OI, EI*[‖]	3.3	6.75	94.4	87.6	74.3	82.2	68.2	108.6	102.6	85.5	93.6	77.1
	K, S_{act} *LT, PH, OI,* EI_{int}[¶]	3.3	0.0	94.4	87.6	74.3	82.2	70.2	108.6	102.6	85.5	93.6	82.0
Moist wood[‡]	K_{act}	3.3	3.75	84.1	56.3	48.0	53.4	44.7	96.7	90.1	55.2	61.0	51.0
	K, S_{act}	3.3	3.75	84.7	57.2	48.4	54.2	45.1	97.5	94.1	55.7	61.9	51.4
	K, S_{act} *LT*	3.3	3.75	84.2	59.9	51.0	56.8	47.6	96.9	90.3	58.7	64.9	54.2
	K, S_{act} *LT, PH, OI*	3.3	3.75	84.9	71.0	60.5	67.4	56.2	97.6	91.0	69.6	76.9	64.0
	K, S_{act} *LT, PH, OI, EI*[‖]	3.3	6.75	85.6	75.0	64.0	69.3	58.7	98.5	92.6	73.6	78.8	65.6
	K, S_{act} *LT, PH, OI,* EI_{int}[¶]	3.3	0.0	85.6	75.0	64.0	69.3	60.5	98.5	92.6	73.6	78.8	69.3

a.r., as-received.
*Case with 2% moisture w.b.
†8% moisture w.b.
‡40% moisture w.b.
§50% moisture w.b.
¶Electricity provided to exchange for 3%LHV_{daf} in the gasifier reactor.

Int. J. Energy Res. (2017) © 2017 The Authors. *International Journal of Energy Research* published by John Wiley & Sons Ltd.
DOI: 10.1002/er

[49–51] with the development of high temperature electrolysis cells, as comparison, a plant efficiency of 55–65%E_{tot} is already achievable with the GoBiGas technology. Therefore, the direct utilisation of electricity as the heat source in the gasifier represents a viable option for a high-efficient power-to-methane process.

Another measure of efficiency when using electricity to enhance the biomethane process is the power-to-gas efficiency (η_{P2G}, Table VII). The power-to-gas efficiency is depended on the reference process used in the calculation because the heat provided can be used either to reduce the combustion of product gas or char (increasing gasification). When product gas re-circulation is substituted by electricity, η_{P2G} is ~85% and gradually increases to values above 105%, if the electricity converted is stored as chemical energy in the gasification products (i.e. char gasification is increased).

For the case with electricity that is produced locally (i.e. *K,S-act LT, PH, Ql* and El_{int}), it is assumed that the level of production corresponds to the total electricity demand of the plant. The biomethane efficiency corresponds to that of the *K,S-act LT, PH, Ql* and *El* case, while the plant efficiency is 71.7% or 61.1% higher with wood pellets or wood chips as the fuel, respectively. These efficiency levels are considerably higher than the current efficiency level of the GoBiGas plant.

The efficiencies presented in the results are based on the LHV of the dry ash-free fuel. Nevertheless, it is common practice on the European biomass market to use LHV based on the as-received fuel for establishing prices. As a comparison with the data from the literature, Table XII summarises the efficiencies of all the plant designs based on the LHVs of both dry ash-free biomass and as-received fresh biomass, with 50% moisture, which corresponds to the moisture content of biomass in the northern hemisphere directly after harvesting.

Table XII also includes a simulation of an intensively dried biomass (2% moisture w.b.), which can be achieved using steam dryers [31,32]. The three biomass cases with different moisture contents (2%, 8% and 40% moisture w.b.) are presented to demonstrate the benefit of investing in a biomass dryer upstream of the gasifier. Using the *K,S-act LT* design as reference, the value of η_{bCH4} based on the LHV of fresh biomass (50% moisture) is increased from 58.7% with natural drying at the storage site (40% moisture w.b.) to 72.8% with dried biomass (8% moisture w.b.), and finally to 74.5% with extensively dried biomass (2% moisture w.b.). Therefore, the benefit of drying the biomass is such that should justify the installation of a drying system.

CONCLUSIONS

The mass and heat balance of the gasification section in the GoBiGas plant were evaluated from the data collected in the first experimental campaign. The efficiency of biomass conversion in the GoBiGas gasifier was evaluated during an experimental series with potassium-activated olivine as the bed material and dried woody biomass (pellets with 8% moisture w.b.) as the fuel. Char gasification in the gasifier was 53.8% (SD, 4.7 pp), yielding a raw gas efficiency of 87.3%LHV_{daf} (SD, 1.9 pp). The fraction of volatile mass converted directly to methane was 34.1%$_{mass}$ (SD, 0.2), which is considered favourable for the biomethane process. The level of fuel conversion ensures high efficiency of the biomethane process, although because of the limitation associated with the design of a relatively small-scale unit, the high heat losses limit the cold gas efficiency. From the heat balance, the heat losses were calculated as 5.2% (SD, 0.6 pp) of the fuels LHV, which is higher than the reference values for biomass boilers. The heat losses were compensated by the combustion of product gas, yielding a cold gas efficiency of 71.7%LHV_{daf} (SD, 1.8 pp).

The activation of the bed material by potassium and sulfur has extended the operational range of the gasifier by reducing the yields of tar, or by enabling operation at lower temperatures. Both these conditions were investigated. The low-temperature case revealed up to 2.5 pp higher cold gas efficiency than the reference case (potassium-activated case), while maintaining the temperature and reducing the tar yield increased the cold gas efficiency by 1.2 pp. Therefore, decreasing the operational temperature while enhancing activation of the bed material with sulfur is an efficient approach to increasing the efficiency of a DFB gasifier. The biomethane efficiency achieved using potassium-sulfur activation and a reduced temperature was 63.3%LHV_{daf}, which approaches the project target of 65%LHV_{daf}, when using dried biomass (8% moisture).

The sensitivity analysis on the GoBiGas gasifier shows that reducing heat losses (to 1% of the energy of the fuel) and increasing pre-heating to 550 °C have the potential to increase the cold gas efficiency by 3 and 6 pp, respectively. These measures combined with a lower operational temperature through activation of the bed material with potassium and sulfur increase the cold gas efficiency to 83.5%LHV_{daf}, which is feasible with existing technologies and represents the state of the art for DFB gasifiers operated with dried biomass (8% moisture w.b.). The biomethane efficiency in these conditions is 71%LHV_{daf}, which is considerably higher than the GoBiGas target.

The penalty associated with using fresh biomass (40% moisture w.b.) rather than dried biomass (8% moisture w.b.) is approximately 16 pp for the cold gas efficiency and 14 pp for the biomethane efficiency, because of the increased combustion of product gas. The benefit of biomass drying prior to gasification was quantified by re-calculating the efficiency on the basis of the LHV as-received of the harvested biomass (50% moisture w.b.), which is used in the trades. Drying to 40%, 8% and 2% moisture contents results in biomethane efficiencies of 55.2%$LHV_{50\%}$, 70.3%$LHV_{50\%}$ and 72.2%$LHV_{50\%}$, respectively. Therefore, drying is crucial for the performance and economics of the plant.

Int. J. Energy Res. (2017) © 2017 The Authors. *International Journal of Energy Research* published by John Wiley & Sons Ltd.
DOI: 10.1002/er

A power-to-methane concept for the conversion of electricity to biomethane by direct heating of the gasifier reactor was evaluated, showing high-potential efficiency. The efficiency of the power-to-methane conversion can reach values as high as 105% (η_{P2G}), in an optimised process where the electricity provides heat to increase the gasification reaction. The overall efficiency of the process, including the electricity converted to methane, is in the range of 68.2%E_{tot} and 58.7%E_{tot} for the dried and moist biomasses, respectively. These efficiencies are significantly higher than those of power-to-methane processes based on electrolysis (rated in the range of 45–55% based on LHV). Therefore, biomass gasification can also play a major role in the conversion of intermittent electricity sources to renewable biofuels.

To explore the potential of a highly optimised stand-alone plant, a design with conversion of electricity that is locally produced at the plant was evaluated. Assuming that the electricity demand of the plant (3.75% of the energy of the fuel) and the electricity sent to the gasifier (3% of the energy of the fuel) are produced from the excess heat in the process, the efficiency of the process is increased to 70.2%E_{tot} with dried biomass (8% moisture) and 60.5% E_{tot} with moist biomass (40% moisture). This option is suitable for large plants (>100 MW_{fuel}), where the installation of a steam cycle is an economically viable option. To achieve higher levels of efficiency, it is necessary to dry further, pre-heat the fuel and lower the operating temperature.

In summary, the fuel conversion and the efficiency in the gasification section of the GoBiGas plant were estimated, revealing the strong potential of dual fluidized bed gasification for large-scale production of advanced biofuels. The data provided represent the first real reference, from a commercial scale plant, at support of the numerous investigations on techno-economic analysis and modelling of energy system.

NOMENCLATURE

Symbols	Unit	Description
a, b, c, d	mol/kg_{daf}	Stoichiometric coefficients
El	MJ_{el}/h	Electricity to the DFB gasifier
El_{tot}	MJ_{el}/h	Total electricity demand in the plant
E_s	MJ/h	Chemical energy in the *s*-th stream calculated from the LHV
H_s	MJ/h	Enthalpy term for the *s*-th stream
$\dot{m}_f$	kg_{daf}/h	Fuel feed to the gasifier
$\dot{m}_{C,PG}$	kg_{daf}/h	Carbon flow in the product gas
$\dot{m}_{C,FG}$	kg_{daf}/h	Carbon flow in the flue gas
$\dot{m}_{C,RME}$	kg_{daf}/h	Carbon flow in the RME
$n_{C,H,O}$	mol/kg_{daf}	Molar yield of the C, H and O
$n_{C,(ch,v,\ rg)}$	mol/kg_{daf}	Molar yield of the carbon in char, volatile and raw gas
$-n_{O,(f,ch,v)}$	mol_O/kg	Stoichiometric oxygen for combustion
η_{RG}	MJ/MJ_{fuel}	Raw gas efficiency
η_{CG}	MJ/MJ_{fuel}	Cold gas efficiency
η_{bCH4}	MJ/MJ_{fuel}	Cold gas efficiency
η_{sect}	MJ/MJ_{tot}	Gasification section efficiency
η_{plant}	MJ/MJ_{totl}	Plant efficiency
η_{P2G}	MJ_{bCH4}/MJ_{el}	Power-to-gas efficiency
Q_{iHD}	MJ/kg_{daf}	Internal heat demand of the gasification reactor
$Q_{l,tot,(comb)}$	MW	Heat losses total and combustor
$Y_{C,f}$	kg_C/kg_{daf}	Carbon yield in the fuel
λ_a	–	Air-to-fuel equivalence ratio
λ_{Otr}	mol_{Otr}/$mol_{O,f}$	Total oxygen transport equivalence ratio
λ_{ch}	mol_{Otr}/$mol_{O,ch}$	Oxygen transport to char equivalence ratio
λ_v	mol_{Otr}/$mol_{O,ch}$	Oxygen transport to volatiles equivalence ratio
X_g	–	Fraction of char gasified
Z_i	–	Fraction of volatile matter converted to the formation of the *i*-th combustible raw gas compound

Subscripts	Terms	Description
i	H_2, CO, CH_4, C_2H_4, C_3H_6, tar, BTX	Raw gas compounds: H_2, CO, CH_4, C_2H_4, C_3H_6, tar (removed in the RME scrubber), BTX (removed in the carbon beds)
s	*f*, *f a.r.*, *ch*, *v*, *syn*, *i*, *RG*, *PG*, PG_{rec}, *CG*, *OC*, *tar*, *RME*, *a*, *st*, *pur*, RME_{mix}, K_{mix}, *bCH4*	Streams: dry ash-free fuel, fuel as received, char, volatiles, syngas, raw gas compound, raw gas, product gas, re-circulated product gas, cold gas, organic compounds, tar, combustion air, steam, purge gas, RME and water, K_2CO_3 and water, biomethane

(*Continues*)

Int. J. Energy Res. (2017) © 2017 The Authors. *International Journal of Energy Research* published by John Wiley & Sons Ltd.
DOI: 10.1002/er

ACKNOWLEDGEMENTS

This work was supported by Göteborg Energi AB, Metso Power AB and the Competency Center of the Svenskt Förgasningscentrum (SFC), in collaboration with the Swedish Energy Agency.

REFERENCES

1. Cooper BL, London JR, Mellon RJ, Behrens MA. Chapter 4: integrated forest biorefineries: product-based economic factors. In *Integrated Forest Biorefineries: Challenges and Opportunities*. The Royal Society of Chemistry, 2013; 98–116.
2. Lange JP. Lignocellulose conversion: an introduction to chemistry, process and economics. *Biofuels, Bioproducts and Biorefining* 2007; **1**(1):39–48.
3. Foust TD, Aden A, Dutta A, Phillips S. An economic and environmental comparison of a biochemical and a thermochemical lignocellulosic ethanol conversion processes. *Cellulose* 2009; **16**(4):547–565.
4. Zinoviev S, Muller-Langer F, Das P, Bertero N, Fornasiero P, Kaltschmitt M, Centi G, Miertus S. Next-generation biofuels: survey of emerging technologies and sustainability issues. *ChemSusChem* 2010; **3**(10):1106–1133.
5. Demirbas A. Biorefineries: current activities and future developments. *Energy Conversion and Management* 2009; **50**(11):2782–2801.
6. Wang B, Gebreslassie BH, You FQ. Sustainable design and synthesis of hydrocarbon biorefinery via gasification pathway: integrated life cycle assessment and technoeconomic analysis with multiobjective superstructure optimization. *Computers & Chemical Engineering* 2013; **52**:55–76.
7. Sikarwar VS, Zhao M, Clough P, Yao J, Zhong X, Memon MZ, Shah N, Anthony EJ, Fennell PS. An overview of advances in biomass gasification. *Energy & Environmental Science* 2016.
8. Zhang LH, Xu CB, Champagne P. Overview of recent advances in thermo-chemical conversion of biomass. *Energy Conversion and Management* 2010; **51**(5): 969–982.
9. Gunnarsson, I. *The GoBiGas Project*; 2011.
10. Gassner M, Marechal F. Thermo-economic optimisation of the polygeneration of synthetic natural gas (SNG), power and heat from lignocellulosic biomass by gasification and methanation. *Energy & Environmental Science* 2012; **5**(2):5768–5789.
11. Bridgwater AV, Toft AJ, Brammer JG. A techno-economic comparison of power production by biomass fast pyrolysis with gasification and combustion. *Renewable and Sustainable Energy Reviews* 2002; **6**(3):181–248.
12. Kalinci Y, Hepbasli A, Dincer I. Biomass-based hydrogen production: a review and analysis. *International Journal of Hydrogen Energy* 2009; **34**(21):8799–8817.
13. Anex RP, Aden A, Kazi FK, Fortman J, Swanson RM, Wright MM, Satrio JA, Brown RC, Daugaard DE, Platon A, Kothandaraman G, Hsu DD, Dutta A. Techno-economic comparison of biomass-to-transportation fuels via pyrolysis, gasification, and biochemical pathways. *Fuel* 2010; **89**:S29–S35.
14. Brown TR, Brown RC. Techno-economics of advanced biofuels pathways. *RSC Advances* 2013; **3**(17):5758–5764.
15. Berdugo Vilches T, Marinkovic J, Seemann M, Thunman H. Comparing active bed materials in a dual fluidized bed biomass gasifier: olivine, bauxite, quartz-sand, and ilmenite. *Energy & Fuels* 2016.
16. Thunman H, Larsson A, Hedenskog M. *Commissioning of the GoBiGas 20MW Bio-methane Plant, TCBiomass*. Chicago: Chicago, 2015.
17. Burman Å. Experiences from the building and commissioning of the GoBiGas-pl. In SFC confernce, Gothenburg, 2016.
18. Biomass CHP station Senden. http://www.4biomass.eu/en/best-practice/project-biomass-chp-station-senden.
19. Pfeifer C, Hofbauer H. Development of catalytic tar decomposition downstream from a dual fluidized bed biomass steam gasifier. *Powder Technology* 2008; **180**(1–2):9–16.
20. Hofbauer H, Rauch R, Loeffler G, Kaiser S, Fercher E, Tremmel H. In Six years experience with the FICFB-gasification process, 12th European conference and technology exhibition on biomass for energy, industry and climate protection, 2002.
21. Larsson A, Seemann M, Neves D, Thunman H. Evaluation of performance of industrial-scale dual fluidized bed gasifiers using the Chalmers 2–4-MWth gasifier. *Energy & Fuels* 2013; **27**(11):6665–6680.
22. Milne TA, Abatzoglou N, Evans RJ, Laboratory NRE. *Biomass Gasifier "Tars": Their Nature, Formation, and Conversion*. National Renewable Energy Laboratory, 1999.
23. Rauch R, Pfeifer C, Bosch K, Hofbauer H, Swierczynski D, Courson C, Kiennemann A. In Comparison of different olivines for biomass steam gasification, Science in Thermal and Chemical Biomass Conversion, Victoria, Canada, 30th August to 2nd September 2004; Victoria, Canada, 2004.
24. Sutton D, Kelleher B, Ross JRH. Review of literature on catalysts for biomass gasification. *Fuel Processing Technology* 2001; **73**(3):155–173.
25. Campoy M, Gómez-Barea A, Fuentes-Cano D, Ollero P. Tar reduction by primary measures in an autothermal air-blown fluidized bed biomass gasifier.

Int. J. Energy Res. (2017) © 2017 The Authors. *International Journal of Energy Research* published by John Wiley & Sons Ltd.
DOI: 10.1002/er

Industrial and Engineering Chemistry Research 2010; **49**(22):11294–11301.
26. Abu El-Rub Z, Bramer EA, Brem G. Review of catalysts for tar elimination in biomass gasification processes. *Industrial and Engineering Chemistry Research* 2004; **43**(22):6911–6919.
27. Aranda G, van der Drift A, Vreugdenhil BJ, Visser HJM, Vilela CF, van der Meijden CM. Comparing direct and indirect fluidized bed gasification: effect of redox cycle on olivine activity. *Environmental Progress and Sustainable Energy* 2014; **33**(3):711–720.
28. Marinkovic J, Thunman H, Knutsson P, Seemann M. Characteristics of olivine as a bed material in an indirect biomass gasifier. *Chemical Engineering Journal* 2015; **279**:555–566.
29. Kirnbauer F, Wilk V, Kitzler H, Kern S, Hofbauer H. The positive effects of bed material coating on tar reduction in a dual fluidized bed gasifier. *Fuel* 2012; **95**(1):553–562.
30. Larsson A, Hedenskog M, Thunman H. Monitoring the bed material activation in the GoBiGas – gasifier. In *Nordic Flame Days Copenhagen*. 2015.
31. Fagernas L, Brammer J, Wilen C, Lauer M, Verhoeff F. Drying of biomass for second generation synfuel production. *Biomass and Bioenergy* 2010; **34**(9): 1267–1277.
32. Alamia A, Ström H, Thunman H. Design of an integrated dryer and conveyor belt for woody biofuels. *Biomass and Bioenergy* 2015, **77** (0), 92–109.
33. Zhang Y, Gong X, Zhang B, Liu W, Xu M. Potassium catalytic hydrogen production in sorption enhanced gasification of biomass with steam. *International Journal of Hydrogen Energy* 2014; **39**(9):4234–4243.
34. Fahmi R, Bridgwater AV, Darvell LI, Jones JM, Yates N, Thain S, Donnison IS. The effect of alkali metals on combustion and pyrolysis of *Lolium* and *Festuca* grasses, switchgrass and willow. *Fuel* 2007; **86**(10–11):1560–1569.
35. McKee DW. Fundamentals of catalytic coal and carbon gasification mechanisms of the alkali metal catalysed gasification of carbon. *Fuel* 1983; **62**(2):170–175.
36. Wang L, Hustad JE, Skreiberg Ø, Skjevrak G, Grønli M. A critical review on additives to reduce ash related operation problems in biomass combustion applications. *Energy Procedia* 2012; **20**:20–29.
37. Heyne S, Thunman H, Harvey S. Extending existing combined heat and power plants for synthetic natural gas production. *International Journal of Energy Research* 2012; **36**(5):670–681.
38. Gassner M, Maréchal F. Thermo-economic process model for thermochemical production of synthetic natural gas (SNG) from lignocellulosic biomass. *Biomass and Bioenergy* 2009; **33**(11):1587–1604.
39. Alamia A, Gardarsdòttir SÒ, Larsson A, Normann F, Thunmann H. Efficiency comparison of large-scale standalone, centralized and distributed thermochemical biorefineries. *Energy Technology* 2016, n/a-n/a.
40. Alamia A, Thunman H, Seemann M. Process simulation of dual fluidized bed gasifiers using experimental data. *Energy & Fuels* 2016; **30**(5):4017–4033.
41. Kroese DP, Brereton T, Taimre T, Botev ZI. Why the Monte Carlo method is so important today. *Wiley Interdisciplinary Reviews: Computational Statistics* 2014; **6**(6):386–392.
42. Karlbrink M. *An Evaluation of the Performance of the GoBiGas Gasificaiton Process*. Chalmers University of Technology, 2015.
43. Heyne S. *Bio-SNG from Thermal Gasification – Process Synthesis*. Chalmers University of Technology: Integration and Performance, 2013.
44. Götz M, Lefebvre J, Mörs F, McDaniel Koch A, Graf F, Bajohr S, Reimert R, Kolb T. Renewable power-to-gas: a technological and economic review. *Renewable Energy* 2016; **85**:1371–1390.
45. Gahleitner G. Hydrogen from renewable electricity: an international review of power-to-gas pilot plants for stationary applications. *International Journal of Hydrogen Energy* 2013; **38**(5):2039–2061.
46. Ursua A, Gandia LM, Sanchis P. Hydrogen production from water electrolysis: current status and future trends. *Proceedings of the IEEE* 2012; **100**(2):410–426.
47. Parthasarathy P, Sheeba KN. Combined slow pyrolysis and steam gasification of biomass for hydrogen generation – a review. *International Journal of Energy Research* 2015; **39**(2):147–164.
48. Jentsch M, Trost T, Sterner M. Optimal use of power-to-gas energy storage systems in an 85% renewable energy scenario. *Energy Procedia* 2014; **46**:254–261.
49. Zoss T, Dace E, Blumberga D. Modeling a power-to-renewable methane system for an assessment of power grid balancing options in the Baltic States' region. *Applied Energy* 2016; **170**:278–285.
50. Ebbesen SD, Jensen SH, Hauch A, Mogensen MB. High temperature electrolysis in alkaline cells, solid proton conducting cells, and solid oxide cells. *Chemical Reviews* 2014; **114**(21):10697–10734.
51. Nechache A, Cassir M, Ringuedé A. Solid oxide electrolysis cell analysis by means of electrochemical impedance spectroscopy: a review. *Journal of Power Sources* 2014; **258**:164–181.

SUPPORTING INFORMATION

Additional Supporting Information may be found online in the supporting information tab for this article.

Int. J. Energy Res. (2017) © 2017 The Authors. *International Journal of Energy Research* published by John Wiley & Sons Ltd.
DOI: 10.1002/er

Paper 3:

Efficiency Comparison of Large-Scale Standalone, Centralized, and Distributed Thermochemical Biorefineries

Efficiency Comparison of Large-Scale Standalone, Centralized, and Distributed Thermochemical Biorefineries

Alberto Alamia,*[a] Stefania Òsk Gardarsdòttir,[a] Anton Larsson,[a, b] Fredrik Normann,[a] and Henrik Thunman[a]

We present a comparison of three strategies for the introduction of new biorefineries: standalone and centralized drop-in, which are placed within a cluster of chemical industries, and distributed drop-in, which is connected to other plants by a pipeline. The aim was to quantify the efficiencies and the production ranges to support local transition to a circular economy based on biomass usage. The products considered are biomethane (standalone) and hydrogen/biomethane and sustainable town gas (centralized drop-in and distributed drop-in). The analysis is based on a flow-sheet simulation of different process designs at the 100 $MW_{biomass}$ scale and includes the following aspects: advanced drying systems, the coproduction of ethanol, and power-to-gas conversion by direct heating or water electrolysis. For the standalone plant, the chemical efficiency was in the range of 78–82.8 % $LHV_{a.r.50\%}$ (lower heating value of the as-received biomass with 50 % wet basis moisture), with a maximum production of 72 MW_{CH_4}, and for the centralized drop-in and distributed drop-in plants, the chemical efficiency was in the range of 82.8–98.5 % $LHV_{a.r.50\%}$ with maximum production levels of 85.6 MW_{STG} and 22.5 MW_{H_2}/51 MW_{CH_4}, respectively. It is concluded that standalone plants offer no substantial advantages over distributed drop-in or centralized drop-in plants unless methane is the desired product.

Introduction

The transition towards a circular economy that is based on biomass products requires the introduction of new biorefineries that respect the targets set in terms of sustainability and economic growth. In particular, thermochemical biorefineries based on the gasification of lignocellulosic biomass and waste can combine a large-scale production with a high conversion efficiency.[1–3] The development of gasification technology over the last few decades has resulted in several demonstration plants (1–32 $MW_{biomass}$)[4–9] with efficiencies from biomass to final product in the range of 50–65 % lower heating value dry ash-free (LHV_{daf}). However, to propel the desired breakthrough of biomass-based products it is necessary to improve the profitability levels of these plants, through the increase of the plant size and efficiency and by identifying economically viable opportunities for the chemical, transport, and energy sectors.

The strategies to be used for the introduction of new gasification plants are not only influenced by the local energy market (prices of feedstock and products) but also by the inherent trade-off between the economy of scale and the logistics of biomass for the plant. In particular, the investment cost for the handling and preparation (which includes drying) of the feedstock is considerable because of the low energy density and high moisture content of the fresh biomass.[10–12] Therefore, the profitability of new plants is affected by the availability of existing infrastructure for biomass handling and of other heat sources for drying, for example, waste heat from existing industrial sites.

The strategies to be applied for the introduction of biomass gasification plants, which are highly dependent upon regional conditions, fall into three main groups: standalone, which produces biofuel or chemicals; centralized drop-in, for a cluster of chemical industries; and distributed drop-in, which involves a connection to a network of chemical plants (Figure 1). Standalone plants[12–16] have their own biomass handling and product distribution facilities, which entail either a pipeline (e.g., biomethane) or a truck/ship (other biochemicals). In contrast to the standalone plants, centralized drop-in plants[17–19] serve a low number of customers located closely (i.e., a cluster of industries) with an intermediate product, which can substitute a fossil equivalent at the customer's site directly. Typically, this intermediate is a nitrogen-free gas with a composition that varies from pure H_2, which is highly desirable for chemical plants based on oil, to a mixture of H_2 and CO, and CO_2, which may also include significant amounts of CH_4 and other hydrocarbons. The distribution pressure is moderate (10–20 bar) so that gases with high dew-points and a significant fraction of CO_2 can be transported. This reduces the complexity of the centralized

[a] A. Alamia, S. Òsk Gardarsdòttir, Dr. A. Larsson, Dr. F. Normann, Prof. H. Thunman
Division of Energy Technology
Chalmers University of Technology
Hörsalsvägen 7, 412-96, Gothenburg (Sweden)
E-mail: alamia@chalmers.se

[b] Dr. A. Larsson
Göteborg Energi AB
Fågelrovägen 16, 418 34 Gothenburg (Sweden)

The ORCID identification number(s) for the author(s) of this article can be found under http://dx.doi.org/10.1002/ente.201600719.

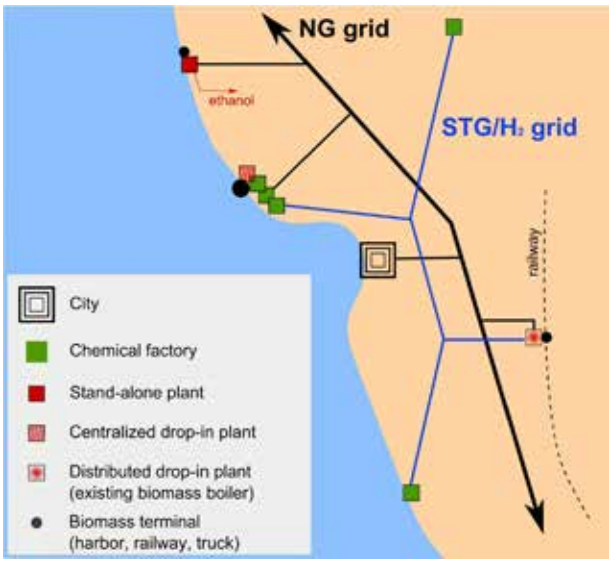

Figure 1. Differences between the three different implementation strategies for biomass gasification, that is, the standalone, centralized drop-in, and distributed drop-in gasification plants.

drop-in gasification plant compared to that of a standalone plant as the final product upgrade is performed by the existing equipment at the premises of the costumer. Further synergies can be achieved by, for example, integrating the steam cycle or utilizing existing methane reformers. However, an infrastructure for biomass handling (storage, drying, transport terminal, etc.) is often missing and needs to be built on an ad hoc basis. Distributed drop-in gasification plants are not integrated physically with the synthesis process at the customer's site but instead produce a nitrogen-free, intermediate product for distribution through a regional pipeline (Figure 1), herein termed "sustainable town gas" (STG). The main advantage of distributed drop-in plants is the possibility to build them at locations favorable for biomass logistics, that is, easily accessible by road, railway, and ship. In particular, existing biomass boilers and pulp mills have the required infrastructures (biomass handling, steam cycles, heat recovery network, and in many cases even dryers) to achieve a high performance through retrofitting or upgrading to gasification plants, although they lack a pipeline connection to the customers' plants. Another potential advantage of decentralization is the redundancy of the regional STG/H_2 pipelines with respect to the national gas grid, which offers flexibility to consumers in terms of seasonal variations of prices and the production of gasification-based products.

We present an analysis of proposed process designs for standalone, centralized drop-in, and distributed drop-in plants with the aim to quantify their efficiencies and production ranges. The results are intended to support the formulation of local strategies for the introduction of gasification processes as part of the transition to a circular economy. The evaluation was performed using process simulations in Aspen Plus based on the design of the GoBiGas plant,[7,20–22] which produces biomethane (also referred to as synthetic natural gas, substitute natural gas, or SNG) from biomass on a commercial scale and represents the state-of-the-art technology for highly efficient gasification.

Methodology

We focus initially on the evaluation of the state-of-the-art standalone biomethane plant operated on a commercial scale, with the introduction of a series of proposed improvements to the process. In the second phase of the study, process designs for distributed drop-in and centralized drop-in plants are analyzed and compared to those for standalone plants with a focus on the achievable efficiencies and product ranges. The process design for the standalone plant was based on that of the GoBiGas plant[7,20,22,23] in Gothenburg, Sweden, which is currently the largest plant in the world that combines biomass gasification technology and methane synthesis. The GoBiGas plant was constructed in 2014 as a demonstration plant with a capacity of 32 $MW_{biomass}$ (20 $MW_{biomethane}$) based on the lower heating value (LHV) of dry ash-free biomass and it uses predried feedstock.[22] The biomethane produced has a methane content $>96\,\%_v$, which is injected into the national natural gas grid. In this investigation, a plant size of 100 $MW_{biomass}$ is used as the reference, in which 100–300 $MW_{biomass}$ would be considered optimal for commercial gasification plants.[24,25] The feedstock has a moisture content of 40 % on a wet basis (w.b.) and the effects of dryers (not included in the GoBiGas design) that are integrated with the heat recovery network and steam cycle are analyzed.

Other aspects investigated for the standalone strategy were: (i) the possibility to introduce power-to-gas technologies to increase the production of methane; and (ii) the coproduction of methane and ethanol. Power-to-gas technologies are of interest because electricity can be added intermittently to a continuous production process, which thereby enables conversion from intermittent renewable energy sources.

Furthermore, the surplus of electricity generated from the excess heat in the process can be converted to methane to recirculate energy in the process. Two power-to-gas technologies were investigated: a traditional process based on the electrolysis of water and the direct heating of the gasifier to reduce char combustion.[22] The coproduction of methane and ethanol was considered as ethanol is the main drop-in alternative to gasoline on the market. The biochemical pathway (syngas fermentation) to ethanol was selected as it offers a high efficiency, tolerates sulfur impurities in the syngas (in contrast to metallic catalysts), and is less affected by inert gases, such as methane. Furthermore, the production technology has recently reached the stage of maturity necessary for industrial applications.[26,27]

The high-energy demand for distillation is a key issue to achieve a high efficiency for ethanol production, and the direct integration of the distillation process into the rest of the plant would lead to an overall low efficiency as extensive streams with high exergy would be used to meet a demand that could instead be achieved using a low-exergy stream.

However, the water/ethanol mixture can be stored in regular tanks, which provides an opportunity to use the distillation process to balance the load of other low-temperature heat sources, for example, a district heating plant, or to balance the electricity demand within the grid. This confers advantages upon the local/regional energy system that can motivate the production of ethanol.

In the investigation of centralized drop-in and distributed drop-in plants, two possible nitrogen-free intermediate products are considered: STG, that is, upgraded syngas from biomass gasification, and hydrogen. The major difference between the two intermediates is the presence in the STG of CH_4 (5–15 $\%_v$), which is a typical product of biomass gasification. As chemical factories reform CH_4 to syngas, its production during gasification is rather a penalty than a benefit, contrary to that in the biomethane process. However, the reforming of renewable methane is questionable as it is a valuable product on the biofuel market. Therefore, the two intermediates taken into consideration represent two extreme choices: (i) STG for supply to industries already equipped with a natural gas reformer and (ii) hydrogen obtained by separation (coproduction) in the biomethane process. The separation of hydrogen in the biomethane process was investigated by using vacuum pressure swing adsorption (VPSA). Both intermediate products can be produced by distributed drop-in and centralized drop-in plants, although STG is considered more suitable for distributed production and distribution because of its lower energy demand for compression.

Investigated designs and system boundaries

We focus on four design classes (Figure 2 and Table 1). The classification is based on the final product of the process. Designs of class A produce biomethane, class B designs produce methane and ethanol, class C designs produce methane and/or STG, and class D designs produce biomethane and hydrogen. The process analysis includes the gasification and gas synthesis as well as the steam cycle for heat recovery and electricity production, which is not included in the current GoBiGas process. The outline of the gasification plant and methane synthesis are common to all the designs and are based on the layout of the GoBiGas plant (outlined in black in Figure 2 and described in greater detail in a later section). Briefly, the gasification plant includes a gasification section that is based on dual fluidized bed (DFB) technology and tar removal stages, and the produced syngas is subsequently compressed and delivered to the premethanation section or to the STG grid (Figure 2c). In the premethanation section, the gas undergoes further cleaning steps (hydrogenation of olefins, removal of H_2S and CO_2), a water gas shift (WGS) reaction, and an initial premethanation reaction. In the final methanation section, the syngas is converted fully to methane in a four-stage direct methanation process and then

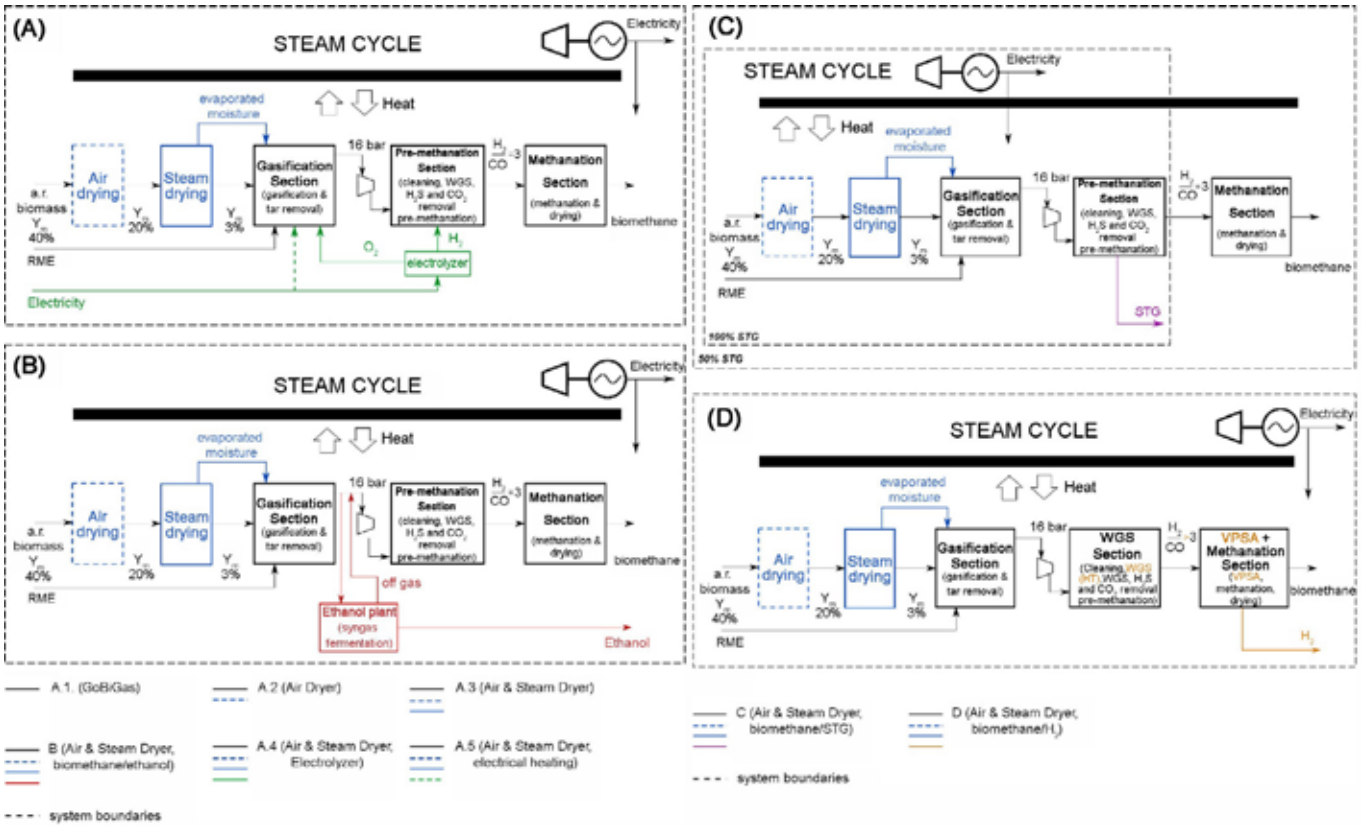

Figure 2. a, b) Designs A.1–5 for a standalone biomethane plant and design B for a plant with the coproduction of ethanol. c, d) Designs C and D for the coproduction of STG/biomethane and H_2/biomethane, respectively, in a distributed/centralized drop-in plant.

Table 1. Designs of the plants used in the present investigation.

Design	Product 1	Product 2	Strategy	Networks	Power-to-gas	Drying
A.1	biomethane	–	standalone	NG[a], electricity	no	none
A.2	biomethane	–	standalone	NG, electricity	no	single-stage[b]
A.3	biomethane	–	standalone	NG, electricity	no	double-stage[c]
A.4	biomethane	–	standalone	NG, electricity	electrolysis	double-stage[c]
A.5	biomethane	–	standalone	NG, electricity	direct heating	double-stage[c]
B	biomethane	ethanol	standalone	NG, electricity, ethanol	no	double-stage[c]
C	STG	biomethane[d]	centralized/ distributed	STG, electricity, NG[d]	no	double-stage[c]
D	hydrogen	biomethane	centralized/distributed	hydrogen, NG, electricity	no	double-stage[c]

[a] NG: natural gas. [b] Air-drying. [c] Air- and steam-drying with moisture recovery as the gasification agent. [d] Optional.

dried to achieve a methane content $>96\,\%_v$. The modifications made to the other designs are highlighted in color (Figure 2a–d).

A detailed list of the investigated designs is given in Table 1. Compared to the GoBiGas design A.1, design A.2 includes additional air-drying of the fuel[28] in which the moisture content is reduced from 40 to 20% w.b. Design A.3 includes additional air-drying, complemented with a steam dryer that recovers the evaporated water as a gasification agent (which thereby reduces the steam demand for the gasifier). Design A.3 is used as the base case for the standalone biomethane plant and for the distributed/centralized drop-in plants. Designs A.4 and A.5 evaluate two power-to-gas concepts. The first concept includes an electrolyzer that feeds hydrogen to the syngas in the premethanation section (A.4). In the second design concept, the gasifier is heated electrically (A.5). The power-to-gas designs can use both the electricity produced from the excess heat in the plant and electricity derived from intermittent energy sources (wind and solar) and drawn from the grid.

The maximum production level of ethanol is obtained by considering the entire syngas flow, although the production can be shifted towards methane, which thereby bypasses the fermentation plant. A similar approach is applied in design C, in which STG is produced in a distributed/centralized drop-in plant (Figure 2c). Design D is used to investigate the coproduction of biomethane and hydrogen by the VPSA separation upstream of the final methanation step. In this case, an additional WGS reactor is introduced at high temperature (400 °C) to maximize the production of hydrogen.

Process layout and modeling

The process simulations were performed by using Aspen Plus using hierarchy blocks with submodels of different process equipment and Fortran routines. The flow-sheet model has been validated against data from the GoBiGas plant[7,22] (Table 2), together with additional measurements brought forward to this work (see later, Table 4). The heat integration in the plant is evaluated and optimized by applying a pinch analysis,[30] in which the heat recovery network is complemented with biomass dryers and a steam cycle for the production of electricity. The overall property method used, unless stated otherwise, is the Peng–Robinson equation of state with Boston–Mathias modification.

Table 2. Experimental data from the GoBiGas plant (gasification section).

DFB gasifier	HT	LT
gasifier bed temperature [°C]	870	820
raw gas temperature [°C]	815	800
combustor temperature [°C]	920	870
max. steam temperature [°C]	550	550
maximum air temperature [°C]	550	550
flue gas temperature [°C]	140	140
fluidization steam [$kg\,kg_{daf}^{-1}$]	0.5	0.5
stoichiometric ratio combustor	1.2	1.2
purge gas (CO_2) flow [$kg\,kg_{daf}^{-1}$]	0.1	0.1
gas composition	HT	LT
H_2 [$vol\,\%_{dry}$]	42.1	39.9
CO [$vol\,\%_{dry}$]	24.1	24.0
CO_2 [$vol\,\%_{dry}$]	23.5[a]	25.3[a]
CH_4 [$vol\,\%_{dry}$]	8.6	7.7
C_2H_2 [$vol\,\%_{dry}$]	0.13	0.13
C_2H_4 [$vol\,\%_{dry}$]	2.0	1.9
C_2H_6 [$vol\,\%_{dry}$]	0.19	0.19
C_3H_6 [$vol\,\%_{dry}$]	0.001	0.001
H_2O [vol%]	6.3[b]	6.3[b]
total tar [$g\,Nm^{-3}$]	10	20.5
BTX [$g\,Nm^{-3}$]	3	7

[a] net of the purge gas; [b] saturated

Process design based on GoBiGas

The layout of design A.1 (GoBiGas) is presented in Figure 3, and all the experimental data used in the simulations are reported in Figure 3 and Tables 2 and 3. The submodel used for the DFB gasifier is based on a previous study[29] in which experimental data (Table 3) were used to calculate a set of fuel conversion variables that describe the gasification and combustion processes. The experimental data are taken from a previous evaluation of the GoBiGas gasifier[22] with full closure of the mass balance, and with an operation range that varies between two operating conditions: high-temperature (HT) operation with gasification at 870 °C and a tar content of 10 $g\,Nm^{-3}$; and low-temperature (LT) operation with gasification at 820 °C and a tar content of 20.5 $g\,Nm^{-3}$. The fuel conversion variables include char gasification X_g, oxygen transport, and the fraction of volatile matter that is convert-

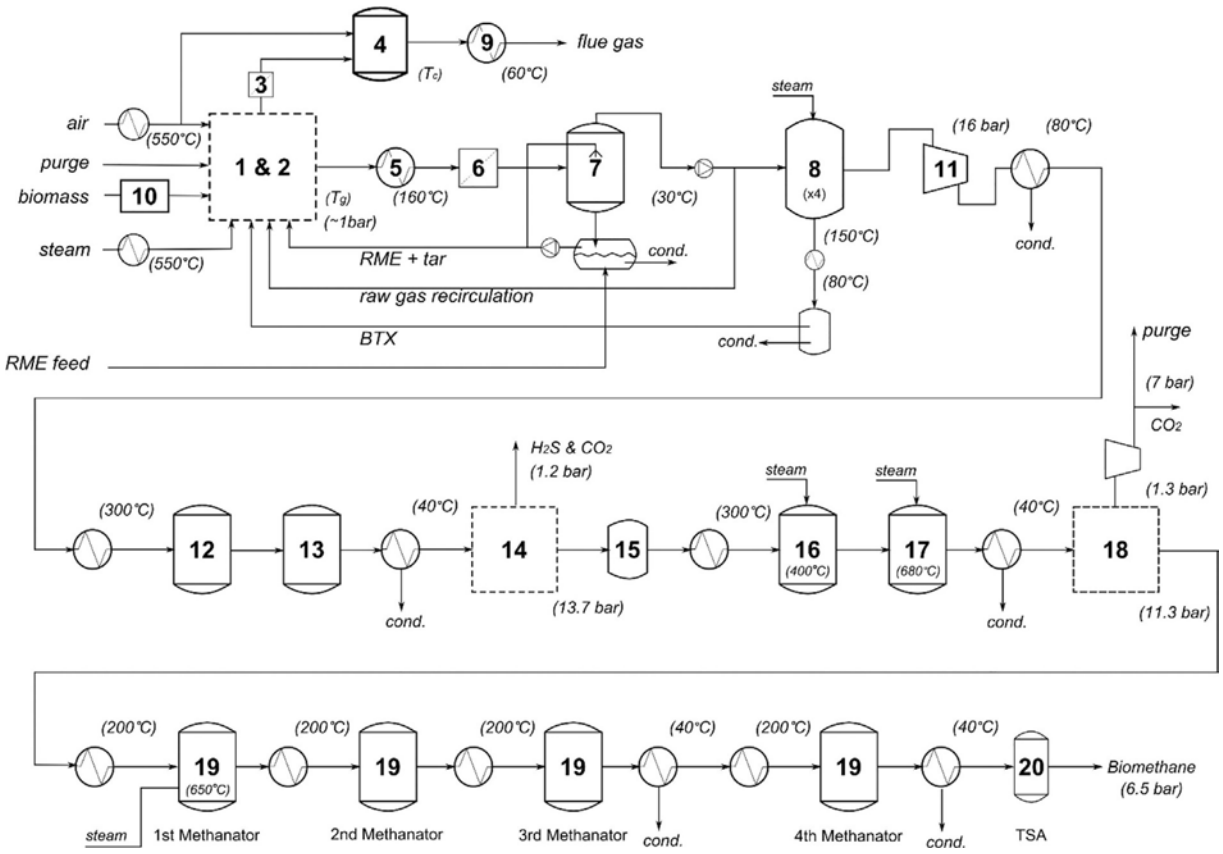

Figure 3. Process flow-sheet of the GoBiGas design at 100 $MW_{biomass}$. Designations: 1 gasifier (separate DFB submodel)[29]; 2 combustor (separate DFB submodel); 3 cyclone; 4 postcombustion chamber; 5 raw gas cooler; 6 raw gas filter; 7 RME scrubber; 8 carbon beds; 9 flue gas train; 10 fuel feeding system; 11 product gas compressor; 12 olefins hydrogenator; 13 COS hydrolyzer; 14 H_2S removal (separate submodel); 15 guard bed; 16 WGS; 17 premethanation; 18 CO_2 removal (separate sub-model); 19 methanation; 20 TSA drying.

ed to each of the energy-carrying compounds of the raw gas. One advantage of this approach is that the heat balance can be extrapolated for different conditions.[22,29] This method enables the transfer of experimental knowledge from smaller facilities to a larger plant, which can differ with respect to heat losses, preheating of ingoing streams, moisture content of the feedstock, and other parameters that affect the efficiency of the process. Compared to the GoBiGas plant (32 $MW_{biomass}$), the heat balance in the flow-sheet (100 $MW_{biomass}$, design A.1) is modified to account for the preheating of the steam and air to a higher temperature (550 °C instead of the 350 °C used in the current operation) and reduced heat losses, from 5.2% of the energy in the fuel[22] (current design) to 0.5–2.5%, compared to the heat losses of the circulating fluidized bed (CFB) boilers of a relevant size.[31]

The flue gas from the combustion side of the DFB gasifier is directed to a postcombustion chamber (**4** in Figure 3), which is then used to combust the off-gases and slipstreams. The sensible heat in the flue gases is then recovered through heat exchange (**9**). The raw gas produced is cooled (**5**), and any particles are removed by passing through a textile-bag filter (**6**), before it enters the tar scrubber (**7**). A continuous flow of rape methyl esters (RME) is fed into the scrubber to avoid saturation by naphthalene, which is the main tar component removed in this stage. The used RME and the extracted tar are fed to the combustor to provide additional heat to the gasification process.

Downstream of the scrubber, a fan controls the gas flow through the gasifier and enables the recirculation of raw gas to the combustor, which thereby provides extra heat to the gasification process if necessary. A minimum level of recirculation of the raw gas is required to stabilize the temperature in the gasification system and to cope with fluctuations in the moisture content of the fuel. Light cyclic hydrocarbons, mainly benzene and small fractions of toluene and xylene (referred to as BTX) remain in the gas at this point and they are removed in the subsequent section through a series of three fixed beds that are filled with active carbon. The plant has four active carbon beds (**8**), which enable the steam regeneration of one bed at all times. The off-gases from the regeneration are condensed to recover heat, and the extracted tar compounds are fed to the combustor. Notably, for large plants, a scrubber might be a suitable alternative to the carbon beds, although this issue is outside the scope of the present study.

The syngas derived from the gasification requires further cleaning and shift stages to achieve the level of purity and

Table 3. Data from GoBiGas plant (tar removal and H_2S and CO_2 removal sections).

Tar cleaning		
cooler temperature [°C]	160	
maximum tar content in raw gas [g Nm^{-3}]		25
fresh RME flow [MW_{RME}/MW_{fuel}]		3.0
temperature of RME scrubber [°C]		35
average flow of steam to carbon bed [kg kg_{BTX}^{-1}]		9.2
temperature of steam to carbon beds [°C]		250
pressure of steam to carbon beds [bar]		3.8
amine processes	H_2S removal	CO_2 removal
absorber pressure [bar]	13.7	11.3
stripper pressure [bar]	1.2	1.3
solvent concentration in CO_2-unloaded solution, MDEA/PZ [wt%]	37.5/0	35.2/6.3
lean solvent loading [mol_{CO_2} $mol_{solvent}^{-1}$]	0.02	0.28
heat requirement for solvent regeneration [MJ $kg_{CO_2}^{-1}$]	2.24	0.83
electricity requirement [MW]	0.05	0.09
cooling requirement [MW]	4.09	2.37
H_2S removal rate [%]	59	–
H_2S concentration in clean gas [ppm]	0.01	–
CO_2 removal rate [%]	56	95
CO_2 concentration in clean gas [$\%_v$]	13.8	2.5
CO_2 final pressure [bar]	1.2	7

composition required for the final synthesis of methane. The pressure in the premethanation section is increased to 16 bar through a six-stage intercooled compressor to meet the requirements for the hydration of olefins and COS (carbonyl sulfide) in reactors **12** and **13**. Notably, the pressure level is not set by the methanation stages, as assumed in some previous studies. The subsequent cleaning steps include the H_2S (**14**) and CO_2 (**18**) separation processes, which rely on selective chemical absorption using amines under pressurized conditions, in which methyl diethanolamine (MDEA) is used in the former process and a MDEA + piperazine (MDEA + PZ) mixture is used in the latter.

The high pressure in the premethanation section is decreased partially in the CO_2 separation stage (Figure 4) to reduce the heat consumption in the reboiler significantly (Table 3).The simulation of the H_2S and CO_2 separation processes is performed separately in two submodels using a rate-based approach, the Aspen Plus built-in electrolyte NRTL method and the Redlich–Kwong equation of state to compute liquid- and vapor-phase properties, respectively. The absorption and stripper columns are modeled as multistage packed columns that use the IMTP™ packing material. The compositions of the solvents and the energy input for solvent regeneration are based on data obtained from the GoBiGas plant.

The removal of the H_2S is modeled according to the work of Bolhàr-Nordenkampf et al.[32] who used a standard absorber–desorber setup with a lean–rich solvent heat exchanger between the columns. The submodel for CO_2 removal (Figure 4) is based on the layout of the GoBiGas plant and includes standard process units as well as additional two-

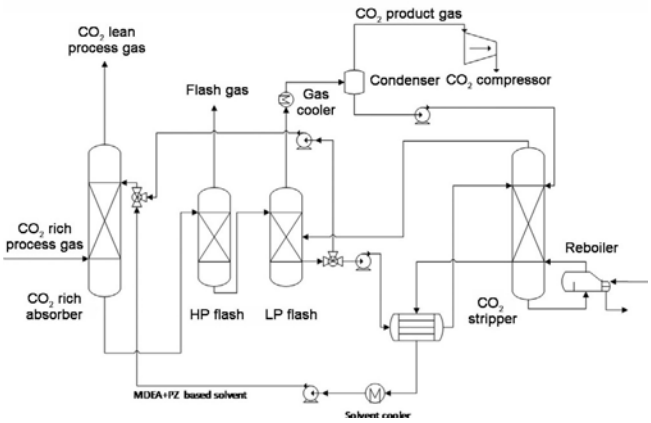

Figure 4. Submodel for the separation of CO_2.

stage flashing of the CO_2-rich solvent between the absorber and the cross-heat exchanger. The CO_2 removed in the first scrubber-absorber is contaminated with H_2S, whereas that removed during the second process is of higher purity and is compressed to 7 bar for use as a purge gas. Both CO_2-containing streams are suitable for use in carbon capture and storage (CCS), which would create a negative CO_2 impact for the use of this biomass.

The gasification plant has the potential to become a carbon-negative facility by combining bioenergy with carbon capture and storage (BECCS).[33] BECCS requires additional on-site compression to 70–110 bar for the transportation and storage of the CO_2.[34] CO_2 storage for climate mitigation is a clear use for the separated CO_2, so the concept of BECCS has been discussed as a promising tool to attain stringent climate mitigation targets.

A guard bed (**15**) is located upstream of the reactors with a sulfur-sensitive catalyst to protect it from possible contamination. The WGS reactor (**16**) is operated at approximately 300 °C, and the H_2/CO ratio is increased from the original value of approximately 1.7 to the optimal value for the synthesis of methane of >3. Thereafter, the syngas is directed to a premethanation reactor, in which some of the CO and CO_2 is converted to CH_4 (**17**) and the C_2 and C_3 hydrocarbons are cracked; as these reactions are strongly endothermic, and the temperature increases to around 680 °C. The methanation process (**19**) is a proprietary Haldor Topsøe technology named TREMP,[35] which is based on the MCR methanation catalyst. The main characteristic of this system is the high temperature increase allowed in a single reactor (up to 500 °C[36]), which results in a very low (or zero) recycle ratio. The fixed-bed design of the reactors enables the recovery of excess heat in the form of high-pressure superheated steam. In the GoBiGas plant (Figure 3), four methanation reactors without recycling are applied, followed by a final drying stage based on temperature swing adsorption (TSA), which then meets the purity target (>96 $\%_v$ methane, <0.5 $\%_v$ CO, <1 $\%_v$ H_2). The methanation reactors are simulated as Gibbs reactors with a maximum temperature in the first stage of <680 °C. Steam is added before the first methanation stage

to avoid carbon formation on the catalyst. The final product is delivered at 6.0–6.5 bar to the compression station (not included in the process analysis), in which the pressure is once again increased to 30 bar to enable injection into the natural gas network.

Additional modeling of process equipment

Dryers

The modeling of the air dryer is based on the work conducted by Holmberg and Ahtila,[28] which involves single-stage drying without recycling, and the modeling of the steam dryer follows the work of Alamia et al.[37] The steam-drying is divided into three stages with steam temperatures of 150, 120, and 150 °C to dry and preheat the biomass. The concept enables a moisture content of <5% w.b. with the extraction of the evaporated moisture in the final two stages to yield a final moisture temperature of around 150 °C. The moisture recovery corresponds to a saving of 0.2–0.25 $kg_{H_2O}\,kg_{daf}^{-1}$ of the gasification steam (drying from 20 to 3–5% w.b.), which represents approximately half of the steam used in the DFB gasifier. The specific work consumption is calculated from the results of the CFD and Aspen simulations of the dryer, as presented previously[37] (Table 4).

Power-to-gas

Power-to-gas processes based on electrolysis are commercially available.[38–40] In a biomethane plant, electrolysis is operated at 10 bar, and the hydrogen is injected after the WGS reactor to adjust the H_2/CO ratio before methanation. Compared to the standalone electrolysis processes, integration in a biomethane plant is particularly favorable because of the existing methanation reactor and the renewable CO and CO_2 already present in the syngas, which otherwise would have to be obtained from other processes. Furthermore, the oxygen can be used in the combustor to reduce the inlet air flow, so the only equipment required is the electrolyzer. In the flowsheet model, the electrolyzer is simulated from data obtained previously with regard to the alkaline electrolyzer[41] module of 3.5 MW_{el} electrical capacity, based on the original Lurgi technology.[42] This represents the state of the art in large-scale alkaline electrolyzers and it is currently used in several plants. The input data used in the simulations are summarized in Table 4. The heat released during the electrolysis process is not accounted for in the pinch analysis because of the low outlet temperature of the cooling stream (<50 °C) associated with the current design of the unit. A retrofit of the current design of the electrolyzer is outside the scope of this work. To calculate the range of operation of the electrolysis process, two cases are investigated: $zero_{El}$, in which only the electricity produced in the plant is converted; and the maximum electricity case (max_{El}), in which electricity from the grid is used to achieve the H_2/CO ratio for methanation without a WGS reactor.

Table 4. Literature data for modeling.

System and parameters	Data
air dryer[28]	
air temperature [°C]	95
specific heat consumption [kJ $kg_{H_2O}^{-1}$]	2900–2750
specific work consumption [kJ $kg_{H_2O}^{-1}$]	20–150
recirculation rate [%]	0–15
steam dryer: three stages[37]	
steam temperatures [°C]	150, 120, 150
specific heat consumption [kJ $kg_{H_2O}^{-1}$]	2310
specific work consumption [kJ $kg_{H_2O}^{-1}$]	352
final biomass temperature [°C]	112
recovered moisture temperature [°C]	150
syngas fermentation[26,27,44–46]	
inlet pressure [bar]	1.8[26]
makeup process water [t t_{eth}^{-1}]	8.5[26]
overall CO conversion [%]	50[44]–80[45]
overall H_2 conversion [%]	45[44]–75[45]
char gasification	
char gasification range [%]	40–70
electrolyzer[41]	
pressure [bar]	10
electricity consumption [kWh $Nm_{H_2}^{-3}$]	4.5
VPSA[47]	
syngas inlet pressure [bar]	13.2
pressure drop of H_2 [bar]	0.1
pressure ratio of CH_4-rich gas	16.5
compression of CH_4-rich gas [bar]	7.5
H_2 recovery [%]	75–95 (max)
high-temperature WGS [°C]	400
steam cycle	
steam pressure [bar]	100
steam temperature [°C]	580
cold utility temperature [°C]	15
minimum vapor fraction in turbine	0.88
number of pressure levels in the plant	2–5
ΔT_{min} [°C]	5–10
turbine isentropic efficiency	0.78–0.93

Power-to-gas conversion through the direct heating of the DFB gasifier can be achieved by introducing a resistance heater into the DFB gasifier or by further preheating the inlet gases.[22] The effect is a reduction of the internal heat demand of the gasifier, which thereby reduces char combustion and increases char gasification. The main advantage of this process over electrolysis is its higher efficiency as almost all the electricity provided is stored in the forms of gasification products and it has lower investment costs. A technical limitation of this technology is the maximum gasification of char that results from the conversion of biomass in the gasifier. This is limited arbitrarily to 70% in the simulations based on the current gasification level in the GoBiGas plant (≈54%[22]) with the assumption that it can be increased by optimizing the reactor design, the catalytic effects of the ash compounds,[20,43] and the heat balance in the DFB reactors. The range of operation is calculated by investigating the $zero_{El}$ case and the maximum gasification case max_{El}.

Ethanol fermentation

Ethanol can be produced by syngas fermentation[27,45,48,49] that uses fermenting organisms that have high tolerances for contaminants, such as sulfur and some tar compounds. The modeling of the fermentation process is based on the LanzaTech design for the steel-manufacturing industry as it currently is the most advanced design in terms of scale reported previously and is already in production in two plants in China,[26,46] with an output capacity of 300 tonnes per year (0.35 MW).[46] The technology used for fermentation to produce syngas from gasification was recently (May 2016) acquired by Aemetis, which is planning the construction of a plant with a capacity of 24 tonnes per year, to be completed in 2017, followed by expansion to 96 tonnes per year.[50] In the LanzaTech process, the syngas is introduced into the bioreactor and mixed with the liquid medium that contains the biocatalyst (the bacterium *Clostridium autoethanogenum*), which is consumed throughout the reactor. The product at the outlet of the reactor is directed to the steadfast separation system (which includes distillation), which recycles the liquid that contains the microorganisms to the bioreactor and separates the main product from the byproducts.[26] As the information available from the process manufacturers is limited, the flow-sheet simulation (Figure 5) is modeled by introducing data from other studies [Eqs. (1)–(4)].

$$4\,CO + 2\,H_2O \rightarrow CH_3COOH + 2\,CO_2 \quad (1)$$

$$4\,H_2 + 2\,CO_2 \rightarrow CH_3COOH + 2\,H_2O \quad (2)$$

$$6\,CO + 3\,H_2O \rightarrow C_2H_5OH + 4\,CO_2 \quad (3)$$

$$6\,H_2 + 2\,CO_2 \rightarrow C_2H_5OH + 3\,H_2O \quad (4)$$

The fermentation process is simulated with a stoichiometric reactor using reactions (1)–(4). The conversion rates of CO and H_2 in the process are set at 50 and 45 %, respectively, according to previous data from studies with a gas that has a similar H_2/CO ratio.[27,44,51,52] However, higher conversion rates (c; for CO, 80 %; and for H_2, 75 %) can be achieved through extensive recycling.[45,46] As a result of a lack of published data, two cases are simulated ($c_{80\%}$ and $c_{50\%}$ in the results) to cover the whole range. The concentration of ethanol in the outlet liquid has not been reported for the demonstration units, which creates uncertainty with regard to the estimate of the distillation energy. Here, the final concentration of ethanol is set within the range of values reported previously: from 0.5[27] to 48 g L^{-1}.[53] The distillation energy is not accounted for in the analysis of the plant as other low-temperature energy sources can be involved and this would require a dynamic analysis of the local/regional system, which is outside the scope of this work. For this reason, the results for the ethanol process are presented based on the ethanol/water mixture that exits the fermentation reactor.

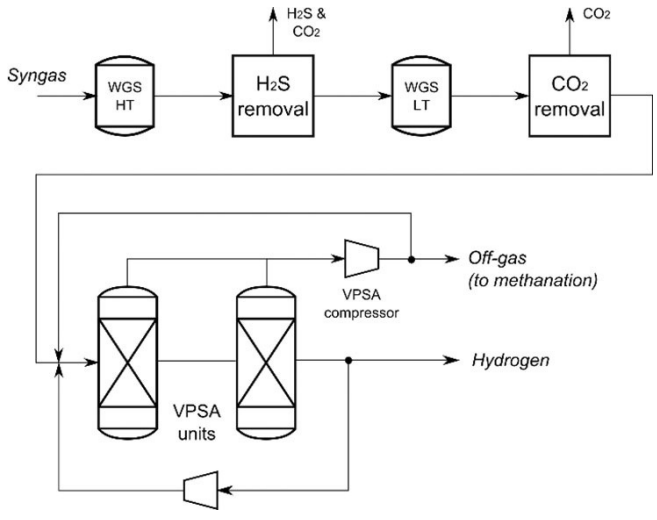

Figure 5. VPSA design scheme (syngas from the COS reactor and heat exchangers and condensers not included).

Vacuum pressure swing adsorption (VPSA)

A VPSA[47,54] unit for hydrogen separation is selected to minimize electricity consumption, if we consider the pressure levels in the process. The hydrogen stream is delivered at 13.1 bar without supplementary compression. Instead, the remaining methane-rich gas is recompressed from 0.8 to 7.5 bar before the final methanation stages.

The VPSA is controlled to allow separation of 75–95 %[47] of the hydrogen in the syngas stream and to have a H_2/CO ratio in the remaining gas stream that matches the requirement for methanation. In the coproduction of hydrogen and methane, the electricity demand in the plant can be a limiting factor because of the increased consumption by the VPSA compressor and the different heat releases in the methanation reactors. Therefore, for design D, we investigated two cases, $zero_{El}$ and max_{H_2}, in which H_2 production is controlled so as to have a zero consumption of electricity in the plant in the first case, and in the second case, electricity from the grid is used to maximize H_2 production. The maximum hydrogen production level is obtained by increasing the WGS and the hydrogen separation in the VPSA system up to the maximum level of 95 %.

STG and methane coproduction

During the production of STG, the excess heat in the process may be insufficient to cover the heat demand of the dryers and for the generation of electricity because of the absence or reduction of the methanation reaction. Therefore, the simulation was performed for two cases: (i) $zero_{El}$, in which combustion is increased to provide heat for the steam cycle to cover the internal electricity demand of the plant and (ii) max_{STG}, in which the DFB gasifier is operated as shown in design A.3 LT and electricity is bought from the grid.

Heat integration and steam cycle

Here, the ideal heat recovery targets are estimated from the analysis of the thermal cascade of the process by setting a minimum temperature difference (ΔT_{min}) for heat exchange and by applying the pinch analysis in line with previous studies.[30,55] The grand composite curves (GCC) are used to represent the heat cascade graphically, which shows the amounts of heat available in the process at the different temperature levels for conditions of ideal heat recovery. To investigate the integration of the steam cycle in the process, the GCC of the process and the steam cycle are plotted against each other by applying the principles of split-GCC graphical analysis.[30]

To optimize the steam cycle steam temperature and pressure levels, the optimal mass flows to maximize the power production are predefined. In the steam cycle, the steam data at the first stage of the turbine are set as constant for all the designs, whereas the other pressure levels are varied depending on the temperature levels in the heat cascade. District heating is not included in the study, and a water stream at 15 °C is used as the cold utility. The isentropic efficiency of the turbine $\eta_{T,is}$ is in the range of 0.78–0.93 and is estimated as a function of mass flow and pressure [Eqs. (5)–(7)], based on previous work.[56] The data used in the steam cycle are summarized in Table 4.

$$\eta_{T,is} = 0.0517\ln(x) + 0.515 \text{ for } x < 500 \quad (5)$$

$$\eta_{T,is} = 0.035\ln(x) + 0.622 \text{ for } x < 500 \quad (6)$$

$$x = \frac{m\ \dot{\Delta}h_{is}}{P_1 - P_2} \quad (7)$$

Process indicators

The performance analysis of a multiproduct plant requires the monitoring of several streams and it can be evaluated by different efficiencies. The evaluation of the outlet streams in this work includes all the chemical products (biomethane, STG, hydrogen, and ethanol) as well as the CO_2 streams for potential carbon storage or other applications. The chemical efficiency η_{ch} (Table 5) is calculated from the yields of chemical products based on the sole biomass energy input. Notably, the efficiency of ethanol production is given on a dry basis and the energy penalty for the distillation is not considered, as discussed above. The electricity in the plant can be produced and delivered to the grid or consumed from the grid; in the definitions of the efficiencies, this is described by the net electricity consumption El_{in} and the net production of electricity El_{out}. The performance of the gasification section is evaluated by the cold gas efficiency η_{CG}, calculated as the energy content in the product gas compared to the energy in the dry as free biomass.

The chemical and total efficiencies (Table 5) can be calculated from the energy input of the biomass (η_{ch}, η_{tot}) or the total energy input that includes the RME flow (η^*_{ch}, η^*_{tot}). In the results, the efficiencies are calculated from the lower heating value of the as-received biomass ($LHV_{a.r.}$) with 50 % w.b. moisture, which corresponds to the average moisture content after harvesting in the northern hemisphere. This biomass is of the lowest market value, which is critical for the economic viability of the plant; further drying to 40 % moisture is assumed to occur naturally if sufficient storage time is allowed before delivery. The results based on the LHV_{daf} are reported for comparison with other studies and are comparable with the efficiencies calculated from the higher heating value (HHV).

The power-to-gas conversion is assessed based on the efficiency η_{P2G}, which is a marginal efficiency that compares the increment of biomethane production from a reference case with the amount of electricity consumed to obtain that increment. This is not an absolute value as it depends on the reference process.

Table 5. Efficiency definitions.

Efficiency	Definition
	based on biomass input
cold gas efficiency	$\eta_{CG} = \frac{E_{CG}}{E_{biom}}$
chemical efficiency	$\eta_{ch} = \frac{E_{CH_4} + E_{STG} + E_{H_2} + E_{ethan}}{E_{biom}}$
total efficiency	$\eta_{tot} = \frac{E_{CH_4} + E_{STG} + E_{H_2} + E_{ethan} + El_{out}}{E_{biom} + El_{in}}$
power-to-gas efficiency	$\eta_{P2G} = \frac{E_{CH_4} - E'_{CH_4}}{El_{in} - E'_{out}}$
	based on all energy inputs
chemical efficiency	$\eta^*_{ch} = \frac{E_{CH_4} + E_{STG} + E_{H_2} + E_{ethan}}{E_{biom} + E_{RME}}$
total efficiency	$\eta^*_{tot} = \frac{E_{CH_4} + E_{STG} + E_{H_2} + E_{ethan} + El_{out}}{E_{biom} + El_{in} + E_{RME}}$

['] Reference process, as in equations.

Results and Discussion

The gas compositions calculated for different stages of the process and the error levels compared to the data obtained

Table 6. Validation of the model versus measurements from the GoBiGas plant (A.1 HT design). The equipment numbers refer to Figure 3.

Outlet reactor	6	7	11	13	15	17	18	Final
H_2 [%$_v$]	41.8	41.8	41.8	40.5	47.9	35.3	48.3	1.9
CO [%$_v$]	23.7	23.7	23.7	24.3	28.5	11.5	14.4	≈0
CO_2 [%$_v$]	24.9	24.9	24.9	25.3	12.0	26.4	1.7	1.1
CH_4 [%$_v$]	7.6	7.6	7.6	7.8	9.2	26.8	35.6	97
C_2H_4 [%$_v$]	2.0	2.0	2.0	0	0	0	0	0
C_3H_6 [%$_v$]	≈0	≈0	≈0	0	0	0	0	0
C_2H_6 [%$_v$]	0	0	0	2.1	2.4	≈0	≈0	≈0
C_3H_8 [%$_v$]	0	0	0	≈0	≈0	≈0	≈0	0
H_2S [ppm]	≈100	≈100	<5	<5	0	0	0	0
BTX [g Nm^{-3}]	7	7	0	0	0	0	0	0
C_7H_{10} [g Nm^{-3}]	13.5	0	0	0	0	0	0	0

Table 7. Results of the simulated designs for a biomass input of 100 MW_{daf} and RME input of 3.3 MW_{RME}. The designs and cases are described in the Methodology and Process layout and modeling sections.

Material products	Design A.1 no drying			Design A.2 air-drying		Design A.3 base case		Design A.4 (LT) electrolysis		Design A.5 (LT) direct heating		Design B (LT) ethanol + CH_4		Design C (LT) STG		Design D (LT) $H_2 + CH_4$	
	HT	LT	750 °C	HT	LT	HT	LT	$zero_{EI}$	max_{EI}	$zero_{EI}$	max_{EI}	$c_{80\%}$	$c_{50\%}$	$zero_{EI}$	max_{STG}	$zero_{EI}$	max_{H_2}
biomethane [MW_{CH_4}]	56.8	57.6	61.3	67	67.9	71.2	72.0	72.8	80.4	73.4	77.2	42.5	49.1	0	0	51	35.6
ethanol [$t\,h^{-1}$][a]	0			0	0	0	0	0	0	0	0	3.41	2.69	0	0	0	0
STG [MW_{STG}][b]	0			0	0	0	0	0	0	0	0	0	0	85.6	91.6	0	0
hydrogen [MW_{H_2}]	0			0	0	0	0	0	0	0	0	0	0	0	0	22.5	42.4
separated CO_2 [$t\,h^{-1}$][c,d]	14.3	15.4	16.0	15.9	16.3	16.4	16.4	16.3	15.4	16.5	17	10.1	10.8	7.1	7.1	20.0	23.3
electricity balance																	
$El_{out} - El_{in}$ [MW_{el}]	6.2	4.7	3.0	3.2	2.4	1.6	1.2	≈0	−12.8	≈0	−3.4	≈0	≈0	≈0	−3.8	≈0	−6.1
El_{demand} [MW_{el}]	4.1	4.1	4.3	4.8	4.7	5.4	5.3	7.1	20.5	7.0	10.5	4.3	4.7	4.5	4.8	6.2	12.1
compressor [MW_{el}]	2.9	2.9	3.0	3.2	3.2	3.4	3.4	3.4	3.5	3.5	3.8	1.6	2.6	3.2	3.4	3.3	3.4
dryers [MW_{el}]				0.35	0.35	0.8	0.8	0.8	0.8	0.8	0.8	0.8	0.8	0.80	0.80	0.8	0.8
El_{P2G} [MW_{el}]								1.2	15	1.2	4.8						
LT heat demands																	
$Q_{reboilers}$ [MW][e]	5.2	5.6	5.8	5.8	6.0	6.1	6.1	6.0	5.6	6.0	6.3	5.1[e]	5.2[e]	2	2.1	7.3	10.0
Q_{dryers} [MW]				6.1	6.1	8.9	8.9	8.9	8.9	8.9	8.9	8.9	8.9	8.9	8.9	8.9	8.9
fuel conversion																	
char gasification	0.4	0.4	0.4	0.45	0.53	0.56	0.61	0.61	0.61	0.6	0.7	0.61	0.61	0.48	0.61	0.58	0.61
recirc. of raw gas [MW]	10.1	4.4	0.9	0.9	0.9	0.9	0.9	0.9	0.9	0.9	0.9	0.9	0.9	0.9	0.9	0.9	0.9
efficiencies																	
η_{CG} [% LHV_{daf}]	67.4	68.1	72.3	79.2	79.8	84.0	84.8	85.7	94.7	86.7	91.0	84.8	84.8	84.8	84.8	84.8	84.8
η_{ch} [% LHV_{daf}]	56.8	57.6	61.3	67	67.9	71.2	72	72.8	80.4	73.4	77.2	67.9	69.1	85.6	91.6	73.5	78
η_{tot} [% LHV_{daf}]	63	62.3	64.3	70.2	70.3	72.8	73.2	72.8	70.5	73.4	73.8	69.7	71.1	85.6	88.2	73.5	73.6
η_{ch} [% $LHV_{a.r.}$][f]	65.3	66.3	70.5	77.1	78	81.9	82.8	83.8	92.5	84.4	88.8	78.1	79.5	98.5	105.4	84.6	89.7
η_{tot} [% $LHV_{a.r.}$][f]	72.5	71.7	73.6	80.8	80.9	83.8	84.2	83.8	81.1	84.4	85.0	80.2	81.8	98.5	101.5	84.6	84.7
η_{P2G} [%]								65[g]	60[g]	118[g]	114[g]				158[h]		74[i]

[a] In solution with water ≈5 $g\,L^{-}$. [b] After H_2S removal. [c] Net of the purge gas. [d] Contains H_2S. [e] No distillation. [f] Based on 50% w.b. moisture biomass. [g] Reference design A.3 LT. [h] Reference design C $zero_{EI}$. [i] Reference design D $zero_{EI}$.

from the GoBiGas plant are given in Table 6. The calculation shows a deviation from the measurements made at the plant in the range of ±10%. Therefore, the flow-sheet model is considered to be reliable for simulations. The results for each design are presented in Table 7, and the production and efficiency ranges and the rates of conversion of electricity to biofuels are compared in Figures 6 and 7.

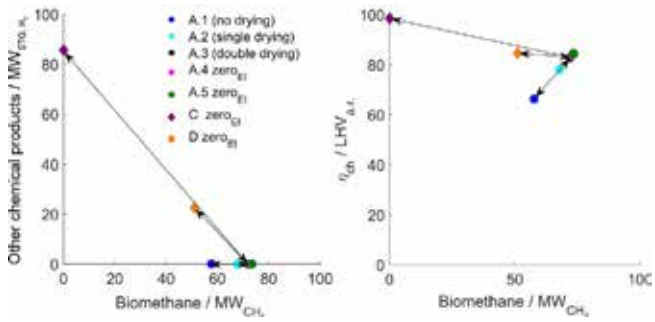

Figure 6. Production ranges of the investigated plant designs.

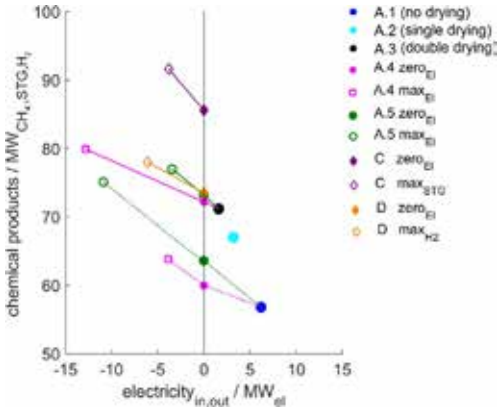

Figure 7. Chemical production versus electricity consumption for plant designs that involve the conversion of electricity to bioproducts. The filled symbols indicate net electricity production level equal to or higher than zero.

Influences of drying and operational conditions of the gasifier

The evaluation of the standalone biomethane designs A.1–A.3 was performed with high-temperature (HT) and low-temperature (LT) operational conditions (Table 7). A comparison of designs A.1, A.2, and A.3 shows that the integration of a drying system in the plant is the parameter that exerts the strongest effect on the chemical efficiency and biomethane production as the variation of the moisture content of the fuel affects the heat balance of the DFB gasifier directly. A major improvement is achieved if we move from design A.1 to design A.2, that is, if we introduce an air dryer (to reduce the moisture content from 40 to 20% w.b.), which corresponds to an increase in cold gas efficiency of the gasifier of around 12 percentage points (pp) and of the chemical

efficiency of around 10 pp to reach 78% $LHV_{a.r.}$. The higher level of methane production is counterbalanced by the slightly lower production of electricity. The increment in production related to the presence of a first drying stage would justify its introduction in any new plant. The introduction of a steam dryer with moisture recovery is more susceptible to the high cost of installation, whereas the advantage on η_{ch} is quantified to be approximately 4% to achieve a chemical efficiency of 82.8% $LHV_{a.r.}$ for design A.3 LT.

The improvements in relation to the GoBiGas demonstration plant (η_{ch} estimated at 57.4% $LHV_{a.r.}$[22]) if different drying strategies are introduced are shown in Figure 6. Here, the gap between designs A.2 and A.3 could be considered as the performance expected for a large-scale standalone plant.

The decrease of the gasification temperature from the HT to the LT case would increase the chemical efficiency of the plant by around 0.8%, which corresponds roughly to the decrease in the internal heat demand of the gasifier. Ongoing research on the catalytic effects of the ash compounds on tar chemistry has revealed the potential to decrease the temperature in the DFB reactor even further.[57] An extrapolation exercise with a gasification temperature of 750 °C and with the same tar content as that under LT conditions but with a decrease of the char gasification to 40% was performed for design A.1 and showed a further improvement in η_{ch} of 3.7%. However, lower temperatures in the reactor are unfavorable for char gasification, which could lead to a level of char conversion that is not feasible for a real process.

Coproduction of biomethane and ethanol

The results obtained for the coproduction of ethanol and biomethane are shown in Table 7 and Figures 6 and 7, in which $c_{80\%}$ and $c_{50\%}$ indicate the cases with rates of conversion of CO up to 80 and 50%, respectively. The yield of ethanol is reported as a mixture with water (with a concentration of $\approx 5\,g\,L^{-1}$). However, a strategy for distillation that involves other low-temperature sources should be incorporated to make this design interesting, otherwise the heat demand for distillation will decrease the chemical efficiency of the plant considerably. The values reported in Table 7 represent the maximum levels of ethanol production achieved by operating the ethanol plant upstream of the methanation section. The maximum production of ethanol is estimated to range from 3.41 ($c_{80\%}$ case) to 2.69 $t\,h^{-1}$ ($c_{50\%}$ case) with coproduction levels of 42.5 and 49.1 MW_{CH_4}, respectively. The production of biomethane can be increased by using a partial bypass of the ethanol plant to achieve up to 100% biomethane (Figure 6).

Drop-in gasification plants for STG and hydrogen production

The simulation of design C is performed for two separate cases: the first, $zero_{El}$, with a STG production of 85.6 MW_{STG}; and the second, max_{STG}, with a maximum production of 91.6 MW_{STG} and an electrical consumption of 3.8 MW_{el}. The composition of the STG resembles that of the raw gas (and is, therefore, dependent upon the operation of the gasifier), with a H_2/CO ratio of approximately 2, methane content if 8%$_v$, and CO_2 content of approximately 12%$_v$. The production of STG has the advantage that it retains the high efficiency of the gasification process because of the minimum requirement of conditioning the gas products. The chemical efficiency of the $zero_{El}$ case is 98% $LHV_{a.r.}$ and it increases to 105.4% $LHV_{a.r.}$ for the max_{STG} case with a total efficiency of 101.5% $LHV_{a.r.}$ ($El_{in} = 3.8\,MW_{el}$).

In addition, the coproduction of hydrogen and methane (design D) is investigated for two cases: $zero_{El}$ and max_{H_2}, in which electricity obtained from the grid is used to maximize H_2 production. In the $zero_{El}$ case, the production levels of H_2 and CH_4 are 22.5 MW_{H_2} and 51 MW_{CH_4} and the chemical efficiency is 84.6% $LHV_{a.r.}$. In the max_{H_2} case, H_2 production is increased to 42.4 MW_{H_2} with a methane production level of 35.6 MW_{CH_4} and an electricity consumption of 6.1 MW_{el}. The chemical efficiency of the plant increases if it changes from exclusively CH_4 production to H_2, although it does not reach the efficiency level seen for STG production (Figure 6b).

Comparison of power-to-gas concepts

Direct heating and electrolysis power-to-gas technologies are investigated in designs A.5 and A.4 based on design A.3. For both A.5 and A.4, two cases are investigated: a $zero_{El}$ case and a maximum electricity case max_{El}. The power-to-gas efficiency is higher for direct heating ($\eta_{P2G} \approx 115\%$), whereas electrolysis achieves an efficiency of $\eta_{P2G} \approx 63\%$. However, the two power-to-gas technologies exhibit different ranges of operation, which depend on the initial design of the plant. In particular, the application of direct heating is quite limited in design A.3 (max_{El} case: $El_{in} = 3.4\,MW_{el}$ and $El_{P2G} = 4.8\,MW_{el}$) as char gasification is already close to the maximum value; instead, electrolysis is favored by the high carbon yield in the raw gas and the conversion range was higher (max_{El} case: $El_{in} = 15\,MW_{el}$ and $El_{P2G} = 12.8\,MW_{el}$). This trend is reversed if these power-to-gas technologies are applied to design A.1, in which direct heating first reduces the product gas recirculation and then leads to an increase in char gasification.

The electricity demand/production and the chemical production of the plants for the two power-to-gas technologies and the other designs that offer the possibility to convert electricity into bioproducts are shown in Figure 7, as in design C (max_{STG} case) and design D (max_{H_2} case). In particular, the power-to-gas efficiency of the overall STG process (calculated using the $zero_{El}$ case as a reference) is even higher than that of direct heating (Table 7), as obtaining the electricity from the grid avoids the combustion of char or product gas for electricity generation, which thereby increases the production of STG. Therefore, electricity can be converted to bioproducts in standalone biomethane plants or distributed drop-in STG plants with similar performance levels. Notably, the maximum chemical efficiency for a standalone plant is achieved for designs A.4 $zero_{El}$ at 84.4% $LHV_{a.r.}$, which represents the maximum efficiency for a conversion of 50% w.b. moisture biomass to biomethane.

Aspects of heat integration

The heat integration in the plant is crucial to achieve high efficiencies. In particular, the use of medium-/low-temperature heat in the dryers and high-temperature heat in the preheaters is important to optimize the heat balance of the DFB gasifier to achieve a high conversion efficiency. In general, the process can be optimized to become self-sustaining by using excess heat from the exothermic steps to maximize the syngas production (chemical efficiency) and to produce some electricity (designs A.1–5, C zero$_{El}$, D zero$_{El}$).

However, all the designs exhibit a heavy demand for low-temperature heat because of the drying step, and the reboilers connected to the H_2S and CO_2 separation steps and the process could benefit from external low-temperature heat sources, such as industrial processes in the vicinity or pulp mills and existing (CHP) plants (local heat integration).

The effect of other low-temperature heat sources can be quantified as an increase in electricity production as shown in Figure 8, in which the GCC for the A.3 (LT) design are plotted together with the corresponding curve obtained after removing the heat demands below 160 °C (≈22.5 MW$_{th}$).

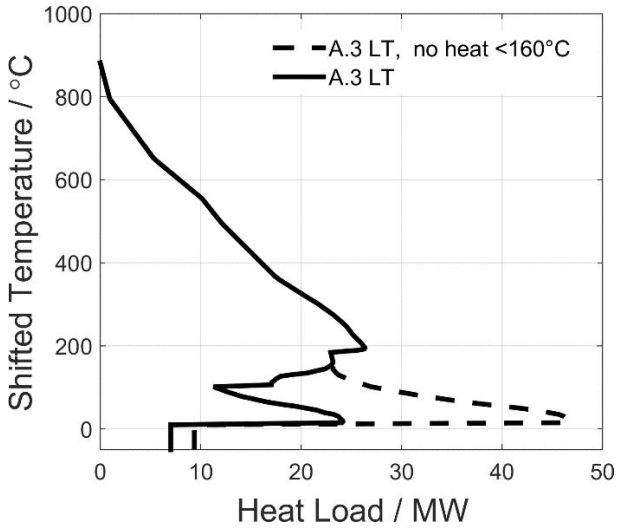

Figure 8. GCC for design A.3 that shows the integration of the steam cycle and biomethane process (which includes cold utility).

The effect is an increase in electricity production in the steam cycle from 6.5 to 9.4 MW$_{el}$. For ethanol coproduction, the opportunity to use excess heat from other processes is crucial to ensure the profitably of the plant as it can be used for distillation, which preserves the high efficiency of the gasification process.

CO_2 as a product

The amounts of CO_2 separated for the investigated plant designs are shown in Figure 9. As expected, design D stands out as having a strong potential to separate the used carbon on-site. Designs A.1–A.3 have similar potentials in which the CO_2 production that increases linearly leads towards higher yields of CH_4. The amount of CO_2 produced at the gasification plant (in the range of 57–186 kt yr^{-1}; cf. Figure 9) is at the low end of what is generally considered feasible for CCS.[34] However, the geographical location of the plant, specifically if it is in proximity to a coastline as well as a harbor and if it is part of an industrial cluster, facilitates the implementation of CCS at the gasification plant.

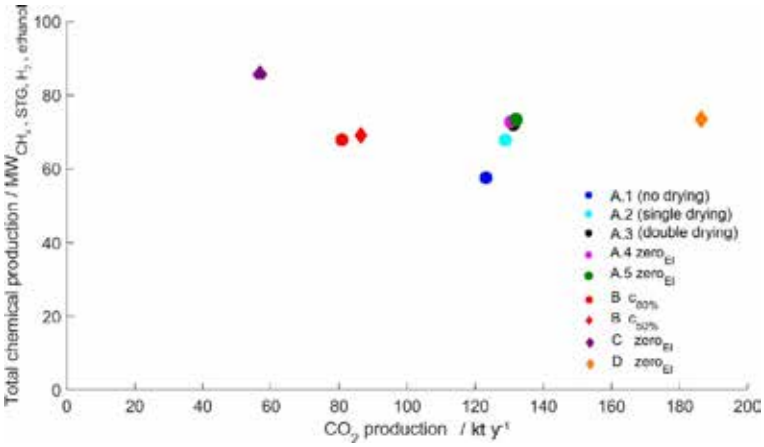

Figure 9. Production ranges of CO_2 as a function of chemical production in the investigated plant designs.

Conclusions

The production ranges and efficiencies are compared between distributed drop-in and centralized drop-in plants and standalone plants for biomass gasification based on dual fluidized bed (DFB) technology. Two intermediate semiproducts for distribution from distributed drop-in and centralized drop-in plants are considered: sustainable town gas (STG; a mixture of CO, H_2, CO_2, and CH_4) and pure H_2 in combination with pure biomethane. The investigation uses the 32 MW$_{biomass}$ standalone GoBiGas plant as reference to consider the scale-up of the technology to 100 MW$_{biomass}$. Measures to improve the efficiency that become feasible at larger scales are investigated, which includes an advanced drying system for the biomass, different operation of the gasifier, and power-to-gas strategies. The considered feedstock is biomass 50 % wet basis (w.b.) moisture, which is dried naturally to 40 % w.b. before it undergoes conversion in the plant.

Our results show that it is possible for standalone plants to increase the chemical efficiency from the current level of 57.4 lower heating value of the as-received biomass (% LHV$_{a.r.}$)[22] to levels within the range of 78–82.8 % LHV$_{a.r.}$.

With large-scale deployment, distributed drop-in and centralized drop-in plants can achieve chemical efficiencies in the ranges of 82.8–98.5 % $LHV_{a.r.}$ for STG/biomethane and 82.8–84.6 % $LHV_{a.r.}$ for H_2/biomethane. The production range for STG/biomethane production ranges from 85.6 MW_{STG} (design C $zero_{El}$) to 72 MW_{CH_4} (design A.3) and for H_2/biomethane it ranges from 22.5 MW_{H_2} and 51 MW_{CH_4} (design D $zero_{El}$) to 72 MW_{CH_4} (design A.3). As a result of the high efficiency levels and the extended range of convenient locations for distributed drop-in and centralized drop-in plants, there is no substantial advantage associated with standalone plants that produce biomethane, unless methane is the desired final product.

The potential of power-to-gas technologies in gasification plants was investigated for standalone plants and compared with the use of electricity to increase production levels in distributed and centralized drop-in plants. The results for the standalone plants show that the direct heating of the DFB gasifier gives a higher conversion efficiency than an electrolysis process, that is, approximately 115 % compared to approximately 63 %. However, the amount of electricity that can be converted into energy bound chemically by direct heating is limited by the rate of char gasification in the gasifier. Thus, in process designs that involve extensive drying (design A.3), the range of applications of direct heating is more limited than electrolysis, and the opposite holds true for designs with low (or zero) drying (design A.1). In distributed drop-in plants, electricity from the grid can be used to boost the chemical production process, which increases the maximum production of STG to 91.6 MW_{STG} (design C max_{STG}) and of H_2 to 42.4 MW_{H_2} (design D max_{H_2}), with power-to-gas efficiencies comparable to or higher than the power-to-gas technologies in standalone plants.

Overall, DFB gasification plants show good flexibility in relation to product output and retain a high efficiency if drying is implemented and heat integration in the plant is optimized. Further economic investigations of the local context are necessary to define introduction strategies for new gasification plants. However, the results of the present study show that distributed and centralized drop-in strategies can be as profitable as or more profitable than standalone biomethane plants, such that they should be considered in an analysis of the local energy system.

Acknowledgements

This work was performed within the Competency Center of Svenskt Förgasningscentrum (SFC), in collaboration with the Swedish Energy Agency and Göteborg Energi. The authors would like to acknowledge the collaboration of Matteo Morandin, Chalmers University of Technology.

Keywords: biomass · biomethane · gobigas · hydrogen · power-to-gas

[1] C. H. Zhou, X. Xia, C. X. Lin, D. S. Tong, J. Beltramini, *Chem. Soc. Rev.* **2011**, *40*, 5588–5617.
[2] L. H. Zhang, C. B. Xu, P. Champagne, *Energy Convers. Manage.* **2010**, *51*, 969–982.
[3] M. Hoogwijk, A. Faaij, B. Eickhout, B. de Vries, W. Turkenburg, *Biomass Bioenergy* **2005**, *29*, 225–257.
[4] V. S. Sikarwar, M. Zhao, P. Clough, J. Yao, X. Zhong, M. Z. Memon, N. Shah, E. J. Anthony, P. S. Fennell, *Energy Environ. Sci.* **2016**, *9*, 2939–2977.
[5] J. Hrbek, *Status report on thermal biomass gasification in countries participating in IEA Bioenergy*, *Task 33*, www.ieabioenergytask33.org, **2016**.
[6] H. Hofbauer, R. Rauch, K. Bosch, R. Koch, C. *APCBEE Procedia*, **2003**, 527–536.
[7] A. Larsson, M. Hedenskog, H. Thunman, presented in part at the *Nordic Flame Days*, Copenhagen, **2015**.
[8] A. Larsson, M. Seemann, D. Neves, H. Thunman, *Energy Fuels* **2013**, *27*, 6665–6680.
[9] Biomass CHP station Senden, http://www.4biomass.eu/en/best-practice/project-biomass-chp-station-senden.
[10] S. Heyne, H. Thunman, S. Harvey, *Int. J. Energy Res.* **2012**, *36*, 670–681.
[11] H. Holmberg, P. Ahtila, *Appl Therm Eng.* **2005**, *25*, 3115–3128.
[12] M. Gassner, F. Marechal, *Energy Environ. Sci.* **2012**, *5*, 5768–5789.
[13] M. Gassner, F. Marechal, *Biomass Bioenergy* **2009**, *33*, 1587–1604.
[14] T. R. Brown, R. C. Brown, *RSC Adv.* **2013**, *3*, 5758–5764.
[15] W. N. Zhang, *Fuel Process. Technol.* **2010**, *91*, 866–876.
[16] C. M. van der Meijden, H. J. Veringa, L. Rabou, *Biomass Bioenergy* **2010**, *34*, 302–311.
[17] P. N. Vennestrøm, C. M. Osmundsen, C. H. Christensen, E. Taarning, *Angew. Chem. Int. Ed.* **2011**, *50*, 10502–10509; *Angew. Chem.* **2011**, *123*, 10686–10694.
[18] I. Hannula, V. Arpiainen, *Biomass Convers. Biorefin.* **2015**, *5*, 63–74.
[19] H. Boerrigter, R. Rauch, *Review of applications of gases from biomass gasification Energy Research of the Netherlands (ECN)*, **2006**.
[20] H. Thunman, A. Larsson, M. Hedenskog, Commissioning of the GoBiGas 20MW plant biomethane plant. Conference:TCBiomass **2015** Chicago, **2015**.
[21] M. Karlbrink, Master of Science Thesis, Chalmers University of Technology, Gothenburg, **2015**.
[22] A. Alamia, A. Larsson, C. Breitholtz, H. Thunman, *Int. J. Energy Res.* **2017**, accepted.
[23] I. Gunnarsson, *The GoBiGas project*, **2011**.
[24] G. Aranda, A. van der Drift, R. Smit, *The Economy of Large Scale Biomass to Substitute Natural Gas (bioSNG) plants*, *Energy Research of the Netherlands (ECN)*, **2014**.
[25] A. L. Soerensen, *Economies of Scale in Biomass Gasification Systems*, *International Institute for Applied Systems Analysis (IIASA)*, **2005**.
[26] R. M. Handler, D. R. Shonnard, E. M. Griffing, A. Lai, I. Palou-Rivera, *Ind. Eng. Chem. Res.* **2016**, *55*, 3253–3261.
[27] J. Daniell, M. Kopke, S. D. Simpson, *Energies* **2012**, *5*, 5372–5417.
[28] H. Holmberg, P. Ahtila, *Biomass Bioenergy* **2004**, *26*, 515–530.
[29] A. Alamia, H. Thunman, M. Seemann, *Energ Fuel.* **2016**, *30*, 4017–4033.
[30] I. Kemp, *Pinch Analysis and Process Integration*, 2nd ed., Elsevier, Oxford, **2007**.
[31] M. K. Bora, S. Nakkeeran, *Int. J. Adv. Res.* **2014**, *2*, 561–574.
[32] M. Bolhàr-Nordenkampf, A. Friedl, U. Koss, T. Tork, *Chem. Eng. Process.* **2004**, *43*, 701–715.
[33] C. Azar, D. J. A. Johansson, N. Mattsson, *Environ. Res. Lett.*, **2013**, *8*, 034004.
[34] J. Kjärstad, R. Skagestad, N.-H. Eldrup, F. Johnsson, *Int. J. Greenhouse Gas Control* **2016**, *54*, 168–184.
[35] H. Topsøe, *From solid fuels to substitute natural gas (SNG) using TREMP™*, **2009**.
[36] H. Topsøe, *From Coal to Clean Energy*, file:///D:/Users/alamia.NET/Downloads/topsoe_from_coal_to_clean_energy_nitrogen_syngas_march_april 2011.pdf.
[37] A. Alamia, H. Ström, H. Thunman, *Biomass Bioenergy* **2015**, *77*, 92–109.

[38] K. P. Brooks, J. Hu, H. Zhu, R. J. Kee, *Chem. Eng. Sci.* **2007**, *62*, 1161–1170.
[39] S. K. Hoekman, A. Broch, C. Robbins, R. Purcell, *Int. J. Greenhouse Gas Control* **2010**, *4*, 44–50.
[40] M. Götz, J. Lefebvre, F. Mörs, A. McDaniel Koch, F. Graf, S. Bajohr, R. Reimert, T. Kolb, *Renewable Energy* **2016**, *85*, 1371–1390.
[41] Pressure Electrolyser, http://elektrolyse.de/wordpress/?page_id=38.
[42] A. J. Appleby, G. Crepy, J. Jacquelin, *Int. J. Hydrogen Energy* **1978**, *3*, 21–37.
[43] J. Marinkovic, H. Thunman, P. Knutsson, M. Seemann, *Chem. Eng. J.* **2015**, *279*, 555–566.
[44] K. Liu, H. K. Atiyeh, R. S. Tanner, M. R. Wilkins, R. L. Huhnke, *Bioresour. Technol.* **2012**, *104*, 336–341.
[45] M. Köpke, C. Mihalcea, J. C. Bromley, S. D. Simpson, *Curr. Opin. Biotechnol.* **2011**, *22*, 320–325.
[46] F. R. Bengelsdorf, M. Straub, P. Durre, *Environ. Technol.* **2013**, *34*, 1639–1651.
[47] D. Johansson, P. A. Franck, T. Berntsson, *Energy* **2012**, *38*, 212–227.
[48] P. C. Munasinghe, S. K. Khanal, *Bioresour. Technol.* **2010**, *101*, 5013–5022.
[49] K. Liu, H. K. Atiyeh, B. S. Stevenson, R. S. Tanner, M. R. Wilkins, R. L. Huhnke, *Bioresour. Technol.* **2014**, *151*, 69–77.
[50] LanzaTech, *Aemetis Acquires License from LanzaTech with California Exclusive Rights for Advanced Ethanol from Biomass*, http://www.lanzatech.com/aemetis-acquires-license-lanzatech-california-exclusive-rights-advanced-ethanol-biomass-including-forest-ag-wastes/.
[51] J. He, W. N. Zhang, *Appl Energ.* **2011**, *88*, 1224–1232.
[52] C. Piccolo, F. Bezzo, *Biomass Bioenergy* **2009**, *33*, 478–491.
[53] J. R. Phillips, E. C. Clausen, J. L. Gaddy, *Appl. Biochem. Biotechnol.* **1994**, *45*, 145–157.
[54] M. T. Ho, G. W. Allinson, D. E. Wiley, *Ind. Eng. Chem. Res.* **2008**, *47*, 4883–4890.
[55] B. Linnhoff, D. W. Townsend, D. Boland, G. F. Hewitt, B. E. A. Thomas, A. R. Guy, R. H. Marsland, *User Guide on Process Integration for the Efficient Use of Energy*, 1st ed., **1982**.
[56] T. Savola, K. Keppo, *Appl. Therm. Eng.* **2005**, *25*, 1219–1232.
[57] T. Berdugo Vilches, "Strategies for controlling solid biomass conversion in dual fluidized bed gasifiers" Licentiate engineer thesis, Chalmers University of Technology, Gothenburg, **2016**.

Manuscript received: November 17, 2016
Revised manuscript received: December 22, 2016
Accepted manuscript online: December 28, 2016
Version of record online: April 4, 2017

Paper 4:

Economic assessment of advanced biofuel production via gasification using real cost data from GoBiGas, a first-of-its-kind industrial installation

Submitted for publication in Energy Science & Engineering

Economic assessment of advanced biofuel production via gasification using real cost data from GoBiGas, a first-of-its-kind industrial installation

Henrik Thunman[1], Christer Gustavsson[2], Anton Larsson[1,3], Ingemar Gunnarsson[3], Freddy Tengberg[3]

[1]Chalmers University of Technology

[2]Bioshare

[3]Göteborg Energi

Abstract

In this paper we describe an economic analysis of the GoBiGas plant, which is a first-of-its-kind industrial installation for advanced biofuel production (ABP) *via* gasification, in which woody biomass is converted to biomethane. The technical evaluation of the demonstration already published confirmed that advanced biofuel production plants could already today be erected using commercially available and widely used components. Thus, significant cost reductions due to learning cannot be expected. Furthermore, since the lion share of the investment lies in the gasification and gas cleaning sections of the process, the estimated cost level for the production of biomethane based on the GoBiGas demonstration plant is expected to be representative for other syngas based advanced biofuels that can replace current fossil fuels produced from oil or natural gas. The analysis shows that a plant capacity of 200 MW biomethane is the most attractive scale for future ABP plants in terms of limiting the cost of production, when excess heat from the ABP is not valorized. For this plant size and today's price of forest residuals, production cost for biomethane is estimated at 600 SEK/MWh, (60€/MWh, 75US$/MWh), which is equivalent to 5.4 SEK/liter gasoline [0.54 €/liter, or 2.5USD per gallon (9.9 SEK/€, 8 SEK/USD)], where the feedstock accounts for about 36%. The most significant factors of uncertainty pertaining to the estimated production costs are timing of the investment, the location of the installation and price of feedstock. Therefore, there is a potential for implementing cost competitive ABP systems, where low-grade feedstocks (e.g. waste-derived woody biomass) are available, and/or where the unit can be integrated with already existing infrastructure. For the latter valorization of excess heat can provide simplification that can significantly lower the specific investment costs for small scale ABPs analogous to small scale combined heat and power plants.

Introduction

In this report, cost data for a first-of-its-kind, industrial-scale plant for advanced biofuel production (ABP), namely the GoBiGas plant are reported. The GoBiGas plant is a direct result of ambitious efforts to replace fossil fuels for renewable alternatives, and it reflects the political goals of both the European Union and the Government of Sweden. The timing of the investment decision followed the trajectory of the Kyoto agreement, as well as local targets to reduce local emissions, such as soot particles, especially from buses. The GoBiGas plant was built by Göteborg Energi, which is an energy company own by the municipality of Gothenburg, and was supported with 222 million SEK by the Swedish Energy Agency. In the GoBiGas process, woody biomass is converted to 20 MW biomethane. However, most of the equipment used would be similar regardless of the type of green chemicals or advanced biofuel for land, sea or air transport to be produced *via* the gasification route An initial breakdown of the

investment cost for the GoBiGas plant based on the project summary has been reported elsewhere [1] and a significant proportion of the investment was related to aspects specific to the site or the project. To generalize the results, a more detailed analysis is performed in the present study, in order to generate a more general and realistic estimate of the production costs of advanced biofuels. This cost breakdown is subtracted from the values given in the ongoing project *Comparative KPI's for integration of biofuel production in CHP processes*, which is funded by the Swedish Energy Agency. In the present study, aggregated cost estimates are presented, complementing a recently published study [1-3] in which the performance and technology were evaluated. Taken together, these provide a comprehensive overview of the technical status and projected production cost for future commercialization of this technology.

As described in the technical review of the GoBiGas project [3], one of the main lessons that has been learned is that: ABP plants can be constructed using commercially available components that have already reached a level of maturity corresponding to the n-th numbered installation. In the GoBiGas project, the major technical component that had not yet reached a mature commercial state was the gasifier. However, the evaluation of the technology, combined with the parallel experience accrued from operation of the semi-industrial plant built at Chalmers, showed that the gasifier could be built using an already existing mature boiler technology. This is in-line with recent modifications made at other plants based on the same gasification technology, but used for heat and power production, and where required availability using intended feedstock - forest residue - has been demonstrated, e.g., the plant in Senden [4]. The reactor design used for the gasifier in the GoBiGas project is predominantly used for heat and power or only heat production in pulp and paper mills and in district heating systems. In Sweden alone, more than 100 of these units have been installed, and around the world more than 1,000 units are in operation. This means that the technology used for these reactors when used in an ABP plant is mature, and that significant cost reductions due to learning cannot be expected.

As shown in previously published studies [1,3] the GoBiGas plant has successfully demonstrated the capability of the technology, and at the time of writing of this report (February 2018), the plant has been in continuous operation in a single run, since the beginning of December 2017, i.e., for more than 1,800 hours, with consistent performance. In total, the gasifier has been operated for more than 15,000 hours, since its commissioning in 2014. Even though the production cost experienced during continuous operation of the plant is in the range of projected production cost at the time of the investment decision, changes in external factors pertaining to the market have made the attainment of profitability challenging. This is partially the result of a failure to reach new targets for climate gas emissions at the COP meeting in Copenhagen in 2009 and the subsequent years' unclear targets for reducing emissions of greenhouse gases. As a consequence, the predicted market for biomethane did not develop as expected, while at the same time fossil fuel prices dropped significantly, affecting the competitiveness of biomethane negatively. Furthermore, regional governmental support systems based on feed-in-tariffs in several European countries, such as Denmark, overlapped the Swedish support system, which is based on tax reductions for both domestic and imported biogas, thus compromising the competitiveness of domestically produced biogas in Sweden. The GoBiGas plant, which was built to demonstrate the feasibility of the technology and was never meant to be profitable as a stand-alone unit, has suffered financially from these events. The total production cost using wood pellets (currently used as feedstock) exceed the price on the regional market for biomethane.

The economic input to the project concluded at an investment of 1,600 MSEK attracted local criticism of the project. However, the cost level of producing biomethane is in line with the costs predicted at the time of the investment decision. When evaluating the investment cost for the project it must be remembered that GoBiGas was built as a demonstration plant with the intention to provide experience

for a second, 5-fold larger, commercial plant, which should cover the investment cost also of the initial demonstration plant. Originally the intention was that the demonstration plant should run in parallel with the commercial plant and share the costs for the personnel and feedstock infrastructure. The operating cost at the demonstration plant was to be sufficiently low to enable cost-competitive production at the commercial scale. However, as described above, the biogas market has not yet grown to the level required for introducing advanced biofuel *via* gasification. This means that the economic basis for start of building a commercial-scale unit is not yet there. The Paris agreement and new local regulations provide some hope that the market for advanced biofuels will increase within the next 5–10 years.

The ambition that the demonstration plant should be operated as part of a commercial production site has added to the complexity of the plant, as this raises the performance requirement. For example, the plant should after the demonstration period be able to operate at full load continuously for 8,000 hours per year for at least 20 years. This places a high demand on reliability, redundancy, and the possibilities for servicing and making replacements of certain parts during operation. The produced gas is fed straight to the high-pressure part of the natural gas grid, and the demands related to the quality of the gas are high (Methane concentration >94%, Hydrogen <2%, Carbon Dioxide <2.5%, Nitrogen <3.5%, Carbon Monoxide <0.1%, Ammonia <20ppm, Dew Point < -8 °C at 70 bar, which can be compared with the average concentrations of the gas produced in the GoBiGas-plant methane 97%, Hydrogen 2%, Carbon Dioxide 0.2%, Nitrogen 0.6% and below the limits for Carbon Monoxide, Ammonia and Dew Point). Here, it should be recognized that the natural gas on the local market has a high Wobbe index compared to most regional markets in Europe. The goal set for the efficiency of conversion of biomass to biomethane was 65% based on the lower heating value. To reach this goal, substantial efforts were made to have a high level of heat integration within the plant. Furthermore, the plant was integrated with the local district heating network, so as to utilize low-grade heat, increase the competitiveness of the plant, and achieve a plant efficiency of 90%. These ambitions are typically expected from a commercial plant rather than from a demonstration plant, where simplification is commonly used to reduce the investment cost, which in turn can lead to unrealistic cost estimates for the scale-up to commercial production. The high level of ambition set for the demonstration GoBiGas plant placed the complexity on a level similar to that expected for a commercial ABP plant, rendering the data on the investment cost for the GoBiGas plant useful for estimating the costs associated with the commercial ABP plant using appropriate scale factors.

The objective of this work was to estimate the production costs for advanced biofuels generated *via* gasification at a commercial scale. To achieve this, investment and operational costs have been estimated based on data from the GoBiGas demonstration plant. Relevant and aggregated reference data and scale-factors for a commercial APB plant have been established based on a detailed study of the investment costs of the GoBiGas plant, in combination with the technical review of the process previously published [1-3].

Reference data and scale-factors

The production cost for a commercial-scale ABP plant is here estimated, based on the investment cost, plant development costs and operating costs, as well with connected assumptions on expected lifetime (LT) and yearly Full Load Hours (FLH) of the plant (Eq. 1). The initial investment cost, as well as part of the operating costs are strongly related to the scale of the plant in terms of production capacity (MW produced biofuel). To estimate the initial investment cost, C_{inv}, and annual operation costs minus the cost of the feedstock, c_{ope}, for a plant with X MW of production capacity (Eqs. 2 and 3), the reference cost and scale factor are estimated based on the GoBiGas plant (20-MW biomethane production capacity).

$$Production\ Cost\ x\ MW = \frac{C_{Inv}+C_{int}+C_{dev}+C_{ope}}{P_{x\ MW}*LT*FLH} \quad \text{Eq. 1}$$

$$C_{Inv\ x\ MW} = C_{Inv,\ ref}\left(\frac{P_{x\ MW}}{P_{ref}}\right)^{Scale\ Factor} \quad \text{Eq. 2}$$

$$c_{ope\ x\ MW} = c_{ope,\ ref}\left(\frac{P_{x\ MW}}{P_{ref}}\right)^{Scale\ Factor} \quad \text{Eq. 3}$$

The initial investment cost for the GoBiGas plant is in this work broken down into individual invoices. Most of the cost has been paid in Swedish crowns (SEK) and the remainder of the cost has been paid in Euros (€). Here, all the costs are given in SEK, as this reflects the cost in the local market during the period of the investment when the average exchange rate was 9.1 SEK for 1.0 €. The cost of each component has been analyzed based on its functionality and level of technological maturity. Thereafter, higher and lower scale factors have been established for each component based on experience gained from other industrial processes in which such components are used. The site that was chosen for the GoBiGas plant entailed the imposition of some restrictions on the project. For example, more or less the entire plant had to be built indoors, and a massive explosion wall had to be built due to the proximity of a production plant for district heating. The site also came with several advantages, including a location close to the local district heating network, the natural gas grid, an existing local system for providing cooling water, and the possibility to recover low-temperature heat for district heating *via* heat pumps. Furthermore, the plant could be incorporated into the existing environmental permit for the neighboring plant used for heat production. Capital tied up in GoBiGas plant feedstock and other inventories are negligible and, therefore, not included in the investment sum. The same is assumed to apply for larger scale units. For all ABP plants that will be built, local conditions and demands will provide numerous challenges or benefits that will add to or reduce the costs of the plant. These costs cannot be predicted using generalized cost estimates.

To generalize the data as much as possible, component-related costs deemed unnecessary by the technical review, together with the costs considered to be specific for this particular plant or project have been subtracted from the established reference data. The same procedure has been carried out for the engineering part of the project, where the different costs related to the construction and building of the plant have been analyzed to establish relevant reference data and scale-factors. Thereby, all the costs arising from constructing a First-of-its-Kind installation have been removed. The costs for additional equipment that would be incorporated into a commercial plant, such as on-site drying and integration of internal electrical production, have been estimated from the costs applying to similar existing commercial industrial installations. In this report, all costs are aggregated to a total plant cost.

To cope with uncertainties related to the scale-up effect on the investment cost, estimates were also performed using a *high* respectively *a low* scale factor, in order to allow comparisons with the base case. To put in perspective this variance in investment cost related to scale-factors it is compared to the historic variance in the initial investment costs of the relevant more mature technology of commercial-scale Combined Heat and Power (CHP) plants. The comparison between the CHP and ABP plant also serves to illustrate how the annual FLH impact the production cost and consequently the profitability of the plant. The initial investment costs for a number of relevant commercial-scale CHP plants built and brought into operation within the past 10 years in Sweden are used for the comparison.

The initial investment costs per MW of installed capacity as a function of the plant size for ABP and CHP respectively are compared, where the initial investment cost for the ABP plants is estimated using

Eq. 2, and the corresponding initial investment cost for the CHP plant is illustrated in an analog way, as well as by plotting actual historic data. For the ABP plants, only the produced biofuel is included in the product capacity. For simplicity, no valorization of side-product streams, such as district heating, are taken into account. For the CHP plants, the heat and power are assigned the same value, and the capacity is calculated as heat plus power. For the initial investment cost of a CHP plant, the reference values for the *low*, *average*, and *high* cases are 900, 1400, and 2500 MSEK, respectively, for a 100-MW plant with scale factors of 0.5, 0.6, and 0.7, respectively. This was considered being representative given the fact that these values lie within the range of the historic values of CHP plants. In the present study, the reference CHP plant is assumed to have an efficiency of 35% electricity and 70% heat based on the lower heating value of the received fuel with a moisture content of 45%. This corresponds to an efficiency of 31% electricity and 63% heat based on delivered dry instead of wet fuel, and is similar to the efficiency number obtained if the efficiency is based on higher heating value; the economic lifetimes of the plants are assumed to be 20 years. In contrast to the advanced fuel production, the product output from the CHP plant is calculated as the sum of the heat and the power, as mentioned above.

The impact of annual FLH on the production cost related to the depreciation cost can be estimated from Eq. 1. The ABP plant is assumed to be operated for 8,000 FLH per year, while different cases are illustrated for the CHP plant, as the operation of this type of plant is more dependent of variations in the energy demand than an ABP plant that can store its product.

The cost related to the interest part of the investment, C_{int}, calculated as the cumulative annuity over the assumed economic lifetime minus depreciation. The interest rate is set at 2.5%, 5%, 7.5% or 10%, which would create an average cost for interest over the period corresponding to 28%, 60%, 96% or 135%, respectively, related to the initial investment cost. Even though the individual parts of an ABP plant are based on mature technologies, combining them into an ABP plant still entails something new. Therefore, a development-related investment cost, C_{dev}, is included. These are equipment and systems updates not covered by regular annual maintenance and are arbitrarily assumed to contribute an additional 10% to the total investment cost during the economic lifetime of the plant.

The operating costs for the GoBiGas plant have been analyzed in detail and are here presented as four different aggregated categories: 1) Personnel cost; 2) Maintenance cost; 3) Consumables and waste products; and 4) Other costs. The scale-factor applied to the investment cost, as well as the different operating costs are summarized in Table 1. The representation of the *Personnel cost*, *Maintenance cost*, and *Other cost*, are usually given as personnel per plant, and two other categories are usually represented in percent of the investment, for which there are tables based on industrial experience available. The alternative representation done, here, is made to give an insight to the actual costs resulting from the GoBiGas-demonstration and how these are expected to be scaled to a commercial sized unit.

Table 1: Aggregated scale-factors for different costs related to the operation of an ABP plant.

Cost	Scale Factor (Low, average, high)	Reference based on 20-MW GoBiGas demonstration plant	Reference based on 20-MW Commercial plant
Initial Investment Cost, $C_{Inv\ 20MW}$		MSEK/20 MW	MSEK/20 MW
- Reactor systems	0.58, 0.68, 0.78	238	238
- Engineering & Connecting and Surrounding systems	0.34, 0.44, 0.54	955	955
- Steam Cycle & Drying	0.67	182	182
Total		1,375	1,375

Operating Costs exclusive feedstock, $c_{ope\ 20MW}$		SEK/MWh[1] $c_{ope\ 20MW}$ /($P_{20\ MW}$ FLH)	SEK/MWh[1] $c_{ope\ 20MW}$ /($P_{20\ MW}$ FLH)
Personnel	0.10	181	181
Maintenance	0.67	89	89
Consumables and waste products	1.00	131.5	55.1
- Electricity		37.6	0
- RME		31.7	0
- Activated Carbon/BTX removal		8.5	10
- Other		53.6	45.1
Other costs	0.67	26.5	26.5
Total		428.0	351.6
	Cost of ingoing fuel	Fuel-related costs in SEK/MWh biogas	
Feedstock cost	SEK/MWh	Dry biomass to biomethane efficiency 55 / 60 / 65 / **70** / 75 %	
Pellets[2]	250	448 / 411 / 379 / **352** / 329	
Forest Residue[3]	170	276 / 253 / 234 / **217** / 203	
Recovered Wood Fuels[4]	110	194 / 178 / 164 / **153** /143	
Recovered Wood Fuels[4]	50	88 / 81 / 75 / **69** / 65	

[1] Based on 8,000 full-load hours per year and a 20-MW biomethane production plant.
[2]Pellets, 10% moisture
[3]Forest residue, 45% moisture.
[4]Recovered wood waste, 18% moisture.

Operation of the GoBiGas plant requires personnel corresponding to about 28 full-time employees, with 3 operators being required on-site at all times. The *Personnel costs* are here estimated as 29 million SEK per year. A low scale factor is assumed, as the number of persons needed to operate a much larger plant is expected to be similar to the number required at the demonstration plant given that there will be a similar level of process complexity.

The *Maintenance cost* category mainly relates to the cost incurred during the revision of the plant. Operation of the GoBiGas plant is stopped each year for about a month to allow for revision, for a plant reaching 8000 full load hour a year the time period between the planned maintenance stops will most likely be extended from the present 12 to 18 months, in-line with the revision period of a pulp mill. About 60% of the revision cost is related to the gasification section of the process, in that the major part of the revision relates to the maintenance of the refractory lining and heat exchangers. The scaling-factor for the maintenance cost is, therefore, assumed to be equal to the ratio of the area to the volume of the reactors (scale-factor of 0.67). About 40% of the maintenance cost is related to the methanation part of the process, where the regular inspection and maintenance of the pressure vessels account for a large proportion of the cost. While a somewhat lower scale-factor could be expected for this part of the process, for the sake of simplicity and to avoid underestimating the maintenance cost, the same scale-factor is applied to the maintenance costs related to both parts of the process.

The category of *Consumables and waste products* includes both the material and energy consumed during operation, as well as the waste products that carry costs for the operation and are based on continuous operation during December 2017. The following materials are used during operation in

addition to the biomass feedstock: nitrogen for purge gas; olivine sand for bed material in the gasifier; rapeseed oil methyl ester (RME) for scrubber liquid to remove tar components; calcium carbonate, which is used as a pre-coating material for the particle filter in the product gas line; potassium carbonate, which is added to control the gas quality in the gasification; activated carbon for adsorbent to remove light aromatic compounds such as BTX (Benzene, Toluene and Xylene) from the product gas; different catalysts used in the methanation section to condition and synthesize the gas to biomethane; and fresh water mainly for steam production. The energy carriers consumed during the production are mainly: electricity, whereof most is used for compression of the gas; and natural gas for heating during start-up the process. The waste products from the plant are: waste water; fly ash; and bottom ash. As described previously [3], the costs for consumables can be significantly reduced through:

(i) the introduction of a steam cycle, which will make the plant self-sufficient for electricity;
(ii) the introduction of a self-cleaning heat exchanger or scrubber agent distilled from inherent tar products, which will eliminate the need for RME;
(iii) inherent regeneration of carbon beds, which would significantly reduce the need for active carbon; and
(iv) the implementation of an optimized heat integration system, which would remove the residual need for natural gas.

In Table 1, both the present costs and the predicted costs for a future commercial plant are given. It should be noted that the cost associated with the removal of aromatic hydrocarbons, which in the GoBiGas plant is accomplished by RME scrubbing and active carbon beds, can be significantly reduced (as described above) by using an alternative strategy; the estimated cost for this is in Table 1 aggregated into the cost for BTX removal for a commercial plant.

The category of *Other costs* includes all the remaining costs, such as overhead costs and license fees. This is a comparatively small category and the scale-factor is arbitrarily assumed to be 0.67.

The chemical efficiency of an ABP plant has previously been evaluated [1,2]. Here, an efficiency of 70% based on the energy of the dry part of the delivered biomass is assumed. It should be noted that while a further increase in efficiency is technically possible, increasing the level to above 70% would probably increase the investment cost; for the sake of simplicity and to avoid increasing the uncertainty of the analysis, this is not considered here. The potential for sellable district heating would be in the order of 10%, subject to that the plant would be located in proximity to a district heating network. Since location is not specified, the heat is not given any value in the analysis.

Results and discussion

As described previously [3], an ABP plant can be constructed from components that are commonly used in commercial processes today. This means that on the component level, the technology has already reached the n-th installation and learning will only be related to the assembly of these parts into a new system, so the cost reduction potential due to further learning is considered to be moderate. In addition, a major part of an ABP plant based on gasification will consist of the same reactor system regardless of the selected product being methane (the biofuel selected here) or any other biofuel, such as methanol, dimethyl ether (DME), mixed alcohols or Fischer-Tropsch crude (which resembles a long distillate from a light crude oil, but without impurities). This means that the cost levels of the GoBiGas plant are representative also for these other types of advanced biofuel plants.

Figure 1 shows the total cost of ABP and CHP plants in relation to the installed capacity. The investment cost of the ABP plant is related to the initial investment cost of the GoBiGas plant, with an estimated range for the scale-factors for the ingoing components. The cost level and variance of the initial

investment costs of CHP plants are also illustrated, where the range of variability is estimated from a number of recently built units (represented as black dots in Figure 1). Even though a biomass-fired CHP plant is of a mature technology that has reached the n-th number of its kind status, the true initial investment costs for the different projects vary considerably. It is clear that the historic data do not follow the expected economy of scale trend for smaller units. The reason for diminishing scale effect for small CHP plants is that electrical efficiency and fuel flexibility are not prioritized for smaller plants, rather reduced initial investment costs. It should be remembered that these plants are designed based on the demand for district heating and not on demands for the production of electricity. Similar effects could be expected for advanced biofuel production, where local conditions offer the possibility to produce advanced biofuels as a side-stream.

When it comes to the larger CHP plants of capacities >80–100 MW, the technical performances of the CHP plants become rather similar, and the variation in cost is mainly linked to non-technology factors, where the time of decision and plant location are the two factors of strongest influences on the cost. For a CHP plant, which by default needs to be located close to a district heating system, the location is often the most important cost-driving factor, as the design of the plant itself and fuel logistics need to be arranged so that the plant visually and environmentally blends into the surroundings. The cost for an ABP plant will be roughly twice that of a CHP plant and will be influenced by similar factors. By comparing the variability in initial investment costs due to non-technology-related factors (based on CHP plants) with the estimated uncertainty related to technology-based factors for an ABP plant, it can be concluded that factors other than the technology itself will have the greatest impact on the initial investment cost for a specific ABP plant (see Fig 2). In Fig 2, the cost is also represented for different currencies, where the cost level in Sweden is linked to the internal European market with the average exchange rate during the erection of the plant of 9.1 SEK per 1.0 €. For a comparison of the US and European markets, the present relationship between the € and US$ of 1.25 US$ per 1.0 € is more relevant. It should be noted that the SEK to € exchange rate has varied ±10% during the GoBiGas project and that for the SEK to US$ exchange rate the variation has been even larger. Therefore, exchange rates representing one non-technical factor that will have a strong influence on the final cost of the project.

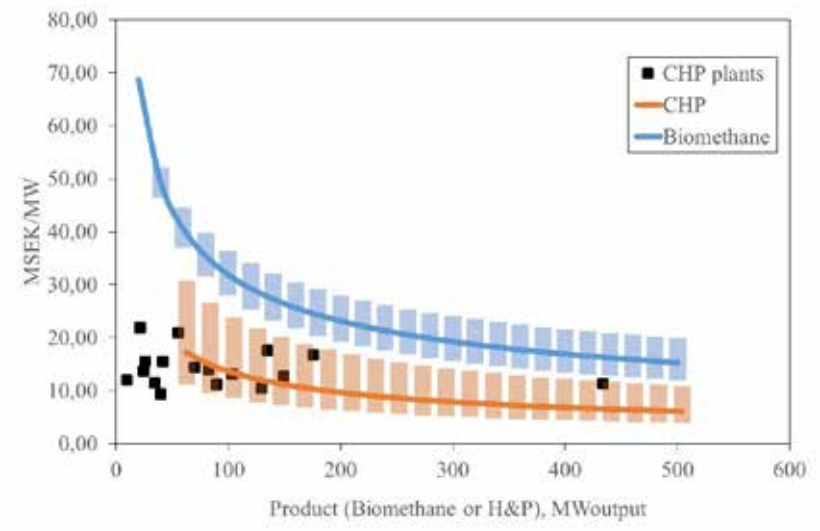

Figure 1: Initial investment cost per capacity (MW product) for advanced biofuel (Biomethane) and CHP plants. The black dots represent the costs for a number of CHP plants built in Sweden after Year 2010.

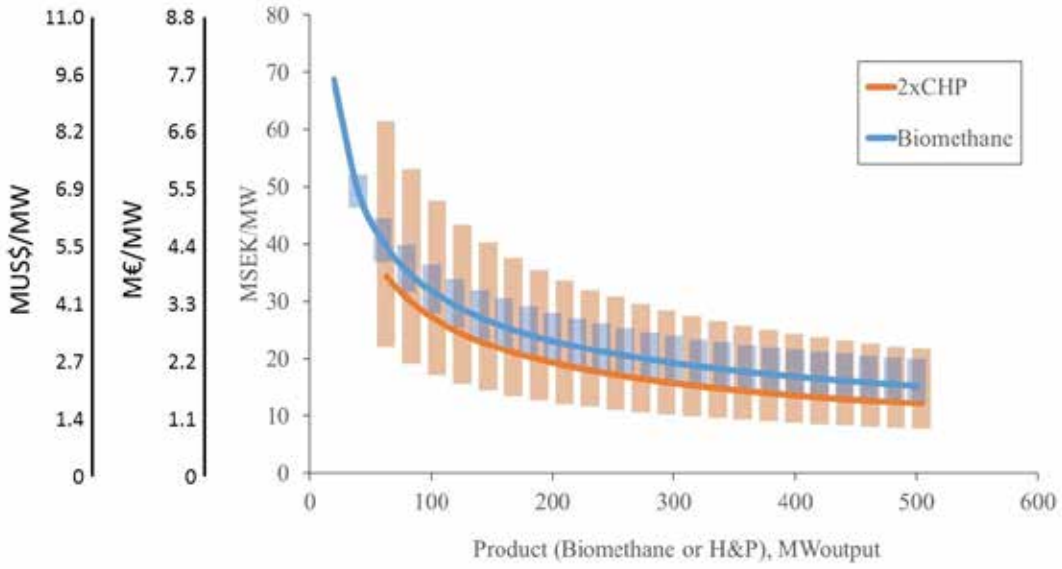

Figure 2: Initial investment cost per capacity (MW product) for an advanced biofuel (biomethane) plant, compared with a 2-fold higher investment cost for a CHP plant, for different currencies. Exchange rates: 9.1 SEK per 1 € (average exchange rate during the project); and 1.25 US$ per 1 €.

ABP plants are associated with large investments when the production has to be at a scale that makes a significant contribution to the transition from fossil fuels to renewable fuels. In the present study, the objective of comparing with the CHP technology is to obtain an indication to how this investment relates to a well-established technology using the same biomass for feedstock, albeit with different production characteristics. To ensure a fair comparison, the depreciation costs associated with the two technologies are divided by the expected production over the economic lifetime of the plant. In Fig 3, four different scenarios are illustrated. In all the cases, the ABP plant is expected to be operated for 8,000 FLH per year, while the CHP plants are operated for 1,000, 2,000, 4,000 and 8,000 FLH per year. We show that for a future situation entailing warmer climate (2,000 FLH), extensive access to intermittent power, extensive variation management strategies, warm winters and energy savings in buildings (1,000 FLH), the relative investment cost for an ABP plant is much less than that for a CHP plant. For CHP plants that reach 4,000 FLH, the relative investment cost will be similar to that of an ABP plant, and if the CHP plant can offset the produced heat and power during the entire year, the relative investment costs for these plants will be significantly lower than those for an ABP plant. With massive introduction of intermittent electrical production (in line with current national targets to the Year 2030), the Nordic electrical mix is expected to come predominantly from wind mills [5]. In such a scenario the number of FLH with satisfactory offset for the electricity will decrease significantly, making the relative investment cost lower for ABP plants than for CHP plants. In Figure 4, the predicted depreciation, including both technical and non-technical uncertainties, for an ABP plant in relation to its lifetime production is illustrated, where the investment cost is estimated at twice that of a CHP plant. The cost is also represented in various currencies (similar to what is shown in Figure 2).

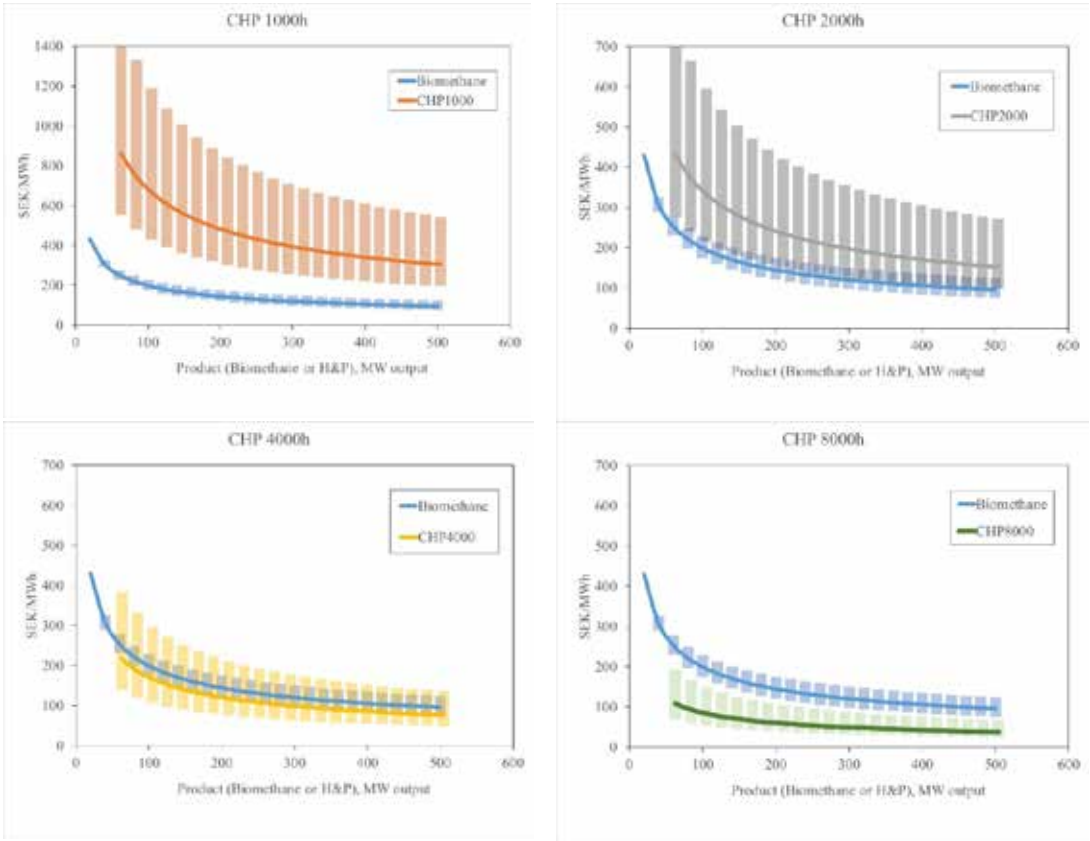

Figure 3: Depreciation *cost divided by the expected production during the technical lifetime of the plant (20 years) for 8000 full-load-hours of the ABP-plant and 1000, 2000, 4000 and 8000 full-load-hours for the CHP-plant. Note that the y-axis for 1,000 full-load-hours of the CHP-plant differs from the other cases.*

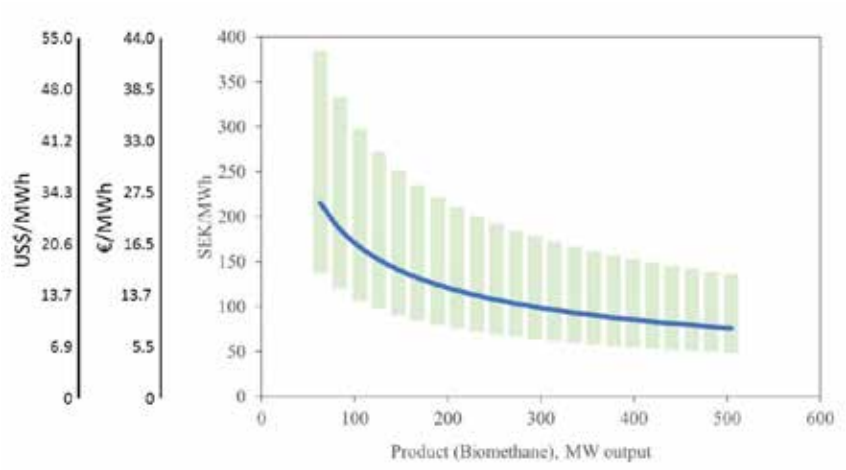

Figure 4: Depreciation *cost for biomethane including non-technical uncertainties divided by the expected production during the technical lifetime of the plant (20 years). Exchange rates: 9.1 SEK per 1.0 € (average exchange rate during the project) and 1.25 US$ per 1.0 €.*

The operating costs for the GoBiGas plant (all costs excluding the investment-related financial costs), are illustrated as a function of the fuel price in Fig 5. The current operating costs for the GoBiGas plant

using wood pellets for feed stock are indicated as an area, where the area is based on variations in feedstock prices, as well as variations in plant operation in terms of availability, load, and efficiency. Previous investigations have shown that it is technically feasible to achieve a chemical efficiency for biomass-to-biomethane conversion of around 70% for the plant, as compared to the current level of 55%–65% (for further details on how to optimize the process, see [1,2]). The operating costs estimated for an 8,000h/year operation, and a biomass-to-biomethane conversion efficiency of 70% are illustrated with a dotted line in Fig 3. A commercial plant could be further optimized in terms of operational costs, mainly by including a steam cycle and removing the need to use large volumes of RME as a scrubbing liquid (see Table 1). The operating costs estimated for a commercial ABP plant are indicated with a solid line in Fig 5.

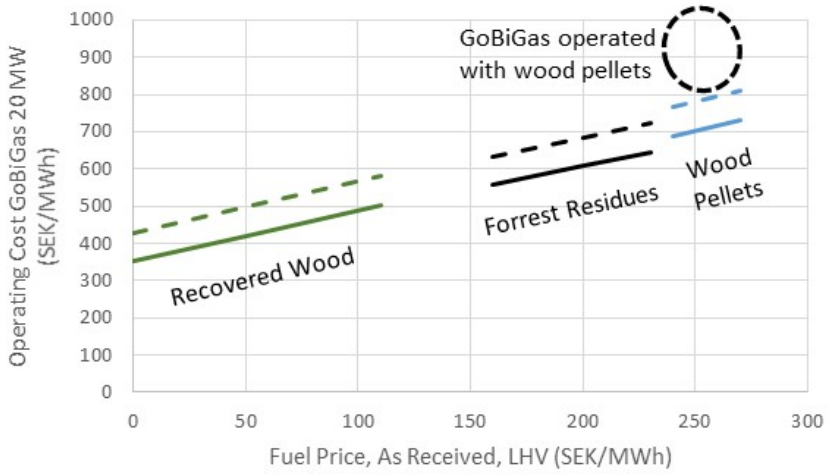

Figure 5 Total operating costs for the GoBiGas plant if optimized and complemented with a dryer, as well as the range of present production costs when using wood pellets. (Fuel price is related to lower heating value of received fuel and as the fuel has different moisture content the lines are not continuous).

Applying the scale-factors for the different costs of the production capacities listed in Table 1, the operating cost including and excluding cost for feedstock was estimated as a function of the production capacity of a plant (see Figs 6 and 7).

The following cases are based on the operating cost for a commercial plant (solid line in Fig 5): In Fig 6, the effects on the operating cost excluding the cost for the feedstock of scaling up the process with different levels of availability are shown. The results show that a lower availability (in terms of the numbers of FLH) will have a very strong impact on the operating costs for plants with capacities of <100 MW. This is mainly related to the personnel costs, which are proportionally higher for smaller scales and are constant regardless of the availability, as the personnel are here assumed to be employed for the full year. Furthermore, the availability will also have a strong impact on the relative investment cost for the production, as exemplified above for CHP plants (Fig. 3).

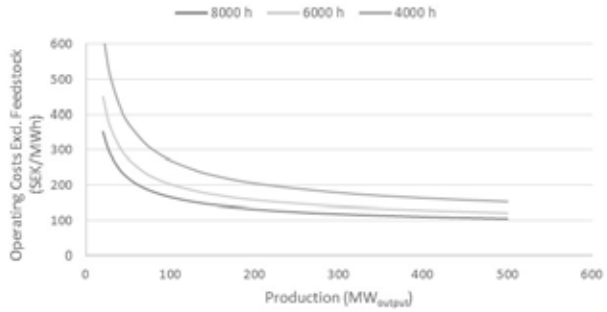

Figure 6: Operating costs excluding feedstock as a function of the production capacity and FLH of the plant.

As shown in Fig 5, the cost of the feedstock has a strong impact on the production cost. Figure 7 shows how the price for the feedstock affects the operating cost as a function of the plant production capacity. As expected, the cost of the feedstock becomes in relative terms more important as the scale of operation increases.

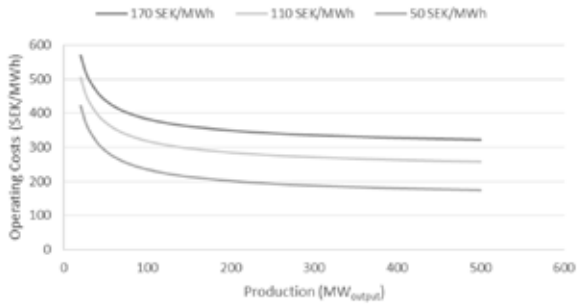

Figure 7. Operating costs as a function of the production capacity of the plant and price of feedstock, assuming an availability of the plant corresponding to 8,000 FLH per year.

Table 2. Estimated total production cost (including investment costs) for biomethane, using forest residues for feedstock (170 SEK/MWh based on lower heating value of received fuel with 45% moisture), 8,000 FLH, 20-year economic lifetime, and 70% plant efficiency.

	Commercial plant 20 MW SEK/MWh	Commercial plant 100 MW SEK/MWh	Commercial plant 200 MW SEK/MWh
Capital cost, depreciation	430	199	145
Capital cost, interest (5%)	258	120	87
Development cost	43	20	15
Operation costs (excluding feedstock)	352	166	132
Feedstock Cost	217	217	217
Total cost	1300	722	596

In Table 2, the estimated total production costs for an ABP plant with 70% efficiency, including capital cost, are given for plants with 20, 100, and 200 MW of biomethane production. A 200-MW ABP is

deemed the optimal size for a plant. As shown in Fig 3 and in Fig 6 and 7, the cost reduction due to economy of scale for plants with capacities above 200 MW plateaus (considering that largest feasible plant size is around 500 MW advance biofuel production), and the benefit of proceeding to a larger scale becomes increasingly uncertain. At this scale of operation the feedstock logistics and handling expenses start to add significant additional costs for most geographic locations, and as it a local specific cost, it is not included in the present analysis. In Table 2, forest residues are chosen as feedstock in all the cases, which would be most relevant for these types of plants in the case of large-scale introduction of advanced biofuels. Here, should be noted that used costs represent forest residue at current price level in the Gothenburg region, which has a market situation where there is an excess of such feedstocks the region. For a smaller plant alternative local feedstocks, such as recovered wood materials, could be an alternative. Under current pricing conditions it offers the potential to reduce the total cost of a 100-MW biomethane plant to the same level as that of a 200-MW biomethane unit using forest residue. If aiming for even smaller scales of operation, cheaper feedstocks would need to be complemented with options for integration with existing industrial infrastructures to reduce the investment cost and provide opportunities for sharing personnel. This could reduce the total production costs to competitive levels, similar to the strategy used for small CHP plants as discussed above. It should also be noted, as evident from the comparison of the resulting feedstock costs for various production efficiencies (Table 1) with the total production cost (including investments), that the influence of plant efficiency has a limited effect on the total cost as long as fuel prices are at or below the price of forest residues.

In summary, the most important factors for reducing the total production costs (including capital costs) are plant availability and scale of operation. The timing of the investment and the location of the plant create the largest uncertainties for the capital cost, which can either increase by up to 95% (30% increase in initial investment cost and 10% interest rate) or shrink by up to 45% (30% decrease in initial investment cost and 2.5% interest rate).

Conclusions

In the GoBiGas project, the production of an advanced biofuel in the form of biomethane has been demonstrated in an industrial scale. By analyzing the investment and production costs at the GoBiGas plant, relevant cost data for future investments in advanced biofuel factories have been compiled. Using forest residues for feedstock at present regional price of 170 SEK/MWh (based on lower heating value of revised moist biomass) this study predicts a production cost for advanced biofuels around 590 SEK/MWh, corresponding to around 5.35 SEK/liter gasoline equivalent, from a commercial plant with a nominal production capacity of 200 MW biomethane, when no excess heat is valorized

Given that the gasification based processes comprise already commercially available components that are used in many existing industrial processes, and the fact that the demonstration plant is designed to meet all regulations pertaining to a commercial plant of this kind, the investment cost is unlikely to decrease dramatically due to learning. Furthermore, the main components of an ABP plant are the same regardless of the end-product, making the result relevant not only for biomethane (as produced at GoBiGas), but also other advanced biofuels, such as methanol, dimethyl ether (DME), mixed alcohols or Fischer-Tropsch products.

In specific cases, the production cost could be reduced further, subject favorable local conditions which could play an important role in providing feasible economic conditions for introducing the technology. The investment cost could also be reduced by taking advantage of investments already made in existing industrial plants and retrofit such plants to produce advanced biofuels, potentially employing simplified process concepts where low investment cost are prioritized over high efficiency when excess

heat from the ABP can be valorized. This can make it feasible to introduce the technology at smaller sizes than what is here deemed the optimal size for a stand-alone unit. However, the greatest opportunity to reduce the overall cost level is to change from biomass to waste-derived feedstocks, where refused derived fuel without impregnated wood and paint are the nearest choice, followed by feeds that are more and more heterogeneous.

These low cost feedstocks represent an exciting opportunity for the GoBiGas plant, which to date has not been adapted to run on these inexpensive alternatives. Having two parallel fuel-feeding systems, the plant is partially prepared for this, however, the absence of an on-site fuel dryer and the required permits for using waste-derived feedstocks has restricted the possibility to explore this possibility. In the longer-term perspective, ABP from waste-derived feedstocks in small dedicated plants, or in plants that are integrated into existing infrastructures so as to ensure a significant reduction in investment costs, is limited. Hence, in the case of extensive introduction of advanced biofuels, they will only have the potential to account for a minor proportion of the total production required. Therefore, in the long term, most of the production of advanced biofuels is expected to come from plants that have an output of around 200 MW utilizing forest residues as feedstock.

Acknowledgment

This work was performed as a part of the Swedish Energy Agency project *Comparative KPI's for integration of biofuel production in CHP processes*, with additional support from the Swedish Gasification Centre (SFC). Måns Collin has contributed to the editing of the paper.

References

1. Alamia, A., A. Larsson, C. Breitholtz, and H. Thunman. 2017. Performance of large-scale biomass gasifiers in a biorefinery, a state-of-the-art reference. Int. J. Energy Res. 41:2001–2019. DOI: 10.1002/er.3758
2. Alamia, A., S. Òsk Gardarsdòttir, A. Larsson, F. Normann, and H. Thunman. 2017. Efficiency comparison of large-scale standalone, centralized, and distributed thermochemical biorefineries. Energy Technol. 5:1435–1448. DOI: 10.1002/ente.201600719
3. Henrik Thunman, Martin Seemann, Teresa Berdugo Vilches, Jelena Maric, David Pallares, Henrik Ström, Göran Berndes, Pavleta Knutsson, Anton Larsson, Claes Breitholtz & Olga Santos. 2017. Advanced biofuel production *via* gasification – lessons learned from 200 man-years of research activity with Chalmers' research gasifier and the GoBiGas demonstration plant. Energy Science & Engineering, doi: 10.1002/ese3.188
4. Kuba, M., Kraft, S., Kirnbauer, F., Maierhans, F., Hofbauer, H. 2017. Influence of controlled handling of solid inorganic materials and design changes on the product gas quality in dual fluid bed gasification of woody biomass. Applied Energy 210 (2018) 230–240. doi.org/10.1016/j.apenergy.2017.11.028
5. Nordic Energy Technology Perspectives 2016, www.iea.org/etp/nordic

Published results:

Relevant references from the associated research activity connected to the research network connected to the GoBiGas demonstration

Relevant references from the associated research activity connected to the research network connected to the GoBiGas demonstration

1/ Process analysis and optimization

1. Advanced Biofuel Production via Gasification - Lessons Learned from 200 man-years of research activity with Chalmers' research gasifier and the GoBiGas demonstration plant, 2018, **https://doi.org/10.1002/ese3.188**
2. Efficiency Comparison of Large-Scale Standalone, Centralized, and Distributed Thermochemical Biorefineries Energy Technology, 2017, **https://doi.org/10.1002/ente.201600719**
3. Performance of large-scale biomass gasifiers in a biorefinery, a state-of-the-art reference International Journal of Energy Research, 2017, **https://doi.org/10.1002/er.3758**
4. Process simulation od dual fluidized bed gasifiers using experimental data, 2016, **https://doi.org/10.1021/acs.energyfuels.6b00122**
5. Well-to-wheel analysis of bio-methane via gasification, in heavy duty engines within the transport sector of the European Union Applied Energy, 2016, **https://doi.org/10.1016/j.apenergy.2016.02.001 0.1002/ese3.188**
6. Improved syngas processing for enhanced Bio-SNG production: A techno-economic assessment, 2016, **https://doi.org/10.1016/j.energy.2016.02.037**
7. Design of an integrated dryer and conveyor belt for woody biofuels, 2015, **https://doi.org/10.1016/j.biombioe.2015.03.022**
8. Initial corrosion attack of 304L and T22 in 2 MW biomass gasifier: a microstructural investigation, 2015, **https://doi.org/10.1179/0960340914Z.000000000101**
9. Heat extraction from a utility-scale oxy-fuel-fired CFB boiler, 2015, **https://doi.org/10.1016/j.ces.2015.03.015**
10. Techno-economic evaluation of a mechanical pulp mill with gasification, 2013, **https://doi.org/10.1016/j.apenergy.2010.10.022**
11. Impact of choice of CO2 separation technology on thermo-economic performance of Bio-SNG production processes, 2013, **https://doi.org/ 10.1002/er.1828**
12. Bio-SNG from Thermal Gasification - Process Synthesis, Integration and Performance. Stefan Heyne, 2013. PhD Thesis, Chalmers University of Technology **ISSN 1404-7098** (https://research.chalmers.se/en/publication/?id=175377)
13. Exergy-based comparison of indirect and direct biomass gasification technologies within the framework of bio-SNG production, 2013, **https://doi.org/10.1007/s13399-013-0079-1**
14. Extending existing combined heat and power plants for synthetic natural gas production, 2011, **https://doi.org/10.1002/er.1828**
15. Highly efficient electricity generation from biomass by integration and hybridization with combined cycle gas turbine (CCGT) plants for natural gas, 2010, **https://doi.org/10.1016/j.energy.2010.06.008**
16. First Experiences with the New Chalmers Gasifier, 2009, Proceedings of the 20th International Conference on Fluidized Bed Combustion, **https://doi.org/10.1007/978-3-642-02682-9_101**

2/ Fuel conversion

1. Bed material as a catalyst for char gasification: The case of ash-coated olivine activated by K and S addition, 2018, **https://doi.org/10.1016/j.fuel.2018.03.079**
2. Influence of bed material, additives and operational conditions on alkali metal and tar concentrations in fluidized bed gasification of biomass, 2018, **https://doi.org/10.1021/acs.energyfuels.8b00159**
3. Effect of ash circulation on the performance of a dual fluidized bed gasification system, 2018, **https://doi.org/10.1016/j.biombioe.2018.04.01**
4. Comparing the structural development of sand and rock ilmenite during long-term exposure in a biomass fired 12 MW th CFB-boiler, 2018, **https://doi.org/10.1016/j.fuproc.2017.11.004**
5. Upscaling Effects on Char Conversion in Dual Fluidized Bed Gasification, 2018, **https://doi.org/10.1021/acs.energyfuels.8b00088**
6. Validation of the oxygen buffering ability of bed materials used for OCAC in a large scale CFB boiler, 2017, **https://doi.org/10.1016/j.powtec.2016.12.048**
7. Experience of more than 1000h of operation with oxygen carriers and solid biomass at large scale, 2017, **https://doi.org/10.1016/j.apenergy.2017.01.032**
8. Alkali-Feldspar as a Catalyst for Biomass Gasification in a 2-MW Indirect Gasifier, 2017, **https://doi.org/10.1021/acs.energyfuels.6b02312**
9. Thermogravimetric and Online Gas Analysis on various Biomass Fuels, 2017, **https://doi.org/10.1016/j.egypro.2017.03.296**
10. Catalytic fast pyrolysis of biomass to produce furfural using heterogeneous catalyst, 2017, **https://doi.org/10.1016/j.jaap.2017.07.022**
11. Enhancement of conversion from bio-syngas to higher alcohols fuels over K-promoted Cu-Fe bimodal pore catalysts, 2017, **https://doi.org/10.1016/j.fuproc.2017.02.010**
12. Co-gasification of coal and biomass: synergy, characterization and reactivity of the residual char, 2017, **https://doi.org/10.1016/j.biortech.2017.07.111**
13. Fast hydrothermal liquefaction of native and torrefied wood, 2017, **https://doi.org/10.1016/j.egypro.2017.03.305**
14. Comparing Active Bed Materials in a Dual Fluidized Bed Biomass Gasifier: Olivine, Bauxite, Quartz-Sand, and Ilmenite, 2016, **https://doi.org/10.1021/acs.energyfuels.6b00327**
15. Impact of Biomass Ash-Bauxite Bed Interactions on an Indirect Biomass Gasifier, 2016, **https://doi.org/10.1021/acs.energyfuels.6b00157**
16. Gasification Reaction Pathways of Condensable Hydrocarbons, 2016, **https://doi.org/10.1021/acs.energyfuels.6b00515**
17. Influence of Fuel Ash Characteristics on the Release of Potassium, Chlorine, and Sulfur from Biomass Fuels under Steam-Fluidized Bed Gasification Conditions, 2016, **https://doi.org/10.1021/acs.energyfuels.6b01470**
18. Characteristics of olivine as a bed material in an indirect biomass gasifier, 2015, **https://doi.org/10.1016/j.cej.2015.05.061**
19. Experimental Investigation of Volatiles–Bed Contact in a 2–4 MW_{th} Bubbling Bed Reactor of a Dual Fluidized Bed Gasifier, 2015, **https://doi.org/10.1021/acs.energyfuels.5b01303**
20. Conversion of Condensable Hydrocarbons in a Dual Fluidized Bed Biomass Gasifier, 2015, **https://doi.org/10.1021/acs.energyfuels.5b01291**
21. An experimental study on catalytic bed materials in a biomass dual fluidised bed gasifier, 2015, **https://doi.org/10.1016/j.renene.2015.03.020**
22. Effects of Steam on the Release of Potassium, Chlorine, and Sulfur during Char Conversion, Investigated under Dual-Fluidized-Bed Gasification Conditions, 2014, **https://doi.org/10.1021/ef501591m**

23. Ash properties of ilmenite used as bed material for combustion of biomass in a circulating fluidized bed boiler, 2014, **https://doi.org/10.1021/ef501810u**
24. Using ilmenite to reduce the tar yield in a dual fluidized bed gasification system, 2014, **https://doi.org/10.1021/ef500132p**
25. Internal tar-CH4 reforming in a biomass dual fluidised bed gasifier, 2014, **https://doi.org/10.1007/s13399-014-0151-5**
26. Evaluation of the performance of industrial-scale dual fluidized bed gasifiers using the Chalmers 2-4 MW_{th} gasifier, 2013, **https://doi.org/10.1021/ef400981j**
27. Using an oxygen-carrier as bed material for combustion of biomass in a 12-MWth circulating fluidized-bed boiler, 2013, **https://doi.org/10.1016/j.fuel.2013.05.073**
28. Transformation and Release of Potassium, Chlorine, and Sulfur from Wheat Straw under Conditions Relevant to Dual Fluidized Bed Gasification, 2013, **https://doi.org/10.1021/ef401703a**
29. Simulation of biomass gasification in a dual fluidized bed gasifier, 2012**,** **https://doi.org/10.1007/s13399-011-0030-2**
30. Characterization of Particulate Matter in the Hot Product Gas from Indirect Steam Bubbling Fluidized Bed Gasification of Wood Pellets, 2011, **https://doi.org/10.1021/ef101710u**
31. Characterization and prediction of biomass pyrolysis products, 2011, **https://doi.org/10.1016/j.pecs.2011.01.001**
32. Separation of drying and devolatilization during conversion of solid fuels, 2004, **https://doi.org/10.1016/j.combustflame.2004.02.008**
33. Thermal conductivity of wood—models for different stages of combustion, 2002, **https://doi.org/10.1016/S0961-9534(02)00031-4**
34. Combustion of wood particles—a particle model for eulerian calculations, 2002, **https://doi.org/10.1016/S0010-2180(01)00371-6**
35. Composition of Volatile Gases and Thermochemical Properties of Wood for Modeling of Fixed or Fluidized Beds, 2001, **https://doi.org/10.1021/ef010097q**

3/ Gas conditioning

1. Fate of Polycyclic Aromatic Hydrocarbons during Tertiary Tar Formation in Steam Gasification of Biomass, 2018, **https://doi.org/10.1021/acs.energyfuels.7b03558**
2. Role of potassium in the enhancement of the catalytic activity of calcium oxide towards tar reduction, 2018, **https://doi.org/10.1016/j.apcatb.2018.02.002**
3. Mechanism and Kinetic Modeling of Catalytic Upgrading of a Biomass-Derived Raw Gas. An Application with Ilmenite as Catalyst, 2016, **https://doi.org/10.1021/acs.iecr.6b00650**
4. Use of alkali feldspar as bed material for upgrading a biomass-derived producer gas from a gasifier, 2016, **https://doi.org/10.1016/j.cej.2016.02.060**
5. Importance of Decomposition Reactions for Catalytic Conversion of Tar and Light Hydrocarbons. An Application with an Ilmenite Catalyst, 2016, **https://doi.org/10.1021/acs.iecr.6b03060**
6. Cu-impregnated alumina silica bed materials for Chemical Looping Reforming of Biomass gasification gas, 2016, **https://doi.org/10.1016/j.fuel.2016.04.024**
7. Reduced Mechanism for Nitrogen and Sulfur Chemistry in Pressurized Flue Gas Systems, 2016, **https://doi.org/10.1021/acs.iecr.5b04670**
8. Time-resolved modeling of gas mixing in fluidized bed units, 2015, **https://doi.org/10.1016/j.fuproc.2015.01.017**

9. Modeling the nitrogen and sulfur chemistry in pressurized flue gas systems, 2015, **https://doi.org/10.1021/ie504038s**
10. Use of CuO,MgAl2O4 and La0.8Sr0.2FeO3,γ-Al2O3 in CLR system for tar removal from gasification gas, 2015, **https://doi.org/10.1002/aic.15034**
11. Chemical Looping Tar Reforming using La, Sr, Fe, containing mixed oxides supported on ZrO2, 2015, **https://doi.org/10.1016/j.apcatb.2015.10.047**
12. Production of Activated Carbon within the Dual Fluidized Bed Gasification Process, 2015, **https://doi.org/10.1021/ie504291c**
13. Using a manganese ore as catalyst for upgrading biomass derived gas Biomass Conversion and Biorefinery, 2015, **https://doi.org/10.1007/s13399-014-0135-5**
14. Modeling the alkali sulfation chemistry of biomass and coal co-firing in oxy-fuel atmospheres, 2014, **https://doi.org/10.1021/ef500290c**
15. Investigation of natural and synthetic bed materials for their utilization in CLR for tar elimination in biomass-derived gasification gas, 2014, **https://doi.org/10.1021/ef500369c**
16. Ilmenite and nickel as catalysts for upgrading of raw gas derived from biomass gasification, 2013, **https://doi.org/10.1021/ef302091w**
17. Producer gas cleaning in a dual fluidized bed reformer - a comparative study of performance with ilmenite and a manganese oxide as catalysts, 2012, **https://doi.org/10.1007/s13399-012-0032-8**
18. Use of nickel oxide as a catalyst for tar elimination in a CLR reactor operated with biomass producer gas, 2012, **https://doi.org/10.1021/ie3028262**
19. Manganese oxide as catalyst for tar cleaning of biomass-derived gas, 2012, **https://doi.org/10.1007/s13399-012-0042-6**
20. Continuous catalytic tar reforming of biomass derived raw gas with simultaneous catalyst regeneration, 2011, **https://doi.org/10.1021/ie200645s**
21. Experimental test on a novel dual fluidised bed biomass gasifier for synthetic fuel production, 2011, **https://doi.org/10.1016/j.fuel.2010.12.035**

4/ Fluid dynamics

1. Bottom-bed fluid dynamics – Influence on solids entrainment, 2018, **https://doi.org/10.1016/j.fuproc.2017.12.023**
2. Control of the solids retention time in a novel multi-staged fluidized bed reactor, 2017, **https://doi.org/10.1016/j.fuproc.2017.06.027**
3. A conversion-class model for describing fuel conversion in large-scale fluidized bed units, 2017, **https://doi.org/10.1016/j.fuel.2017.01.090**
4. The role of fuel mixing on char conversion in a fluidized bed, 2017, **https://doi.org/10.1016/j.powtec.2016.10.060**
5. Mass transfer under segregation conditions in fluidized beds, 2017, **https://doi.org/10.1016/j.fuel.2017.01.021**
6. Magnetic tracking of a fuel particle in a fluid-dynamically down-scaled fluidised bed, 2017, **https://doi.org/10.1016/j.fuproc.2017.03.018**
7. Solids circulation in circulating fluidized beds with low riser aspect ratio and varying total solids inventory, 2017, **https://doi.org/10.1016/j.powtec.2016.09.028**
8. Experimental characterization of axial fuel mixing in fluidized beds by magnetic particle tracking, 2017, **https://doi.org/10.1016/j.powtec.2016.12.093**
9. On the dynamics of instabilities in two-fluid models for bubbly flows, 2017, **https://doi.org/10.1016/j.ces.2017.03.063**

10. Influence of surrounding conditions and fuel size on the gasification rate of biomass char in a fluidized bed, 2016, **https://doi.org/10.1016/j.fuproc.2016.01.002**
11. Measuring fuel mixing under industrial fluidized-bed conditions – A camera-probe based fuel tracking system, 2016, **https://doi.org/10.1016/j.apenergy.2015.11.024**
12. Experimental and numerical investigation of the dynamics of loops seals in a large-scale DFB system under hot conditions, 2015, **https://doi.org/10.1002/aic.14887**
13. Diversity of chemical composition and combustion reactivity of various biomass fuels, 2015, **https://doi.org/10.1016/j.fuel.2015.01.047**
14. Magnetic tracer-particle tracking in a fluid dynamically down-scaled bubbling fluidized bed, 2015, **https://doi.org/10.1016/j.fuproc.2015.06.016**
15. Influence of bulk solids cross-flow on lateral mixing of fuel in dual fluidized beds, 2015, **https://doi.org/10.1016/j.fuproc.2015.09.017**
16. Challenges and Opportunities in the Eulerian Approach to Numerical Simulations of Fixed-bed Combustion of Biomass, 2015, **https://doi.org/10.1016/j.proeng.2015.01.293**
17. The crucial role of frictional stress models for simulation of bubbling fluidized beds, 2015, **https://doi.org/10.1016/j.powtec.2014.09.050**
18. Experimental quantification of lateral mixing of fuels in fluid-dynamical down-scaled bubbling fluidized bed, 2014, **https://doi.org/10.1016/j.apenergy.2014.09.075**
19. Experimental evaluation of lateral mixing of bulk solids in a fluid-dynamically down-scaled bubbling fluidized bed, 2014, **https://doi.org/10.1016/j.powtec.2014.04.091**
20. A computationally efficient particle submodel for CFD simulations of fixed bed conversion, 2013, **https://doi.org/10.1016/j.apenergy.2012.12.057**
21. CFD simulations of biofuel bed conversion. A submodel for the drying and devolatilization of thermally thick wood particles, 2013, **https://doi.org/10.1016/j.combustflame.2012.10.005**
22. Heat transfer effects on particle motion under rarefied conditions, 2013, **https://doi.org/10.1016/j.ijheatfluidflow.2013.04.012**
23. Estimation of gas phase mixing in packed beds, 2008, **https://doi.org/10.1016/j.combustflame.2007.05.006**
24. Stresses in a Cylindrical Wood Particle Undergoing Devolatilization in a Hot Bubbling Fluidized Bed, 2008, **https://doi.org/10.1021/ef700658k**
25. Estimation of Solids Mixing in a Fluidized-Bed Combustor, 2002, **https://doi.org/10.1021/ie020173s**

5/ Measurement method development

1. Online Measurements of Alkali Metals during Start-up and Operation of an Industrial-Scale Biomass Gasification Plant, 2018, **https://doi.org/10.1021/acs.energyfuels.7b03135**
2. Influence of potassium chloride and other metal salts on soot formation studied using imaging LII and ELS, and TEM technique, 2018, **https://doi.org/10.1016/j.combustflame.2017.11.020**
3. Experimental studies of nitromethane flames and evaluation of kinetic mechanisms, 2018, **https://doi.org/10.1016/j.combustflame.2017.12.011**
4. Experimental Investigation of Potassium Chemistry in Premixed Flames, 2017, **https://doi.org/10.1016/j.fuel.2017.05.013**
5. A novel multi-jet burner for hot flue gases of wide range of temperatures and compositions for optical diagnostics of solid fuels gasification/combustion, 2017, **https://doi.org/10.1063/1.4979638**

6. Development of an alkali chloride vapor-generating apparatus for calibration of ultraviolet absorption measurements, 2017, **https://doi.org/10.1063/1.4975590**
7. Modeling of Alkali Metal Release during Biomass Pyrolysis, 2017, **https://doi.org/10.1016/j.proci.2016.06.079**
8. Terahertz spectroscopy for real-time monitoring of water vapor and CO levels in the producer gas from an industrial biomass gasifier, 2014, **https://doi.org/10.1109/TTHZ.2014.2357344**
9. Method for online measurement of the CHON composition of raw gas from biomass gasifier, 2014, **https://doi.org/10.1016/j.apenergy.2013.08.032**
10. Online Measurement of Elemental Yields, Oxygen Transport, Condensable Compounds, and Heating Values in Gasification Systems, 2014, **https://doi.org/10.1021/ef501433n**
11. Assessment of the SPA method for sampling biomass-derived tar in industrial environments, 2013, **https://doi.org/10.1021/ef401893j**
12. Assessment of the Solid-Phase Adsorption Method for Sampling Biomass-Derived Tar in Industrial Environments, 2013, **https://doi.org/10.1021/ef401893j**
13. Post-flame gas-phase sulfation of potassium chloride, 2013, **https://doi.org/10.1016/j.combustflame.2013.01.010**.
14. Biomass pyrolysis in a heated-grid reactor: Visualization of carbon monoxide and formaldehyde using Laser-Induced Fluorescence, 2011, **https://doi.org/10.1016/j.jaap.2011.06.008**
15. Na and K released from burning particles of brown coal and pine wood in a laminar premixed methane flame using quantitative Laser-Induced Breakdown Spectroscopy, 2011, **https://doi.org/10.1366/10-06108**
16. On-line monitoring of fuel moisture-content in biomass-fired furnaces by measuring relative humidity of the flue gases, 2011, **https://doi.org/10.1016/j.cherd.2011.03.018**
17. Optical and mass spectrometric study of the pyrolysis gas of wood particles, 2003, **https://doi.org/ 10.1366/000370203321535141**

6/ Biomass resources and environmental impacts

1. Future demand for forest-based biomass for energy purposes in Sweden, 2017. **http://dx.doi.org/10.1016/j.foreco.2016.09.018**
2. The potential role of forest management in Swedish scenarios towards climate neutrality by mid century, 2017. **https://doi.org/10.1016/j.foreco.2016.07.015**
3. Carbon balances of bioenergy systems using biomass from forests managed with long rotations: Bridging the gap between stand and landscape assessments, 2017. **https://doi.org/10.1111/gcbb.12425**
4. Status and prospects for renewable energy using wood pellets from the southeastern United States, 2017. **https://doi.org/10.1111/gcbb.12445**
5. How to Analyse Ecosystem Services in Landscapes — a systematic review, 2017. **https://doi.org/10.1016/j.ecolind.2016.10.009**
6. Bioenergy production and sustainable development: science base for policy-making remains limited, 2017. **https://doi.org/10.1111/gcbb.12338**
7. The role of biomass to replace fossil fuels in a regional energy system: The case of west Sweden, 2016, **https://doi.org/10.2298/TSCI151216113K**
8. Assessment of biomass energy sources and technologies: The case of Central America, 2016**, https://doi.org/10.1016/j.rser.2015.12.322**
9. Opportunities to encourage mobilization of sustainable bioenergy supply chains, 2016, **https://doi.org/10.1002/wene.237**

10. Policy institutions and forest carbon. Reply to “Rethinking forest carbon assessments to account for policy institutions”, 2016, **https://doi.org/10.1038/nclimate3093**
11. Forests and forest management plays a key role in mitigating climate change. Reply to “Europe’s forest management did not mitigate climate warming”, 2016, **https://doi.org/10.1126/science.aad7270**
12. May we have some land use change, please?, 2016, **https://doi.org/10.1002/bbb.1656**
13. The climate effect of increased forest bioenergy use in Sweden: evaluation at different spatial and temporal scales, 2015, **https://doi.org/10.1002/wene.178**
14. Bioenergy and climate change mitigation: an assessment, 2014, **https://doi.org/10.1111/gcbb.12205**
15. How do Sustainability Standards Consider Biodiversity?, 2014, **https://doi.org/10.1002/wene.118**
16. Modeling potential freshwater ecotoxicity impacts due to pesticide use in biofuel feedstock production: the cases of maize, rapeseed, salix, soybean, sugarcane and wheat, 2014. **https://doi.org/10.1021/es502497p**
17. The prospects of cost reductions in willow production in Sweden, 2013, **https://doi.org/10.1016/j.biombioe.2012.11.013**
18. How much land based greenhouse gas can be achieved without compromising food security and environmental goals?, 2013, **https://doi.org/10.1111/gcb.12160**
19. Bioenergy and land use change—state of the art, 2013, **https://doi.org/10.1002/wene.41**
20. The climate benefit of Swedish ethanol – present and prospective performance, 2012, **https://doi.org/10.1002/wene.17**
21. Meeting Sustainability Requirements for SRC bioenergy: Usefulness of existing tools, responsibilities of involved stakeholders, and recommendations for further developments, 2012, **https://doi.org/10.1007/s12155-012-9217-z**
22. Bioenergy’s contribution to climate change mitigation – a matter of perspectives, 2012. **https://doi.org/10.1002/bbb.1343**

7/ Catalytic synthesis and lignin cracking

1. The effect of rosin acid on hydrodeoxygenation of fatty acid, 2018, **https://doi.org/10.1016/j.jechem.2018.01.023**
2. Investigating the effect of Fe as a poison for catalytic HDO over sulfided NiMo alumina catalysts, 2018, **https://doi.org/10.1016/j.apcatb.2018.01.027**
3. Hydroconversion of rosin acids into value-added fuel components over NiMo catalysts with varying support, 2018, **https://doi.org/10.1002/ese3.70**
4. Hydrothermal Liquefaction of Kraft Lignin in Sub-Critical Water: The Influence of the Sodium and Potasium Fraction, 2018, **https://doi.org/10.1007/s13399-018-0307-9**
5. Effect of dimethyl disulfide on activity of NiMo catalysts used in hydrodeoxygenation of oleic acid, 2017, **https://doi.org/10.1021/acs.iecr.6b04703**
6. The storage stability of Bio-oils derived from the catalytic conversion of softwood kraft lignin in subcritical water, 2016, **https://doi.org/10.1021/acs.energyfuels.6b00087**
7. Effect of pH on kraft lignin depolymerisation in sub-critical water, 2016, **https://doi.org/10.1021/acs.energyfuels.6b00462**
8. Using 2D NMR to characterize the structure of low and high molecular weight fractions of bio-oil obtained from LignoBoost™, kraft lignin depolymerized in subcritical water, 2016, **https://doi.org/10.1016/j.biombioe.2016.09.004**

9. Thermal stability of low and high Mw fractions of bio-oil derived from lignin conversion in subcritical water, 2016, **https://doi.org/10.1007/s13399-016-0228-4**
10. Effect of thermal treatment on hydrogen uptake and characteristics of Ni-, Co-, and Mo-containing catalysts, 2015, **https://doi.org/10.1021/acs.iecr.5b02510**
11. Catalytic Depolymerisation and Conversion of Kraft Lignin into Liquid Products Using Near-Critical Water, 2014, **https://doi.org/10.1016/j.supflu.2013.11.022**
12. The effect of temperature on the catalytic conversion of kraft lignin using near-critical water, 2014, **https://doi.org/10.1016/j.biortech.2014.06.051**
13. Pyrolysis oils from CO2 precipitated Kraft lignin, 2011, **https://doi.org/10.1039/c1gc15818j**

8/ Lignin separation processes

1. Local filtration properties of Kraft lignin - The influence of residual xylan, 2017. **https://doi.org/10.1016/j.seppur.2017.01.068**
2. Parameters affecting the cross-flow filtration of dissolved lignoboost kraft lignin, 2016, **https://doi.org/10.1080/02773813.2015.1025284**
3. Lignin separation from kraft black liquor by combining ultrafiltration and precipitation: a study of solubility of lignin with different molecular properties, 2016, **https://doi.org/10.3183/NPPRJ-2016-31-02-p270-278**
4. Investigation and Characterization of lignin precipitation in the LignoBoost process, 2013, **https://doi.org/10.1080/02773813.2013.838267**
5. Precipitation and filtration of lignin from black liquor of different origin, 2007, **https://doi.org/10.3183/NPPRJ-2007-22-02-p188-193**

9/ Biochemical processes

1. Sustaining fermentation in high-gravity ethanol production by feeding yeast to a temperature-profiled multifeed simultaneous saccharification and co-fermentation of wheat straw, 2017, **https://doi.org/10.1186/s13068-017-0893-y**
2. Enhancement of anaerobic lysine production in Corynebacterium glutamicum electrofermentations, 2017, **https://doi.org/10.1016/j.bioelechem.2017.06.001**
3. Nutrients from anaerobic digestion effluents for cultivation of the microalga Nannochloropsis sp. – Impact on grown, biochemical composition and the potential for cost and environmental impact savings, 2017, **https://doi.org/10.1016/j.algal.2017.08.007**
4. Combined genome and transcriptome sequencing to investigate the plant cell wall degrading enzyme system in the thermophilic fungus Malbranchea cinnamomea, 2017, **https://doi.org/10.1186/s13068-017-0956-0**
5. Membrane engineering of S. cerevisiae targeting sphingolipid metabolism, 2017, **https://doi.org/10.1038/srep41868**
6. ALD5, PAD1, ATF1 and ATF2 facilitate the catabolism of coniferyl aldehyde, ferulic acid and p-coumaric acid in Saccharomyces cerevisiae, 2017, **https://doi.org/10.1038/srep42635**
7. A glucoronoyl esterase from Acremonium alcalophilum cleaves native lignin-carbohydrate ester bonds, 2016, **https://doi.org/10.1002/1873-3468.12290**
8. Toward a sustainable biorefinery using high-gravity technology. Biofuels, Bioproducts and Biorefining, 2016, **https://doi.org/10.1002/bbb.1722**

9. Integrating microalgal production with industrial outputs – reducing process inputs and quantifying the benefits, 2016, **https://doi.org/10.1089/ind.2016.0006**
10. Impact of the supramolecular structure of cellulose on the efficiency of enzymatic hydrolysis, 2015, **https://doi.org/10.1186/s13068-015-0236-9**
11. Short-term adaptation during propagation improves the performance of xylose-fermenting Saccharomyces cerevisiae in simultaneous saccharification and co-fermentation, 2015, **https://doi.org/10.1186/s13068-015-0399-4**
12. Lignocellulosic ethanol production at high-gravity: Challenges and perspectives, 2014, **https://doi.org/10.1016/j.tibtech.2013.10.003**
13. Comparison of strategies to overcome the inhibitory effects in a high-gravity fermentation of lignocellulosic hydrolysates, 2014, **https://doi.org/10.1016/j.biombioe.2014.03.060**
14. The chemical nature of phenolic compounds determines their toxicity and induces distinct physiological responses in Saccharomyces cerevisiae in lignocellulose hydrolysates, 2014, **https://doi.org/10.1186/s13568-014-0046-7**
15. Performance and bacterial enrichment of bioelectrochemical systems during methane and acetate production, 2014, **https://doi.org/10.1016/j.ijhydene.2014.05.038**
16. Flocculation causes inhibitor tolerance in Saccharomyces cerevisiae for second-generation bioethanol production, 2014, **https://doi.org/ 10.1128/AEM.01906-14**
17. The influence of HMF and furfural on redox-balance and energy-state of xylose-utilizing Saccharomyces cerevisiae, 2013, **https://doi.org/10.1186/1754-6834-6-22**
18. Lipidomic profiling of Saccharomyces cerevisiae and Zygosaccharomyces bailii reveals critical changes in lipid composition in response to acetic acid stress, 2013, **https://doi.org/10.1371/journal.pone.0073936**
19. Engineering glutathione biosynthesis of Saccharomyces cerevisiae increases robustness to inhibitors in pretreated lignocellulosic materials, 2013, **https://doi.org/10.1186/1475-2859-12-87**
20. Evolutionary engineering strategies to enhance tolerance of xylose utilizing recombinant yeast to inhibitors derived from spruce biomass, 2012. **https://doi.org/10.1186/1754-6834-5-32**
21. Simultaneous saccharification and co-fermentation for bioethanol production using corncobs at lab, PDU and demo scales, 2012, **https://doi.org/10.1186/1754-6834-6-2**

10/ Energy model changes and CO_2 reduction

1. Thermal energy storage in district heating: Centralised storage vs. storage in thermal inertia of buildings, 2018, **https://doi.org/10.1016/j.enconman.2018.01.068**
2. Improving the flexibility of coal-fired power generators: Impact on the composition of a cost-optimal electricity system, 2018, **https://doi.org/10.1016/j.apenergy.2017.10.085**
3. The effect of high levels of solar generation on congestion in the European electricity transmission grid, 2017, **https://doi.org/10.1016/j.apenergy.2017.08.143**
4. Electric road systems in Norway and Sweden-impact on CO2 emissions and infrastructure cost, 2017, **https://doi.org/10.1109/ITEC-AP.2017.8080779**
5. Managing the costs of CO2 abatement in the cement industry, 2017, **https://doi.org/10.1080/14693062.2016.1191007**

6. An economic assessment of distributed solar PV generation in Sweden from a consumer perspective – The impact of demand response, 2017, **https://doi.org/10.1016/j.renene.2017.02.050**
7. Geographic aggregation of wind power—an optimization methodology for avoiding low outputs, 2017, **https://doi.org/10.1002/we.1987**
8. Impact of electricity price fluctuations on the operation of district heating systems: A case study of district heating in Göteborg, Sweden, 2017, **https://doi.org/10.1016/j.apenergy.2017.06.092**
9. Impact of thermal plant cycling on the cost-optimal composition of a regional electricity generation system, 2017, **https://doi.org/10.1016/j.apenergy.2017.04.018**
10. Spacial and dynamic energy demand of the E39 highway – Implications on electrification options, 2017, **https://doi.org/10.1016/j.apenergy.2017.02.025**
11. Demonstrating load-change transient performance of a commercial-scale natural gas combined cycle power plant with post-combustion CO2 capture, 2017, **https://doi.org/10.1016/j.ijggc.2017.05.011**
12. Value of wind power – Implications from specific power, 2017, **https://doi.org/10.1016/j.energy.2017.03.038**
13. Solar photovoltaic-battery systems in Swedish households – Self-consumption and self-sufficiency, 2016, **https://doi.org/10.1016/j.apenergy.2016.08.172**
14. Distributed solar and wind power – Impact on distribution losses, 2016, **https://doi.org/10.1016/j.energy.2016.06.029**
15. Demand response potential of electrical space heating in Swedish single-family dwellings, 2016, **https://doi.org/10.1016/j.buildenv.2015.11.019**
16. CO2 emissions abatement in the Nordic carbon-intensive industry - An end-game in sight?, 2015, **https://doi.org/10.1016/j.energy.2014.12.029**
17. Post-combustion CO2 capture applied to a state-of-the-art coal-fired power plant-The influence of dynamic process conditions, 2015, **https://doi.org/10.1016/j.ijggc.2014.12.001**
18. A geospatial comparison of distributed solar heat and power in europe and the US, 2014, **https://doi.org/10.1371/journal.pone.0112442**
19. Linkages between demand-side management and congestion in the European electricity transmission system, 2014, **https://doi.org/10.1016/j.energy.2014.03.083**
20. Thermo-economic optimization of hybridization options for solar retrofitting of combined-cycle power plants, 2014, **https://doi.org/10.1115/1.4024922**
21. Challenges to integrate CCS into low carbon electricity markets, 2014, **https://doi.org/10.1016/j.egypro.2014.11.785**
22. Dampening variations in wind power generation-The effect of optimizing geographic location of generating sites, 2014, **https://doi.org/10.1002/we.1657**